

A N N U A L   R E P O R T

1 9 7 1

U. S. WATER CONSERVATION LABORATORY  
Southwest Branch  
Soil and Water Conservation Research Division  
Agricultural Research Service  
United States Department of Agriculture  
Phoenix, Arizona

---

FOR OFFICIAL USE ONLY

This report contains unpublished and confidential information concerning work in progress. The contents of this report may not be published or reproduced in any form without the prior consent of the research workers involved.

## TABLE OF CONTENTS

	<u>Title</u>	<u>Page</u>
Introduction		v
SWC-018-gG-4	Increasing and conserving agricultural and rural water supplies	
Ariz.-WCL 61-4	Measurement and calculation of unsaturated conductivity and soil-water diffusivity	1-1
Ariz.-WCL 65-2	Materials and methods for water harvesting and water storage in the State of Hawaii	2-1
Ariz.-WCL 66-2	Irrigation outlet structures to distribute water onto erosive soils	3-1
Ariz.-WCL 67-1	Flow measurement in open channels with critical depth flumes	4-1
Ariz.-WCL 67-2	Physical and chemical characteristics of hydrophobic soils	5-1
Ariz.-WCL 67-4	Waste-water renovation by spreading treated sewage for groundwater recharge	6-1
Ariz.-WCL 68-1	Evaporation of water from soil	7-1
Ariz.-WCL 68-2	Fabricated-in-place, reinforced linings and ground covers	8-1
Ariz.-WCL 68-3	Column studies of chemical, physical, and biological processes of waste-water renovation by percolation through the soil	9-1
Ariz.-WCL 68-5	Assessing the energy environment of plants	10-1
Ariz.-WCL 70-3	Design and performance of trickle irrigation systems	11-1

	<u>Title</u>	<u>Page</u>
Ariz.-WCL 71-1	Relative changes in transpiration and photosynthesis induced by soil water depletion in a constant environment	12-1
Ariz.-WCL 71-2	The effect of irrigation regimes and early cut-off of irrigation water on the yield of high population cotton	13-1
Ariz.-WCL 71-3	Heat and light transfer in ponds	14-1
Ariz.-WCL 71-4	Measurement and prediction of the solubility behavior of the calcium mineral constituents of soils	15-1
Ariz.-WCL 71-5	Water vapor movement through mulches under field conditions	16-1
Ariz.-WCL 71-6	Use of floating materials to reduce evaporation from water surfaces	17-1
Ariz.-WCL 71-7	Water adsorption properties of soil surfaces coated with organic compounds	18-1
Ariz.-WCL 71-8	The effect of air entrapment on water movement in soils	19-1
Ariz.-WCL 71-9	One-dimensional flow in scaled heterogeneous porous media	20-1
Ariz.-WCL 71-10	Assessment of biostimulation and eutrophication of reclaimed waste water	21-1
Ariz.-WCL 71-11	Chemical treatment of irrigation water for the prevention of clogging and the removal of flow obstructions in trickle irrigation systems	22-1
Ariz.-WCL 71-12	Lower cost water harvesting systems	23-1

	<u>Title</u>	<u>Page</u>
Ariz.-WCL 71-15	Soil clogging during intermittent infiltration with secondary sewage effluent	24-1
Appendix I	Summation of Important Findings	AI-1
Appendix II	List of Publications	AII-1
Appendix III	Summary Table of Status of Research Outlines	AIII-1

## CHANGES IN PERSONNEL

The Laboratory has been strengthened during 1971 by the addition of three new members. They are as follows.

M. J. Jones, Agricultural Aid (NYC)  
F. Leon, Jr., Laboratory Aid (NYC)  
J. Robinson, Laboratory Aid (NYC)

During 1971 there were three departures. They are as follows.

F. Leon, Jr., Laboratory Aid (NYC)  
J. Robinson, Laboratory Aid (NYC)  
K. K. Watson, Research Civil Engineer, Visiting Scientist  
from Australia

## LABORATORY STAFF

### Professional:

L. E. Myers, B.S., M.S., P.E., Research Hydraulic Engineer and Director  
H. Bower, B.S., M.S., Ph.D., P.E., Research Hydraulic Engineer  
D. A. Bucks, B.S., M.S., Agricultural Engineer  
K. R. Cooley, B.S., M.S., Ph.D., Research Hydrologist  
W. L. Ehrler, B.A., M.S., Ph.D., Research Plant Physiologist  
L. J. Erie, B.S., M.S., P.E., Agricultural Engineer  
D. H. Fink, B.S., M.S., Ph.D., Soil Scientist  
G. W. Frasier, B.S., M.S., Research Hydraulic Engineer  
R. G. Gilbert, B.S., M.S., Ph.D., Soil Scientist  
S. B. Idso, B.Phys., M.S., Ph.D., Soil Scientist  
R. D. Jackson, B.S., M.S., Ph.D., Research Physicist  
B. A. Kimball, B.S., M.S., Ph.D., Soil Scientist  
J. C. Lance, B.S., M.S., Ph.D., Soil Scientist  
F. S. Nakayama, B.S., M.S., Ph.D., Research Chemist  
R. J. Reginato, B.S., M.S., Soil Scientist  
J. A. Replogle, B.S., M.S., Ph.D., P.E., Research Hydraulic Engineer  
R. C. Rice, B.S., M.S., P.E., Agricultural Engineer  
K. K. Watson, B.E., M.E., Ph.D., Research Civil Engineer  
F. D. Whisler, B.S., M.S., Ph.D., Soil Scientist

Technicians :

E. D. Escarcega, Hydrologic Technician  
O. F. French, B.S., M.S., Agricultural Research Technician  
L. P. Girdley, Engineering Draftsman  
J. R. Griggs, Physical Science Technician  
M. L. Jones, Agricultural Aid (NYC)  
F. Leon, Jr., Laboratory Aid (NYC)  
R. S. Linebarger, B.S., Hydrologic Technician  
J. M. R. Martinez, Engineering Aid  
H. L. Mastin, Physical Science Technician  
J. B. Miller, B.S., Physical Science Technician  
S. T. Mitchell, B.S., Physical Science Technician  
K. G. Mullins, B.S., Physical Science Technician  
J. M. Pritchard, Physical Science Technician  
B. A. Rasnick, B.A., Physical Science Technician  
J. Robinson, Laboratory Aid (NYC)  
M. S. Riggs, Laboratory Technician (Salt River Project)  
R. Valdez, Mathematics Aid

Administrative, Clerical, and Maintenance:

O. J. Abeyta, Gardener  
I. G. Barnett, Janitor  
E. D. Bell, General Machinist  
E. E. De La Rosa, Maintenance Worker  
B. E. Fisher, Library Technician  
C. G. Hiesel, General Machinist  
R. C. Klapper, Maintenance Worker Foreman  
A. H. Morse, B. Ed., Secretary (Dictating Machine Transcribing)  
M. E. Olson, Clerk-Stenographer  
L. J. Orneside, Clerk-Stenographer  
M. A. Seiler, Clerk-Stenographer  
M. F. Witcher, Clerk-Stenographer

TITLE: MEASUREMENT AND CALCULATION OF UNSATURATED  
CONDUCTIVITY AND SOIL WATER DIFFUSIVITY

CRIS WORK UNIT: SWC-018-gG-4 CODE NO.: Ariz.-WCL-61-4

INTRODUCTION:

The objectives and need for study for this project were given in the 1961 Annual Report of the U.S. Water Conservation Laboratory. Annual Reports for 1962, 1963, and 1965 reported work concerning conductivity and soil water diffusivity measurements at several porosities and temperatures. The 1966 report concerned deviations from Darcy's law for flow of water through fine pores. The 1967 and 1968 reports contain data on the flow of various polar and nonpolar liquids, and salt solutions of different concentrations through two ceramic plates in an attempt to elucidate the effect of structuring of polar molecules and electrokinetic effects on flow through very fine pores. This report clarifies some points in the methods of calculating unsaturated hydraulic conductivities from pore size distribution data. This constitutes a terminal report as this project was terminated during 1971.

Methods for calculating the hydraulic conductivity of unsaturated soil from the water content-pressure head relation have been proposed by Childs and Collis-George (1950), Marshall (1958), and Millington and Quirk (1959, 1960, 1961). This report shows that, when a matching factor is used, the calculation procedures for the Marshall and the Millington and Quirk methods are similar except for the exponent of the pore interaction term, and a statistical value for the exponent is determined.

The conductivities are obtained by dividing the water content-pressure head relation into  $n$  equal water content increments, obtaining the pressure head  $h$  at the midpoint of each increment, and calculating the conductivity using the equation

$$k_i = \frac{30\gamma^2}{\rho g \eta} \frac{\epsilon_i^p}{n^2} \sum_{j=1}^m [(2j + 1 - 2i) h_j^{-2}] \quad (1)$$

where  $k_i$  is the hydraulic conductivity ( $\text{cm min}^{-1}$ ) corresponding to the  $i$ th water content increment,  $\gamma$  is the surface tension of water,  $\rho$  the density of water,  $g$  the gravitational constant, and  $\eta$  the viscosity. The number 30 is a composite of the constant  $1/8$  from Poiseuille's equation, 4 from the square of  $r = 2\gamma/h$ , where  $r$  is the pore radius, and 60 converts from seconds to minutes. The term  $\epsilon$  represents the water-filled porosity, usually taken as the volumetric water content. The exponent of  $\epsilon$ ,  $p$ , is a constant whose value depends upon the method of computation. The summation indices are  $j$  and  $i$ , and  $m$  is the number of increments for which the calculation is to be made.

The difference between M and MQ methods lies in the values of  $p$  and  $n$ . For the M method  $p = 2$  and  $n$  is the number of water content increments from zero to the water content in question. For the MQ method  $p = 4/3$  and  $n = n_t$  the total number of water content increments from zero to the saturated water content.

Consider the M method, with  $p = 2$  and  $n$  dependent on the water content increment. We have  $(\epsilon_i/n)^2$ . Now  $\epsilon_i = \epsilon_1 - (n_t - n) \Delta\epsilon$ , and  $\Delta\epsilon = \epsilon_1/n_t$ . Therefore,  $\epsilon_i/n = \epsilon_1/n_t$  is constant for any water content. The Marshall equation is then

$$k_i = A \sum_{j=i}^m [(2j + 1 - 2i) h_j^{-2}] \quad (2)$$

with  $A = (30\gamma^2/\rho g \eta)(\epsilon/n)^2$ , where any  $\epsilon$  and its corresponding  $n$  can be used.

The MQ method requires  $p = 4/3$  and  $n = n_t$ , a constant. Thus,

$$k_i = B \epsilon_i^{4/3} \sum_{j=i}^m [(2j + 1 - 2i) h_j^{-2}] \quad (3)$$

with  $B = (30\gamma^2 / \rho g \eta) (1/n_c^2)$ .

As earlier work has shown, both the M and MQ methods require a matching factor to adequately represent experimental data. Using the ratio of the measured to the calculated saturated conductivity  $k_s/k_1$  as the matching factor, we have

$$k_i = k_s (\epsilon_i/\epsilon_1)^p \frac{\sum_{j=i}^m [(2j+1-2i) h_j^{-2}]}{\sum_{j=1}^m [(2j-1) h_j^{-2}]} \quad (4)$$

where  $p = 0$  for the Marshall formulation (the pore interaction term  $(\epsilon/n)^2$  cancels when the ratio is formed) and  $p = 4/3$  for Millington and Quirk. Since both the M and MQ derivations are based upon an idealized capillary tube model, the value of  $p$  appears arbitrary. It is of interest, then, to determine the value of  $p$  for which Equation [4] will best predict experimental conductivities.

Data were selected from the literature on the basis of having  $k$  values over a wide range of water contents and a detailed water content-pressure head relation. The data were obtained in a laboratory under conditions that allowed the conductivity, water content, and pressure head to be measured on the same sample.

Values of  $p$  were calculated by an iterative procedure that minimized the sums of squares of  $(k_{meas} - k_{calc})/k_{meas}$ . These values, saturated hydraulic conductivity and saturated water content values, are presented in Table 1. For four materials the average value of the exponent is nearly 1.

Although not perfect, the conductivities calculated from laboratory-determined  $h - \epsilon$  relations reasonably predict conductivities measured in the field. These results support the use of calculation methods for obtaining the hydraulic conductivity-water content relation for field soils.

## SUMMARY AND CONCLUSIONS :

Two methods for calculating hydraulic conductivities of porous materials were examined and simplified. In particular, the methods proposed by Marshall and by Millington and Quirk were shown to be similar except for the pore interaction term. Using a matching factor, equations for the two methods differ only by the exponent of the pore interaction term, being 0 for Marshall's method and 4/3 for Millington and Quirk's. Data for four porous materials, for which the hydraulic conductivities, pressure heads, and water contents were determined on the same sample, were used in a statistical procedure to obtain a best fit value for the exponent. For the four materials, an exponent of 1 adequately predicted the measured conductivities. With this exponent, hydraulic conductivities for a field soil were calculated from a laboratory-determined pressure head-water content relation. Calculated and measured conductivities agreed to within the limit of error of measurement. These results support the use of calculation methods for obtaining the hydraulic conductivity-water content relation for field soils.

## REFERENCES:

1. Childs, E. C., and N. Collis-George. The permeability of porous materials. Proc. Roy. Soc., London, A, 201, 392-405. 1950.
2. Marshall, T. J. A relation between permeability and size distribution of pores. J. Soil Sci., 9, 1-8. 1958.
3. Millington, R. J., and J. P. Quirk. Permeability of porous media. Nature, 183, 387-388. 1959.
4. Millington, R. J., and J. P. Quirk. Transport in porous media. Trans. Intern. Congr. Soil Sci., 7th, Madison, 1.3, 97-106. 1960.
5. Millington, R. J., and J. P. Quirk. Permeability of porous solids. Trans. Faraday Soc., 57, 1200-1206. 1961.

PERSONNEL: Ray D. Jackson

CURRENT TERMINATION DATE: 1971

Table 1. Values of the exponent  $p$ , saturated hydraulic conductivity, and saturated water content for four porous materials.

Porous material	$p$	$k_s$ ( $\text{cm min}^{-1}$ )	$\epsilon$ ( $\text{cm}^3 \text{ cm}^{-3}$ )
1 - 5 mm sand	0.82	1.05	0.30
Botany sand	0.90	1.116	0.35
50-500 $\mu$ sand	1.24	0.267	0.40
Guelph loam	0.74	0.021	0.52

TITLE: MATERIALS AND METHODS FOR WATER HARVESTING AND  
WATER STORAGE IN THE STATE OF HAWAII

CRIS WORK UNIT: SWC-018-gG4

Code No.: Ariz.-WCL 65-2

INTRODUCTION:

Treatments and procedures at the Maui catchments remained the same as described in previous annual reports. A new asphalt-fiberglass covering was installed on the Kukaiau catchment in June 1971. Also in June 1971, critical depth flumes were installed on three small watersheds of non-irrigated sugar cane and two small watersheds of pineapple.

RESULTS AND DISCUSSION:

Kukaiau Catchment: The elastomeric reservoir lining is performing satisfactorily. Several small seam failures occurred, but these were easily repaired by ranch personnel. Seams in the chlorinated polyethylene sheeting started failing rapidly early in 1971. The sheeting was removed and an asphalt-fiberglass covering installed in June 1971. A description of the installation is presented in the 1971 annual report titled "Fabricated-In-Place, Reinforced Linings and Ground Covers."

Maui Catchments: All plots were considered in satisfactory condition when inspected in June 1971. Several seams were starting to fail on the Hypalon sheeing on Plot 1. The sheeting itself appeared to be weathering satisfactorily. The butyl and asphalt-fiberglass plots were in excellent condition. There were 3 or 4 plants growing through the fiberglass but these were easily removed. Trouble is still being encountered with plugging of the meters on the water measuring system. It appears that the meters and screens will require cleaning on a bimonthly schedule or more often to insure reliability of the data.

Analysis has been started of the runoff data collected from the plots for the period of 24 June 1966 through 27 September 1969. This runoff data is from the critical depth flumes on the plots and was recorded on charts with water stage recorders. The charts on the

recorders were changed weekly and the data recorded usually represented 5 to 50 runoff events per chart. Analysis of this volume of data was delayed until a chart reader and Wang calculator was purchased.

Preliminary analysis of the rainfall data shows that the major portion of the precipitation at the test site occurs as showers less than 5 mm in size and with intensities of less than 10 mm per hour. Measured runoff from the grass plot for the period of 24 June 1966 through 27 September 1969 by weeks is presented in Table 1. Total runoff from the plot averaged approximately 15 percent for this period. This quantity of runoff is larger than was expected, especially when considering the size and intensity of the individual rainfall events. One observation from the runoff results is that the majority of the runoff occurs during the winter and early spring months. Further analysis of the data will be done to evaluate runoff by individual rainfall event. Conversion of analog to digital data for the butyl and asphalt plots has not been completed.

Studies were initiated in the spring of 1971 to measure runoff and erosion from small watersheds of non-irrigated sugar cane and pineapple. In May 1971, five sites approximately 5 acres in size were selected. Two of the sites were on sugar cane in a 100 to 200 inch rainfall zone on the island of Hawaii. The other three sites are on the island of Oahu, two pineapple and one sugar cane in an approximately 100 inch rainfall zone.

Runoff from the sites will be measured with critical depth flumes equipped with water stage recorders. The flumes were prefabricated at the U.S. Water Conservation Laboratory, partially disassembled and air freighted to the islands. In June 1971 the flumes were installed by personnel from the USWCL staff with assistance by Soil Conservation Service. The downstream ends of two flumes had to be supported on trestles which were also prefabricated and shipped with the flumes. At one site a bulldozer was provided to move the

soil. At the other four sites all excavation and backfilling was done by hand with shovels, picks, and a wheelbarrow.

Each site will be equipped with a weighing raingage. The data from the raingages and water stage recorders will be recorded on punched paper tape at 5 minute intervals for later processing by computer. Final installation of the raingages and water stage recorders will be completed in early 1972. Maintenance of the recorders will be performed by SCS personnel augmented by periodic visits by USWCL personnel.

#### SUMMARY AND CONCLUSIONS:

The elastomeric reservoir lining on the Kukaiiau water harvesting unit is in good condition. There were small seam failures which were repaired by ranch personnel. A new asphalt-fiberglass covering was installed on the catchment in June 1971 to replace the chlorinated polyethylene sheeting which was failing.

Treatments at the Maui test sites were in satisfactory condition when visited in June 1970. Several seams were starting to fail on the Hypalon sheeting. They butyl and asphalt-fiberglass plots were in excellent condition. Trouble is still being encountered with plugging of meters and screens on the water measuring systems.

Analysis was started of the runoff data from the plots for the period 24 June 1966 through 27 September 1969. The majority of the individual precipitation events for this period occurred as small showers of less than 5 mm each and intensities of less than 10 mm per hour. Total runoff from the grass plot for this period averaged approximately 15 percent and occurred primarily in the winter and early spring.

Studies were initiated to measure runoff and erosion from approximately 5 acre watersheds of non-irrigated sugar cane and pineapple. In June 1971 critical depth flumes were installed on the five sites. Final instrumentation will be completed in 1972.

PERSONNEL: L. E. Myers and G. W. Frasier.

CURRENT TERMINATION DATE: July 1972

Table 1. Rainfall and runoff results from the grass plot at Maui test site by weeks.

Chart Date	Rainfall	Runoff		Chart Date	Rainfall	Runoff	
	(mm)	(mm)	(%)		(mm)	(mm)	(%)
24 Jun 66	55.8	0	0				
1 Jul 66	25.4	0	0				
8 Jul 66	43.3	0	0				
18 Jul 66	40.4	0	0				
25 Jul 66	11.0	<u>1</u> /	-				
1 Aug 66	29.5	0	0				
9 Aug 66	23.5	0	0				
15 Aug 66	54.3	0	0				
22 Aug 66	49.2	0	0				
29 Aug 66	<u>2</u> /	-	-				
5 Sep 66	82.0	0	0				
12 Sep 66	47.6	0	0				
19 Sep 66	1.6	0	0				
27 Sep 66	13.6	0	0				
3 Oct 66	52.3	0	0				
10 Oct 66	159.7	<u>1</u> /	-				
17 Oct 66	<u>2</u> /	-	-				
24 Oct 66	8.7	0	0				
31 Oct 66	58.0	0	0				
9 Nov 66	24.5	0	0				
14 Nov 66	13.5	0	0				
21 Nov 66	45.6	0	0				
28 Nov 66	6.0	0	0				
5 Dec 66	<u>2</u> /	-	-				
12 Dec 66	28.1	0	0				
19 Dec 66	22.1	0	0	<u>1</u> /	Malfunction of water stage recorder		
26 Dec 66	86.9	24.2	27.8	<u>2</u> /	Malfunction of raingage		
30 Dec 66	88.1	10.3	11.7				
Total for 1966	<u>900.0</u>	<u>34.5</u>	<u>3.8</u>				

Table 1. Continued.

Chart Date	Rainfall		Runoff		Chart Date	Rainfall		Runoff	
	(mm)	(mm)	(%)	(mm)		(mm)	(mm)	(%)	
5 Jan 67	5.7	0	0	1 Aug 67	62.2	4.8	7.7		
9 Jan 67	27.0	4.4	16.3	7 Aug 67	297.0	<u>1</u> /	-		
16 Jan 67	13.0	0	0	14 Aug 67	53.0	0	0		
24 Jan 67	33.7	6.9	20.5	21 Aug 67	14.4	0	0		
30 Jan 67	8.2	0	0	28 Aug 67	3.2	0	0		
6 Feb 67	83.5	20.8	24.9	5 Sep 67	27.3	0	0		
13 Feb 67	36.4	0.9	2.5	12 Sep 67	19.1	0	0		
20 Feb 67	41.3	9.2	22.3	18 Sep 67	18.2	0	0		
27 Feb 67	28.7	4.4	15.3	26 Sep 67	22.4	0	0		
6 Mar 67	20.6	0	0	2 Oct 67	12.5	0	0		
14 Mar 67	26.3	8.5	32.3	9 Oct 67	9.5	<u>1</u> /	-		
20 Mar 67	266.5	146.1	54.8	16 Oct 67	0	0	0		
28 Mar 67	53.2	15.1	28.4	24 Oct 67	36.9	<u>1</u> /	-		
3 Apr 67	55.2	13.5	24.5	30 Oct 67	85.7	5.3	6.2		
10 Apr 67	14.8	<u>1</u> /	-	6 Nov 67	67.8	3.1	4.6		
17 Apr 67	5.2	0	0	13 Nov 67	21.7	<u>1</u> /	-		
25 Apr 67	9.6	0	0	20 Nov 67	247.0	12.3	5.0		
1 May 67	8.7	0	0	29 Nov 67	102.7	<u>1</u> /	-		
8 May 67	20.0	0	0	4 Dec 67	75.5	11.8	15.6		
16 May 67	53.2	0.8	1.5	11 Dec 67	17.9	<u>1</u> /	-		
23 May 67	8.5	0	0	18 Dec 67	31.7	<u>1</u> /	-		
29 May 67	3.9	0	0	27 Dec 67	60.6	1.3 <sup><u>1</u></sup> /	2.1		
6 Jun 67	8.3	0	0	Total for	<u>1892.1</u>	<u>291.2</u>	<u>15.4</u>		
13 Jun 67	1.5	0	0	1967					
19 Jun 67	30.2	0	0						
26 Jun 67	84.1	0	0						
5 Jul 67	59.4	0	0						
11 Jul 67	40.0	0	0						
18 Jul 67	95.2	21.6	22.7						
24 Jul 67	56.7	1.7	3.0						

Table 1. Continued.

Chart Date	Rainfall			Runoff			Chart Date	Rainfall			Runoff				
	(mm)	(mm)	(%)	(mm)	(mm)	(%)		(mm)	(mm)	(%)	(mm)	(mm)	(%)		
1 Jan 68	145.3	<u>1</u> /	-	2 Aug 68	22.1	0	0	8 Jan 68	11.3	0	0	8 Aug 68	51.0	0	0
17 Jan 68	<u>2</u> /	-	-	16 Aug 68	6.5	0	0	23 Jan 68	28.9	0	0	23 Aug 68	38.6	0	0
23 Jan 68	28.9	0	0	30 Aug 68	36.8	0	0	6 Feb 68	19.9	0	0	6 Sep 68	11.0	0	0
6 Feb 68	19.9	0	0	20 Sep 68	86.3	<u>1</u> /	-	13 Feb 68	28.7	<u>1</u> /	-	13 Sep 68	23.2	0	0
13 Feb 68	28.7	<u>1</u> /	-	27 Sep 68	24.7	0	0	21 Feb 68	9.3	0	0	4 Oct 68	4.1	0	0
21 Feb 68	9.3	0	0	4 Oct 68	4.1	0	0	1 Mar 68	60.7	9.5	15.7	11 Oct 68	24.2	0	0
7 Mar 68	306.8	127.9	41.7	11 Oct 68	24.2	0	0	7 Mar 68	306.8	127.9	41.7	18 Oct 68	51.1	<u>1</u> /	-
17 Mar 68	<u>2</u> /	-	-	18 Oct 68	51.1	<u>1</u> /	-	17 Mar 68	<u>2</u> /	-	-	27 Oct 68	21.4	0	0
21 Mar 68	<u>2</u> /	25.0	-	27 Oct 68	21.4	0	0	21 Mar 68	<u>2</u> /	25.0	-	1 Nov 68	2.0	0	0
29 Mar 68	10.2	0	0	1 Nov 68	2.0	0	0	29 Mar 68	10.2	0	0	8 Nov 68	61.3	<u>1</u> /	-
4 Apr 68	<u>2</u> /	13.8	-	8 Nov 68	61.3	<u>1</u> /	-	4 Apr 68	<u>2</u> /	13.8	-	15 Nov 68	1.7	<u>1</u> /	-
11 Apr 68	<u>2</u> /	15.1	-	15 Nov 68	1.7	<u>1</u> /	-	11 Apr 68	<u>2</u> /	15.1	-	22 Nov 68	254.1	70.1	27.6
17 Apr 68	89.8	77.6	86.4	22 Nov 68	254.1	70.1	27.6	17 Apr 68	89.8	77.6	86.4	1 Dec 68	61.9	11.0	17.8
25 Apr 68	<u>2</u> /	1.7	-	1 Dec 68	61.9	11.0	17.8	25 Apr 68	<u>2</u> /	1.7	-	5 Dec 68	100.2	19.9	19.9
3 May 68	<u>2</u> /	0	0	5 Dec 68	100.2	19.9	19.9	3 May 68	<u>2</u> /	0	0	13 Dec 68	53.8	2.8	5.2
10 May 68	<u>2</u> /	0	0	13 Dec 68	53.8	2.8	5.2	10 May 68	<u>2</u> /	0	0	20 Dec 68	156.0	<u>1</u> /	-
14 May 68	6.5	0	0	20 Dec 68	156.0	<u>1</u> /	-	14 May 68	6.5	0	0	27 Dec 68	158.6	68.3	43.1
23 May 68	11.7	0	0	27 Dec 68	158.6	68.3	43.1	23 May 68	11.7	0	0	Total for	1731.7	387.1	22.4
31 May 68	0.9	0	0	Total for	1731.7	387.1	22.4	31 May 68	0.9	0	0	1968			
6 Jun 68	39.6	0	0	6 Jun 68	39.6	0	0	6 Jun 68	39.6	0	0				
14 Jun 68	46.1	0	0	14 Jun 68	46.1	0	0	14 Jun 68	46.1	0	0				
21 Jun 68	18.3	0	0	21 Jun 68	18.3	0	0	21 Jun 68	18.3	0	0				
27 Jun 68	3.3	0	0	27 Jun 68	3.3	0	0	27 Jun 68	3.3	0	0				
4 Jul 68	25.8	0	0	4 Jul 68	25.8	0	0	4 Jul 68	25.8	0	0				
11 Jul 68	37.2	0	0	11 Jul 68	37.2	0	0	11 Jul 68	37.2	0	0				
19 Jul 68	40.5	0	0	19 Jul 68	40.5	0	0	19 Jul 68	40.5	0	0				
25 Jul 68	70.7	0	0	25 Jul 68	70.7	0	0	25 Jul 68	70.7	0	0				

Table 1. Continued.

Chart Date	Rainfall		Runoff		Chart Date	Rainfall		Runoff	
	(mm)	(mm)	(%)	(mm)		(mm)	(mm)	(%)	
7 Jan 69	92.2	21.2	23.0	1 Aug 69	75.3	<u>1</u> /	-		
10 Jan 69	4.7	0	0	10 Aug 69	91.5	<u>1</u> /	-		
17 Jan 69	5.4	0	0	15 Aug 69	64.1	<u>1</u> /	-		
24 Jan 69	308.8	87.9	28.5	22 Aug 69	64.0	0	0		
2 Feb 69	66.7	2.3	3.4	29 Aug 69	74.4	<u>1</u> /	-		
7 Feb 69	278.4	55.9	20.1	5 Sep 69	56.6	<u>1</u> /	-		
16 Feb 69	106.6	7.7	7.2	12 Sep 69	29.5	0	0		
21 Feb 69	79.0	<u>1</u> /	-	20 Sep 69	47.2	15.0	31.8		
1 Mar 69	61.6	<u>1</u> /	-	Total for	<u>2172.0</u>	<u>298.0</u>	<u>13.7</u>		
7 Mar 69	158.1	28.4	18.0	1969					
16 Mar 69	120.2	33.0	27.5						
21 Mar 69	86.0	7.8	9.1						
29 Mar 69	227.4	21.6	9.5						
4 Apr 69	74.4	10.3	13.8						
11 Apr 69	24.0	<u>1</u> /	-						
18 Apr 69	23.8	<u>1</u> /	-						
25 Apr 69	121.6	<u>1</u> /	-						
4 May 69	1.9	0	0						
9 May 69	42.2	0	0						
16 May 69	11.3	0	0						
23 May 69	63.3	.6	0.9						
29 May 69	6.2	0	0						
7 Jun 69	36.0	0	0						
13 Jun 69	1.7	0	0						
22 Jun 69	15.1	0	0						
27 Jun 69	73.7	0	0						
5 Jul 69	72.6	0	0						
11 Jul 69	49.2	0	0						
18 Jul 69	129.2	6.3	4.9						
25 Jul 69	48.7	<u>1</u> /	-						

TITLE: IRRIGATION OUTLET STRUCTURE TO DISTRIBUTE WATER  
ONTO EROSION SOILS

CRIS WORK UNIT: SWC-018-gG4 CODE NO.: Ariz.-WCL-66-2

INTRODUCTION:

For need of study, see Annual Report for 1966.

OBJECTIVES:

To obtain design criteria for low-cost irrigation outlets that will distribute large streams of water without excessive erosion.

PROCEDURE:

The major activity on this project has been to construct outlets at farm sites where erosion problems exist, observe their operation, determine their weaknesses, then repair or reconstruct them and continue to observe their performance and longevity.

RESULTS AND DISCUSSION:

Inspections throughout the year indicated no cases of failure due to faulty design, other than on the Cannon Ranch, where some of the original structures were built and a firm bond was not made between the dissipator box and the rest of the structure. In this case, bermuda grass grew through the cracks and will eventually ruin the structure.

On the Sparr Ranch, S-2 was rebuilt because of a leak in the original tile outlet next to the ditch, which allowed water to undermine the structure. S-3 also needed repair because of damage by machinery.

The SS-2 structure on the Spencer and Spencer Ranch, which was coated by a clay emulsion in 1970 because weeds were growing through the walls and ruining it, is in excellent condition at the end of the 1971 year.

Ten erosion-preventive structures were built by the owner at the Scarborough Ranch in conjunction with an automated irrigation system, under the direction of Dr. Howard Haise. Water flow is partly dissipated by the automatic rubber pillows, and then is

distributed onto an apron.

Two structures were built at the T. P. Ranch, principally for the purpose of making a movie. The John Deere Company filmed the movie, which is being shown throughout the United States and other countries. The movie showed our pre-fabricated form for making the dissipator box, and then showed the complete process of pouring the concrete and construction of the outlet structure.

The outlet structures for jack gates at the Wheeler and Woodhouse Ranches appeared to be doing the required erosion-prevention job. Results at the Wheeler Ranch are masked by the original pile-up of concrete and rocks hauled into the original erosion hole. This hindrance will be removed the first time the bermuda grass is replanted.

A new structure servicing a jack gate at the Currie Ranch was built by the owner during the summer, upon our recommendation. It involves a 4-ft drop onto a platform, where the water is dissipated by concrete blocks set at the edge of the platform in a semi-circle, approximately 15 ft from the outlet. The erosion is non-existent, to date.

Additional work should be conducted on structures to prevent erosion from 3-ft-wide jack gates which emit up to 20 cfs of irrigation water.

#### SUMMARY AND CONCLUSIONS:

Inspections of structures showed no cases where design was faulty, as far as erosion prevention was concerned. Structure failures were due to machinery damage. If this damage is to be minimized, the structures will have to be reinforced and/or made heavy enough to withstand machinery damage. The inexpensive course of action is to be more careful when making turns with the machinery. Research on erosion-preventive structures on jack gates needs to be expanded. The structures now built are preventing erosion, but so

many different outlet situations exist that each one is a design problem in itself.

PERSONNEL: Leonard J. Erie, J. A. Replogle, D. A. Bucks, and Orrin F. French.

CURRENT TERMINATION DATE: December 1971.

TITLE: FLOW MEASUREMENT IN OPEN CHANNELS WITH CRITICAL  
DEPTH FLUMES.

CRIS WORK UNIT: SWC-018-gG-4 CODE NO.: Ariz.-WCL-67-1

INTRODUCTION:

Summaries of studies on several critical-depth flumes with cross-sectional shapes that were trapezoidal, triangular or circular, appear in previous reports (see Annual Reports for 1966-1970). Technical Papers "Flow Measurement with Critical Depth Flumes" (1969) and "Critical Depth Flumes for Determining Flow in Canals and Natural Channels" (1970) were followed by a presentation entitled "Tailoring Critical-Depth Measuring Flumes" before the Instrument Society of America, Pittsburgh, Pennsylvania, May 1971. The first paper presented some theoretical aspects for predicting the calibration results for flumes and also summarized the effects of installation anomalies; the second paper proposed sizes for several common ditch shapes frequently constructed; and the third described methods of incorporating the head loss effects, based on boundary layer development, into more accurate prediction techniques.

PROCEDURE:

The laboratory calibration techniques have been previously described. For comparison purposes, a discharge table was first computed for an ideal frictionless flow through each flume. The computations were repeated, incorporating the effects of roughness and velocity distribution. A curve of a type of calibration coefficient was calculated by comparing the roughness results with the ideal discharge calculations. The laboratory measurements were also compared to the ideal discharge rates. A direct comparison of the computed and laboratory-derived calibration-coefficient curves then indicated the success of the fit for the flow range.

RESULTS:

A total of 16 flume configurations have been laboratory calibrated and the results compared with computer predictions

made according to the procedure described in Annual Report 1970. Five more flume designs have been constructed and installed in Arizona and Hawaii. Laboratory calibration of these flumes was considered unnecessary because of the success of the computer predictions of the 16 flumes.

Tables 1-16 list the laboratory calibration data and other derived flow information for each flume. Tables 17-21 list computed values only because no laboratory calibration was made on these five flumes. Table 22 summarizes the basic dimensions of all the flumes including the maximum depth,  $Y_{\max}$ , and the maximum discharge rate,  $Q_{\max}$ . Figure 1 defines most of the symbols and column headings of the tables.

Referring to Tables 1-21 and Figure 1, the column headings from left to right are as follows:

1. Flow depth,  $Y_1$ , at distance  $X_1$ .
2. Discharge rate,  $Q$ , in cfs.
3. Critical depth in the throat section,  $L_3$ .
4. Froude number at the point of depth measurement,  $Y_1$ .
5. Ideal fluid discharge rate, cfs.
6. Discharge coefficient, column 2 divided by ideal discharge rate.
7. Average velocity,  $V_1$ , in the approach section,  $L_1$ .

In general, all cases of deviation from expected behavior could be traced to problems involved in accurately determining the flow area of the flume throat, either because of insufficient support of the flume throat walls, or of warpage of the materials of which the flume was constructed. Flume 2, Table 2, deviated -5% below expected for flow depths less than 1/3 foot. However, this depth to length of throat ratio is outside the 1:20 range currently recommended for use with this method of head loss calculation.

Flume 3, the first of the triangular flumes constructed is satisfactory except in the flow depth range exceeding 1 foot.

Excess deflection of the flume throat, added to insufficient throat length to achieve parallel flow resulted in 3% more discharge than expected. Flume 4 of similar sizing had added support and added outlet sections and is satisfactory almost to the full depth despite a relatively short throat length, L3. Added outlet sections appear to help compensate for short throat lengths. Short throat length, and not deflection, appears responsible for the behavior of Flume 5. A longer throat and added outlet sections bring the results into line.

Flume 10 operated satisfactorily until the PVC plates used in the throat section began to take up water and warped enough to prevent ready determination of the flow area. The last half of Table 10 reflects this problem. The plates were laid into an existing flume constructed of galvanized sheet steel and held down by non-hardening mastic material and modeling clay. The plates warped in two directions when moisture remained behind the plates over night.

The most surprising results occurred with pilot studies of flumes No. 15 and 16. These flumes are constructed with the contraction extending into the channel from one wall only. These flumes could be constructed in existing concrete channels at minimum cost. The discharge tables checked out as if the asymmetric condition did not exist.

Flumes 17-21 are designs that have been installed in Arizona and Hawaii by our own and other agencies.

#### FIELD INVESTIGATIONS:

Five of the flumes that were laboratory calibrated have been placed into field measurement service. These are flumes number 3, 5, 7, 9, and 11 of Table 22. Five more designs, installed with computer calibration only, have been in service for periods ranging from 6 months to over 3 years. The most universal problem is plugging of the stilling well depth-sensing pipelines. Bed load sediments appear to progress into the flume as a type of

sand dune and covers the outlet hole so that depth of flow cannot be detected and the flow area is changed. Suspended sediments are only a minor problem in that the stilling wells eventually fill with sediments but the time-frame is so long that routine annual or semi-annual cleaning is all that is required. However, in some streams the bed load depth through some flumes may change as much as several inches or even more than a foot during a single storm. This, of course, incapacitates the flume.

Flume number 11, Table 22, is of the type used on an Arizona watershed named Monument Tank. A particularly severe storm produced enough runoff to wash large quantities of 1/2- to 2-inch flat shale-like rocks from the desert surface into the channels being measured by these flumes. Two of the flumes operated normally with only minor sedimentation observed. Another had about 3 or 4 inches of coarse sand and gravel deposited in the approach section while a fourth flume had about 1½ feet of the shale-like gravel and some 6-inch diameter boulders deposited in the approach section and converging section. In all cases the throat sections were clear.

Similar experience was observed on another Arizona watershed managed by the Southwest Watershed Research Center, Tucson, on flume number 20, Table 22, designated by them as K-3B. Large bedloads could not pass the flume, depositing more than a foot of sand and gravel in the approach and converging sections.

The University of Arizona Flume Number 17, Table 22, designated by the U of A as Arcadia Flume, showed tendencies of depositing sand in the approach section, depending on the storm and on the way the recession flow occurred. Most of the sediments appeared to be deposited during the recession period. A nearly continuous source of sand moves into and down the channel and long periods of flow below 1.5 feet deep (80 cfs) produce an average velocity in the approach section of less than about 2.5 feet per second.

Flume number 18 (U of A designation is "Highschool" flume), Table 22, on the other hand, has stayed quite clear. This watershed probably peaks quickly, has a rock lined stable channel with little or no apparent source of sediment, and flows deeper than 1.5 feet for a longer portion of the storm than does number 17.

It appears logical that the movement of sediment through a flume is a function of the tractive force, the size of particles, and the quantity of particles. High upstream velocities bring down more bedload than low velocities, but the particle sizing can also be expected to be larger.

Another study is being initiated to investigate these relationships and to determine flume designs that facilitate movement of sediment. This will be conducted under a separate Research Outline.

#### SUMMARY AND CONCLUSIONS:

Sixteen models of critical-depth flumes have been laboratory calibrated in efforts to verify analytical methods of accurately predicting their calibration. Results on flumes of rectangular, triangular and trapezoidal cross-sectional shapes establish that the calibration can be predicted to within  $\pm 2\%$  for a minimum to maximum depth of flow range of about 1:20. Conformance to standard sizes, a long-standing limitation to use of critical-depth flumes, is unnecessary. Computer techniques permit tailoring of the flume to the channel and flow conditions so that, in most cases, a design configuration can be selected to avoid the problems of submerged-flow operation, common to many previous applications of critical-depth flumes.

The computational procedure involves the application of hydrodynamics to the calculation of the drag force exerted by a flowing fluid on one side of a flat plate which has been warped to the shape of the flume throat. This drag force is incorporated into the appropriate energy equations to predict the flume calibration. These equations were solved by iteration techniques on digital computers.

The procedure was applied to the sixteen flumes having a range in roughness heights from hydraulically smooth to 0.005 feet. All anomalies from the predicted flow were satisfactorily explained by inaccuracies in determining the flume dimensions or to insufficient restraint against deflection of the flume walls.

The flumes can be constructed by a wide variety of methods, permitting the use of the most economical local materials and techniques. Construction criteria are not rigorous, requiring dimensional accuracy in the throat section of the flume to be approximately the same as that desired in the resulting discharge rate, while all other dimensions can be about  $\pm 10\%$ . Rough-dimensioned, hand-plastered construction is usually sufficient except in the throat section.

Modeling techniques applied to small flumes calibrated in the laboratory to obtain prototype discharges agree well with the computer-generated calibrations and indicate that size is no particular limitation. The largest flume in operation that was designed by the technique has a capacity of 1900 cfs and the smallest operates at a maximum capacity of 0.25 cfs.

PERSONNEL: John A. Replogle and C. G. Hiesel.

CURRENT TERMINATION DATE: Terminated 1971.

Table 1. Laboratory data for Flume Number 1 appears in columns 1 and 2. Remaining columns derive from these. Symbols are defined in Figure 1. Table 22 provides additional dimensional data.

FLUME DIMENSIONAL DATA:      B1= 1.500                      Z1= .0000  
 SILL HEIGHT= .000              B3= 1.000                      Z3= .0000  
 X1= .500              L2= 1.500              L3= 3.000              K= .00050000

Y1 FT	Q CFS	CRITICAL DEPTH·FT	FROUDE NO·AT Y	IDEAL Q	DISC· COEF·	V1
.181	.2444	.130	.373	.2682	.9112	.90
.184	.2522	.132	.375	.2749	.9173	.91
.224	.3363	.161	.372	.3693	.9107	1.00
.232	.3538	.167	.372	.3892	.9089	1.01
.243	.3822	.175	.375	.4172	.9160	1.04
.346	.6696	.250	.386	.7089	.9445	1.29
.409	.8660	.295	.389	.9110	.9505	1.41
.462	1.031	.333	.385	1.094	.9426	1.48
.510	1.226	.368	.395	1.269	.9664	1.60
.597	1.553	.431	.395	1.607	.9666	1.73
.703	1.969	.507	.392	2.053	.9590	1.86
.782	2.360	.565	.401	2.409	.9798	2.01
.908	2.890	.656	.392	3.014	.9589	2.12
.988	3.264	.713	.390	3.421	.9542	2.20

Table 2. Laboratory data for Flume Number 2 appears in columns 1 and 2. Remaining columns derive from these. Symbols are defined in Figure 1. Table 22 provides additional dimensional data.

FLUME DIMENSIONAL DATA:      B1= 1.500                      Z1= .0000  
 SILL HEIGHT= .000              B3= 1.000                      Z3= .0000  
 X1= .500              L2= 1.500              L3= 8.000              K= .00050000

Y1 FT	Q CFS	CRITICAL DEPTH·FT	FROUDE NO·AT Y	IDEAL Q	DISC· COEF·	V1
.220	.2685	.158	.305	.3594	.7470	.81
.240	.3160	.173	.315	.4095	.7716	.87
.339	.5592	.244	.333	.6875	.8134	1.09
.462	.9360	.333	.350	1.094	.8557	1.35
.472	.9680	.341	.350	1.129	.8570	1.36
.576	1.323	.416	.355	1.523	.8688	1.53
.670	1.679	.484	.359	1.910	.8789	1.67
.771	2.102	.557	.365	2.358	.8914	1.81
.882	2.573	.637	.365	2.885	.8918	1.94

Table 3. Laboratory data for Flume Number 3 appears in columns 1 and 2. Remaining columns derive from these. Symbols are defined in Figure 1. Table 22 provides additional dimensional data.

FLUME DIMENSIONAL DATA:      B1= .666                      Z1= .5773  
 SILL HEIGHT= .000              B3= .000                      Z3= .5773  
 X1= .500              L2= 2.310              L3= 2.333              K= .00005000

Y1 FT	Q CFS	CRITICAL DEPTH·FT	FROUDE NO·AT Y	IDEAL Q	DISC· COEF·	V1
.227	.0303	.182	.066	.0327	.9260	.16
.339	.0863	.272	.099	.0896	.9627	.29
.415	.1460	.333	.119	.1492	.9784	.38
.515	.2487	.415	.140	.2574	.9661	.50
.627	.4173	.506	.167	.4237	.9849	.64
.725	.6012	.587	.186	.6126	.9813	.76
.896	1.036	.729	.218	1.051	.9861	.97
1.001	1.385	.816	.237	1.394	.9933	1.11
1.201	2.212	.983	.267	2.223	.9951	1.35
1.371	3.183	1.127	.297	3.123	1.0192	1.59
1.514	4.144	1.248	.318	4.031	1.0279	1.77
1.569	4.374	1.295	.313	4.420	.9897	1.77
1.669	5.088	1.380	.322	5.183	.9817	1.87
1.724	5.647	1.427	.334	5.635	1.0021	1.97
1.845	6.773	1.530	.349	6.714	1.0087	2.12
1.962	8.014	1.631	.364	7.871	1.0181	2.27
2.056	9.056	1.712	.374	8.884	1.0193	2.37

Table 4. Laboratory data for Flume Number 4 appears in columns 1 and 2. Remaining columns derive from these. Symbols are defined in Figure 1. Table 22 provides additional dimensional data.

FLUME DIMENSIONAL DATA:							
		B1=	.666		Z1=	.5773	
SILL HEIGHT=	.000	B3=	.000		Z3=	.5773	
X1=	.500	L2=	2.310	L3=	2.333	K=	.00005000
		L4=	2.310	L5=	2.333		
Y1	Q	CRITICAL FROUDE		IDEAL	DISC.		
FT	CFS	DEPTH·FT	NO·AT Y	Q	COEF·	V1	
.691	.5190	.559	.175	.5422	.9571	.70	
.795	.7514	.645	.197	.7745	.9701	.84	
.802	.7526	.651	.194	.7920	.9502	.83	
.957	1.187	.779	.221	1.243	.9550	1.01	
.960	1.193	.782	.221	1.253	.9521	1.01	
1.747	5.741	1.447	.331	5.831	.9845	1.96	
1.829	6.480	1.517	.340	6.565	.9870	2.05	
1.890	7.097	1.569	.348	7.146	.9931	2.13	
2.153	10.08	1.796	.378	10.01	1.0069	2.45	

Table 5. Laboratory data for Flume Number 5 appears in columns 1 and 2. Remaining columns derive from these. Symbols are defined in Figure 1. Table 22 provides additional dimensional data.

FLUME DIMENSIONAL DATA:      B1= .167                      Z1= .5773  
 SILL HEIGHT= .000              B3= .002                      Z3= .5773  
 X1= .125              L2= .577              L3= .583              K= .00005000

Y1 FT	Q CFS	CRITICAL DEPTH·FT	FROUDE NO·AT Y	IDEAL Q	DISC· COEF·	V1
.095	.0035	.076	.105	.0039	.8785	.16
.108	.0048	.086	.118	.0054	.8936	.19
.148	.0108	.119	.153	.0118	.9127	.28
.167	.0148	.134	.169	.0160	.9238	.33
.207	.0259	.167	.201	.0275	.9421	.43
.266	.0498	.217	.243	.0520	.9587	.58
.295	.0653	.241	.261	.0676	.9661	.65
.335	.0918	.275	.287	.0936	.9812	.76
.416	.1623	.343	.330	.1629	.9960	.95
.476	.2335	.395	.361	.2304	1.0133	1.11
.509	.2801	.424	.376	.2745	1.0205	1.19

Table 6. Laboratory data for Flume Number 6 appears in columns 1 and 2. Remaining columns derive from these. Symbols are defined in Figure 1. Table 22 provides additional dimensional data.

FLUME DIMENSIONAL DATA:							
SILL HEIGHT=	.000	B1=	.167	Z1=	.5773		
X1=	.125	B3=	.002	Z3=	.5773		
		L2=	.577	L3=	1.167	K=	.00005000
		L4=	.577	L5=	.583		
Y1	Q	CRITICAL	FROUDE	IDEAL	DISC.		
FT	CFS	DEPTH·FT	NO·AT Y	Q	COEF·	V1	
.146	.0103	.117	.150	.0114	.9064	.28	
.221	.0302	.179	.207	.0326	.9250	.46	
.242	.0383	.197	.222	.0409	.9359	.51	
.305	.0702	.249	.263	.0736	.9545	.67	
.344	.0955	.282	.283	.1001	.9547	.75	
.378	.1227	.311	.302	.1274	.9630	.84	
.439	.1811	.363	.330	.1871	.9681	.98	
.474	.2200	.394	.342	.2285	.9628	1.05	
.478	.2244	.397	.344	.2329	.9636	1.05	
.507	.2649	.422	.359	.2717	.9749	1.13	

Table 7. Laboratory data for Flume Number 7 appears in columns 1 and 2. Remaining columns derive from these. Symbols are defined in Figure 1. Table 22 provides additional dimensional data.

FLUME DIMENSIONAL DATA:      B1= .666                      Z1= .5773  
 SILL HEIGHT= .000              B3= .006                      Z3= .5808  
 X1= .500              L2= 3.000              L3= 3.000              K= .00000500

Y1 FT	Q CFS	CRITICAL DEPTH·FT	FROUDE NO·AT Y	IDEAL Q	DISC· COEF·	V1
.185	.0188	.147	.057	.0211	.8940	.13
.190	.0201	.151	.058	.0225	.8927	.13
.279	.0528	.222	.083	.0578	.9138	.22
.497	.2318	.399	.139	.2431	.9535	.48
.558	.3080	.449	.151	.3249	.9478	.55
.620	.3995	.500	.163	.4235	.9434	.62
.623	.4088	.502	.165	.4286	.9537	.63
.657	.4756	.530	.175	.4900	.9706	.69
.725	.6090	.586	.188	.6282	.9694	.77
.844	.8880	.685	.208	.9230	.9624	.91
.869	.9500	.706	.211	.9940	.9563	.93
1.077	1.667	.879	.248	1.715	.9721	1.20
1.078	1.674	.880	.249	1.719	.9739	1.20
1.110	1.794	.907	.252	1.852	.9686	1.23
1.166	2.039	.954	.261	2.100	.9710	1.30
1.236	2.367	1.013	.271	2.437	.9711	1.38
1.309	2.744	1.074	.281	2.823	.9720	1.47
1.341	2.920	1.101	.285	3.003	.9723	1.51
1.349	2.975	1.108	.287	3.049	.9757	1.52
1.442	3.534	1.187	.299	3.617	.9769	1.63

Table 8. Laboratory data for Flume Number 8 appears in columns 1 and 2. Remaining columns derive from these. Symbols are defined in Figure 1. Table 22 provides additional dimensional data.

FLUME DIMENSIONAL DATA:      B1= .750                      Z1= 1.0000  
 SILL HEIGHT= -.025              B3= .008                      Z3= .2679  
 X1= .500              L2= 1.500              L3= 4.000              K= .00005000

Y1 FT	Q CFS	CRITICAL DEPTH·FT	FROUDE NO·AT Y	IDEAL Q	DISC· COEF·	V1
.209	.0094	.164	.024	.0145	.6521	.05
.389	.0506	.308	.042	.0638	.7940	.12
.514	.1082	.408	.053	.1254	.8626	.17
.547	.1256	.435	.054	.1460	.8605	.18
.563	.1369	.448	.056	.1566	.8742	.19
.633	.1838	.504	.060	.2085	.8814	.22
.700	.2427	.558	.065	.2668	.9096	.25
.821	.3618	.655	.071	.3947	.9165	.29
.961	.5525	.767	.079	.5818	.9497	.35
1.100	.7770	.879	.084	.8120	.9568	.39
1.229	1.030	.982	.089	1.068	.9641	.43
1.395	1.421	1.116	.094	1.462	.9720	.48
1.479	1.646	1.183	.096	1.690	.9740	.51
1.598	2.006	1.279	.099	2.048	.9797	.54
1.710	2.390	1.369	.102	2.422	.9866	.58

Table 9. Laboratory data for Flume Number 9 appears in columns 1 and 2. Remaining columns derive from these. Symbols are defined in Figure 1. Table 22 provides additional dimensional data.

FLUME DIMENSIONAL DATA:      B1= .666                      Z1= .5040  
 SILL HEIGHT= .000              B3= .006                      Z3= .5040  
 X1= .500              L2= 2.000              L3= 2.000              K= .00050000

Y1 FT	Q CFS	CRITICAL DEPTH·FT	FROUDE NO·AT Y	IDEAL Q	DISC· COEF·	V1
.162	.0108	.128	.041	.0133	.8067	.08
.165	.0110	.131	.040	.0139	.7903	.08
.218	.0228	.173	.054	.0275	.8299	.13
.272	.0417	.217	.069	.0474	.8809	.19
.299	.0521	.238	.074	.0598	.8722	.21
.400	.1099	.320	.097	.1229	.8941	.31
.430	.1320	.344	.104	.1471	.8973	.34
.444	.1435	.356	.107	.1593	.9008	.36
.478	.1732	.383	.114	.1914	.9047	.39
.564	.2644	.453	.131	.2894	.9137	.49
.580	.2839	.466	.134	.3103	.9147	.51
.587	.2943	.472	.137	.3198	.9202	.52
.597	.3055	.480	.138	.3336	.9156	.52
.650	.3801	.523	.148	.4130	.9204	.58
.721	.5006	.582	.162	.5359	.9341	.67
.752	.5540	.607	.167	.5958	.9298	.70
.787	.6272	.636	.174	.6682	.9386	.74
.824	.7030	.666	.180	.7503	.9369	.78
.875	.8220	.708	.189	.8730	.9416	.84
.938	.9900	.761	.200	1.041	.9512	.92

Table 10. Laboratory data for Flume Number 10 appears in columns 1 and 2. Remaining columns derive from these. Symbols are defined in Figure 1. Table 22 provides additional dimensional data.

FLUME DIMENSIONAL DATA:      B1= .666                      Z1= 1.7321  
 SILL HEIGHT= .050              B3= .000                      Z3= 1.7321  
 X1= .500              L2= 2.330              L3= 1.667              K= .00050000

Y1 FT	Q CFS	CRITICAL DEPTH·FT	FROUDE NO·AT Y	IDEAL Q	DISC· COEF·	V1
.108	.0140	.086	.047	.0153	.9151	.09
.152	.0334	.121	.074	.0361	.9252	.16
.182	.0542	.146	.093	.0568	.9539	.21
.239	.1081	.192	.125	.1131	.9560	.32
.294	.1859	.237	.156	.1912	.9725	.42
.353	.2962	.286	.184	.3044	.9730	.53
.404	.4174	.328	.205	.4295	.9717	.63
.455	.5680	.370	.226	.5822	.9756	.73
.524	.8110	.428	.250	.8360	.9699	.85
.595	1.136	.488	.276	1.159	.9799	.98
.671	1.586	.553	.306	1.580	1.0036	1.14
.705	1.794	.582	.315	1.795	.9993	1.20
.714	1.863	.589	.319	1.855	1.0043	1.22
.654	1.481	.538	.300	1.479	1.0013	1.11
.606	1.205	.497	.283	1.215	.9915	1.01
.460	.5933	.375	.232	.5987	.9910	.75
.335	.2642	.271	.179	.2664	.9917	.51
.257	.1355	.207	.140	.1359	.9970	.36
.156	.0363	.125	.077	.0385	.9419	.17
.151	.0343	.121	.076	.0355	.9661	.16

Table 11. Laboratory data for Flume Number 11 appears in columns 1 and 2. Remaining columns derive from these. Symbols are defined in Figure 1. Table 22 provides additional dimensional data.

FLUME DIMENSIONAL DATA:            B1= 1.000                            Z1= 1.0000  
 SILL HEIGHT= .000                    B3= .000                                Z3= 1.0000  
 X1= 2.000                    L2= 3.000                    L3= 7.000                    K= .00005000

Y1 FT	Q CFS	CRITICAL DEPTH·FT	FROUDE NO·AT Y	IDEAL Q	DISC· COEF·	V1
.298	.1002	.239	.092	.1125	.8905	.25
.365	.1682	.293	.110	.1876	.8967	.33
.424	.2479	.341	.126	.2738	.9053	.41
.511	.4043	.412	.149	.4391	.9207	.52
.571	.5530	.462	.167	.5819	.9503	.61
.614	.6460	.497	.172	.6997	.9232	.65
.618	.6635	.500	.174	.7113	.9327	.66
.693	.8890	.562	.190	.9520	.9342	.75
.776	1.188	.631	.206	1.270	.9353	.86
.862	1.561	.702	.223	1.661	.9397	.97
.945	1.984	.772	.238	2.102	.9440	1.07
1.021	2.431	.835	.252	2.562	.9487	1.17
1.095	2.911	.898	.263	3.066	.9493	1.26
1.190	3.615	.978	.278	3.797	.9520	1.38
1.290	4.450	1.063	.292	4.673	.9522	1.50
1.306	4.483	1.076	.287	4.824	.9293	1.48
1.264	4.185	1.041	.286	4.434	.9437	1.46
1.146	3.265	.941	.270	3.447	.9473	1.32
1.062	2.687	.870	.258	2.835	.9479	1.22
.980	2.171	.801	.243	2.307	.9411	1.11
.906	1.778	.739	.231	1.887	.9423	1.02
.832	1.428	.677	.218	1.517	.9410	.93
.740	1.045	.601	.198	1.125	.9287	.81
.676	.8370	.548	.187	.8940	.9365	.73
.579	.5606	.468	.166	.6028	.9300	.61
.516	.4141	.416	.150	.4501	.9201	.52
.417	.2403	.336	.126	.2625	.9153	.40
.362	.1662	.291	.111	.1837	.9047	.33
.219	.0437	.175	.067	.0518	.8435	.16

Table 12. Laboratory data for Flume Number 12 appears in columns 1 and 2. Remaining columns derive from these. Symbols are defined in Figure 1. Table 22 provides additional dimensional data.

FLUME DIMENSIONAL DATA:      B1= 1.000                      Z1= 1.0000  
 SILL HEIGHT= .037              B3= .073                      Z3= 1.0000  
 X1= 2.000              L2= 3.000              L3= 7.000              K= .00050000

Y1 FT	Q CFS	CRITICAL DEPTH·FT	FROUDE NO·AT Y	IDEAL Q	DISC· COEF·	V1
.105	.0098	.079	.029	.0155	.6293	.06
.182	.0378	.140	.057	.0493	.7664	.14
.253	.0706	.197	.068	.1020	.6922	.18
.321	.1417	.252	.096	.1750	.8095	.29
.361	.1869	.284	.106	.2295	.8144	.33
.519	.4520	.413	.143	.5388	.8388	.52
.576	.5867	.460	.156	.6913	.8486	.59
.655	.8140	.525	.174	.9420	.8638	.69
.725	1.061	.583	.191	1.206	.8799	.79
.799	1.367	.644	.207	1.529	.8941	.89
.882	1.743	.713	.221	1.949	.8944	.98
.955	2.159	.774	.236	2.371	.9105	1.09
1.031	2.636	.838	.250	2.866	.9196	1.19
1.110	3.161	.905	.261	3.444	.9178	1.28
1.171	3.638	.956	.272	3.936	.9243	1.36
1.249	4.324	1.022	.285	4.624	.9350	1.47
1.286	4.631	1.054	.289	4.975	.9308	1.50

Table 13. Laboratory data for Flume Number 13 appears in columns 1 and 2. Remaining columns derive from these. Symbols are defined in Figure 1. Table 22 provides additional dimensional data.

FLUME DIMENSIONAL DATA:      B1= .833                      Z1= 1.0000  
 SILL HEIGHT= .000              B3= .333                      Z3= 1.0000  
 X1= .500              L2= 3.000              L3= 3.000              K= .00000500

Y1 FT	Q CFS	CRITICAL DEPTH-FT	FROUDE NO-AT Y	IDEAL Q	DISC- COEF-	V1
.113	.0451	.082	.234	.0507	.8890	.42
.166	.0889	.123	.250	.0991	.8968	.53
.233	.1715	.176	.278	.1840	.9319	.69
.357	.4059	.276	.321	.4180	.9711	.95
.450	.6444	.353	.340	.6666	.9666	1.11
.511	.8400	.405	.354	.8670	.9686	1.22
.614	1.255	.492	.379	1.279	.9814	1.41
.715	1.748	.578	.398	1.778	.9832	1.57
.811	2.298	.660	.412	2.346	.9794	1.72
.862	2.638	.704	.421	2.688	.9815	1.80
.971	3.435	.799	.435	3.514	.9775	1.96
1.037	4.013	.856	.446	4.081	.9833	2.06
1.116	4.762	.925	.458	4.829	.9861	2.18

Table 14. Laboratory data for Flume Number 14 appears in columns 1 and 2. Remaining columns derive from these. Symbols are defined in Figure 1. Table 22 provides additional dimensional data.

FLUME DIMENSIONAL DATA:      B1= 1.000                      Z1= 1.0000  
 SILL HEIGHT= .463              B3= .962                      Z3= 1.0000  
 X1= 2.000              L2= 3.000              L3= 7.000              K= .00500000

Y1 FT	Q CFS	CRITICAL DEPTH·FT	FROUDE NO·AT Y	IDEAL Q	DISC· COEF·	V1
.311	.5676	.221	.099	.6408	.8858	.41
.371	.7810	.266	.118	.8690	.8988	.51
.454	1.108	.330	.141	1.241	.8927	.63
.532	1.522	.391	.165	1.653	.9207	.76
.594	1.852	.440	.179	2.025	.9147	.85
.620	2.030	.460	.187	2.193	.9258	.89
.667	2.334	.498	.199	2.515	.9281	.96
.746	2.894	.561	.216	3.111	.9303	1.08
.835	3.585	.634	.232	3.868	.9269	1.20
.905	4.270	.691	.249	4.529	.9429	1.31
.882	4.045	.672	.244	4.305	.9396	1.28
.815	3.439	.617	.230	3.689	.9321	1.18
.758	2.994	.571	.219	3.207	.9334	1.10
.683	2.443	.511	.202	2.630	.9289	.99
.608	1.969	.451	.186	2.114	.9313	.88
.523	1.472	.384	.163	1.602	.9186	.75
.452	1.135	.328	.145	1.231	.9217	.64
.377	.8120	.271	.121	.8940	.9081	.52
.310	.5683	.220	.099	.6372	.8918	.41
.270	.4396	.190	.085	.5041	.8721	.34
.180	.2132	.124	.052	.2577	.8273	.20
.136	.1328	.093	.037	.1640	.8095	.13
.126	.1170	.086	.033	.1452	.8055	.12

Table 15. Laboratory data for Flume Number 15 appears in columns 1 and 2. Remaining columns derive from these. Symbols are defined in Figure 1. Table 22 provides additional dimensional data.

FLUME DIMENSIONAL DATA:      B1= .989                      Z1= 1.0100  
 SILL HEIGHT= .008              B3= .416                      Z3= 1.0240  
 X1= .667              L2= 1.500              L3= 3.000              K= .00050000

Y1 FT	Q CFS	CRITICAL DEPTH·FT	FROUDE NO·AT Y	IDEAL Q	DISC· COEF·	V1
.564	1.158	.445	.352	1.190	.9727	1.29
.273	.2614	.205	.268	.2875	.9092	.73
.274	.2722	.206	.278	.2895	.9403	.75
.266	.2541	.200	.272	.2740	.9274	.73
.145	.0829	.105	.227	.0928	.8925	.47
.197	.1454	.145	.250	.1588	.9155	.59
.223	.1815	.166	.257	.1984	.9148	.64
.332	.3918	.253	.293	.4157	.9425	.86
.379	.5053	.291	.303	.5366	.9416	.94
.416	.6106	.322	.314	.6441	.9479	1.01
.492	.8660	.385	.334	.9010	.9615	1.15
.569	1.177	.449	.352	1.212	.9708	1.29
.637	1.497	.506	.367	1.534	.9761	1.41
.717	1.905	.574	.377	1.970	.9670	1.52
.791	2.382	.637	.394	2.433	.9791	1.65
.792	2.382	.638	.393	2.439	.9765	1.65
.888	3.089	.721	.412	3.130	.9869	1.82
1.020	4.139	.835	.424	4.254	.9729	1.98

Table 16. Laboratory data for Flume Number 16 appears in columns 1 and 2. Remaining columns derive from these. Symbols are defined in Figure 1. Table 22 provides additional dimensional data.

FLUME DIMENSIONAL DATA:      B1=    .989                      Z1= 1.0100  
 SILL HEIGHT=    .008      B3=    .666                      Z3= 1.0110  
 X1=    .667      L2= 1.500      L3= 3.000                      K= .00050000

Y1 FT	Q CFS	CRITICAL DEPTH·FT	FROUDE NO·AT Y	IDEAL Q	DISC· COEF·	V1
.907	4.122	.754	.528	4.285	.9618	2.35
.796	3.147	.656	.514	3.277	.9602	2.17
.710	2.486	.581	.501	2.602	.9554	2.01
.643	2.035	.523	.490	2.137	.9524	1.89
.556	1.513	.448	.472	1.608	.9407	1.72
.473	1.103	.377	.455	1.181	.9341	1.55
.414	.8520	.327	.441	.9200	.9261	1.42
.340	.5883	.266	.423	.6413	.9173	1.26
.124	.0934	.092	.323	.1136	.8222	.63

Table 17. Computed calibrations and derived flow information for Flume 17. Symbols are defined in Figure 21. Table 22 provides additional dimensional data.

FLUME DIMENSIONAL DATA:						
SILL HEIGHT=		.000	B1= 17.000	B3= 11.000	Z1= 2.0000	Z3= 2.0000
X1= 1.000	L2= 9.000	L3= 16.000	L4= 6.000	L5= .000	K= .00050000	
Y1	Q	CRITICAL	FROUDE	IDEAL	DISC.	
FT	CFS	DEPTH·FT	NO·AT Y	Q	COEF·	V1
.500	12.53	.339	.356	14.34	.8734	1.39
1.000	40.20	.718	.392	43.22	.9300	2.11
1.500	80.33	1.108	.413	84.38	.9519	2.67
2.000	132.7	1.507	.429	137.7	.9636	3.15
2.500	197.6	1.913	.443	203.5	.9709	3.59
3.000	275.6	2.326	.456	282.3	.9761	3.99
3.500	367.1	2.744	.468	374.6	.9800	4.37
4.000	472.7	3.166	.478	480.9	.9831	4.72
4.500	593.1	3.592	.488	601.7	.9856	5.06
5.000	728.8	4.021	.498	737.8	.9878	5.39
5.500	880.5	4.453	.507	889.6	.9896	5.71
6.000	1049	4.888	.515	1058	.9913	6.02
6.500	1234	5.325	.523	1243	.9928	6.32
7.000	1437	5.764	.531	1445	.9941	6.62
7.500	1658	6.206	.539	1665	.9953	6.90
8.000	1898	6.649	.546	1904	.9965	7.18

Table 18. Computed calibrations and derived flow information for Flume 18. Symbols are defined in Figure 21. Table 22 provides additional dimensional data.

FLUME DIMENSIONAL DATA:						
			B1= 9.000		Z1= 1.5000	
SILL HEIGHT=	.000		B3= 6.000		Z3= 1.5000	
X1= 1.000	L2= 5.000	L3= 10.000		K= .00050000		
	L4= 5.000	L5= .000				
Y1	Q	CRITICAL	FROUDE	IDEAL	DISC.	
FT	CFS	DEPTH·FT	NO·AT Y	Q	COEF·	V1
.500	7.364	.353	.390	8.085	.9108	1.51
1.000	23.71	.740	.425	24.90	.9521	2.25
1.500	47.98	1.141	.448	49.59	.9675	2.84
2.000	80.39	1.551	.466	82.38	.9759	3.34
2.500	121.4	1.969	.483	123.7	.9813	3.80
3.000	171.5	2.394	.497	174.0	.9854	4.23
3.500	231.2	2.824	.511	233.9	.9885	4.63
4.000	301.1	3.257	.523	303.8	.9910	5.01
4.500	381.7	3.695	.535	384.3	.9932	5.38
5.000	473.4	4.135	.545	475.7	.9951	5.73

Table 19. Computed calibrations and derived flow information for Flume 19. Symbols are defined in Figure 21. Table 22 provides additional dimensional data.

FLUME DIMENSIONAL DATA:						
			B1= 16.000		Z1= 3.0000	
SILL HEIGHT=	.000		B3= 11.000		Z3= 3.0000	
X1= 1.000		L2= 8.000	L3= 10.000		K= .00050000	
		L4= 5.000	L5= .000			
Y1	Q	CRITICAL	FROUDE	IDEAL	DISC.	
FT	CFS	DEPTH·FT	NO·AT Y	Q	COEF·	V1
.500	13.69	.355	.406	15.09	.9071	1.56
1.000	44.52	.746	.444	46.81	.9508	2.34
1.500	90.73	1.152	.469	93.81	.9671	2.95
2.000	153.0	1.568	.488	156.7	.9760	3.47
2.500	232.2	1.991	.506	236.4	.9819	3.95
3.000	329.5	2.421	.521	334.1	.9861	4.39
3.500	446.0	2.856	.535	450.7	.9894	4.80
4.000	582.8	3.294	.548	587.4	.9921	5.20
4.500	741.0	3.736	.560	745.1	.9945	5.58
5.000	921.7	4.182	.571	924.9	.9965	5.94

Table 20. Computed calibrations and derived flow information for Flume 20. Symbols are defined in Figure 21. Table 22 provides additional dimensional data.

FLUME DIMENSIONAL DATA:      B1= 3.000                      Z1= 1.5000  
 SILL HEIGHT= .000              B3= 1.500                      Z3= 1.0000  
 X1= 1.000              L2= 8.000              L3= 12.000              K= .00050000

Y1 FT	Q CFS	CRITICAL DEPTH·FT	FROUDE NO·AT Y	IDEAL Q	DISC· COEF·	V1
.500	1.904	.345	.277	2.153	.8843	1.01
1.000	6.779	.731	.306	7.301	.9284	1.50
1.500	14.85	1.131	.324	15.68	.9469	1.88
2.000	26.51	1.536	.337	27.68	.9576	2.20
2.500	42.12	1.946	.347	43.66	.9648	2.49
3.000	62.04	2.357	.355	63.95	.9700	2.75
3.500	86.58	2.771	.361	88.88	.9741	2.99
4.000	116.1	3.185	.366	118.8	.9773	3.22
4.500	150.8	3.600	.371	153.8	.9799	3.43
5.000	190.9	4.016	.375	194.4	.9820	3.63
5.500	236.9	4.433	.378	240.8	.9839	3.82
6.000	288.8	4.850	.382	293.1	.9855	4.01
6.500	347.0	5.267	.384	351.6	.9869	4.18
7.000	411.7	5.684	.387	416.6	.9881	4.35

Table 21. Computed calibrations and derived flow information for Flume 21. Symbols are defined in Figure 21. Table 22 provides additional dimensional data.

FLUME DIMENSIONAL DATA:      B1= 3.000                      Z1= 2.0000  
 SILL HEIGHT= .000              B3= 1.000                      Z3= 2.0000  
 X1= .500              L2= 2.830              L3= 3.000              K= .00005000

Y1 FT	Q CFS	CRITICAL DEPTH-FT	FROUDE NO-AT Y	IDEAL Q	DISC- COEF-	V1
.100	.1039	.067	.186	.1145	.9077	.32
.200	.3468	.141	.212	.3659	.9476	.50
.300	.7226	.218	.232	.7519	.9610	.66
.400	1.243	.297	.250	1.283	.9687	.81
.500	1.920	.377	.267	1.972	.9737	.95
.600	2.767	.458	.283	2.830	.9774	1.09
.700	3.795	.540	.298	3.871	.9803	1.23
.800	5.018	.623	.312	5.106	.9827	1.36
.900	6.446	.707	.325	6.547	.9846	1.49
1.000	8.093	.791	.337	8.205	.9863	1.61
1.100	9.968	.875	.349	10.09	.9878	1.74
1.200	12.08	.960	.360	12.22	.9891	1.86
1.300	14.45	1.045	.371	14.59	.9902	1.98
1.400	17.08	1.131	.381	17.23	.9913	2.10
1.500	19.98	1.217	.391	20.13	.9923	2.21

Table 22. Summary of basic dimensions of flumes designed and constructed. Flumes 1 through 16 were laboratory calibrated (see Tables 1 through 16).

Flume Identification	B1	B3	Z1	Z3	X1	L1	L2	L3	L4	L5	S	K	Y1 max	Q max
	(ft)	(ft)	-	-	(ft)	(ft)	(cfs)							
RECTANGULAR														
1. 3' throat	1.50	1.000	0	0	.5	3.00	1.50	3.00	0	0	0	.0005	1.5	6.2
2. 8' throat	1.50	1.000	0	0	.5	3.00	1.50	8.00	0	0	0	.0005	1.5	5.9
TRIANGULAR														
3. 60°-3-pce,L	.666	0	.5773	.5773	.5	2.33	2.31	2.33	0	0	0	.00005	2.0	8.1
4. 60°-5-pce,L	.666	0	.5773	.5773	.5	2.33	2.31	2.33	2.31	2.33	0	.00005	2.0	8.1
5. 60°-3-pce,S	.167	.0023	.5773	.5773	.125	.583	.577	.583	0	0	0	.00005	.5	.25
6. 60°-5-pce,S	.167	.0023	.5773	.5773	.125	.583	.577	.583	.577	.583	0	.00005	.5	.25
7. 60°-Fibergl.	.677	.006	.5773	.5808	.5	3.00	3.00	3.00	0	0	0	.000005	1.5	3.9
8. 30°-Portable	.750	0	1.000	.2680	.5	1.50	1.67	4.00	0	0	0	.00005	2.0	3.3
9. 54°-Brawley	.666	.006	.5040	.5040	.5	2.00	2.00	2.00	0	0	0	.0005	1.0	1.2
10. 120°-PVC	.666	0	1.732	1.732	.5	2.00	2.33	1.80	0	0	0	.00005	1.0	4.5
11. 90°-Alum.	1.00	0	1.000	1.000	2.0	6.00	3.00	7.00	0	0	0	.00005	4.0	87.3
12. 90°-Coated	1.00	.073	1.000	1.000	2.0	6.00	3.00	7.00	0	0	.037	.0005	4.0	88.9
TRAPEZOIDAL														
13. USBR Type	.833	.333	1.000	1.000	.5	3.00	3.00	3.00	0	0	0	.000005	1.8	14.8
14. Bottom Sill	1.00	.962	1.000	1.000	2.0	6.00	3.00	7.00	0	0	.463	.005	3.5	82.6
15. Uni-sill-1	.989	.416	1.010	1.024	.667	4.00	1.50	3.00	1.50	1.00	.008	.0005	1.5	10.1
16. Uni-sill-2	.989	.666	1.010	1.011	.667	5.00	1.50	3.00	1.50	1.00	.008	.0005	1.5	12.5
TRAPEZOIDAL, FIELD INSTAL.														
17. Tucson-A	17.0	11.00	2.000	2.000	1.0	16.0	9.00	16.0	6.00	0	0	.0005	8.0	1900
18. Tucson-H	9.00	6.00	1.500	1.500	1.0	10.0	5.00	10.0	5.00	0	0	.0005	5.0	470
19. Tucson-R	16.0	11.00	3.000	3.000	1.0	10.0	8.00	10.0	5.00	0	0	.0005	5.0	910
20. K-3B	3.00	1.500	1.500	1.000	1.0	15.0	8.00	12.0	0	0	0	.0005	7.0	410
21. Hawaii	3.00	1.000	2.000	2.000	.5	3.00	2.83	3.00	0	0	0	.00005	1.5	20.0

4-28

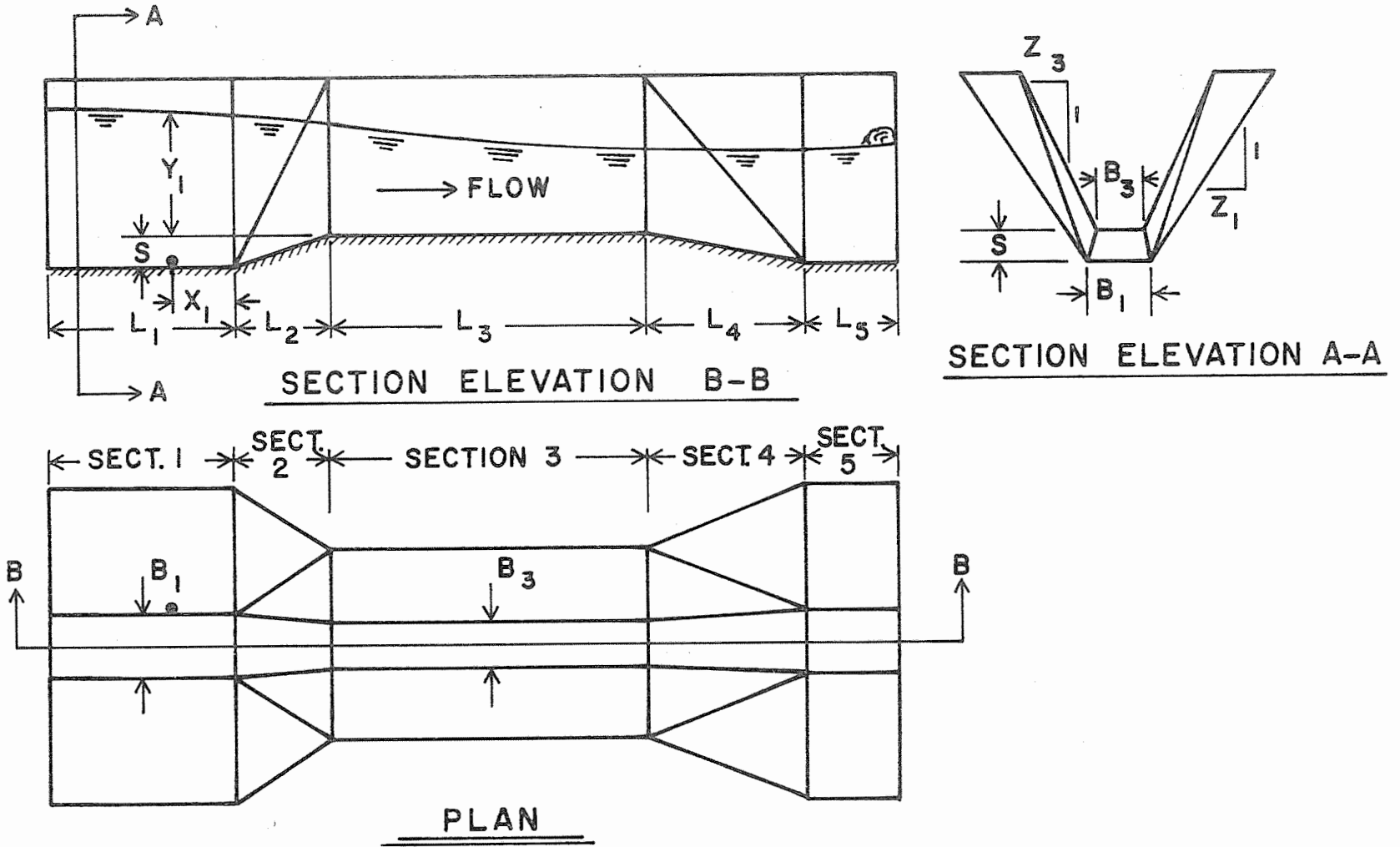


Figure 1. General layout of flumes. Table 22 provides the indicated dimensions for each flume.

TITLE: PHYSICAL AND CHEMICAL CHARACTERISTICS  
OF HYDROPHOBIC SOILS

CRIS WORK UNIT: SWC-018-gG-4 CODE NO.: Ariz.-WCL 67-2

PART A. ADSORPTION ISOTHERMS

A three constant empirical equation for describing Type-II adsorption isotherms was presented in the 1970 Annual Report:

$$\ln(W) = A + B \ln[(p/p_0)^{-c} - 1] \quad (1)$$

where W equals the amount of adsorbate and  $p/p_0$  is the relative vapor pressure. In 1971 the two constant form of this equation (i.e.  $c = 1$ ) was tested on several adsorption isotherms. Typical results are shown in Figure 1. The two constant form divides the isotherms into two or more linear segments with one or more short segments at vapor pressures below the inflection point and one long segment at vapor pressures beyond this point. At low vapor pressures the two constant equation reduces to the Freundlich equation,  $W = a(p/p_0)^b$ , and thence to Henry's linear relation between pressure and adsorption (i.e., for  $b = 1$ ).

The three constant form of equation (1) was also tested on several other sigmoidal relations common to agronomic research. Two examples appear in Figures 2 and 3.

PART B. CLAY-WATER SYSTEMS

Previously (Annual Report 1970) it was shown that a number of Na- and Li-montmorillonite clays exhibit linear swelling with respect to the d-spacing vs. total water content, and that this swelling conforms to the equation:

$$d = [9.4 - \frac{ua}{S_i}] + [u(1 - \frac{b}{S_i})]W_t \quad (2)$$

where d is the d-spacing of the expanded montmorillonite in Angstroms; 9.4A is the thickness of the individual clay sheets;

$S_i$  is the internal surface area of the swelling portion;  $W_t$  is the total weight of water present;  $a$  is a constant portion of water associated with non-free-swelling clay surfaces;  $b$  also relates to a portion of water associated with non-free-swelling surfaces, but which portion increases linearly as the total water content in the system increases; and  $u$  is a units conversion factor. The following is a summary statement of information which may be obtained utilizing this linear swelling of 2:1 type clays in water, in conjunction with the theoretical equation for describing the phenomenon.

1. Surface Area. The internal surface area ( $S_i$ ) of the swelling clay portion directly appears in both the intercept and slope of equation (2).
2. Quantitative Clay Evaluation. The amount of montmorillonite present in clay-type mixtures may be determined using equation (2) by assuming a value for the surface area of the montmorillonite portion present (e.g.  $800 \text{ m}^2/\text{g}$ ).
3. Ion Distribution. The distribution of the several exchangeable ions in multi-ionic systems may be deduced from the slopes and "jump-spacing" of d-spacing vs. water content plots.
4. Water Distribution. Equation (2) may be used to differentiate the total water present in such swelling systems among free-swelling interlattice, non-free-swelling interlattice, and extra-packet void regions.
5. Charge Density. The extent of the jump-spacing of swelling Na-montmorillonites is affected directly by the charge density of the clay lattices.
6. Charge Location. The presence or absence of a jump-spacing for Na-montmorillonite in a water system is controlled by

the location of the charge, whether tetrahedral or octahedral, respectively.

7. Salt Activity. Increasing salt activity decreases clay swelling, which has been shown to affect the  $b$  term of equation (2); thus salt affects the distribution of water in the system.
8. Structure Factors. Interaction between clay edge sites and planar surfaces controls the distribution of water between interlamellar and void regions, and thus should affect the  $(b)$  parameter of equation (2).

PERSONNEL: Dwayne H. Fink

CURRENT TERMINATION DATE: December 1971

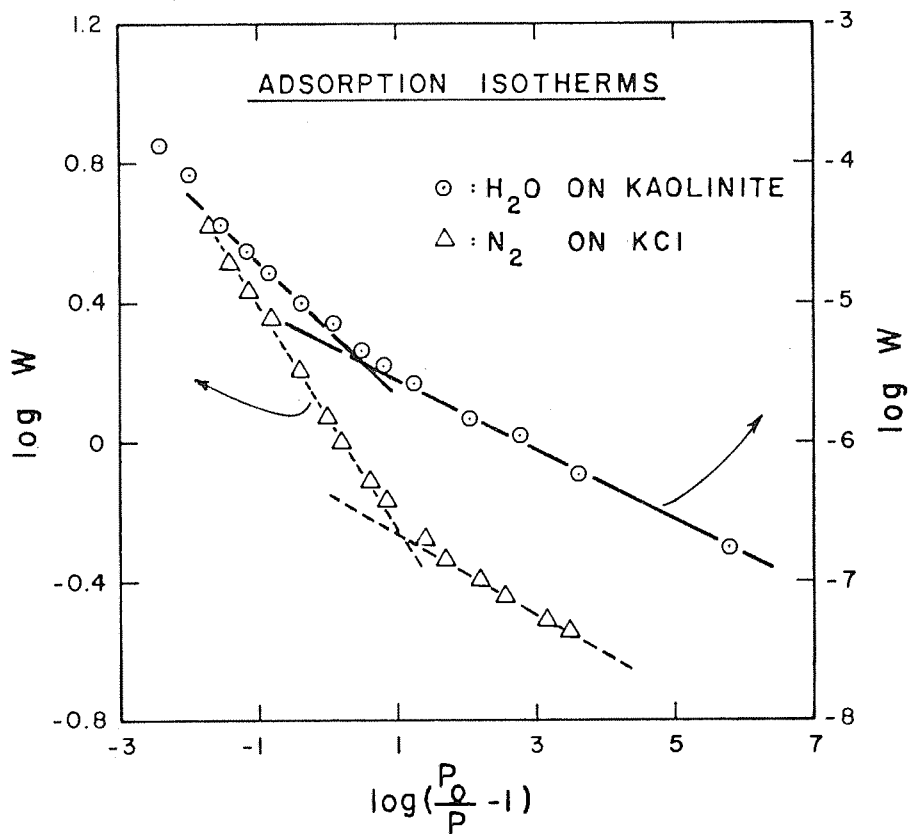


Figure 1. Adsorption isotherms of water on Li-kaolinite (data of Martin, R. T. Clays and Clay Minerals 6:259. 1959), and N<sub>2</sub> on KCl crystals (data of Keenan, A. G., and Holmes, J. M. J. Phys. and Colloid Chem. 53:1309. 1949), both plotted according to the two constant form of equation (1).

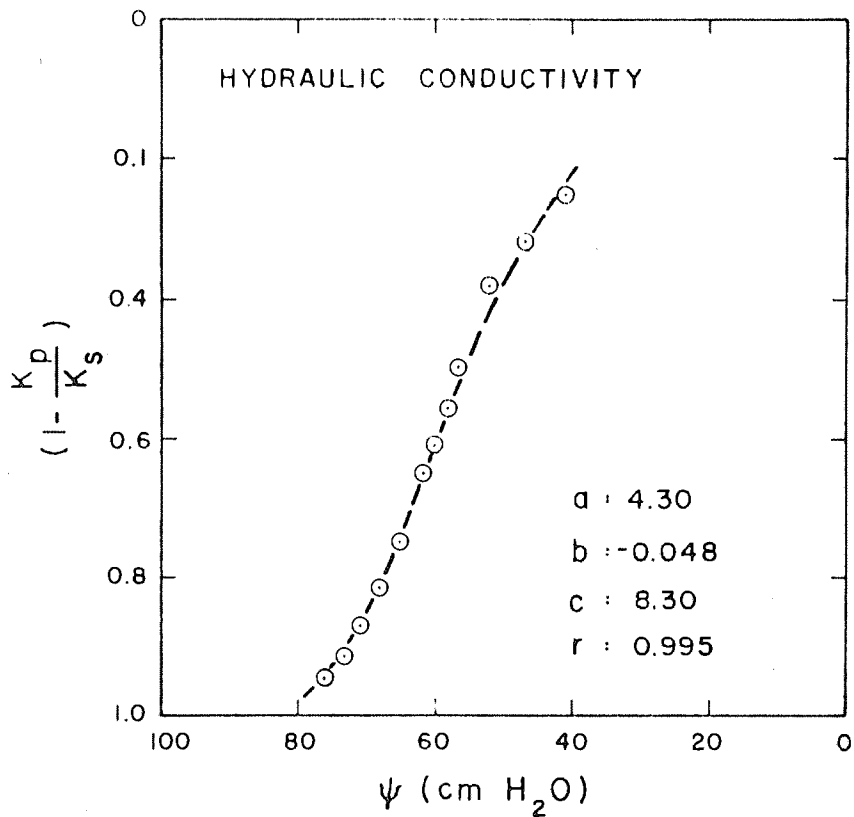


Figure 2. Hydraulic conductivity of 50-500  $\mu$  sand (unpublished data of R. Jackson). Circles represent data; dashed line was calculated using the relation:

$$\log \psi = a + b \log \left[ \left( \frac{1}{1 - \frac{K_p}{K_s}} \right)^c - 1 \right]$$

where  $\psi$  = water suction;  $K_s$  = saturated hydraulic conductivity and  $K_p$  = hydraulic conductivity of unsaturated <sup>p</sup>system.

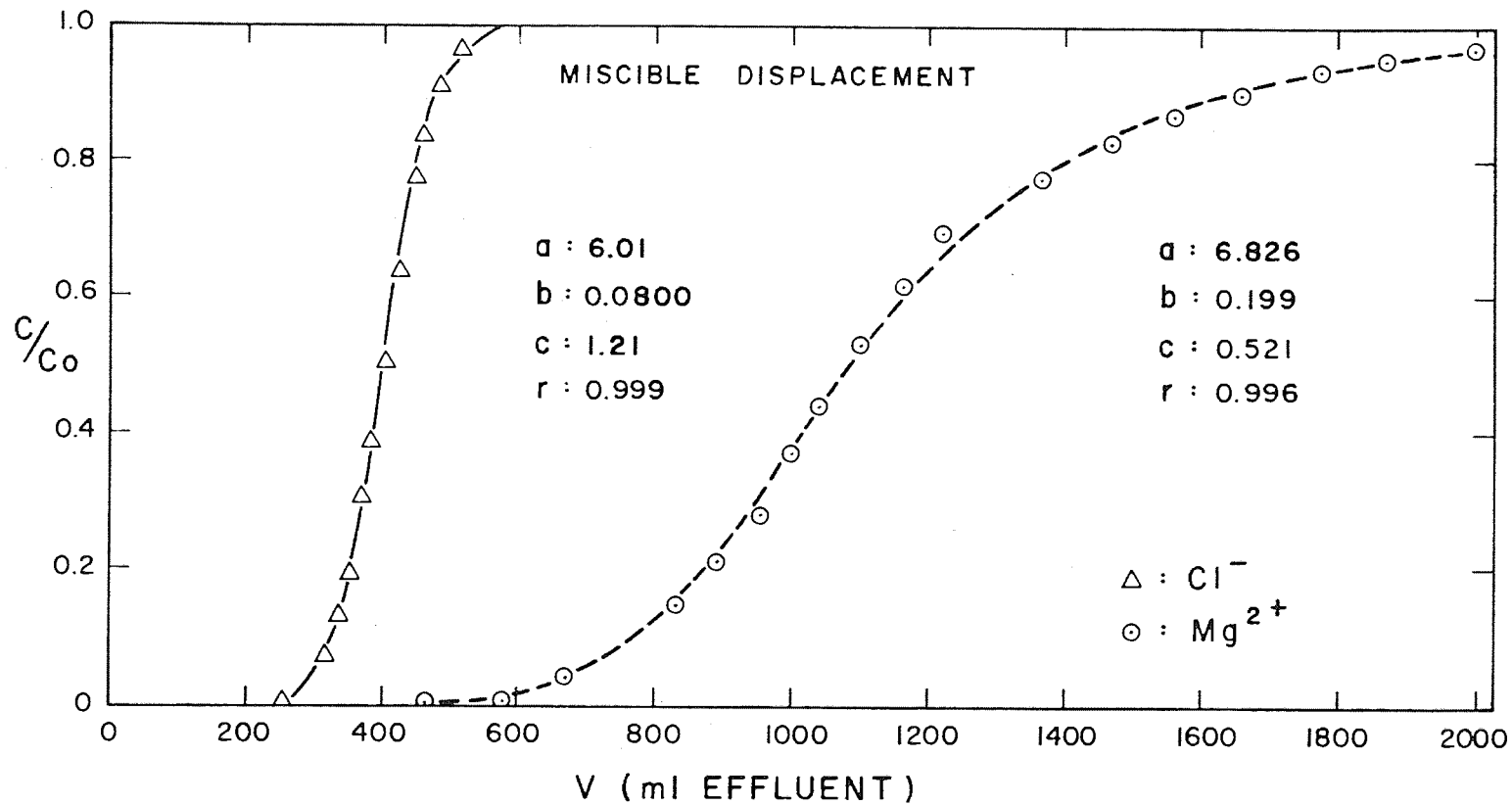


Figure 3. Breakthrough curves for Cl<sup>-</sup> and Mg<sup>2+</sup> ions with displacement of 0.1 N Ca-acetate by 0.1 N MgCl<sub>2</sub> in Ca-saturated Oakley sand (data of Bigger, J. W. and Nielsen, D. R. SSSAP 27:623. 1963). Symbols represent data; lines were calculated using the relation:

$$\log(V) = a + b \log[(C/Co)^c - 1]$$

where V is the volume of effluent; Co is the concentration of ion in the influent, and C is the concentration measured in the effluent.

TITLE: WASTE-WATER RENOVATION BY SPREADING TREATED SEWAGE  
FOR GROUND-WATER RECHARGE

CRIS WORK UNIT: SWC-018-gG-4 CODE NO.: Ariz.-WCL-67-4

INTRODUCTION:

The year of 1971 was the fourth full year of operation of the Flushing Meadows Project, which is an experimental project for renovating secondary sewage effluent by ground-water recharge with infiltration basins. The project is located in the Salt River bed about 1½ miles downstream (west) from the 91st Avenue Phoenix Sewage Treatment Plant. The project was constructed in 1967 and the basins have been inundated according to various flooding and dry-up schedules since September 1967.

The excellent cooperation with the Salt River Project, which received a grant from the Environmental Protection Agency (then Federal Water Quality Administration) for partial support of the project, was continued in 1971. The grant terminated in December 1969, at which time the financial support for the laboratory technician was assumed by the Salt River Project.

The operation of the basins in 1971 was aimed at removing nitrogen from the soil beneath the basins that had apparently accumulated during several years of predominantly long inundation periods. With sequences of relatively long inundation periods (for example, 2 to 3 weeks inundation and 10 to 20 days dry up), considerable nitrogen was removed from the waste water as it percolated through the soil. However, the removal efficiency gradually decreased with time, probably because of ammonium buildup in the soil. A sequence of relatively short inundation periods (for example, a few days inundation followed by about 5 days dry up) could create conditions favorable for nitrification of this ammonium and thus "rejuvenate" the soil beneath the basins as to their nitrogen-removing capability. For this reason, four basins were operated in 1971 with short, frequent inundation

periods, whereas two basins were continued to be flooded with relatively long inundation periods.

To facilitate orderly presentation of the results, the report is divided into three sections:

- I. Infiltration studies.
- II. Water quality studies.
- III. Future projects.

## I. INFILTRATION STUDIES

### 1. Recharge Basin Management.

A plan of the Flushing Meadows Project showing infiltration basins, observation wells, and experimental ponds, is shown in Figure 1.

The basins entered the year 1971 in essentially bare-soil condition (except basin 2 which is covered with a gravel layer), after the basins were "shaved" with a front-end loader on 29 October 1970. The secondary effluent went through its usual winter cycle with black appearance and high suspended solids concentrations in the 50- to 100-mg/liter range.

On February 1971, all basins except basin 2 were again cleaned with a front-end loader, which left the basins in bare-soil condition. The sedimentation basins formed by the gravel dam at the head of each infiltration basin (Figure 1) were deepened to obtain longer detention times and more complete settling of solids in the sedimentation basins.

Uniform inundation and dry-up schedules were used for the basins in January and February. In March, cycles of short, frequent inundations (2 days wet--5 days dry) were started for basins 1, 2, 5, and 6 and long inundation periods (several weeks wet, 10 to 20 days dry) were used for basins 3 and 4. These schedules were maintained for the rest of the year. The different schedules were used to investigate the possibility of lowering the ammonium nitrogen

content of the renovated water by short, frequent inundation periods. A few inundation periods in excess of 1 month were held for basins 3 and 4 to study the behavior of fecal coliform densities in the renovated water.

On 20 October, experiments were started in the 91st Avenue Treatment Plant to evaluate the effect of higher loading of the treatment facilities on the quality of the secondary effluent. This caused a sharp increase in the suspended solids content of the effluent. For this reason, basins 1, 2, 5, and 6 were not flooded from the end of October to the beginning of December. Throughout the entire fall and winter, the secondary effluent had a high suspended solids content and was of a black appearance.

The short, frequent inundations promoted growth of grasses in basins 1, 5, and 6. Basin 1 was burned periodically to maintain bare-soil conditions, but a dense vegetation was allowed to develop in basins 5 and 6. The vegetation consisted of bermudagrass in strips of about 3 ft wide along the basin banks and Mexican sprangletop in the rest of the basins. At the end of the year, basins 1, 3, and 4 were in bare soil, basins 5 and 6 were covered by bermuda and sprangletop straw, and basin 2 still had the gravel layer.

## 2. Infiltration Rates

The infiltration rates for basins 1, 2, 5, and 6, which were inundated with short, frequent floodings, remained fairly constant throughout the entire year (Figure 2). Infiltration rates decreased essentially linearly with time during the long flooding periods for basins 3 and 4 (July-December, Figure 2), but the dry ups yielded complete recovery of the infiltration rates. Throughout the year, inundation depths of 13 inches were employed.

The accumulated infiltration curves (Figure 3) show that sequences of long inundation and dry-up periods yielded much higher annual infiltration amounts than did short, frequent inundations, as previously predicted (see Annual Report 1970). Basins

3 and 4 yielded an average infiltration of 350 ft for the year, whereas an average of about 160 ft/year were obtained with the short, frequent flooding cycles of basins 1, 2, 5, and 6.

The effect of the surface condition of the basins on infiltration can be determined by dividing the accumulated infiltration for 1971 by the original or "bench-mark" infiltration rates. These were the infiltration rates measured in September 1967 when the basins were inundated for the very first time. Thus, the bench-mark infiltration rates reflect the infiltration "potential" of the basins as affected by original soil conditions. After dividing the accumulated infiltration for 1971 by the bench-mark infiltration rate to eliminate the effect of soil variability between the basins, the highest ratio was arbitrarily set at 100 and the other ratios adjusted accordingly to obtain relative indexes of infiltration as calculated below.

Basin	Accumulated infiltration in 1971  ft	Bench-mark infiltration rate  ft/day	Accumulated infiltration/ bench-mark infiltration rate	Relative index of infil- tration
1 (bare soil)	130	3.2	40.6	79
2 (gravel)	148	4.0	37.0	72
5 (grass)	200	3.9	51.3	100
6 (grass)	155	3.1	50.0	98

The results show that the highest relative indexes of infiltration were obtained for basins 5 and 6 in which grass developed in spring and summer. The bare soil basin was next and the lowest relative index of infiltration was yielded by the gravel-covered basin. The same order of infiltration indexes has been observed in previous years.

### 3. Effect of Rainfall on Infiltration Recovery

The rainfall in the Phoenix area is about 7 inches per year. Thus, when the basins are drying to restore infiltration rates, there is usually no interference from rainfall. This may not be true in other areas with higher rainfall.

To study the effect of rain on infiltration recovery, certain areas in basins 3 and 4 were sprinkled during the long dry up in September and the beginning of October (see Figure 2), using renovated sewage water from WCW. "Showers" of about 0.75 inch in 45 minutes were applied with sprinklers. Three, 6, 8 and 10 days after the start of the dry-up period, infiltration rates in the dry and sprinkled areas were measured with cylinder infiltrometers. The cylinders were about 8 inches in diameter and they were driven about 6 inches into the soil. Water depths of 6 inches were maintained in the cylinders and the infiltration rates were measured until final infiltration rates were established. Each time six infiltrometers were used and the average for the six was determined.

The resulting averages (Figures 4 and 5) show that the areas that received no sprinkling displayed the typical S-shaped infiltration recovery curve as previously observed. The infiltration rates increased rapidly from the third to the sixth day after the start of a dry-up period, after which they increased only slightly.

The areas that received four sprinklings showed a decrease in infiltration after the first irrigation. This decrease continued until sprinkling was stopped. The infiltration recovery in basin 3 was then about the same as that of the dry area, whereas the recovery in basin 4 took about 7 days longer.

One 0.75-inch sprinkling was given to a portion of the dry areas 14 days after the start of the dry up. This also resulted in a reduction in the infiltration rate. The recovery rate was about the same as that in the wet areas. A 0.4-inch rain that

occurred 22 days after the start of the dry up caused a small decrease in the infiltration rate in basin 3, but had no effect on the infiltration for basin 4 (Figures 4 and 5).

Rainfall during the first stages of the dry up may delay the infiltration recovery more than when it occurs at the end of the dry period. Dry ups during rainy periods will probably not give much infiltration recovery and it may be better to continue the inundation under those conditions. In humid areas, inundations and dry ups should be scheduled with the weather forecast in mind.

#### 4. Pond Seepage Studies

The seepage from the unlined East Pond (Figure 1), which receives renovated sewage water from the East Well, gradually increased from about 0.1/day to about 0.2 ft/day during 1971 (Figure 6). The pond was treated with a chemical sealant on 14 October 1970, which reduced the seepage from about 0.4 ft/day to 0.1 ft/day (see Annual Report 1970).

The permanent effluent pond was dry for most of 1971 due to a pump failure. No seepage data are reported for this pond.

## II. WATER QUALITY STUDIES

### 1. Sampling, Observation Wells, and Analytical Techniques

Sampling schedules and techniques in 1971 were essentially the same as described for 1970 and 1969 (see Annual Report 1969). The observation wells (see Figure 1 for location), which are cased and open at the bottom, are 20 ft deep, except the East Center Well (ECW) which is 30 ft deep, and the West Center Well (WCW) which is 100 ft deep. The East Well (EW) is 250 ft deep, but water is obtained from 10 ft to 30 ft depth where the casing is perforated. The static ground-water table was at a depth of about 9 ft throughout 1971.

All nitrogen analyses were performed with the Technicon Auto Analyzer. This apparatus was also used in the end of the year to determine phosphate-phosphorus concentrations. The Beckman 915

Total Organic Carbon analyzer was made operational. Routine use of this instrument started in April 1971. Fecal coliform densities were determined with the membrane filter technique.

## 2. Chemical Oxygen Demand and Total Organic Carbon

The water samples were analyzed for COD until about 1 June, and for TOC starting 20 April. The results during the period of overlap were used to construct Figure 7, which shows the relation between TOC and COD for secondary effluent, renovated water from the wells, and renovated water in the experimental ponds (pumped from the East Well). Regression analysis yielded the equation

$$\text{TOC} = 0.252 \text{ COD} + 1.297$$

and a correlation coefficient of 0.8332.

COD-values for the secondary effluent and the renovated water from wells ECW, 1-2, and 5-6 are shown in Figure 8 and the TOC-values in Figure 9. The TOC-content of the effluent reached some high values after 20 October, undoubtedly due to the overloading experiments at the 91st Avenue Treatment Plant. The TOC content of the renovated water generally ranged from 0 to 8 ppm. Since the  $\text{BOD}_5$  of this water was seldom above 1 ppm (see previous annual reports), the organic carbon must be in a form that resists biodegradation. There may be some tendency of the TOC-content to increase when newly infiltrated water reaches the observation well (see, for example, TOC rises in ECW following start of inundation periods on 24 June, 17 August, and 16 October).

COD- and TOC-values for the renovated water from the other wells (1, 7, EW, WCW, and 8) are shown in Tables 1 and 2. The 91st Avenue Well is located about  $1\frac{1}{2}$  miles east of the Flushing Meadows Project and it yields native ground water from about the 100- to 200-ft depth level. The TOC-content of the renovated water from these wells generally ranged between 0 and 5 ppm. These values are somewhat below the TOC-content of the renovated

water from the wells inside the basin area (Figure 9).

### 3. Nitrogen

Total nitrogen (calculated as ammonium N + 1 ppm organic N) of the secondary effluent, which was the influent for the Flushing Meadows Project, generally ranged between 20 and 40 ppm with most of the low values occurring in the summer months (Figure 10).

The source of water pumped from ECW is effluent that has infiltrated in basins 3 and 4. The schedules of long inundations and dry ups used for these basins during the entire year (Figure 2) yielded the characteristic nitrate-N peaks in the renovated water (Figure 10). These peaks are due to the arrival of effluent water that was held as capillary water in the upper layers of the soil during the preceding dry up. Because of predominantly aerobic conditions in those soil layers during dry up, the nitrogen in this capillary water was converted to nitrate. Then, when a new inundation was started, the nitrified effluent was pushed down by the newly infiltrating water, causing a nitrate peak in the water from the observation well when it reached the intake of that well.

The ammonium-N levels in the water from ECW were mostly between 15 and 20 ppm, which is considerably higher than the ammonium-N concentrations observed a few years ago when sequences of long inundation periods were first started (see previous Annual Reports). Thus, continued use of long inundation periods for removing nitrogen apparently causes an ammonium buildup in the renovated water. This buildup is probably due to saturation of the ammonium adsorption complex in the soil, so that more ammonium remains in the water after oxygen for nitrification is no longer available.

The ammonium-N levels in the water from wells 1-2 and 5-6 were also high at the end of 1970, due to the long inundation periods employed for those basins in the years 1969 and 1970. However, the schedule for basins 1, 2, 5 and 6 was changed to one of short, frequent inundation periods in 1971. This inundation

schedule was effective in reducing the ammonium-N content of the renovated water, as evidenced by the downward trend of the ammonium-N curve for the renovated water from well 1-2 and well 5-6 shown in Figures 11 and 12. This decrease in ammonium nitrogen was not obtained in the water from ECW because long inundation periods were maintained in basins 3 and 4 in 1971.

After the sequence of short, frequent inundations was started in basins 1, 2, 5 and 6, an increase in nitrate-N was observed in the renovated water from wells 1-2 and 5-6. This occurred mainly in the month of March (Figures 11 and 12) and was due to the more aerobic conditions in the upper soil layers with the short, frequent inundations, and resulting conversion of ammonium-N stored in the soil during the previous sequences of long flooding periods to nitrate-N.

The release of nitrate-N in March and the subsequent nitrate-N levels were less for well 5-6 than for well 1-2. This may be due to the residual effects of vegetation, which were present in basins 5 and 6 in 1970 and 1969, and to the development of new vegetation in basins 5 and 6 during spring and summer 1971. Basins 1 and 2 have always been essentially free from vegetation, except for native vegetation that was allowed to develop in basin 1 during 1968. The decaying roots of the old vegetation and the active root system of the new vegetation may have aided in the denitrification process. Vegetation may also have been the reason that the ammonium-N concentrations in the water from well 5-6 were lower than those in the water from well 1-2 at the end of the year.

Nitrate-N and ammonium-N concentrations for the water from wells 1, 7, 8, EW, WCW, and 91st Avenue are shown in Tables 3 and 4, respectively. All wells yielded renovated sewage water, except the 91st Avenue Well which is a regular irrigation well and pumps native ground water. Well 8 and WCW started to yield more saline water during the course of the year (see Dissolved Salts), indicating

that a mixture of renovated sewage water and native ground water was probably obtained from these two wells.

As the renovated sewage water moves below the ground water to the outlying or deeper wells, the nitrate peaks are attenuated by dispersion. Well 7 yielded higher nitrate-N concentrations than Well 1. The nitrate-N concentrations in EW water were in the 3-12 ppm range. The nitrate-N concentrations in WCW showed a few small "peaks." Ammonium-N concentrations in the renovated water from the outlying wells were generally in the 5-12 ppm range. Well 8 and WCW continued to yield water with low ammonium-N concentrations (Table 4).

Organic nitrogen concentrations, determined in December 1971 for the effluent and the renovated water from various wells, were as follows:

Effluent	2.8 ppm
Well 1	0.6 ppm
Well 1-2	0.9 ppm
ECW	0.7 ppm
Well 5-6	1.3 ppm
Well 7	0.4 ppm
Well 8	0.5 ppm
EW	0.8 ppm
WCW	0.4 ppm

The organic-N content of the effluent was on the high side because of the high suspended solids content of the effluent in the winter. The organic N content of the renovated water is about 0.7 ppm. The TOC content of the renovated water was about 4 ppm, yielding a C/N-ratio of about 6 for the organic fraction in the renovated water.

#### 4. Phosphates

Phosphate-P concentrations of the effluent generally ranged from about 7 ppm to 12 ppm, with most of the lower values occurring in the summer (Figure 13). The average P-concentration of the

effluent in 1971 was 9.6 ppm. This is slightly less than the average for 1970, which was 11.5 ppm.

The phosphate-P concentrations for the shallow well within the recharge basin area (1-2, ECW, and 5-6) were generally in the 2-7 ppm range, with not much difference between the wells (Figure 14). These P-concentrations were about the same as in 1969 and 1970, indicating that the P-content in the renovated water from the wells within the basin area may have reached a constant level.

The average phosphate-P concentration of the water from well 7 was about 4 ppm, of the water from well 1 about 2 ppm, and of the water from well 8 essentially zero (Figure 14). The values for wells 1 and 7 are slightly below those obtained in 1970, indicating that also for the outlying wells, the P-concentrations may have reached a stable level. The P-concentrations for well 8 were still low, but this may be partly due to the fact that the water yielded by this well is a mixture of native ground water and renovated sewage water.

Phosphate-P concentrations for WCW, EW, and the 91st Avenue Well are shown in Table 5. The P-levels in WCW are still very low. Those in EW are more like the P-concentrations in the water from wells 1 and 7.

#### 5. Fluorides

The average fluoride concentration of the effluent was 4.1 ppm (Table 6). The concentration in the renovated water decreased with increased underground travel of the water. The average F-concentrations in the water from the wells within the basin area were between 1.9 and 2.5 ppm, and those in the water from wells 1, 7, and EW between 1.6 and 2.2 ppm. Well 8 and WCW yielded lower F-concentrations (Table 6).

#### 6. Boron

Boron concentrations generally fluctuated around 1 mg/liter in the effluent and in the renovated water (Table 7). Thus, the

boron levels, which were about 0.5 mg in 1968 and 1969, and 0.75 mg/liter in 1970, continued to increase. Boron is not removed from the effluent water as it moves through the sands and gravels of the Salt River bed. Boron concentrations in excess of 0.5 mg/liter may be objectionable in irrigation water if the water is used to irrigate such boron-sensitive crops as citrus.

#### 7. Dissolved Salts

The total dissolved salts content of the effluent in the renovated water was usually in the 1000 to 1200 ppm range (Table 8). The salt content of well 8 gradually increased from about 1200 to 2200 ppm. Well 8 was pumped for several hours each time a sample for coliform analysis was taken and this pumping may have drawn in native ground water, particularly if the renovated sewage water had not advanced much beyond well 8. The same may have happened to WCW, where the salt content also increased (Figure 15). The nitrate-N content of the water from WCW fluctuated between 0 and 5 ppm (Figure 15). Periodic high nitrate-N concentrations would unmistakably indicate that renovated sewage water was indeed pumped from WCW.

#### 8. pH

The pH of the effluent ranged between 7.6 and 8.2 with an average of 7.9 (Table 9). The average pH of the renovated water was around 7.0, except for well 1 where the average pH of the water was 7.6. The lower pH of the renovated water is probably due to CO<sub>2</sub>-production by the soil micro-organisms.

#### 9. Fecal Coliform Density

The fecal coliform density in the effluent was generally of the order of 10<sup>6</sup>/100 ml (Figure 16) and between 0 and 100/100 ml for the renovated water from ECW (Figure 17). For the renovated water from well 7 and EW, which are located outside the basin area, the fecal coliform densities were in the range of 0 to 10/100 ml most of the time (Figures 18 and 19, respectively).

The fluctuations in the fecal coliform density of the renovated water from ECW, which is water that infiltrated in basins 3 and 4, can be directly traced to the inundation periods in those basins. The time required for the infiltrated water to travel from basins 3 and 4 to the intake of ECW can be calculated from the infiltration rates (see Annual Report 1969). These calculations show that it takes about 3 to 5 days for the water that infiltrated at the start of a new inundation period to reach ECW. The calculated arrival times of the newly infiltrated water are indicated with a downward arrow in Figure 17 for each inundation period. Each time, the rise in fecal coliform density coincides with the arrow, indicating that the increase in fecal coliform density was caused by the arrival of newly infiltrated water. With continued flooding, however, the fecal coliform density decreased in the water from ECW and reached essentially zero in 2 or 3 weeks. The fluctuations in fecal coliform density for the renovated water from well 7 and EW (Figures 18 and 19) are similar to those for the water from ECW.

The increase in fecal coliform density in the renovated water after the start of a new inundation period is probably due to the absence of clogging of the surface soil in the basin and reduced bacterial activity in the soil profile when inundation is started. With continued inundation, however, the soil surface in the basins becomes more clogged, which increases the filtering action. Also, the continued supply of nutrients entering the soil with the sewage water stimulates bacterial activity, and hence the competition among microbes in the soil beneath the basins. Both factors would result in increased removal and mortality of fecal coliform bacteria in the soil.

The rate of removal of fecal coliform bacteria in the soil was studied by obtaining water samples from different depths in basin 3 for the two long inundation periods in the last 3 months of the year. Cylindrical ceramic cups about 5 x 10 cm in size with pores of about 30 to 40 micron and a bubbling pressure of 70- to 90-cm

water, were installed at 3-cm, 10-cm, 36-cm, and 60-cm depths (one cup for each depth). Water samples were obtained by applying a vacuum to these cups. Some coliforms were filtered out as the water moved through the ceramic. For secondary effluent, about  $\frac{1}{2}$  the fecal coliform bacteria were removed in this manner. For the water sampled in the soil, the coliform removal by filtering was probably less because of the lower suspended solids content of the effluent water after it has moved some distance through the soil.

The results (Figure 16) show that almost all fecal coliform bacteria were removed in the first 60 cm of the soil, even though the actual values may be in error because filtering through the ceramic cup removed some of the coliforms from the water. At 60 cm, the coliform density started to decrease on about 26 October. Figure 17 shows that the fecal coliform density in the water from ECW decreased again on about 1 November, or about 5 days later. This is just about the time required for the water to travel from the 60-cm depth level in the soil beneath the basins to the intake of ECW.

Fecal coliform densities in the deep West Center Well and the remote well 8 were zero, except for a few positive values for WCW in November (Table 10). External infection of the water in the wells by dust or insects is not impossible and may explain the positive values. Well 8 was no longer sampled in the second half of the year to reduce pumping the well and resulting encroachment of native ground water.

#### 10. Profile Studies of Nitrogen and Organic Carbon

Water samples from the ceramic cups at depths of 3 cm, 10 cm, 36 cm, and 60 cm in basins 3 were analyzed for nitrate, nitrite, ammonium and TOC. The first sample analyzed was taken at the start of the dry-up period on 3 November. No other samples could be taken during the dry up because of the low water content of the soil. The next samples were obtained during the subsequent flooding period, 11 November - 21 December.

Nitrogen. At the beginning of the dry period, there was no nitrate-N in the soil water (Table 11). Also, ammonium-N decreased with depth from a concentration about equal to that of the effluent to essentially zero at 60 cm (Table 12). This is probably due to adsorption to the clay and organic exchange complex in the soil and to fixation in organic matter. Nitrite is absent at the start of the dry period (Table 13).

The next sample was taken on 18 November, 1 week after the start of a new inundation period. At that time, there was considerable nitrate-N in the water and some of the nitrates from the top 10 cm had already been leached out (Table 11). The nitrate-N concentration at 60 cm was still fairly low, indicating that nitrate formation is concentrated in the surface layers of the soil, which are aerobic during the dry-up period. Ammonium concentrations were lower on 18 November than in the beginning of the dry up, probably due to nitrification and adsorption of ammonium to clay and organic fraction (Table 12). Also, considerable nitrite occurred on that day, indicating denitrification.

During the remainder of the flooding period, nitrate-N was leached down to greater depth and eventually disappeared entirely from the 60-cm soil layer (Table 11). Undoubtedly, oxygen depletion prevented the formation of nitrates. The same was true for nitrite, which also disappeared (Table 13). Ammonium-N continued to decrease with depth during the remainder of the flooding period, probably due to adsorption and fixation. There was a gradual increase of ammonium-N with time for all depths, probably due to saturation of the exchange complex with ammonium. The ammonium-N concentration in the water at 60 cm was lower than that in the water from ECW (Figure 10). If this was not a local effect, there must have been an increase in the ammonium-N content as the water moved from 60-cm depth below the basin to the 30-ft depth of ECW.

The results of the profile studies are in agreement with the nitrogen regimes proposed in previous reports to explain the nitrogen behavior in the renovated water from ECW and other observation wells. These regimes include adsorption of ammonium by the cation exchange complex of the soil and fixation to organic matter during prolonged flooding, nitrification of adsorbed ammonium in the upper soil layers during dry up, denitrification in micro-anaerobic environments in the upper soil layers during dry up, leaching of nitrate to ground water when flooding is resumed, nitrification of ammonium in the upper soil layers during the early stages of the inundation period when oxygen is still available in the soil, and denitrification where nitrate and organic carbon are present under anaerobic conditions.

Total Organic Carbon. Total Organic Carbon in the soil water generally decrease with depth (Table 14). The TOC-value at 60 cm was mostly in the 2- to 10-ppm range, which is about the same as that for the renovated water from ECW. Thus, most of the organic carbon reduction takes place in the upper soil profile. Occasionally, however, TOC-values are not reduced in the first 60 cm as the effluent water moves through the soil (see 13 November, 1 December, and 14 December in Table 14, for example). This may be due to changes in the bacterial population in the soil, for example, from a predominantly aerobic population at the beginning of an inundation period to an anaerobic population as inundation continues and oxygen will be depleted in the soil.

#### 11. Metals

Metal concentrations in the effluent and renovated water were determined by the U. S. Soils Laboratory (Beltsville, Maryland) using atomic adsorption spectrometry. Mercury was consistently below 1 ppb, but this was attributed to adsorption of mercury to the plastic bottles in which the samples were shipped.

The results (Table 15) show that the concentrations of zinc and copper were considerably lower in the renovated water than in

the effluent. Some lead was also removed by the soil filtration process, but cadmium levels stayed about the same.

The high concentration of Zn in ECW- and WCW-water may have been caused by the galvanized pipe through which the submerged pumps discharged their water (the other wells are sampled with a bailer or a portable submersible pump on a plastic hose). Well 8 and WCW yielded also some native ground-water (see Total Salts), which may explain the higher Cd and Pb concentrations in the water from these wells.

The metal concentrations in the renovated water were below the maximum limits of surface water criteria for public water supplies, with the exception of lead. These limits are 5000 ppb for zinc, 1000 ppb for copper, 10 ppb for cadmium, and 50 ppb for lead.

### III. FUTURE PROJECTS

The Flushing Meadows Project has demonstrated that renovated sewage water suitable for unrestricted irrigation, primary contact recreation, and other purposes can be obtained at reasonable cost by soil filtration in the Salt River bed. Using a system of infiltration basins along both sides of the river bed and wells in the center of the river bed to pump the renovated water, the total cost of the renovation process was estimated at about \$5/acre-foot at the pump. Because of the favorable results, plans for two larger projects are under development. These projects are the 23rd Avenue Project and the Rio Salado Project.

The 23rd Avenue Project would renovate secondary effluent (activated sludge process) from the 23rd Avenue Sewage Treatment Plant in Phoenix at a rate of about 15 mgd or 45 acre-feet/day. An existing oxidation pond of about 40 acres on the north side of the Salt River bed would be subdivided by three dikes into four intermittently inundated basins (Figure 20). Wells for pumping the renovated water would be located in the center dike (Figure 20).

The renovated sewage water would be delivered to an irrigation district for unrestricted use. The soil and hydrogeologic conditions at the project site are similar to those at the Flushing Meadows Project, except that the static ground-water is at greater depth (about 50 ft compared to about 10 ft for the Flushing Meadows Project). A project plan, including objectives, needs for project, and a plan of operation was prepared for the City of Phoenix, who then incorporated the material in an application for a research development and demonstration grant from the Environmental Protection Agency. The grant application was mailed on 14 June 1971. The total cost of the project for the grant period was \$784,630, of which \$411,520 would be covered by the grant.

The Rio Salado Project is a long-range plan to convert most of the Salt River bed from Granite Reef to Gillespie Dam (a 40-mile stretch) into a series of aquatic parks with resorts, scenic drives, etc., and housing and industrial developments. The plan was proposed by the School of Architecture of Arizona State University in 1967. The project would depend on the completion of flood control works on the Salt River system. Renovated sewage water would be a likely source of water for the project. The Rio Salado Project is now administered by the Rio Salado Steering Committee under the Valley Forward Association. A preliminary planning study by the firm of Daniel, Mann, Johnson, and Mendenhall of Los Angeles is almost completed. The study was financed by municipalities and other institutions of the Salt River Valley.

#### SUMMARY AND CONCLUSIONS:

Continued use of long inundation periods in 1969 and 1970 to minimize the nitrate-nitrogen level in the renovated water caused a gradual increase of the ammonium-nitrogen level in the renovated water at the Flushing Meadows Project. This project is an experimental ground-water recharge facility in the Salt River bed west of Phoenix, installed in 1967 to study renovation of secondary

sewage effluent by soil filtration. To determine if a sequence of short, frequent inundations could reverse the increasing trend in the ammonium level of the renovated water, four basins were flooded according to a 2-days-wet-5-days-dry schedule. Inundation periods of several weeks rotated with dry-ups of 10 to 20 days were used for the remaining two basins as a control.

The short, frequent inundations were indeed effective in lowering the ammonium content of the renovated water, apparently because of the resulting predominantly aerobic conditions in the upper soil layers. This led to conversion of adsorbed and fixed ammonium in the soil to nitrates, which were then leached out by the infiltrated effluent water. The resulting nitrate levels in the renovated water were considerably higher below the two non-vegetated basins than below the two vegetated basins, indicating that residual or active root zones contributed to denitrification. The ammonium-nitrogen levels in the renovated water below the four basins receiving short, frequent flooding decreased gradually over the year from about 15 ppm to about 5 ppm, whereas the ammonium-nitrogen level in the renovated water below the two basins flooded for long periods remained high (generally between 15 and 20 ppm, compared to a total nitrogen content of 20-40 ppm in the effluent.

Thus, long flooding periods to minimize the nitrogen in the renovated water can not be used indefinitely because of a gradual buildup of the ammonium levels in the renovated water. Sequences of long inundations should therefore be periodically interrupted with cycles of short, frequent inundations to reduce the ammonium level in the renovated water. Vegetation in the recharge basins during the period of short, frequent inundations apparently is effective in minimizing the release of nitrates from the soil.

Infiltration rates in the recharge basins were about the same as in previous years. The accumulated infiltration in 1971 for the two basins receiving long inundations were 310 ft and 396 ft, respectively, whereas the four basins receiving short frequent

inundations had an annual infiltration of 130, 148, 155, and 200 ft. This agreed with previous conclusions that maximum annual infiltration amounts are obtained with flooding periods of about 20 days, alternated with dry ups of about 10 days in the summer and 20 days in the winter.

Taking soil differences between the four basins that received short, frequent inundations into account, the two vegetated basins had the highest infiltration rates with relative infiltration indexes of 98 and 100. Next came the basin that was kept in bare soil with an index of 79. The gravel-covered basin had the lowest infiltration with an index of 72.

The analyses for chemical oxygen demand were replaced by analyses for total organic carbon in April 1971. Regression analysis showed that  $TOC = 0.252 COD + 1.297$ , with a correlation coefficient of 0.8332. TOC for the effluent was generally in the 10-30 ppm range. This was reduced to an average of about 4 ppm (range 0-8 ppm) for the renovated water from the wells between the basins, and to slightly lower values for the renovated water from the outlying wells.

The phosphate-phosphorus concentration in the effluent for 1971 generally ranged from 7 to 12 ppm with an average of 9.6 ppm. This was reduced to a general range of 2 to 7 ppm for the renovated water from the wells between the basins, and to a general range of 0 and 4 ppm for the wells outside the basins. The 1971 phosphate levels in the renovated water from the various wells were about the same as in 1970.

The average fluoride concentration in the effluent was 4.1 ppm. This was reduced to 1.9-2.5 ppm for the renovated water from the wells inside the basin area, and to 1.6-2.2 ppm for the wells outside the basin area.

Boron levels were around 1 ppm in both effluent and renovated water. This compares to about 0.75 ppm in 1970 and about 0.5 ppm

in 1968 and 1969. Thus, the increasing trend in boron concentration in effluent and renovated water continued in 1971.

Average metal concentrations in the effluent were 193 ppb zinc, 123 ppb copper, 7.7 ppb cadmium, and 82 ppb lead. Mercury was essentially absent, but this may have been due to adsorption of mercury to the plastic bottles in which the samples were stored. The average zinc concentration in the renovated water from wells without galvanized plumbing was 36 ppb. The copper concentration in the renovated water was also considerably lower than that in the effluent, i. e., 17 ppb. Some of the lead was also removed by the soil filtration process, but the cadmium level stayed about the same. The metal concentrations in the renovated water were well below the maximum limits for municipal water supply, except lead which was 16 ppb above the limit of 50 ppb.

Dissolved salts continued to be in the 1000- to 1200-ppm range for the effluent and the renovated water. The pH of the effluent usually ranged between 7.6 and 8.2 with an average of 7.9. The pH of the renovated water was generally around 7.0, probably due to CO<sub>2</sub> production by the soil microflora.

Fecal coliform density in the effluent was of the order of 10<sup>6</sup> per 100 ml. This was generally reduced to a range of 0-100 per 100 ml for the renovated water from the 30-ft deep well in the center of the basin area, and to 0-10 per 100 ml for the 20-ft deep well 100 ft away from the basins. The 100-ft deep well in the center of the basin area and the 20-ft deep well 300 ft away from the basin remained essentially negative for fecal coliforms. Almost all of the fecal coliform removal took place in the first 3 ft of soil.

Fluctuations in the fecal coliform density in the renovated water from the 30-ft well in the center of the basin area could be directly traced to the flooding cycles. When a new flooding period was started, fecal coliform bacteria were apparently able to penetrate the soil and cause densities of 100 to 500 per 100 ml in the

renovated water. With continued flooding, however, fecal coliform density at this depth went down to zero in a few weeks, probably because the clogging of the soil surface yielded better filtering. Also, the continued supply of nutrients carried into the soil by the effluent probably caused an increase in the microbial population in the soil, and, hence, a more competitive environment.

PERSONNEL: Herman Bower, R. C. Rice, E. D. Escarcega, and  
M. S. Riggs.

CURRENT TERMINATION DATE: December 1973.

Table 1. COD in mg/l for various wells (1971).

<u>Date</u>	<u>1</u>	<u>7</u>	<u>EW</u>	<u>WCW</u>	<u>8</u>	<u>91st Ave</u> *
27 Jan	16	18	8	9	8	-
17 Feb	10	5	6	8	17	-
31 Mar	17	17	21	11	13	-
28 Apr	16	16	15	8	12	-
26 May	22	21	21	14	18	28

\* native ground water

Table 2. Total organic carbon in mg/l for various wells (1971).

<u>Date</u>	<u>1</u>	<u>7</u>	<u>EW</u>	<u>WCW</u>	<u>8</u>	<u>91st Ave. *</u>
27 Jan	4.8	3.3	3.8	1.9	2.7	-
17 Feb	5.2	-	5.2	2.2	-	-
31 Mar	-	-	-	-	-	-
28 Apr	-	-	-	-	-	-
26 May	3.5	5.0	6.0	3.1	3.0	1.0
24 Jun	3.9	0.7	3.0	0	0	-
28 Jul	4.4	3.8	4.4	0.7	1.6	-
17 Sep	8.3	6.2	7.2	4.7	4.2	-
20 Oct	3.1	3.5	3.1	1.6	1.0	-
17 Nov	1.9	0	1.6	0	0	-
15 Dec	0.1	0.6	0	0	0	-

\* native ground water

Table 3. Nitrate-nitrogen concentrations in mg/l for various wells (1971).

<u>Date</u>	<u>1</u>	<u>7</u>	<u>8</u>	<u>EW</u>	<u>WCW</u>	<u>91st Ave. *</u>
27 Jan	7.7	7.8	4.3	8.4	0.5	-
17 Feb	1.3	4.7	2.0	8.3	0.4	-
31 Mar	13.4	32.1	0.5	10.0	0.3	-
28 Apr	10.4	19.7	0.8	6.9	0.2	-
26 May	10.9	16.9	0.7	3.3	3.5	4.8
24 Jun	6.0	9.0	0.4	14.7	0.7	-
28 Jul	2.6	17.7	0.9	4.2	4.5	-
17 Sep	0.4	12.5	0.6	7.0	4.2	-
20 Oct	3.3	20.4	0.9	12.3	0.3	-
17 Nov	5.1	17.0	0.2	12.2	0.1	-
15 Dec	7.9	18.2	0.5	8.3	3.6	-

\* native ground water

Table 4. Ammonium-nitrogen concentrations in mg/l for various wells (1971).

<u>Date</u>	<u>1</u>	<u>7</u>	<u>8</u>	<u>EW</u>	<u>WCW</u>	<u>91st Ave.*</u>
27 Jan	5.1	6.4	0.3	9.5	0.3	-
17 Feb	5.3	7.1	0.4	8.6	0.5	-
31 Mar	5.4	10.5	0.6	10.3	0.6	-
28 Apr	6.4	11.4	0.5	9.3	0.4	-
26 May	6.6	10.6	0.4	10.2	0.3	0.4
24 Jun	7.9	3.9	0.4	10.2	0.5	-
28 Jul	11.1	9.6	0.6	11.0	0.5	-
17 Sep	12.4	4.8	0.2	13.1	0.2	-
20 Oct	14.6	6.8	0.1	12.5	0.1	-
17 Nov	12.9	6.5	0.4	11.0	0.4	-
15 Dec	11.2	5.1	0.2	9.2	0.2	-

\* native ground water

Table 5. Phosphate-phosphorus concentration in mg/l for various wells (1971).

<u>Date</u>	<u>WCW</u>	<u>EW</u>	<u>91st Ave. *</u>
27 Jan	0.1	6.2	-
17 Feb	0.1	3.6	-
31 Mar	0	6.8	-
28 Apr	0.1	7.6	-
26 May	0	7.8	0.1
24 Jun	0.4	5.6	-
28 Jul	0	5.4	-
17 Sep	0	3.8	-
20 Oct	0.1	3.0	-
17 Nov	0	2.0	-
15 Dec	0	1.7	-

\* native ground water

Table 6. Fluoride concentration in mg/l for effluent and wells (1971).

<u>Date</u>	<u>Effl.</u>	<u>Date</u>	<u>1</u>	<u>1-2</u>	<u>ECW</u>	<u>5-6</u>	<u>7</u>	<u>8</u>	<u>EW</u>	<u>WCW</u>	<u>91st Ave.*</u>
12-15 Jan	4.4	27 Jan	1.3	2.0	2.3	2.0	2.3	0.8	1.9	0.5	-
15-19 Jan	4.4										
18-19 Mar	4.0	31 Mar	1.8	1.5	2.1	1.8	1.9	1.3	2.1	1.1	-
23-26 Mar	3.8										
26-31 Mar	3.2	26 May	0.8	1.3	2.2	2.6	1.5	0.7	1.8	0.2	0.3
30-31 Mar	3.9										
1- 2 Apr	3.2	28 Jul	1.9	2.3	2.6	3.2	3.0	1.0	2.6	0.5	-
6- 8 Apr	4.5										
14-16 Apr	4.1	17 Sep	1.9	2.2	2.3	2.7	2.4	0.7	2.0	0.4	-
16-23 Apr	4.1										
23-29 Apr	4.6	17 Nov	1.7	1.9	2.6	2.6	2.2	0.8	1.8	0.6	-
11-14 May	4.8										
14-21 May	4.3										
21-27 May	4.5	Av.	1.6	1.9	2.4	2.5	2.2	0.9	2.0	0.6	0.3
25-26 May	3.5										
1- 3 Jun	3.8										
8-10 Jun	4.7										
15-18 Jun	5.2										
24-25 Jun	4.8										
25-30 Jun	4.8										
1- 2 Jul	4.8										

\* native ground water

6-28

Table 6 (continued). Fluoride concentration in mg/l for effluent and wells (1971).

<u>Date</u>	<u>Effl.</u>	<u>Date</u>	<u>Effl.</u>
3- 9 Jul	3.5	10-17 Dec	4.4
9-16 Jul	3.9	17-21 Dec	4.0
16-23 Jul	3.5	27-29 Dec	3.9
26-30 Jul	3.9		
27-28 Jul	3.8	Av.	4.1
2- 5 Aug	3.9		
10-12 Aug	4.1		
17-20 Aug	3.8		
20-27 Aug	3.7		
1- 3 Sep	4.1		
3- 9 Sep	3.3		
15-16 Sep	4.9		
16-17 Sep	4.4		
22-24 Sep	4.3		
15-22 Oct	4.5		
22-29 Oct	4.6		
1- 2 Nov	2.7		
17-18 Nov	4.9		
1- 3 Dec	4.6		
3-10 Dec	3.8		

6-29

Table 7. Boron concentration in mg/l for effluent and wells (1971).

<u>Date</u>	<u>Effl.</u>	<u>1</u>	<u>1-2</u>	<u>ECW</u>	<u>5-6</u>	<u>7</u>	<u>8</u>	<u>EW</u>	<u>WCW</u>
17 Feb	-	0.78	0.80	0.78	0.72	0.72	-	-	-
28 Apr	0.89	-	-	-	-	-	1.02	0.92	0.96
24 Jun	-	1.08	1.13	1.02	1.06	1.03	-	-	-
17 Sep	-	-	-	-	-	-	1.02	0.87	0.97
20 Oct	0.90	0.92	0.89	0.83	0.83	-	-	-	-
15 Dec	0.77	-	-	-	-	0.79	1.32	0.79	1.00

Table 8. Total salt concentration in mg/l for effluent and wells (1971).

<u>Date</u>	<u>Effl.</u>	<u>1</u>	<u>1-2</u>	<u>ECW</u>	<u>5-6</u>	<u>7</u>	<u>8</u>	<u>EW</u>	<u>91st Ave.*</u>
27 Jan	-	1024	1094	1094	1107	1030	1216	1043	-
17 Feb	-	992	1018	973	1011	934	-	960	-
30-31 Mar	1216	1184	1280	1184	1210	1286	1619	1184	-
27-28 Apr	1216	1222	1216	1165	1184	1248	1600	1203	-
25-26 May	1261	1280	1216	1229	1216	1267	1587	1216	2291
24 Jun	1210	1261	1222	1280	1236	1248	1600	1254	-
27-28 Jul	1216	1216	1165	1120	1216	1267	1664	1126	-
16-17 Sep	1024	1114	1088	1030	1088	1152	1568	1126	-
20 Oct	1152	1114	1197	1056	1088	1190	1792	1139	-
17 Nov	-	1120	1024	998	1101	1235	1984	1229	-
14-15 Dec	1024	1107	960	960	992	1088	2170	1037	-

\* native ground water

Table 9. pH of effluent and water from wells (1971).

<u>Date</u>	<u>Effl.</u>	<u>1</u>	<u>1-2</u>	<u>ECW</u>	<u>5-6</u>	<u>7</u>	<u>8</u>	<u>EW</u>	<u>91st Ave.*</u>
27 Jan	-	7.5	6.9	7.2	7.3	7.5	7.2	7.0	-
17 Feb	-	7.5	7.0	7.2	7.4	7.1	-	7.0	-
30-31 Mar	8.1	7.7	6.9	7.0	7.0	6.9	7.3	6.9	-
27-28 Apr	7.8	7.3	6.8	6.8	7.0	6.6	7.1	6.8	-
25-26 May	8.0	7.4	7.0	7.2	7.1	6.9	7.3	7.1	7.1
24 Jun	-	7.3	6.7	6.9	6.8	6.8	7.1	6.8	-
27-28 Jul	8.2	7.6	7.0	7.1	7.0	7.0	7.3	7.2	-
16-17 Sep	7.6	7.2	6.8	6.9	6.7	6.7	7.0	6.7	-
20 Oct	7.9	7.8	7.0	7.1	6.9	6.8	7.1	6.8	-
17 Nov	-	8.0	7.3	7.2	7.3	7.2	7.4	7.1	-
14-15 Dec	7.8	8.1	7.2	7.1	7.1	6.9	7.2	6.9	-
Av.	7.9	7.6	7.0	7.1	7.0	6.9	7.2	6.9	

\* native ground water

Table 10. Fecal coliform for West Center Well and Well 8 (1971).

<u>Date</u>	<u>WCW</u>	<u>8</u>	<u>Date</u>	<u>WCW</u>	<u>8</u>
6 Jan	-	0	21 July	0	-
27 Jan	-	0	4 Aug	0	-
10 Feb	-	0	18 Aug	0	-
24 Feb	-	0	1 Sep	0	-
10 Mar	-	0	15 Sep	0	-
24 Mar	-	0	29 Sep	0	-
7 Apr	-	0	13 Oct	0	-
21 Apr	-	0	28 Oct	0	-
5 May	0	-	10 Nov	6.5	-
26 May	0	0	17 Nov	2.0	-
9 Jun	0	-	23 Nov	0	-
23 Jun	0	-	1 Dec	0	-
30 Jun	0	-	8 Dec	0	-
			15 Dec	0	-
			22 Dec	0	-

Table 11. Nitrate-N concentrations in mg/l for effluent and water samples from ceramic cups at depths of 3 cm, 10 cm, 36 cm, and 60 cm in basin 3 (1971).

	3 Nov	18 Nov	22 Nov	30 Nov	1 Dec	3 Dec	6 Dec	8 Dec	9 Dec	14 Dec	16 Dec	21 Dec
Effluent	0.3	0		0.2		0.2	0	0	0.2	0	0	0.1
3 cm	0	22.3	0.1	0	0.5	0.1	0	0	0.1	0	0	0
10 cm	0	93.3	15.6	0	0.4	0	0	0	0	0	0	0
36 cm	0	88.6	16.6	0.9	0.6	0	0	0	0	0	0	0
60 cm	0	6.3	81.1	18.5	19.5	9.4	0.1	0	0	0	0	0

48-9

Table 12. Ammonium-N concentrations in mg/l for effluent and water samples from ceramic cups at depths of 3 cm, 10 cm, 36 cm, and 60 cm in basin 3 (1971).

	3 Nov	18 Nov	22 Nov	30 Nov	1 Dec	3 Dec	6 Dec	8 Dec	9 Dec	14 Dec	16 Dec	21 Dec
Effluent	30.6	38.8		30.3		36.6	28.5	36.5	37.9	37.6	38.2	36.7
3 cm	25.6	4.5	8.8	19.8	19.2	21.9	25.4	26.4	27.6	31.0	31.3	34.0
10 cm	9.7	6.4	3.5	1.7	1.5	1.7	1.9	2.2	2.1	2.2	2.4	3.7
36 cm	8.1	2.9	2.1	1.5	1.2	1.5	1.4	1.6	1.4	1.3	1.5	2.1
60 cm	0.1	0.8	0.6	0.2	0.2	0.4	0.3	0.7	0.5	0.1	0.2	9.8

6-35

Table 13. Nitrite-N concentrations in mg/l for effluent and water samples from ceramic cups at depths of 3 cm, 10 cm, 36 cm, and 60 cm in basin 3 (1971)

	3 Nov	18 Nov	22 Nov	30 Nov	1 Dec	3 Dec	6 Dec	8 Dec	9 Dec	14 Dec	16 Dec	21 Dec
Effluent	0.4	0.5		0.2		0	0	0	0	0.1	0.1	0.1
3 cm	0	0.1	0.1	0	0	0	0	0	0	0.1	0.1	0.1
10 cm	0	3.3	0.4	0	0	0.1	0	0	0	0.1	0	0.1
36 cm	0	10.4	0.4	0	0	0.1	0	0	0	0.1	0	0.1
60 cm	0	0.1	1.4	0.3	0.1	0.1	0	0	0	0.1	0	0

63-9

Table 14. Total organic carbon in mg/l for effluent and water samples from ceramic cups at depths of 3 cm, 10 cm, 36 cm, and 60 cm in basin 3 (1971).

	3 Nov	18 Nov	22 Nov	30 Nov	1 Dec	3 Dec	6 Dec	8 Dec	9 Dec	14 Dec	16 Dec	21 Dec
Effluent	24.1	42.2		20.3		13.5	9.9	13.1	12.0	17.6	14.3	11.7
3 cm	14.8	29.8	28.8	18.3	10.0	11.7	8.3	8.5	7.8	11.9	6.1	6.6
10 cm	10.8	11.6	17.4	14.6	24.2	8.7	6.5	6.4	6.0	9.0	2.8	1.8
36 cm	10.8	14.1	7.4	19.6	30.0	9.6	4.9	4.4	6.3	8.6	3.7	3.6
60 cm	9.4	2.4	2.1	19.6	23.2	5.4	6.2	3.0	2.8	20.0	2.9	3.4

6-37

Table 15. Metal concentrations in parts per billion for effluent and renovated water from wells (1971).

	22 Oct	3 Nov	17 Nov	1 Dec	15 Dec	29 Dec	Av.
<u>Zinc</u>							
Effluent	197	401	55	49	124	330	193
1-2	73	49	27	12	17	29	35
ECW	120	123	70	270	39	27	108
7	63	80	40	11	15	12	37
8	39	32	20	9.1	8.0	7.0	19
WCW	391	232	214	130	142	700	185
<u>Copper</u>							
Effluent	71	291	28	23	179	144	123
1-2	24	23	16	9.5	10	16	16
ECW	29	26	18	12	9.2	6.3	17
7	23	25	20	12	13	9.5	17
8	12	9.5	11	10	12	9.5	11
WCW	16	11	12	11	12	12	12
<u>Cadmium</u>							
Effluent	9.0	9.2	7.7	5.7	7.2	7.5	7.7
1-2	8.3	6.8	7.4	6.8	6.4	7.7	7.2
ECW	7.5	7.1	7.1	6.6	7.7	7.1	7.2
7	8.3	7.4	7.2	7.2	7.2	6.3	7.3
8	11	13	13	12	13	13	13
WCW	12	13	12	13	13	14	13
<u>Lead</u>							
Effluent	83	99	75	63	86	86	82
1-2	80	63	63	51	63	75	66
ECW	75	75	63	75	63	46	66
7	63	63	75	63	63	69	66
8	99	125	113	113	136	125	119
WCW	86	113	118	125	125	130	116

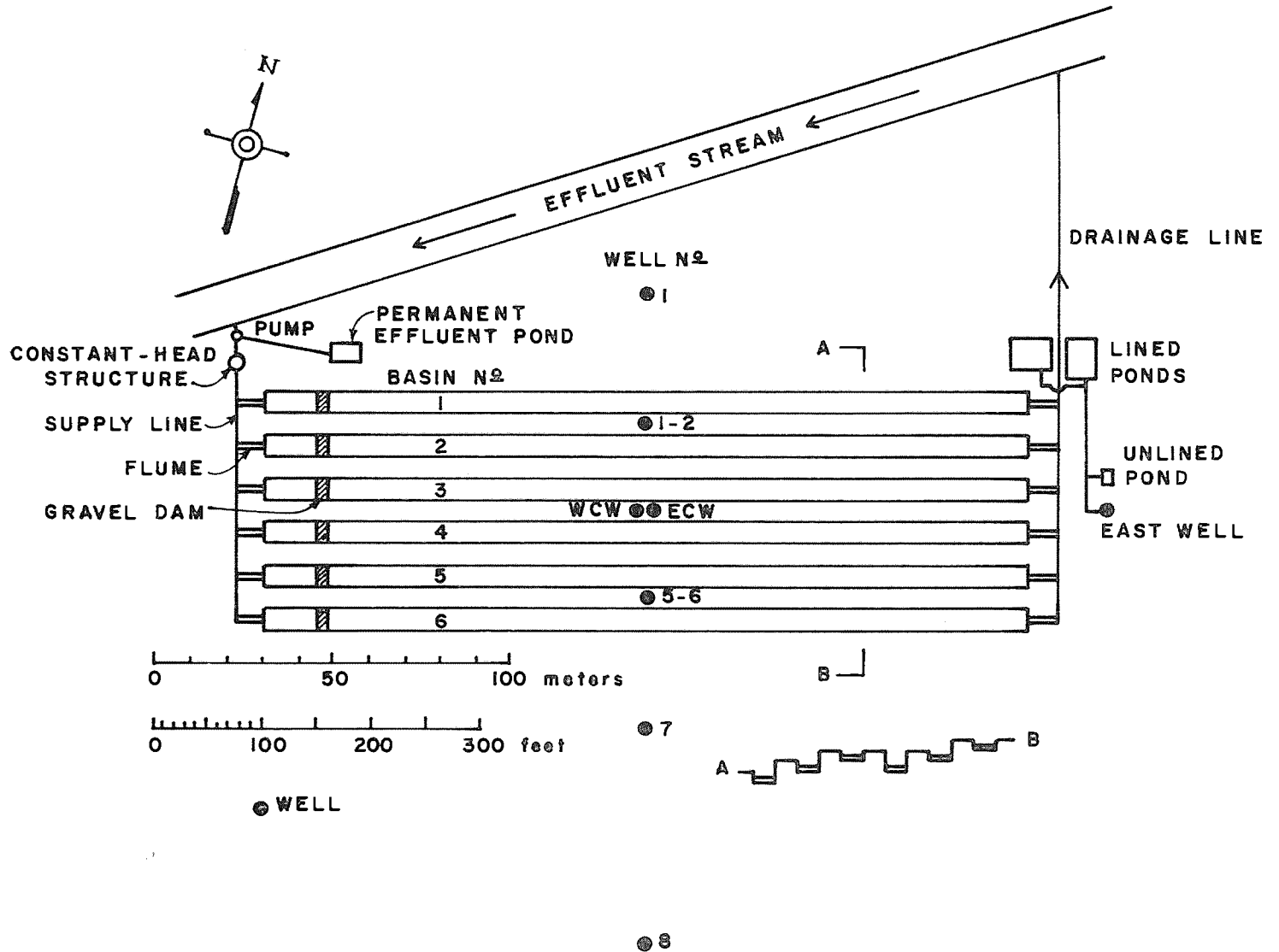


Figure 1. Schematic of Flushing Meadows Project.

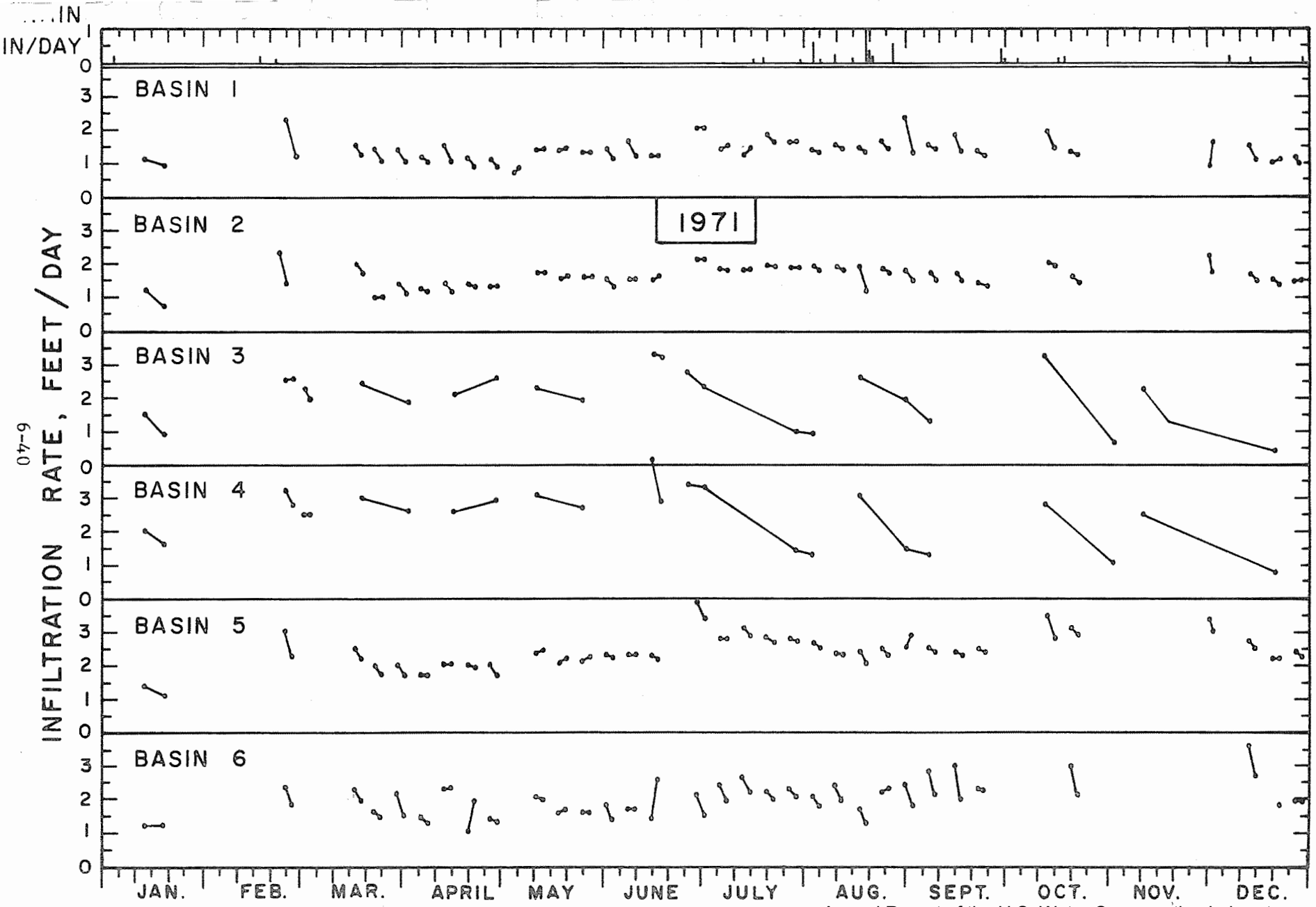


Figure 2. Infiltration rates in recharge basins and rainfall.

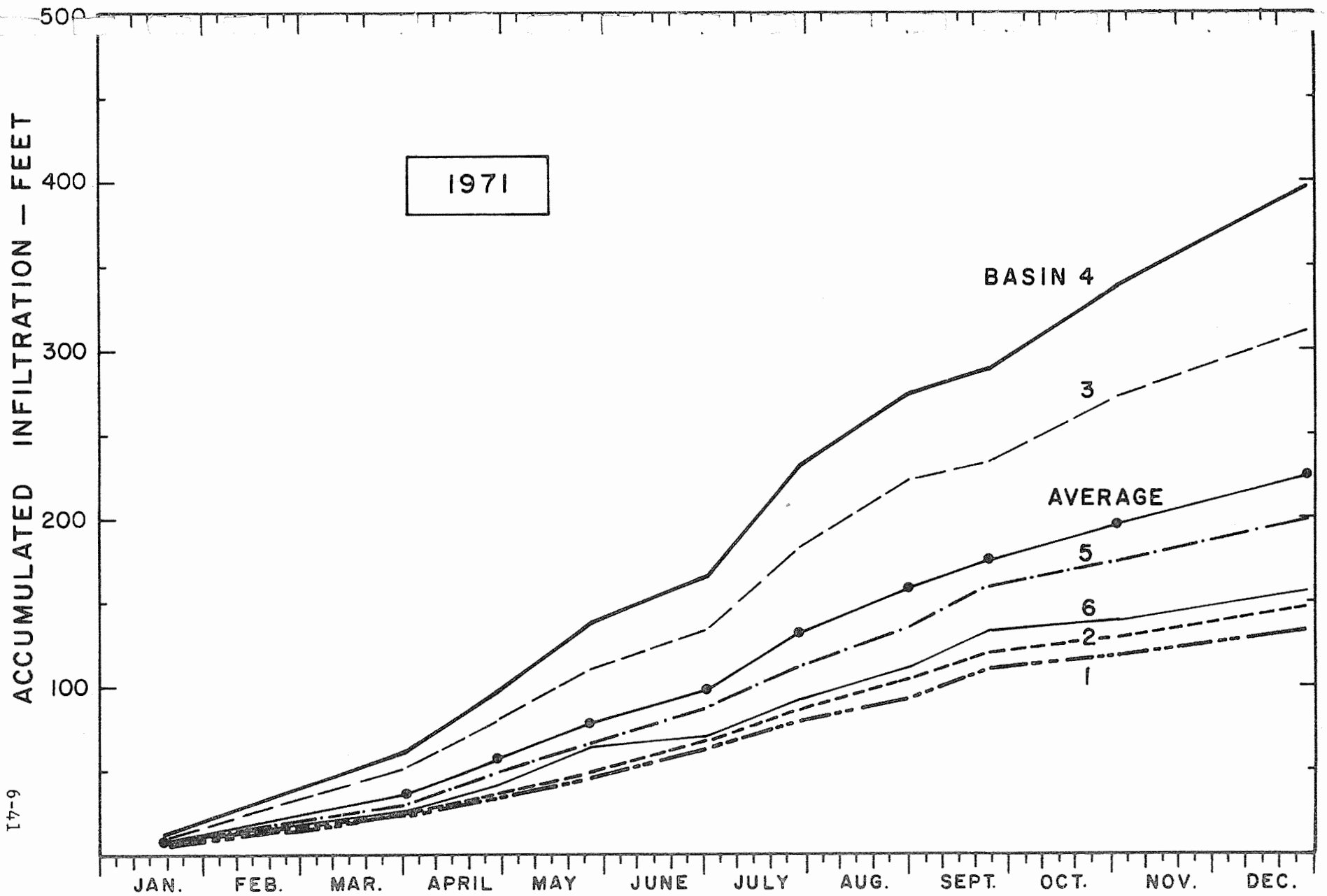


Figure 3. Accumulated infiltration in recharge basins. Annual Report of the U.S. Water Conservation Laboratory

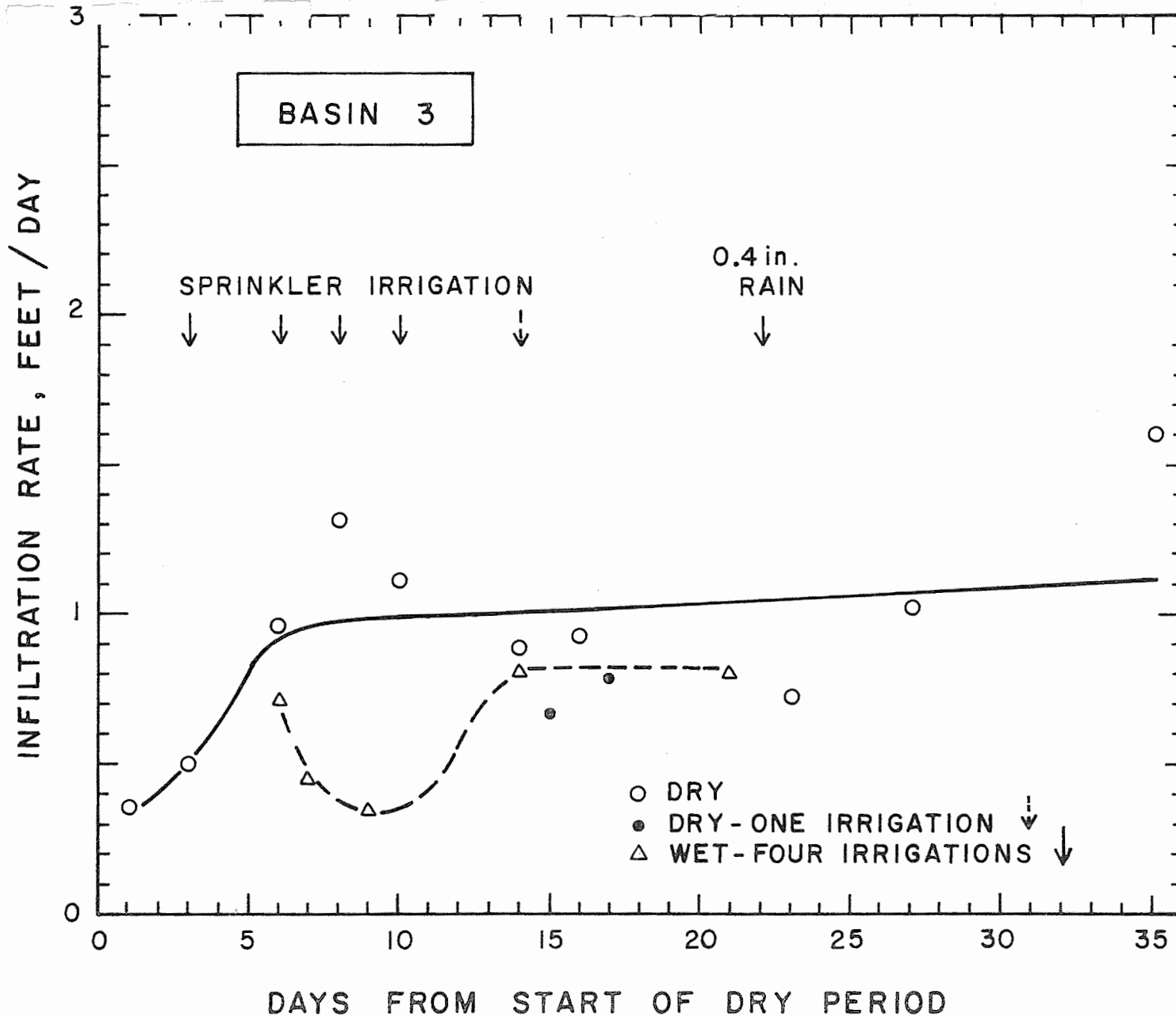


Figure 4. Effect of sprinkler irrigation during dry up on infiltration recovery in basin 3. Annual Report of the U.S. Water Conservation Laboratory

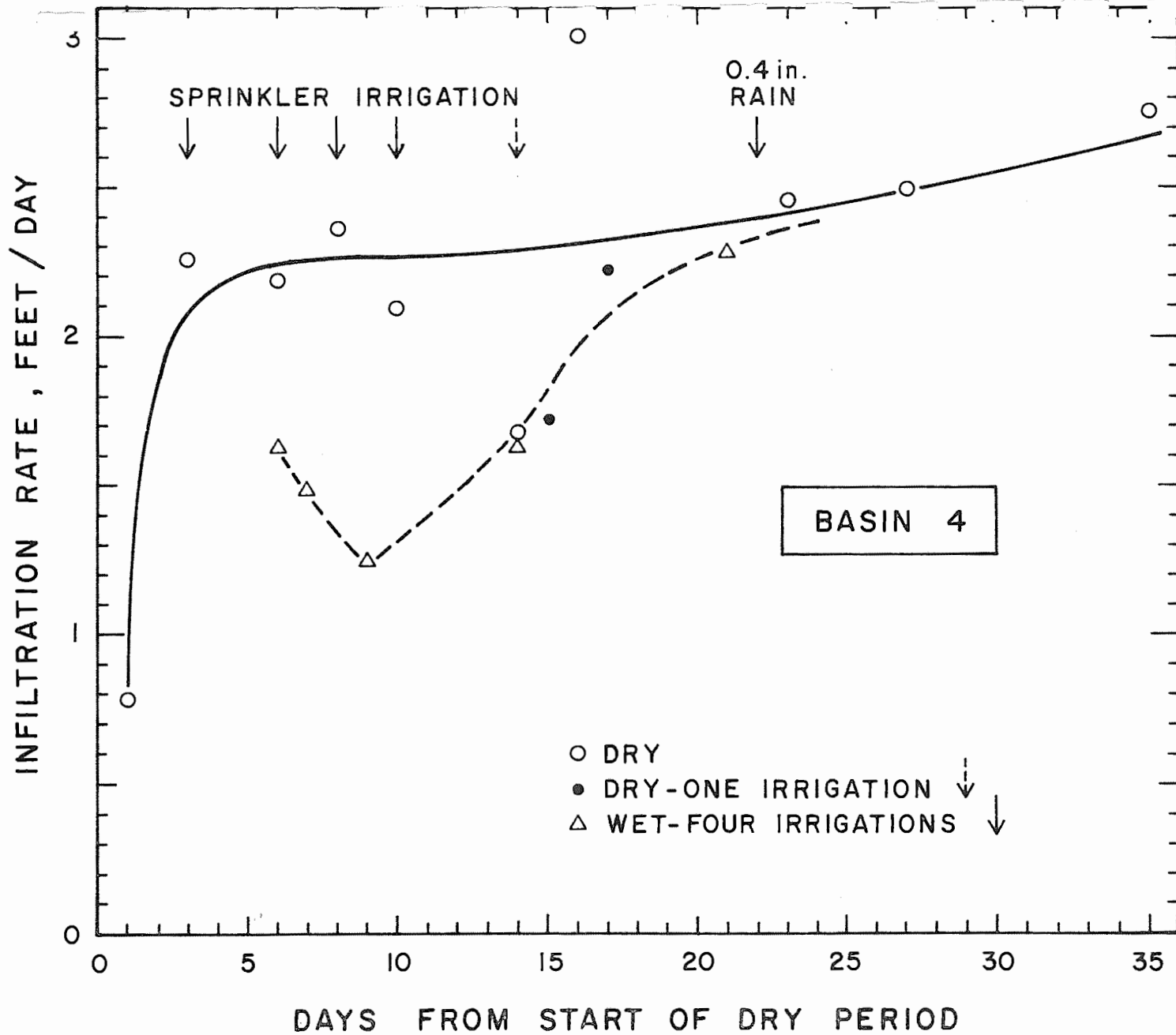


Figure 5. Effect of sprinkler irrigation during dry up on infiltration recovery in basin 4.

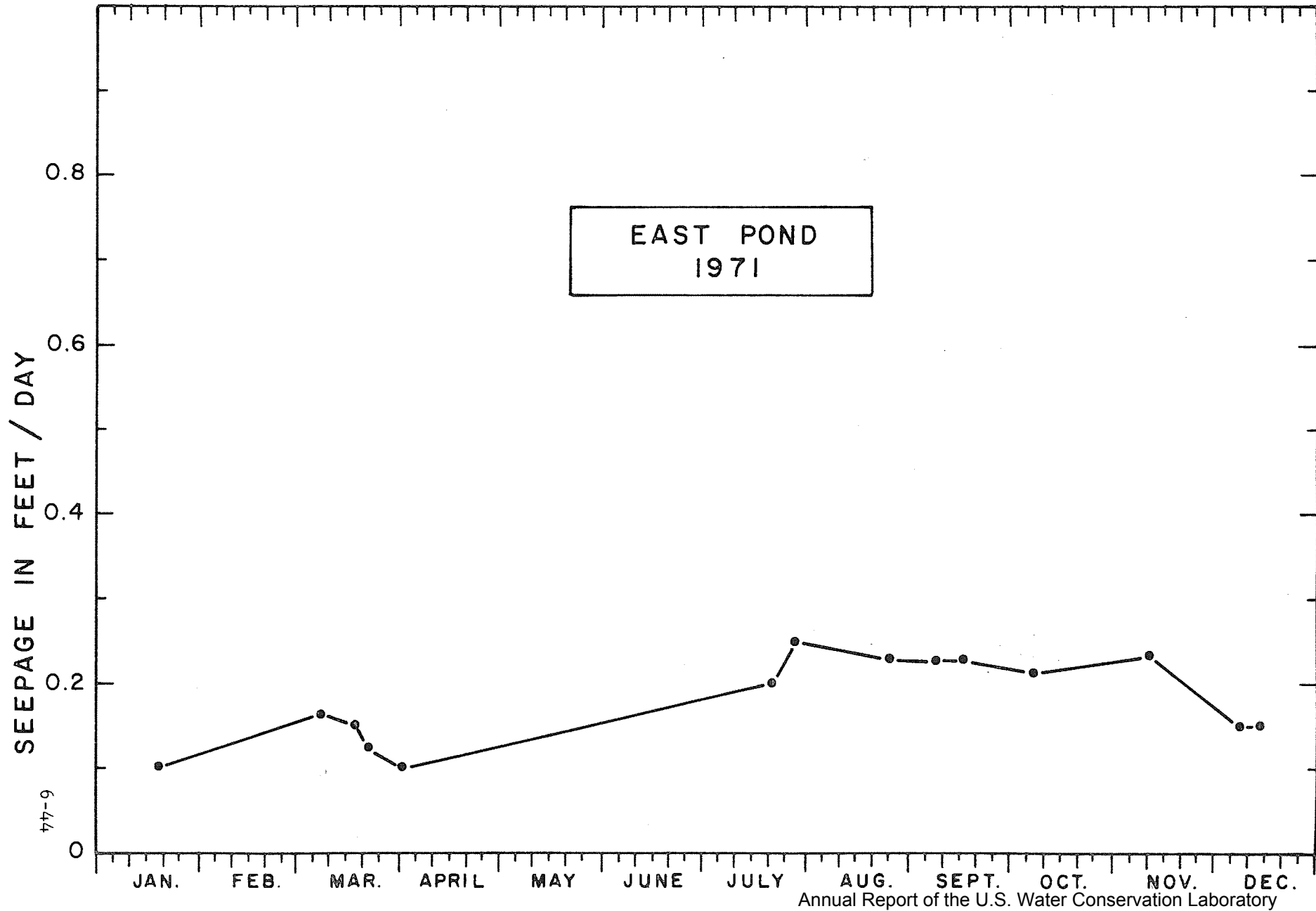


Figure 6. Seepage rates in unlined east pond.

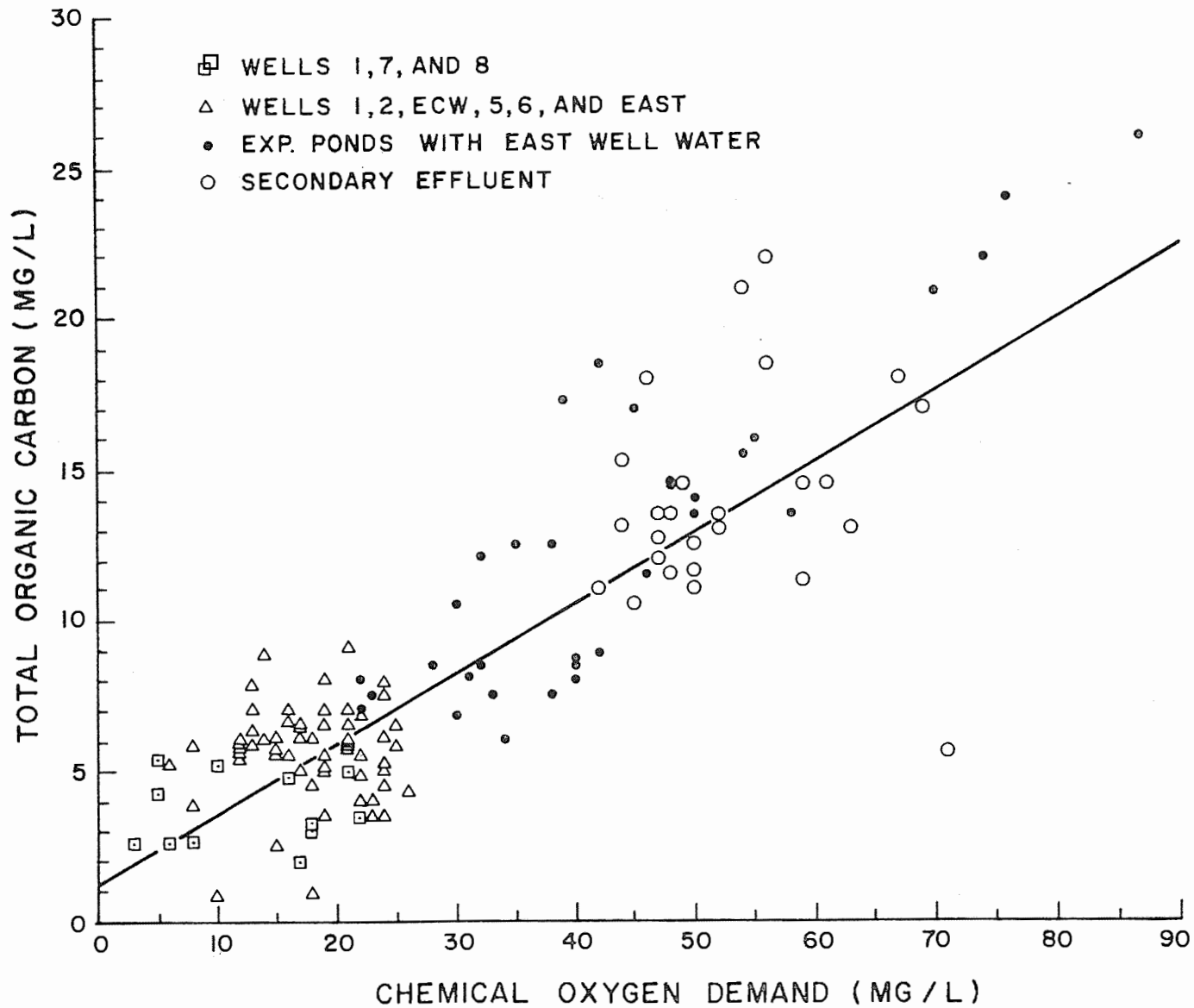


Figure 7. Relation between TOC and COD for various waters.

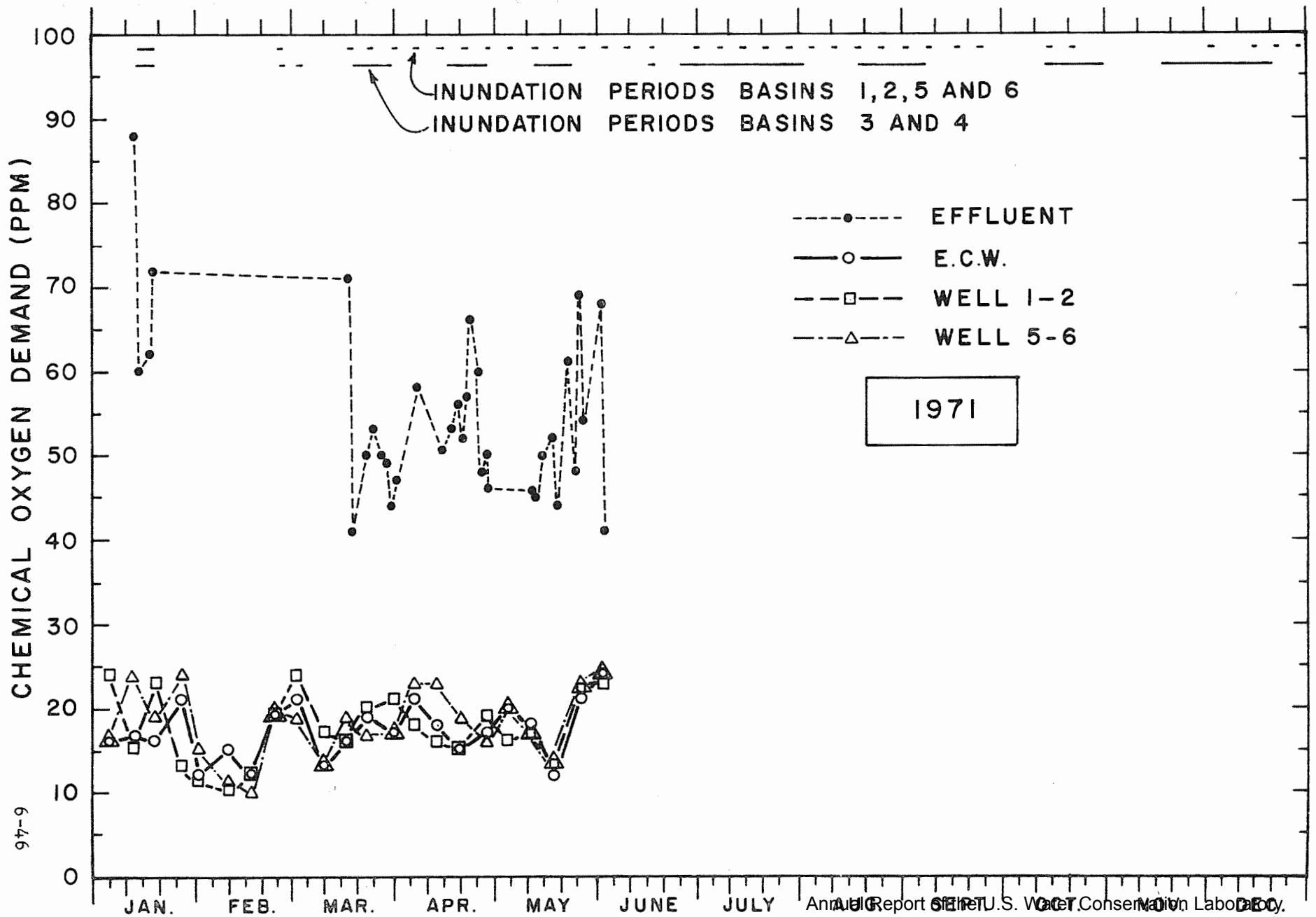


Figure 8. COD of effluent and renovated water.

TOTAL ORGANIC CARBON (PPM)

6-47

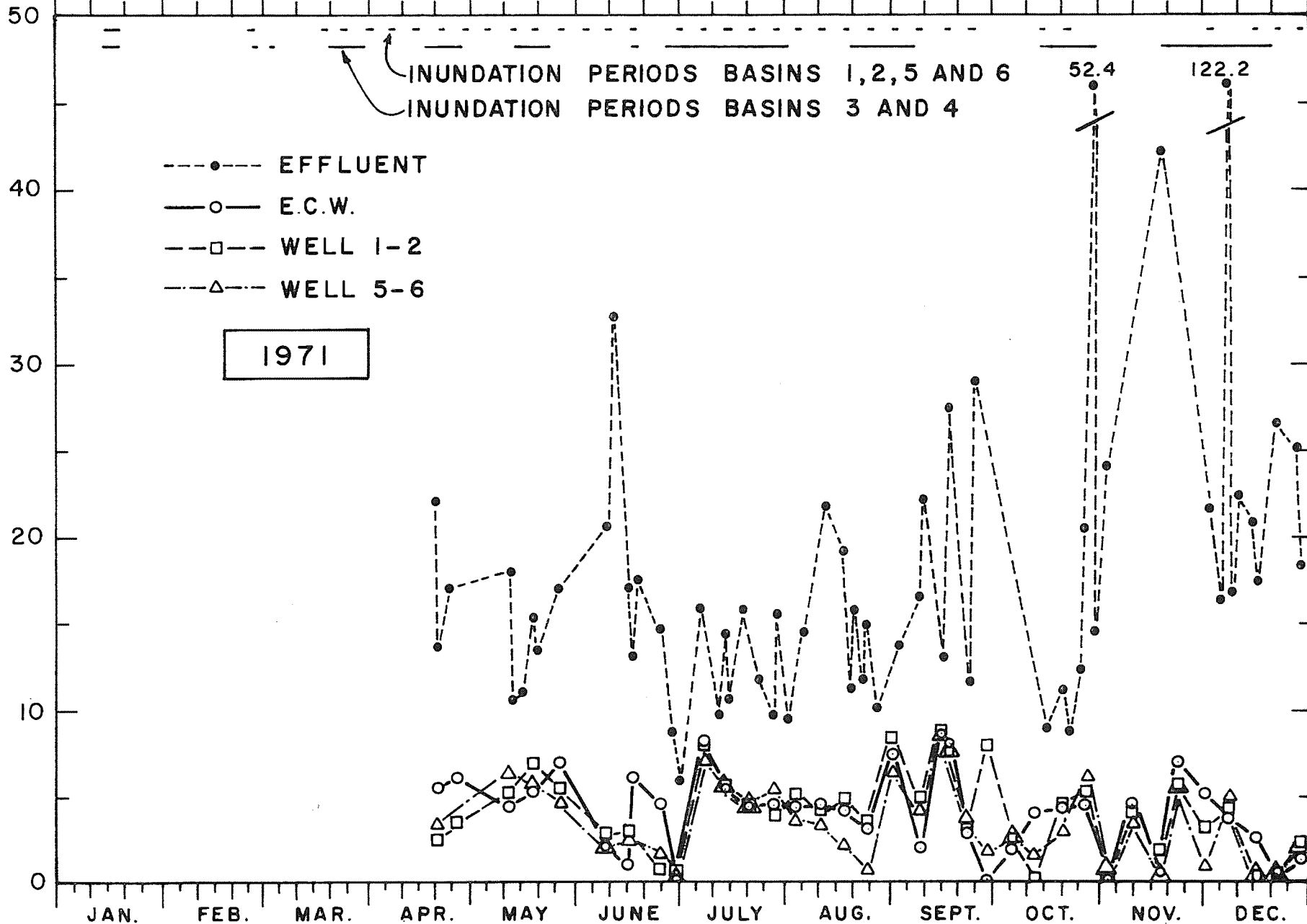


Figure 9. TOC of effluent and renovated water.

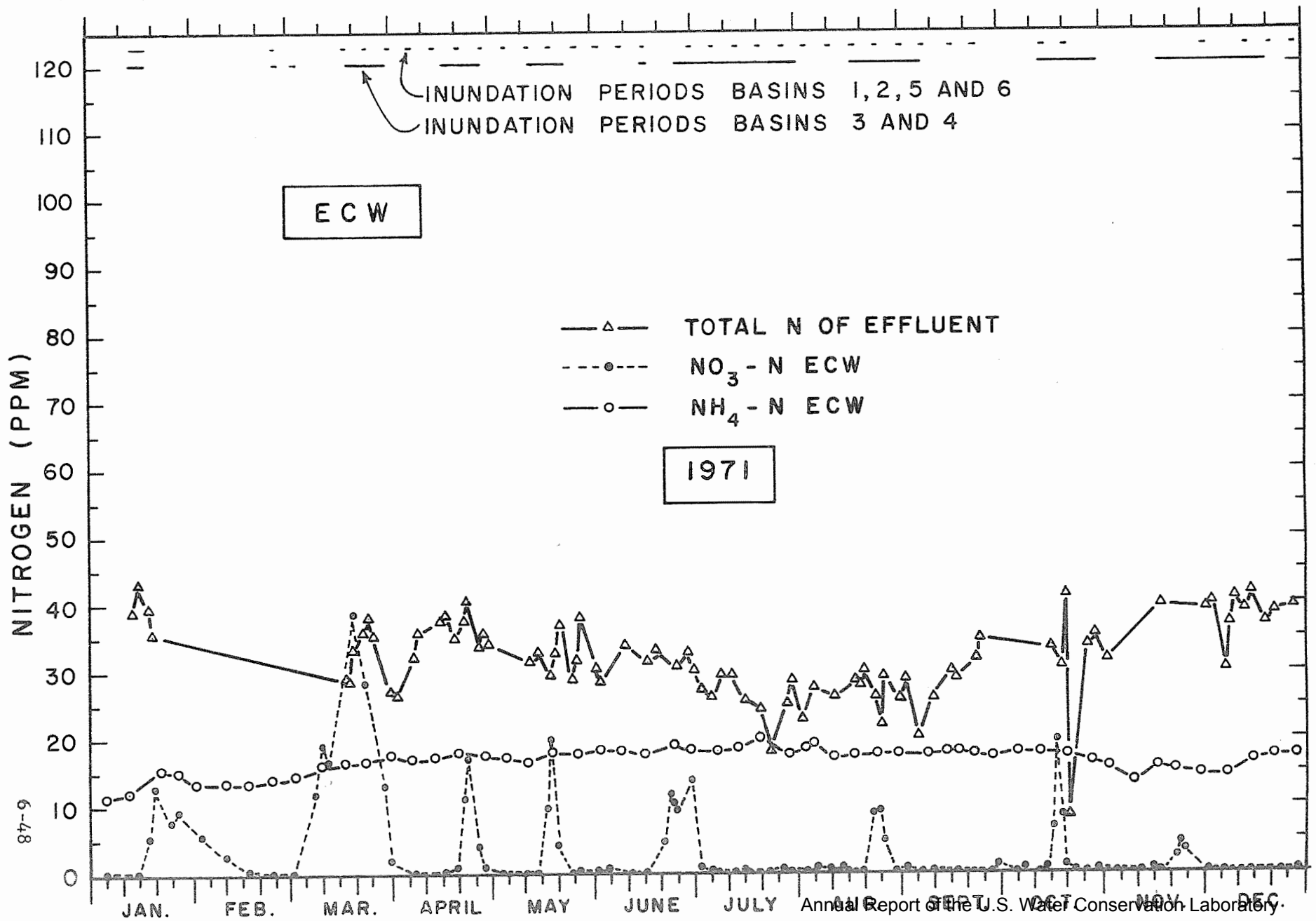


Figure 10. Total nitrogen in effluent and nitrate-N and ammonium-N in renovated water from ECW.

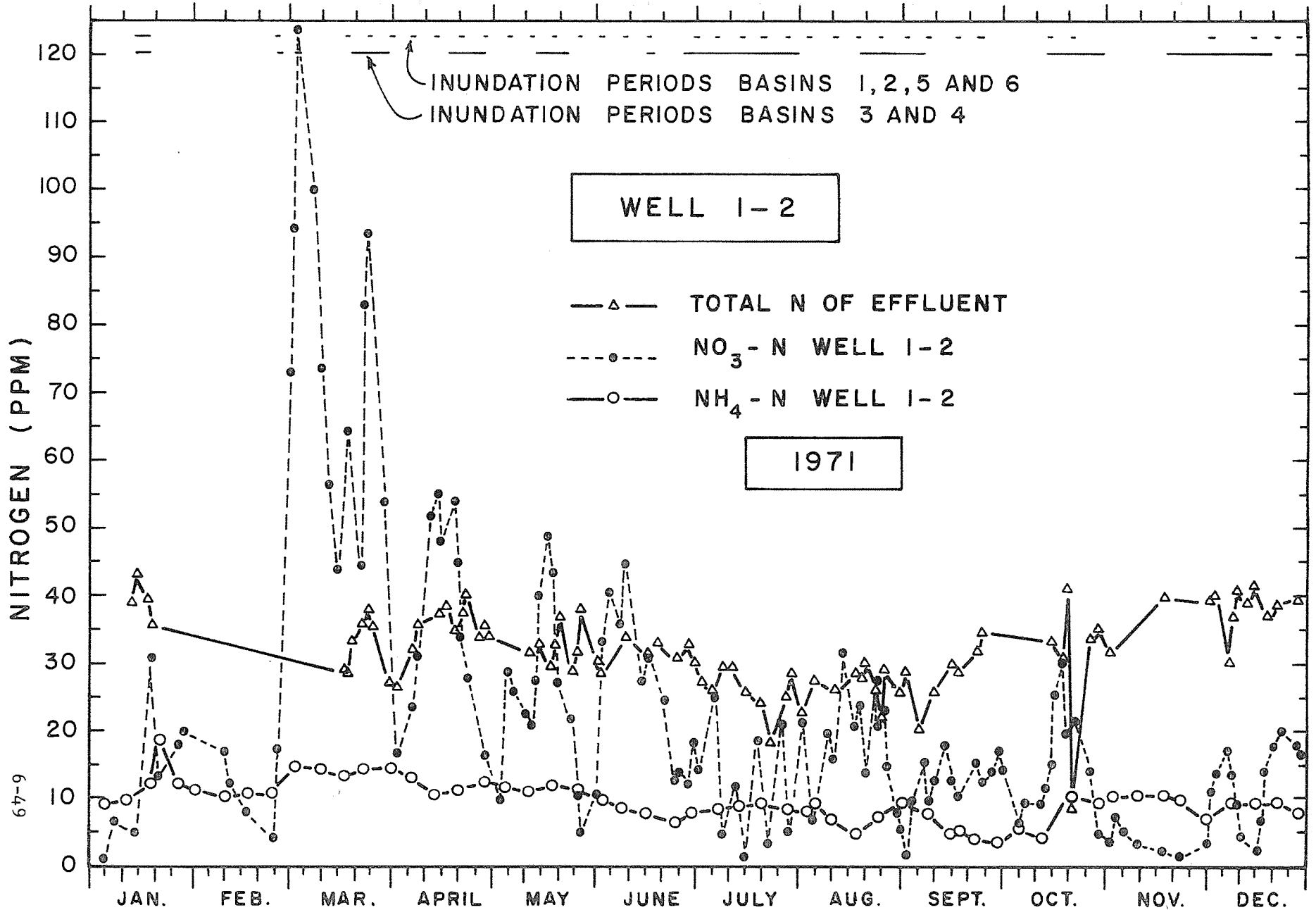


Figure 11. Total nitrogen in effluent and nitrate-N and ammonium-N in renovated water from well 1-2. Annual Report of the U.S. Water Conservation Laboratory

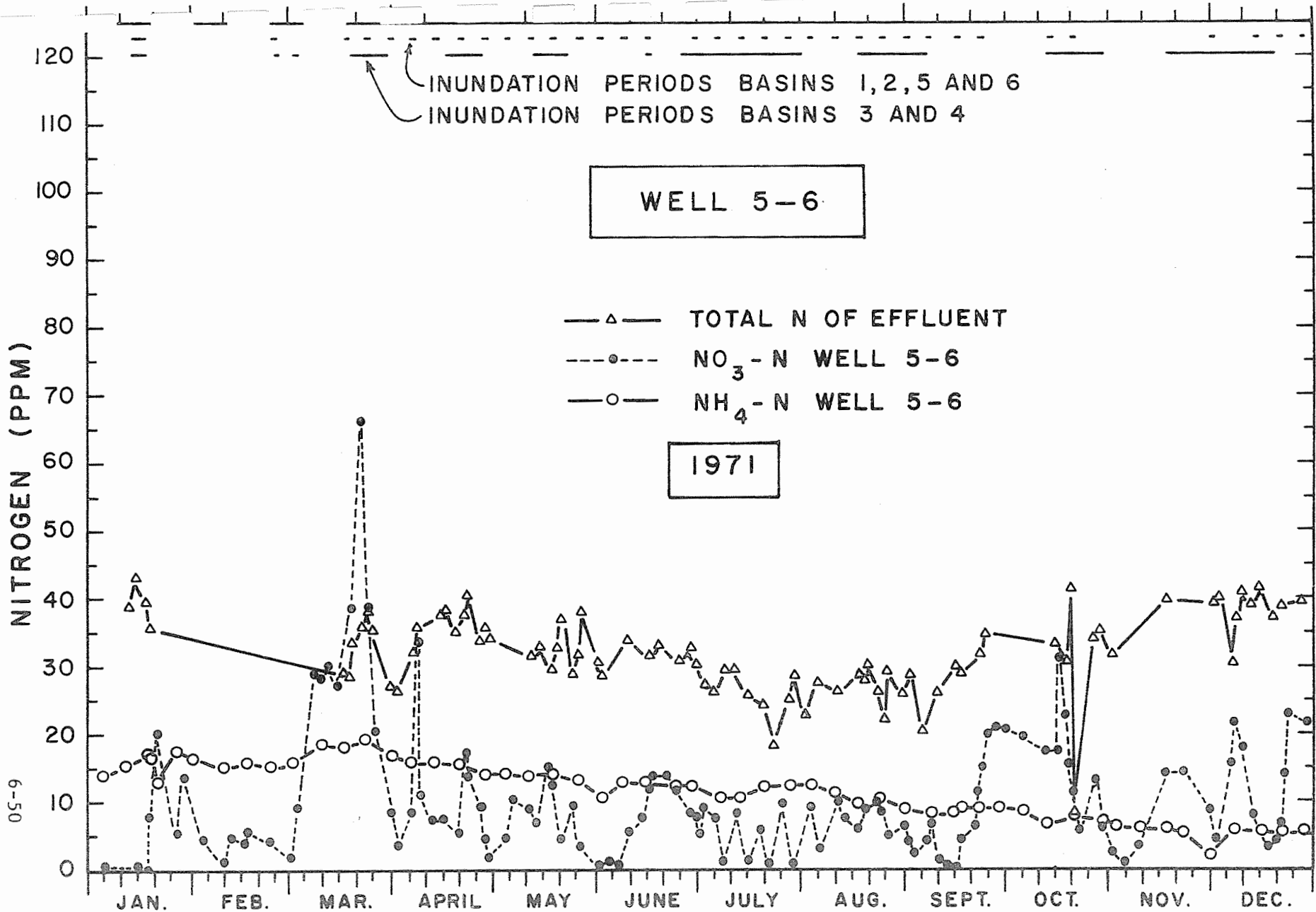


Figure 12. Total nitrogen in effluent and nitrate-N and ammonium-N in renovated water from well 5-6. Annual Report of the U.S. Water Conservation Laboratory

PHOSPHATE PHOSPHORUS (PPM)

---●--- EFFLUENT  
—○— E.C.W.  
---□--- WELL 1-2  
---△--- WELL 5-6

1971

20  
10  
0

JAN. FEB. MAR. APR. MAY JUNE JULY AUG. SEPT. OCT. NOV. DEC.

15-51

Figure 13. Phosphate-P concentrations in effluent and renovated water from ECW and wells 1-2 and 5-6.

Annual Report of the U.S. Water Conservation Laboratory

PHOSPHATE PHOSPHORUS (PPM)

---○--- EFFLUENT  
—○— WELL 1  
---□--- WELL 7  
---△--- WELL 8

1971

6-52

20

10

0

JAN. FEB. MAR. APR. MAY JUNE JULY AUG. SEPT. OCT. NOV. DEC.

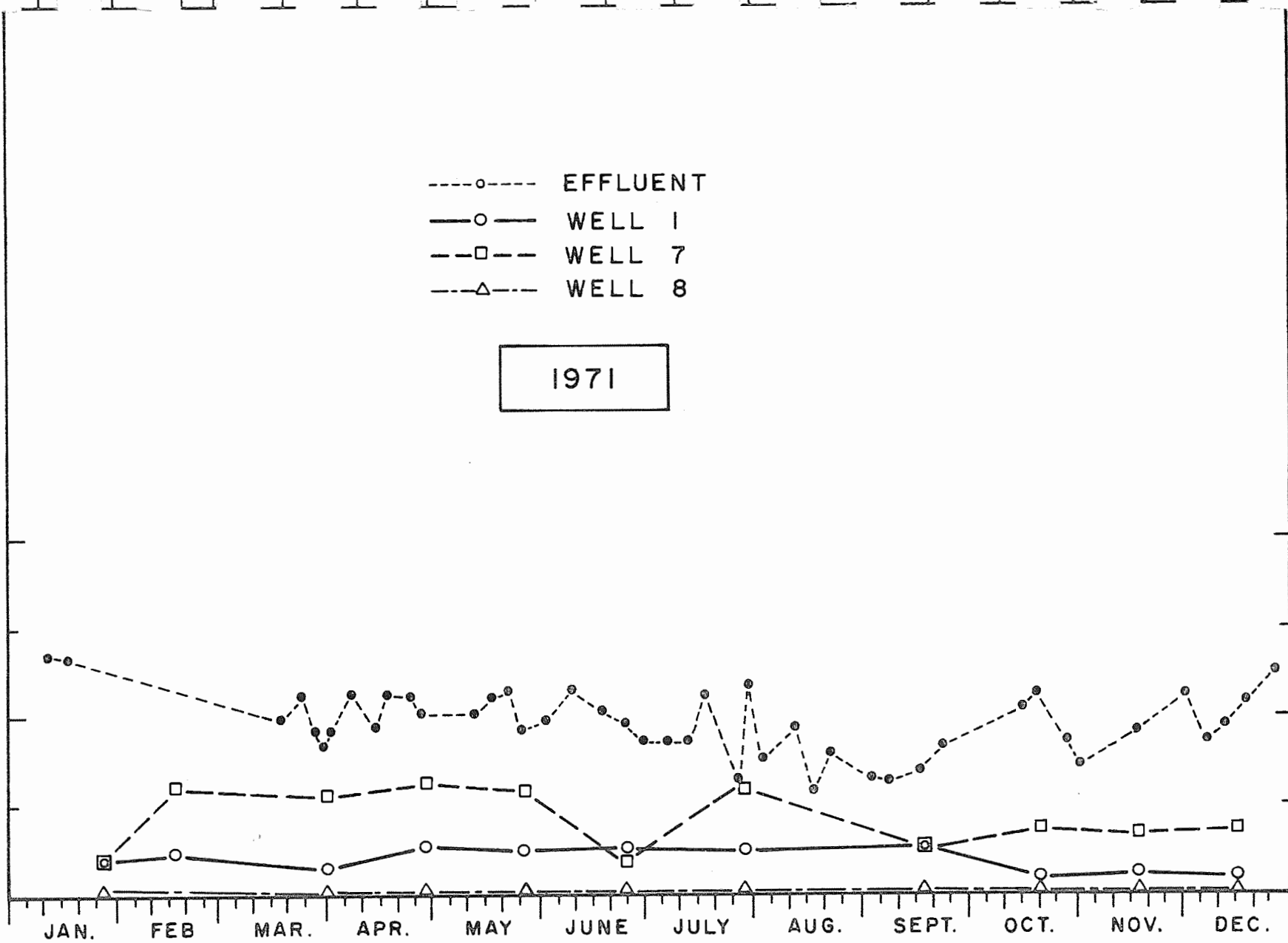


Figure 14. Phosphate-P concentrations in effluent and renovated water from wells 1, 7, and 8.

NO<sub>3</sub>-N, PPM

SALT CONCENTRATION, PPM

WEST CENTER WELL  
1971

ES-9

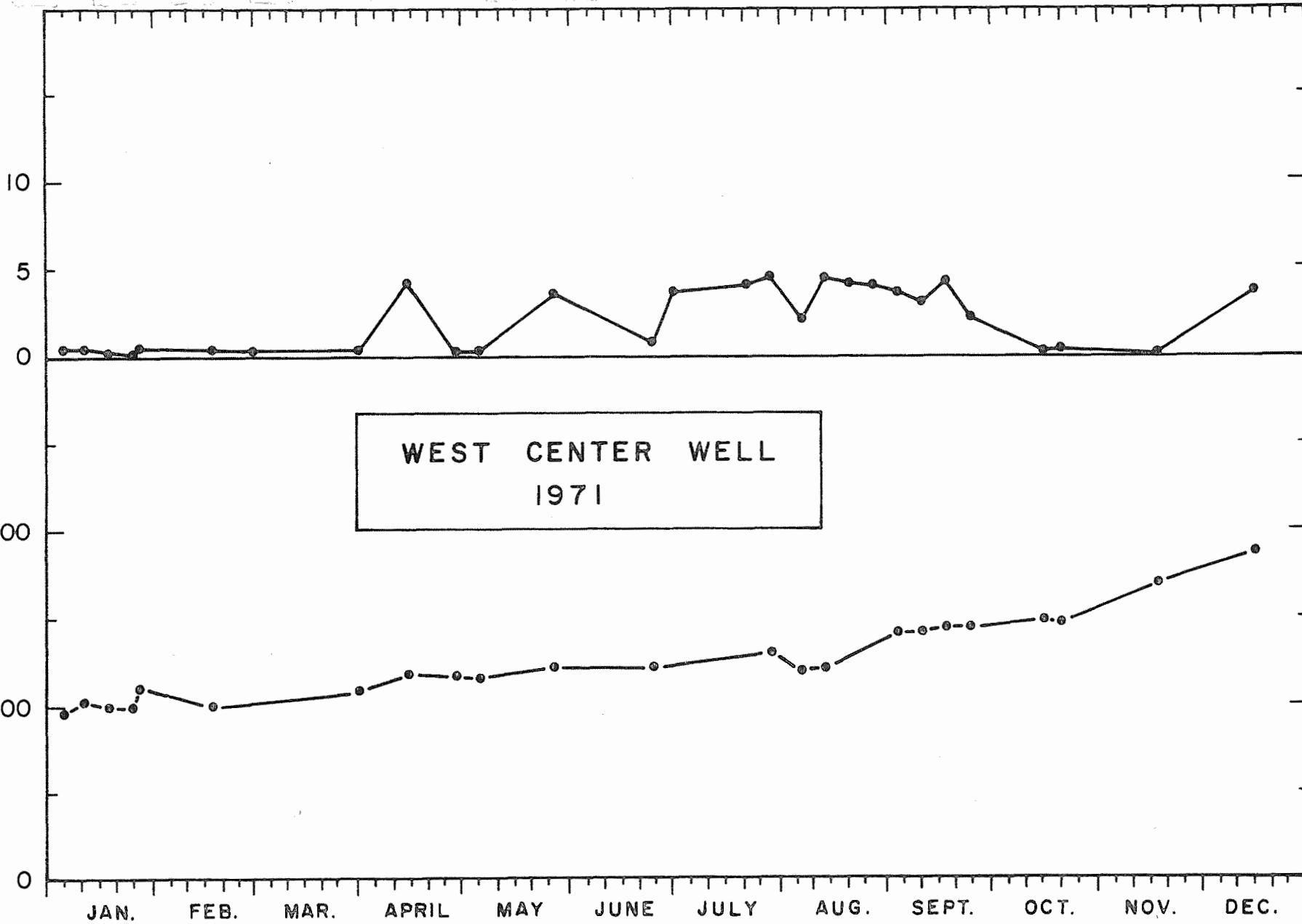


Figure 15. Total salts and nitrate-N concentrations in water from WCW. Annual Report of the U.S. Water Conservation Laboratory

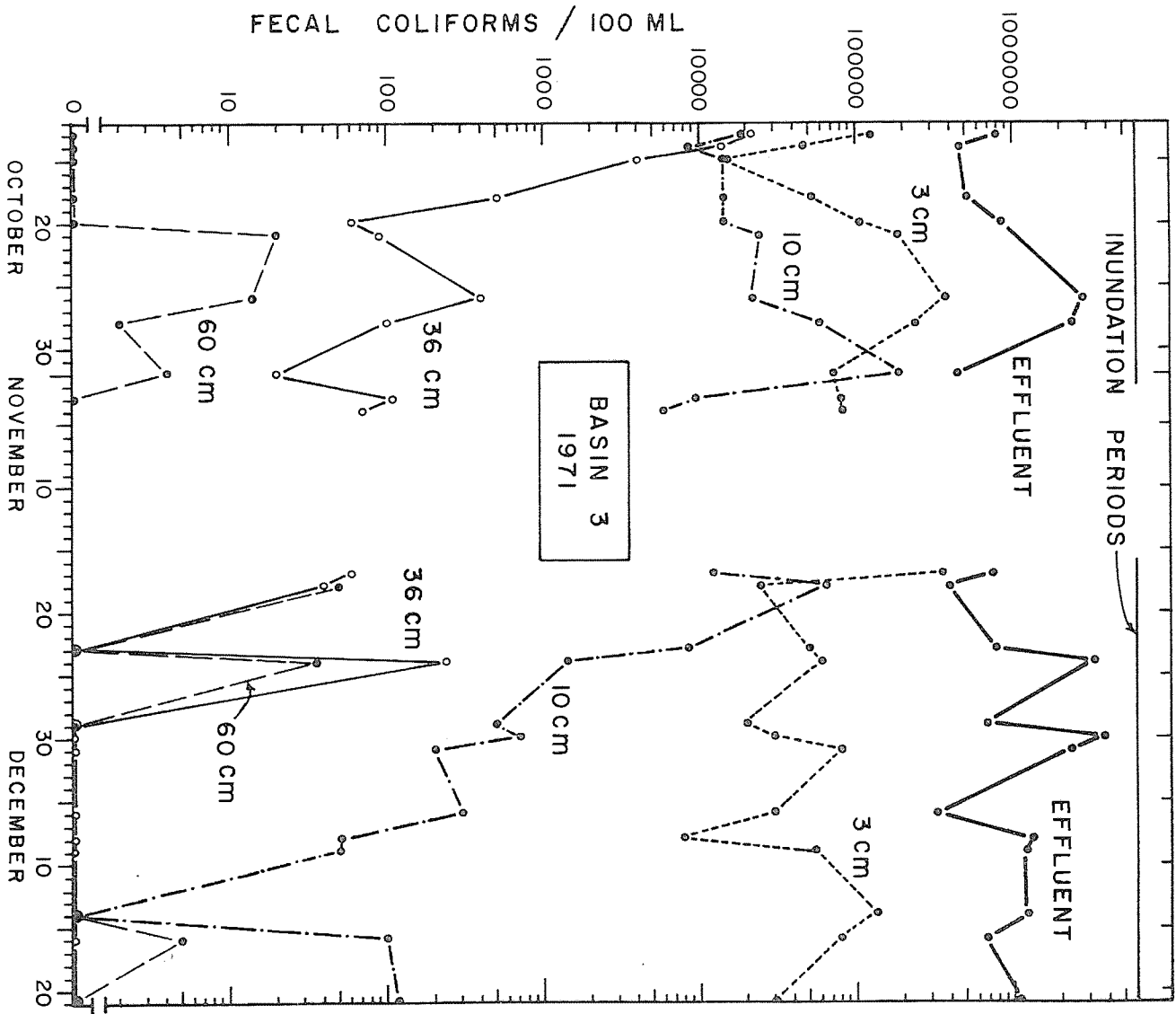


Figure 16. Fecal coliform densities in effluent and water from ceramic cups at different depths.

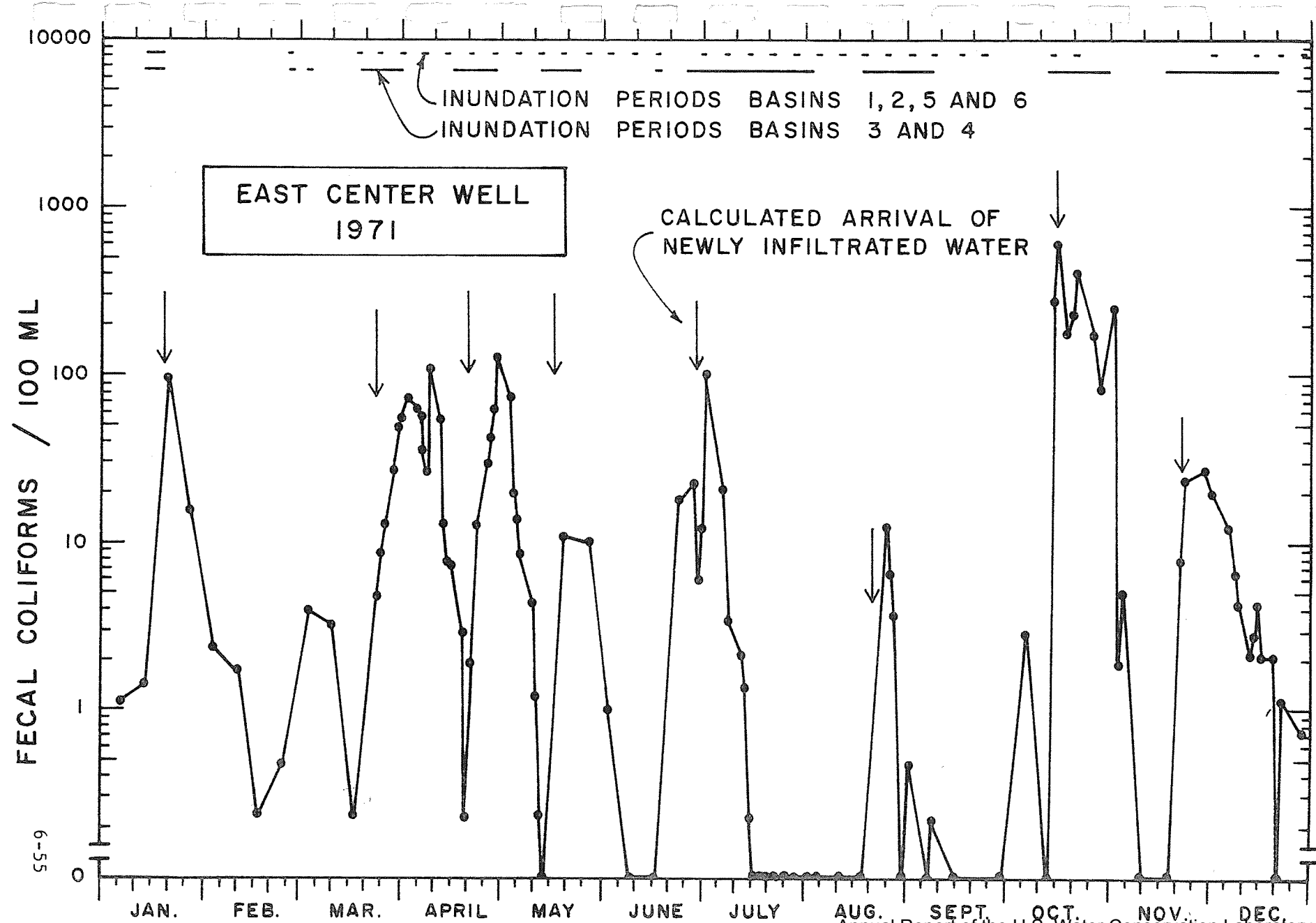


Figure 17. Fecal coliform densities in renovated water from ECW. Annual Report of the U.S. Water Conservation Laboratory

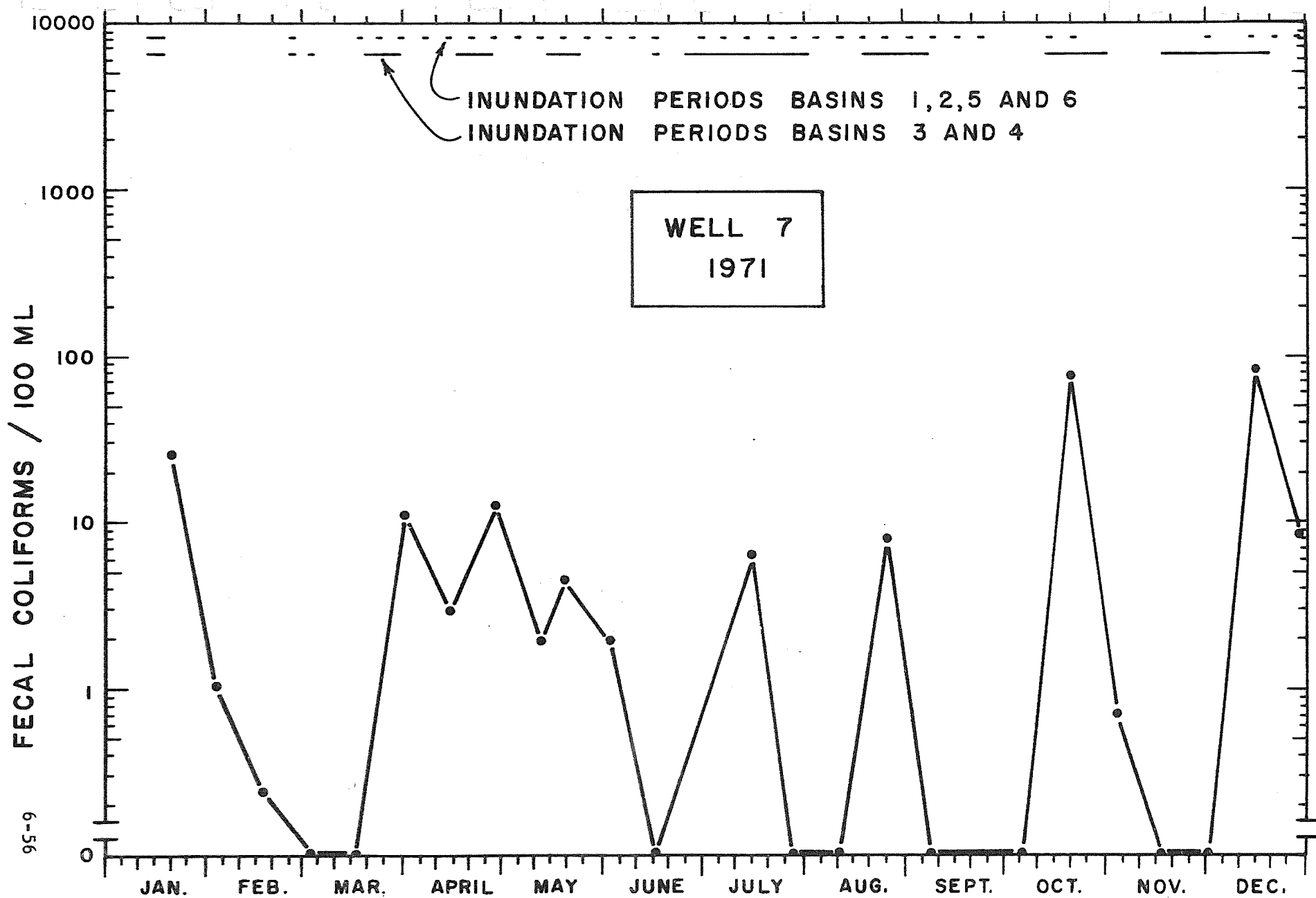


Figure 18. Fecal coliform densities in renovated water from well 7. Annual Report of the U.S. Water Conservation Laboratory

95-9

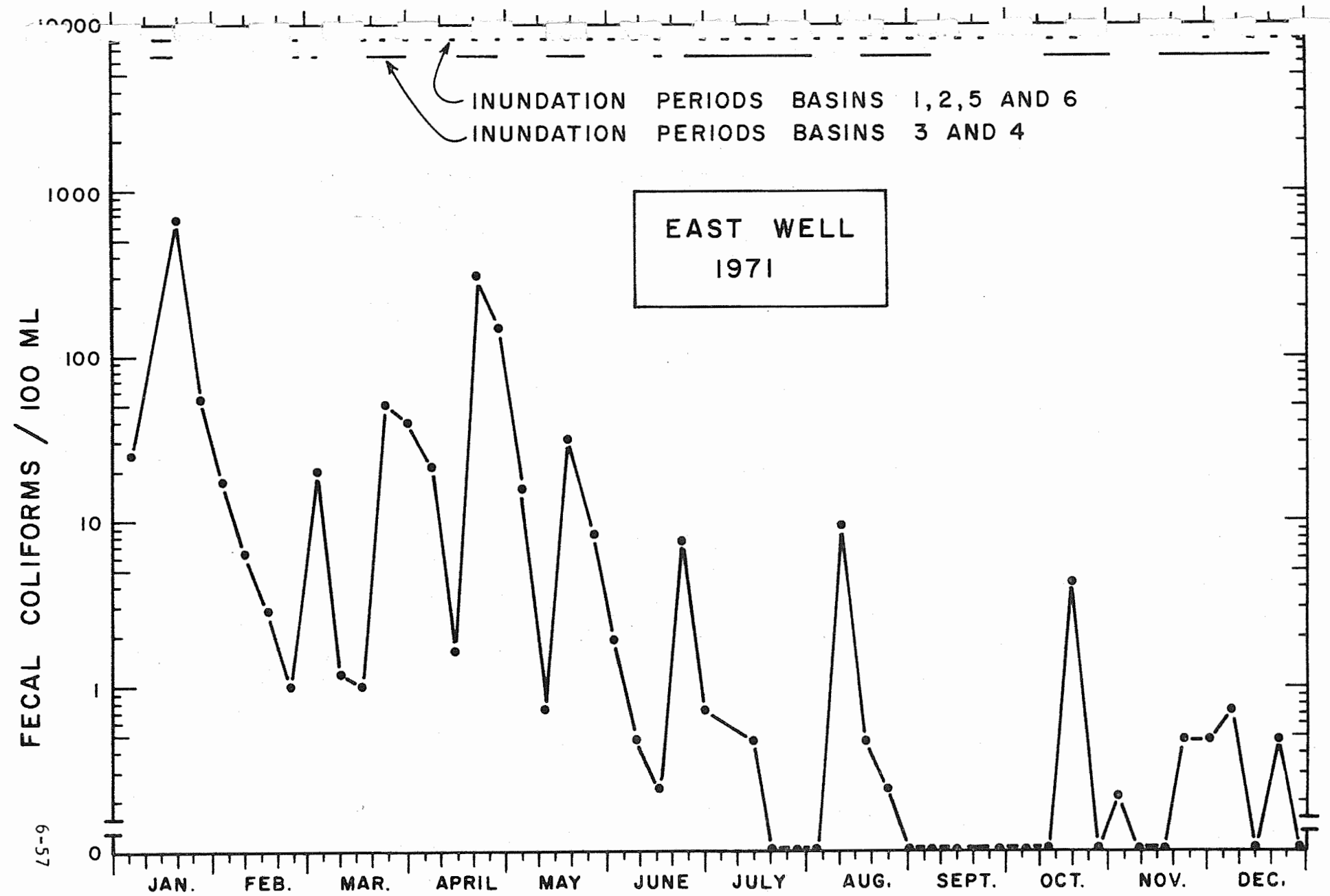
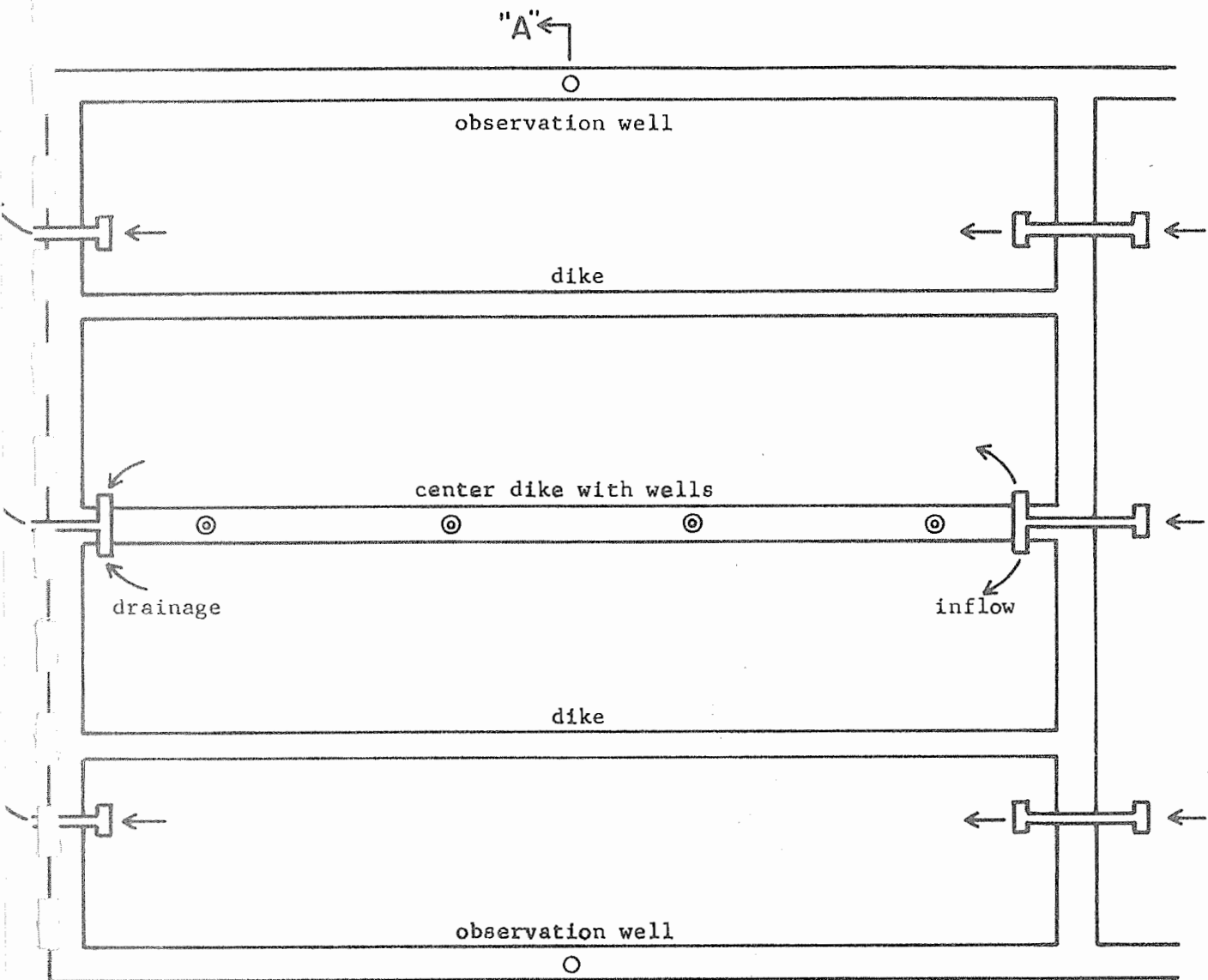


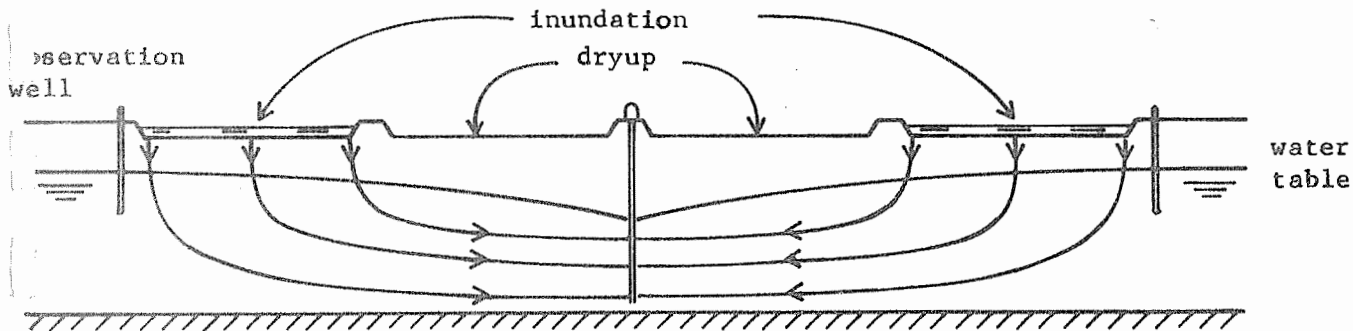
Figure 19. Fecal coliform densities in renovated water. Annual Report of the U.S. Water Conservation Laboratory



"A" ←  
PLAN

0 500 feet

A horizontal scale bar with tick marks, labeled "0" at the left end and "500 feet" at the right end.



CROSS SECTION "A-A"

Figure 20. Schematic of 23rd Avenue Project.

TITLE: EVAPORATION OF WATER FROM SOIL

CRIS WORK UNIT: SWC-018-gG-4

CODE NO.: Ariz.-WCL-68-1

INTRODUCTION:

The objective and need for the research documented in this outline appears in the USWCL 1969 Annual Report. A field experiment was conducted during 1970 in which soil-water content and soil temperatures were measured as a function of depth and time under high evaporating conditions. A brief description of this experiment was presented in the 1970 Annual Report. In March 1971 a similar, but more detailed experiment was conducted. Concurrently, an experiment was initiated by Dr. K. K. Watson, visiting scientist from Australia, to measure quantitatively the hydraulic conductivity profile at the field experiment site. This experiment utilized numerous pressure transducers for pressure potential measurements and the gamma-ray transmission apparatus, described in the 1969 and 1970 Annual Reports, to measure water content profiles. These data have not yet been analyzed. The following report presents a general overview of the two evaporation experiments and a description of some results. Additional data analysis is currently underway.

In a natural environment, the soil surface undergoes tremendous diurnal changes in water content and temperature. Atmospheric conditions such as radiation, windspeed, air temperature and humidity, and other factors influence the physical conditions of the soil surface and determine the course of evaporation. The rate of water movement to the surface at a particular time is determined by the ability of the soil to conduct water, the evaporative demand at the surface, the temperature of the soil-water system, and the temperature gradients acting upon the water at the time. These various factors change with time. Some, notably the temperature and temperature gradient, change markedly during the course of a day. At night the temperature gradient causes water to move towards the surface, while during the day it acts to oppose upward flow caused by water content gradients. These complex interactions are only

superficially understood. Classical theories of soil-water movement have, for the most part, ignored the effects of temperature and temperature gradients. During the past two decades the theories of simultaneous movement of heat and water and the thermodynamics of irreversible processes have been applied with some success to the movement of soil-water in nonisothermal systems. For the most part, tests of these theories have been restricted to the laboratory.

A currently held hypothesis concerning the drying of soil is that, if a moist soil is exposed to initially high evaporative conditions, the dry layer that rapidly forms will reduce subsequent evaporation and the cumulative evaporation may in the long run be less than that for a soil initially exposed to low evaporative conditions. This hypothesis has been confirmed in the laboratory, but has not been demonstrated to hold under field conditions.

It has long been recognized that any means of reducing evaporative losses of water from soil must somehow alter the mechanisms of water movement in the surface zone. From studies concerning these mechanisms the concept of three stages of drying emerged. These stages are: (1) When the soil is sufficiently moist, evaporation is determined solely by atmospheric conditions; (2) At intermediate water contents the ability of the soil to conduct water is the limiting factor, with atmospheric conditions no longer as important; (3) The third stage is characterized by extremely slow water movement and is dominated by adsorptive forces acting over molecular distances at the solid-liquid interfaces in the soil.

In the laboratory experiments a distinct break in the evaporation-water content curves delineated the change from the first to the second stage. The change from the second to the third stages was gradual. Generally, evaporation versus time plots for field soils do not show distinct breaks. Evaporation data from this laboratory for one soil for several seasons of the year indicate that the three stages of drying could not be definitely delineated.

Further clarification of the evaporation process and tests of the various theories rests upon obtaining data from measurement of the pertinent parameters in the field under naturally varying environmental conditions. This report presents an overview of two field experiments, carried out during two different seasons, in which soil water content profiles were measured at half-hourly and hourly intervals for periods of 1-2 weeks after irrigation. Concurrently, evaporation rates, soil temperatures and pertinent meteorological parameters were measured. The main emphasis to date concerns diurnal soil water content changes, soil water content profiles, soil water flux at several depths and times, as related to the evaporation process. Analysis currently underway involve diurnal salt movement and the effect of meteorological conditions on soil water movement.

#### EXPERIMENTAL PROCEDURES:

Two experiments were conducted. The first was from 10-17 July 1970. This experiment was briefly described in the 1970 Annual Report. Some information is repeated here in order to compare the results from two different seasons of the year. Ten cm of water was applied to the field and lysimeters on the afternoon of 10 July. The meteorological conditions during these seven days were characterized by clear skies and light winds. There was an exception from 0330 to 0600 on 16 July when winds were gusty. Maximum and minimum air temperatures ranged from 40 to 44 C and 17 to 30 C respectively.

The second, and more extensive experiment, was conducted during March and April, 1971. On the afternoon of 2 March the field was irrigated with 10 cm of water. Soil-water content measurements were made from 5 to 18 March, 25 March and 8 April. Generally, skies were clear and winds were light. Maximum and minimum air temperatures ranged from 17 to 24 C and -2 to 5 C, respectively. High winds and mostly cloudy skies prevailed on 5 and 13 March.

Field Site and Lysimeters. The experimental site was a 72 x 90-m field at the U.S. Water Conservation Laboratory. Three weighing

lysimeters are located within the field. The soil, Adelanto loam, is reasonably uniform to about 100 cm and has been cultivated numerous times during past years. Prior to the experiments to be described here the field was disked, leveled, and divided into three plots, each plot surrounding a lysimeter. At the start of both experiments the lysimeters and the borders were irrigated with 10 cm of water. After irrigation the lysimeter weight loss, and hence evaporation, was monitored at half-hourly intervals throughout the experiment.

Measurement of Soil-Water Content. Soil-water contents were measured gravimetrically. In July, soil cores were taken to 10 cm and sectioned into 1 cm increments. Five sites were sampled and the depth increments composited. A separate sample was taken for the 0-.5 increment. Samples were taken at hourly intervals from 0500 11 July to 2200 17 July.

During March 1971 samples were taken of the 0-.5 cm increment and in 1 cm increments to 5 cm and 2 cm increments from 5 to 9 cm. Samples were taken at half-hourly intervals from 2300 4 March 1971 to 0130 19 March 1971, 2300 24 March to 0130 26 March and 2300 7 April to 0130 9 April. Six sites were sampled each time and composited for each depth increment. In both experiments the time between the beginning of sampling until the samples were weighed and placed in the oven (at 110 C) was less than 15 minutes.

Errors inherent in the gravimetric measurement of soil water content arise from site differences, sectioning of cores, weighing and recording data. Site differences and sectioning errors were minimized by compositing samples from six sites. All weighings were made to 0.01 g on a direct reading balance. To reduce scatter the water content data were smoothed by a 1-2-3-2-1 weighted running average procedure. This method proved to be quite satisfactory. A sample of the original and smoothed data are presented in the Results section. All water contents were converted to the volumetric basis by multiplying by the bulk density.

Auxiliary Measurements. In addition to evaporation and soil water content, soil temperature profiles and various meteorological parameters were measured. During July thermocouples were placed at the soil surface, and at 1, 2, 4, 8, 16, 32, 64 and 128 cm depths. In March these depths and temperatures at depths 0.5, 3, 5 cm were measured.

The meteorological parameters measured were, solar and net radiation, reflected solar radiation, windspeed at several heights above the surface, and vapor pressure and air temperature at two heights above the soil. All meteorological data and soil temperatures were recorded on punched paper tape by a data acquisition system.

Physical Data for Adelanto Loam. A discussion of the results of these experiments require a knowledge of several physical parameters of Adelanto loam, namely, the water characteristic, the vapor pressure isotherm, the hydraulic conductivity and the soil-water diffusivity. Data from both laboratory and field measurements of these parameters have been collected for Adelanto loam during the past decade.

Figure 1 represents the water characteristic for Adelanto loam. These data were taken in the same experimental field as the current experiments except at 20 cm depth. Data for pressures less than -15 bars and the graph of relative humidity versus water content (Figure 2) were measured in the laboratory. From the water characteristic of Figure 1 the hydraulic conductivity was calculated and is shown in Figure 3. The matching factor was obtained from saturated hydraulic conductivity data obtained in the experimental field. From the hydraulic conductivity and water characteristic data, soil-water diffusivities were calculated, and are represented by the straight line in Figure 4. The symbols in the figure represent laboratory measured vapor diffusion coefficients. The dotted line indicates the sum of the liquid and vapor diffusivities.

## RESULTS AND DISCUSSION:

Diurnal Soil-Water Content Changes. Figure 5 depicts the soil-water content in the 0-0.5 cm layer at half-hourly intervals during March 1971. These data show the wide range of water contents encountered in this layer during the course of a day. A 50% reduction in water content occurred between 0600 and 1400 on 7 March. Following a recovery of volumetric water content from .097 to .19 during the night, a rapid drying of this layer again occurred. This pattern was exhibited by the 0-.5 layer for all days of measurement. In the figure the up arrows indicate the time of sunrise and the down arrows indicate sunset. Water loss began about 1-2 hours before sunrise and rewetting began about 2-4 hours before sunset.

Figure 5 serves to show the results of the smoothing procedure. The circles represent the measured volumetric water content (obtained from multiplying the measured gravimetric data by the bulk density), whereas the solid line connects the points calculated by the smoothing procedure. Only smoothed data will be presented in subsequent figures.

The amplitude of the diurnal water content changes decreases with depth as shown in Figure 6. Five days' data are presented to show the differences in diurnal patterns as the soil dried. For day 3 after irrigation, water contents are shown for three depths. Data for the other 5 increments lay in between the extremes shown. In the 0-.5 cm increment the water content was .35 before sunrise and decreased to .24 at sunset. Recovery began at sunset and increased to .295 the following morning (data for day 4 are not shown). At the 7-9 cm depth the water content decreases from .305 to .275 during the day, but showed only a small recovery at night. During this period water was being evaporated from the surface and was also draining to deeper depths. However, data in a subsequent figure will show that the net 24-hour flux at 9 cm for day 3 was upward towards the surface.

By day 9 (11 March 1971) the water content in the 0-.5 cm layer has decreased considerably, exhibiting a range of .093-.038 with the maximum occurring near sunrise and the minimum about 2 hours before sunset. The diurnal change is evident, but with decreasing amplitude, for every measurement day, including the 37th and final day of the experiment.

The lines for 0.5 to 1 cm were calculated from the data for 0-.5 and 0-1 cm increments. Errors in measurement at the two depths, not removed in smoothing, can be magnified in the calculation. Nevertheless, the calculated lines correspond very well with the other data. The minimum water content for the 0.5-1 cm layer lagged behind that of the 0-0.5 cm layer for four of the days shown in Figure 5. For day 9 the minimum was near sunset, about 2 hours later than the minimum for 0-0.5 cm. On subsequent days the minimum occurs earlier and at day 37 occurs at nearly the same time as for the 0-0.5 layer. No time lags were evident on day 3.

The amplitude of the diurnal fluctuation decreased with depth, and with time. On day 9 the 1-2 cm layer dried during the afternoon and rewet at night, whereas at deeper depths fluctuations occurred at various times during the day. However, the deeper layers exhibited a net decrease in water content from midnight to midnight. The range in water contents at the 7-9 cm layer was 0.008 on day 9, compared to 0.03 on day 3.

Mechanisms of Water Flow. Figure 4 shows the calculated liquid diffusivities and the measured and estimated vapor diffusivities for Adelanto loam. Vapor diffusion evidently is the predominant water transfer mechanism below 0.10 water content. The range 0.10 and 0.15 water content is a transition stage within which the mechanism changes from vapor to liquid.

The water content for the 0-0.5 cm layer changes from about 0.235 to 0.10 in about 8 hours on day 5 (Figure 5). The corresponding diffusivity decreased by a factor of about 30 (Figure 4). The hydraulic conductivity change was greater than four orders of

magnitude for this water content change (Figure 3).

From Figure 4 and 5 it is evident that the water transfer mechanism went from predominantly liquid flow, through the intermediate zone to predominantly vapor and back to predominantly liquid flow in the course of a 24-hour period. By day 7 the mechanisms were intermediate to predominantly vapor.

In Figure 6, for day 3, the water moved in the liquid phase at all depths. By day 9 vapor diffusion was the major mechanism in the 0-.5 and .5-1 layers, while liquid flow predominates below 1 cm. On days 16 and 23 liquid flow predominated only below 3 and 5 cm respectively. By day 37 vapor diffusion predominated in the entire 0-9 cm layer.

The above statements are based on the classical concepts of isothermal soil-water diffusivity. A quantitative examination of flow mechanisms in this system, utilizing the theory of simultaneous transfer of heat and water is underway. It is anticipated that information on liquid, vapor, and temperature induced flow mechanisms, and the associated coefficients will be obtained.

Soil-Water Flux. The diurnal changes in soil-water content are a consequence of the evaporative loss of water to the atmosphere. Evaporation rates vary with the season of the year and hence water content and flux profiles within the surface zone should be different for the different seasons. In this and the following section evaporation rates, cumulative evaporation, water content and flux profiles are compared for two seasons.

The evaporation rate ( $\text{cm day}^{-1}$ ) for the July 1970 and March 1971 experiments are presented in Figure 7. Also shown are the soil water flux data at the 9 cm depth. The flux at 9 cm was calculated from the flux at the surface (obtained from the lysimeters) and the water content changes in the 0-9 cm layer. For both experiments the flux per 24 hours at 9 cm was upward towards the evaporating surface. For day 11 (13 March) the flux at 9 cm was almost equal to the evaporation rate at the surface. This indicates essentially no net

loss of water from the 0-9 cm layer for this day. Day 11 was characterized by high gusty winds during the afternoon and evening. The average windspeed for the 24-hour period was more than twice that of the surrounding days. For the July experiment, the flux at 9 cm was almost equal to the evaporation rate on day 6. Between 0300 and 0600 hours high, gusty winds prevailed. In both cases the water contents of the surface few cm's were in the range within which vapor diffusion predominates. Thus, the soil should have been well within the second, if not the third stage of drying. This point is being currently investigated in more detail. However, it is evident that atmospheric conditions can markedly influence soil drying even when the soil has a dry surface layer.

As the 0-9 layer dried further the flux at 9 cm approached the evaporation rate. On day 23 they were nearly equal, while on day 37 the flux at 9 cm was actually higher than at the surface. Of course, this latter condition would usually not hold for additional days, since the soil continues to dry.

Figure 8 shows the cumulative water loss at the surface and the cumulative flux at 9 cm. More water was lost from the entire soil profile during seven days in July than were lost during sixteen days in March. Also more water was lost from the 0-9 cm layer during the seven July days than sixteen March days. On day 1 of the July experiment more water was lost in the 0-9 cm layer than was evaporated, indicating drainage below 9 cm for the time immediately following irrigation.

At the end of 7 days in July, 69% of the total water evaporated originated in the 0-9 cm layer. After 16 days in March 66% came from the 0-9 cm layer.

Soil Water Content and Flux Profiles. In Figure 7 it can be seen that the evaporation rates on day 4 for the July and March experiments were nearly the same. Soil-water flux profiles were calculated for these two days and are presented in Figure 9. Profiles for four, six-hour periods were calculated for both days. For

these calculations flow downward was taken as positive. The July data, represented by dashed lines, indicate flow was upward except for the 9 cm depth during the early morning hours (open circles). The flux upward increased in magnitude with time until 1800. For the period 1800-2400 the flux above 3 cm was less in magnitude than for the daylight periods, but was greater below 3 cm.

For the March data a wide range of flux values occurred. The values for the periods 0000-0600 and 1800-2400 indicate water was moving up at all depths and the water content was increasing at all depths. For the 0600-1200 period, high upward flux occurred above 3 cm's, while below 3.5 cm the flux was downward, indicating flow below 9 cm. By the 1200-1800 period all flow was upward, with more being lost in the upper layers than was being replenished at night. The downward flux during 0600-1200 probably was caused by the relatively large temperature gradients that occurred during this time. If so, then thermal induced liquid flow is of considerably greater magnitude than has been predicted to date.

The water content profiles for these two days are shown in Figure 10. It is obvious that, even though the daily evaporation rates for the two days were nearly equal, the water contents for 6 March were considerably greater than for 14 July. Five time periods are shown for each day. For July the water content at all depths steadily decreased with time until 1800. A small increase can be observed for the period 1800-2400. In March there was much more water content fluctuation with time. The water content decreased with time until 1800. The profile for 2400 shows that an increase in water content, back to about the 1200 values, occurred.

The data for July shows that the 0-1 cm layer was so dry that vapor diffusion would have been the major transfer mechanism, whereas liquid flow would have prevailed in this layer on 6 March. The hydraulic conductivity in the 0-1 cm layer would have been at least 4 orders of magnitude greater for 6 March than 14 July (Figure 3) and the diffusivity would have been at least 1 order of magnitude

greater (Figure 4). Yet, the evaporation rate for these days was nearly equal. It is evident that atmospheric conditions played a prominent role in the evaporation process at all times during the drying of Adelanto loam.

From Figure 8 we find that day 4 for July (14th) and day 8 for March (10th) had nearly the same cumulative evaporation. The flux profiles for four time periods for these two days are compared in Figure 11. The profiles for 10 March show less spread than the 6 March data shown in Figure 9, and they were more similar to the 14 July data. The profiles for the time periods 0000-0600 and 1800-2400 were quite similar for the two days. The profiles for the daylight periods for March showed less flux upward than those for July. This was reflected in the evaporation rates for the two days (0.313 cm for 14 July and 0.123 cm for 10 March).

The similarity of the water content profiles for 14 July and 10 March can be seen in Figure 12. To preserve clarity only three time periods are shown for each day. The profiles for 0000 hours for the two days are nearly identical. For 14 July the profile becomes drier with time of day as reflected in the higher evaporation rate.

Drying Patterns and Cumulative Loss. A comparison of diurnal water content changes for three depth increments for two days is shown in Figure 13. Data in Figure 8 indicates that the cumulative loss from the 0-9 cm layer was nearly the same on 14 July and 12 March, the 4th and 10th days after irrigation, respectively. The values of water content and the diurnal changes were remarkably similar for the two days, especially for the 0-0.5 and 7-9 cm increments. For the 1-2 cm increment the July data were about 0.02 higher in water content for the first 12 hours. However, the evaporation rate for 14 July was about 4 times that of 12 March.

The similarity of the water contents and water content gradients for these days indicate that the water flux due to "isothermal" driving forces would be of similar magnitude. Although the

"isothermal" diffusivities are temperature dependent, this factor alone cannot account for the four-fold greater evaporation rate on 14 July than on 12 March. Evidently temperature induced driving forces were the cause of the greater evaporation rate. The data in Figures 12 and 13 indicate that the drying patterns in time and depth are more a result of the total loss of water than on the rate of loss. This contradicts the hypothesis that an initially high evaporation rate may in the long run reduce cumulative water loss to the atmosphere.

The Three Stages of Drying. Examination of the evaporation rates in Figure 7 shows that the rate for July decreased continuously from the first day after irrigation. During March the rate increased for three days after irrigation and then decreased continuously, having nearly the same values as the July data. The high winds prevalent on day 3 in March were probably responsible for the high evaporation rate on that day. Assuming that the rate would have been somewhat lower if the wind had been moderate, it is tempting to conclude that on day 3 for March, the second stage of drying began. In March day 3 was the first water content sampling day. Part of the data are shown in Figure 6. It is difficult to draw inferences from Figure 6 concerning daily evaporation rates. To circumvent this, the average daily water contents were calculated for both experiments and are shown in Figure 14. Data for day 1 in July are not shown because data were not available for the full 24-hour period. On day 2 for July the water contents for the various depths were quite different; whereas, day 3 for March shows a rather uniform water content with depth. By day 4 in March the average water contents exhibit some drying of the upper layers. Data for days 1 and 2 for March would be needed to allow a firm conclusion on the beginning of the second stage of drying. During those days the soil was too wet for gravimetric sampling.

Much has been written concerning the three stages of drying, yet available criteria to determine the transition from one stage

to another are only qualitative. It would be advantageous if the stages could be related to soil physical parameters such as those shown in Figures 1, 2, 3 and 4. A theoretical equation utilizes the parameters  $D_o$  and  $\beta$ , the soil-water diffusivity at the "air dry" water content and the slope of the logarithm of the diffusivity versus water content relation. From Figure 4 a value of  $D_o$  was taken to be  $0.1 \text{ cm}^2/\text{hr}$  for the "air dry" diffusivity and  $\beta = 38$ . The initial evaporation rate for July was about  $1 \text{ cm/day}$ , and for March about  $0.5 \text{ cm/day}$ . The calculated time of transition between the first and second stages was 4 and 10 days respectively. If  $D_o$  was reduced by a factor of 10, the times would be 2 days for July and 5 days for March. These times do not appear realistic when the data in Figures 7 and 14 are considered.

The third stage of drying begins when the water content of the soil surface becomes "air dry." Water movement at these low water contents is influenced by adsorptive forces. For Adelanto loam, the water content corresponding to a monomolecular layer was about 0.03 volumetric water content. From Figure 2, this water content corresponds to a relative vapor pressure of about 0.33.

Assuming that capillary condensation, and hence capillary flow, begins at a relative pressure at about .8, adsorptive forces would influence water movement for water contents below 0.06. For the lack of better criteria, it will be assumed that the third stage of drying begins when the surface dries to 0.06 volumetric water content. Figure 14 shows that the average water content of the 0-.5 cm layer was below 0.06 from the fourth day after irrigation. Figure 13 shows that the water content was below 0.06 from about 0945 hours for the remainder of the 24-hour period. For days 5, 6 and 7 the water content was always below this value. If the criteria is correct, then the July data was in the third stage of drying from day 4 on. Figure 7 shows that the evaporation rates for days 4-7 in July were very close or slightly higher than for March. The data in Figure 5 indicate that water contents in the 0-0.5 layer

was always greater than 0.06, except for three hours at midday on day 7. The average water content for the 0-0.5 layer during March is not less than 0.06 until day 11 (Figure 14). By this time the evaporation rate (Figure 7) is less than 0.1 cm per day. It is obvious that the criteria used here to determine the transition from the second to the third stage of drying is not appropriate when data from two seasons of the year are compared.

#### SUMMARY AND CONCLUSIONS:

In the surface zone of a field soil the soil water content exhibits a marked diurnal variation. During the course of a day some water moves to the surface and escapes into the atmosphere, and some may move downward into the lower soil profile. The net water movement results from a complex interaction of soil-water pressure, vapor pressure, and temperature gradients. In two experiments, soil-water contents to 9 cm were measured in 1 cm increments at half-hour intervals for 16 days during March 1971, and at hourly intervals for 7 days during July 1970. Data from these experiments showed the drying of the surface during the day and the subsequent rewetting at night. The effect of drying of the surface layers on evaporation is discussed. The soil water regime under naturally occurring environmental conditions was so dynamic that the three stages of drying could not be delineated. The hypothesis that a rapid drying of the surface will, in the long run, reduce total evaporation loss appears not to be valid. The extrapolation of laboratory data on the evaporation process to the diurnally changing environment may lead to erroneous conclusions.

PERSONNEL: Ray D. Jackson, R. J. Reginato, B. A. Kimball,  
F. S. Nakayama, and K. K. Watson

CURRENT TERMINATION DATE: December 1973

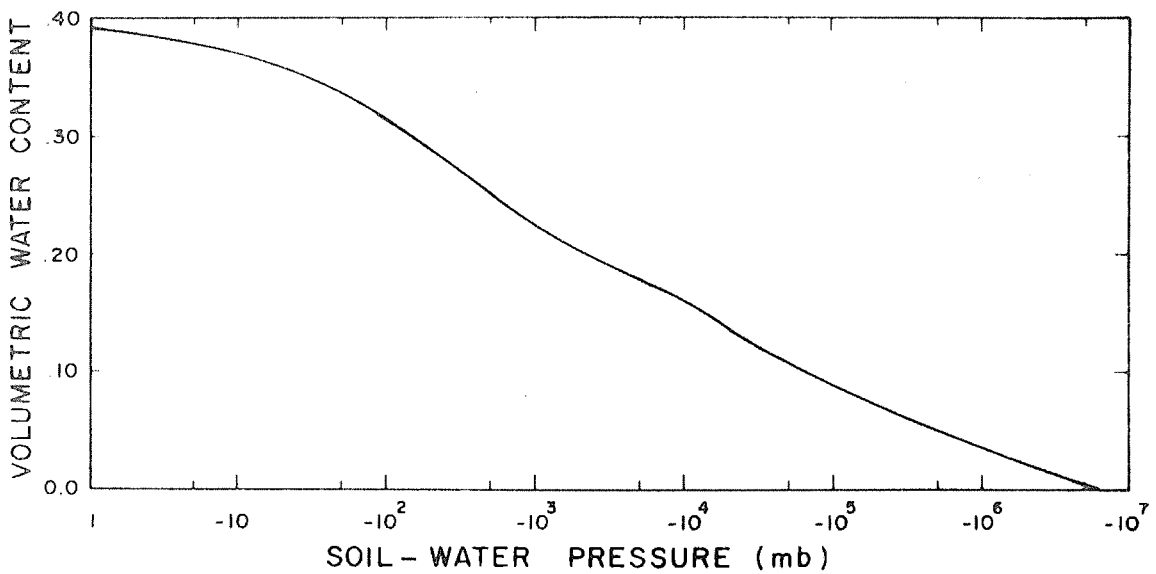


Figure 1. Water characteristic curve for Adelanto loam.

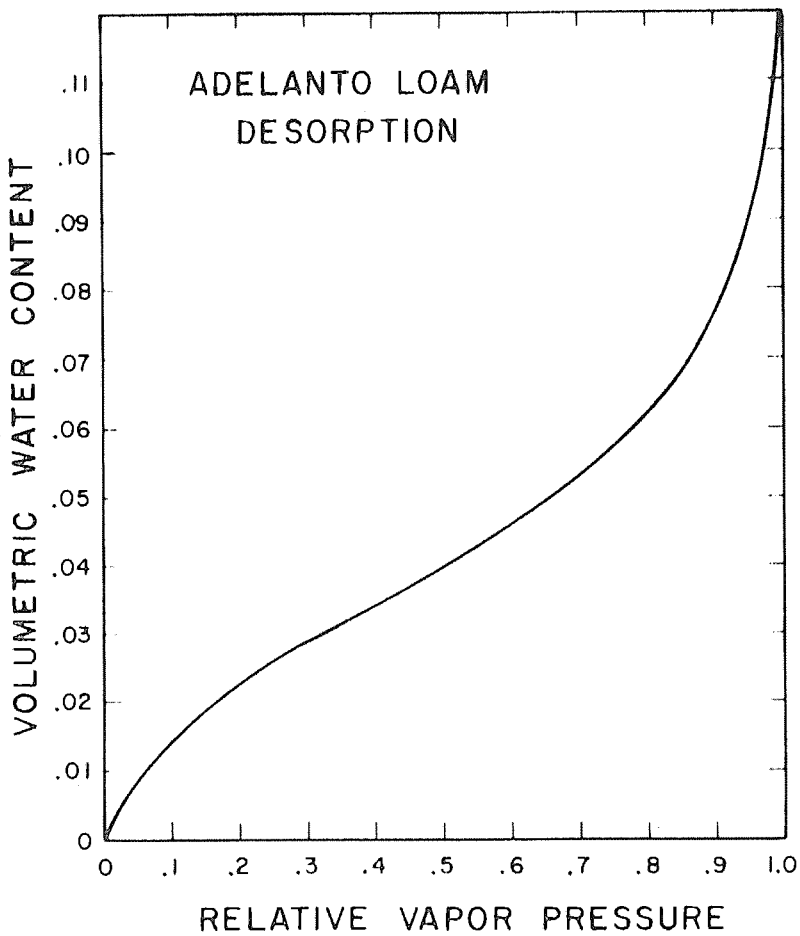


Figure 2. Volumetric water content versus relative vapor pressure.

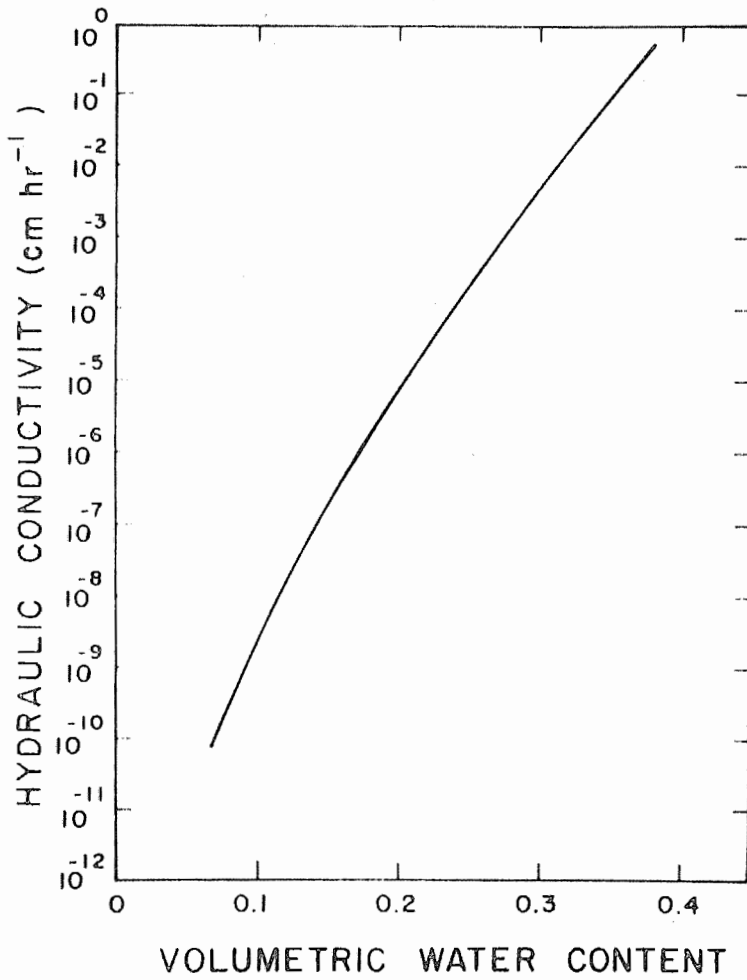


Figure 3. Calculated hydraulic conductivities for Adelanto loam.

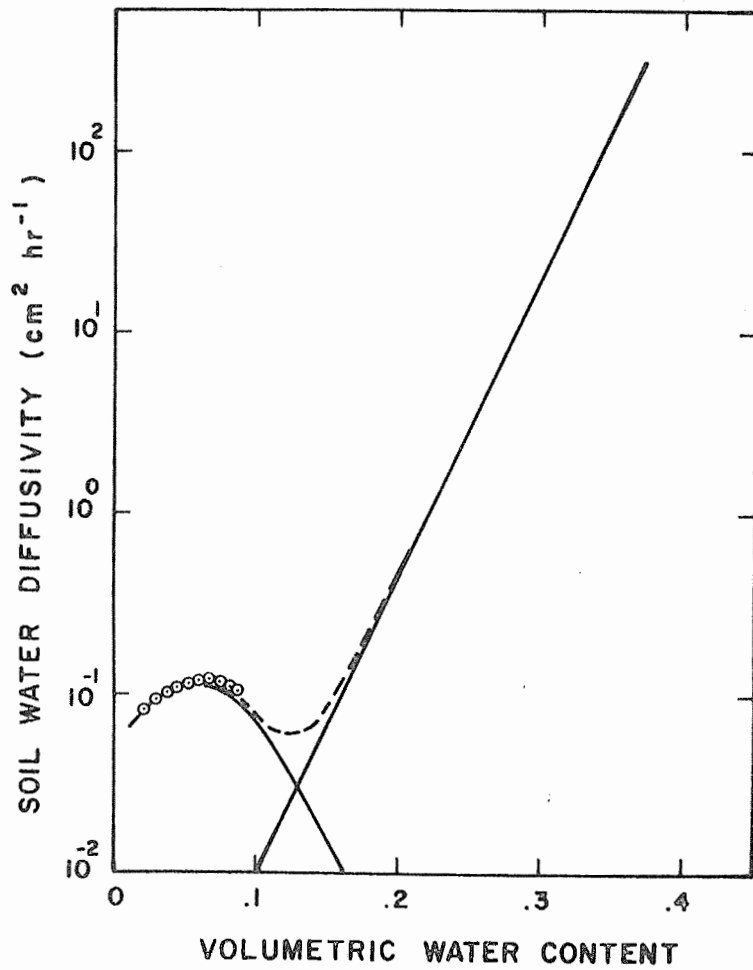


Figure 4. Calculated and measured soil-water diffusivities for Adelanto loam.

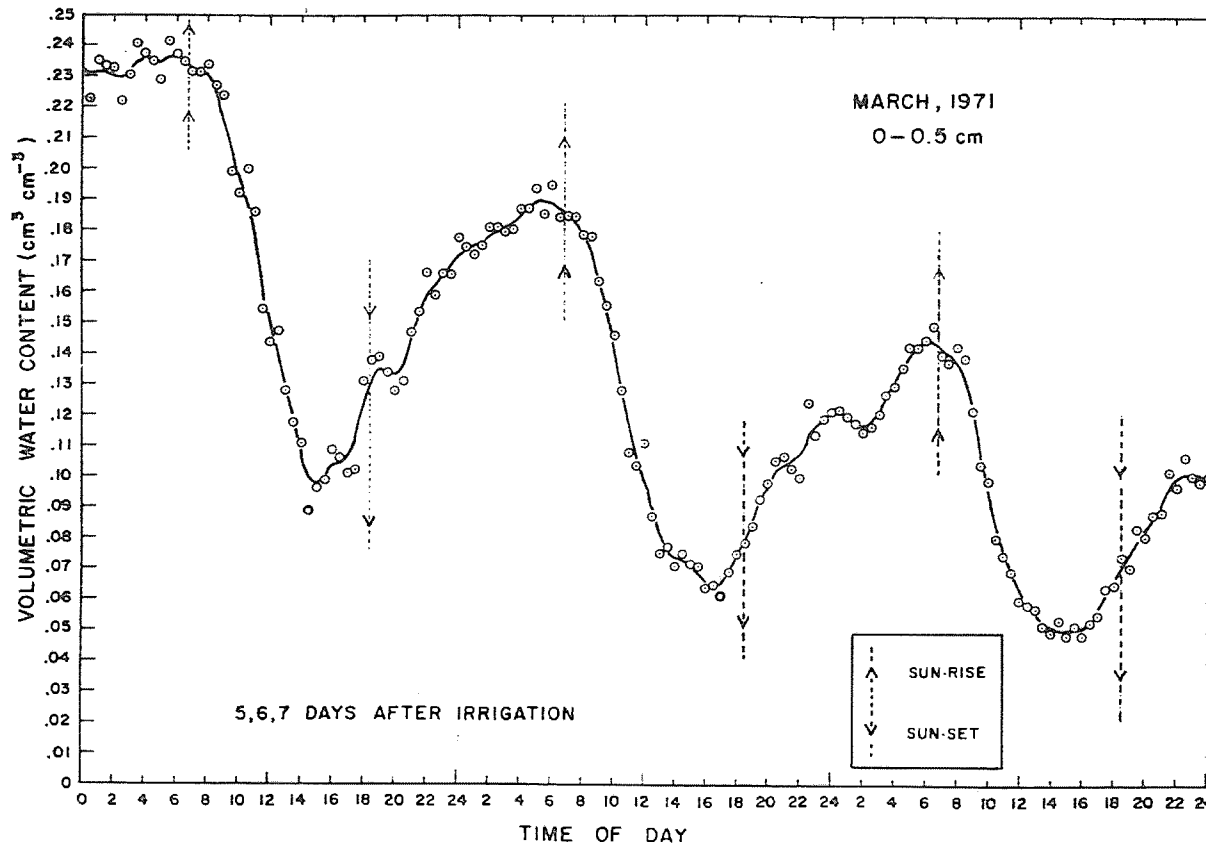
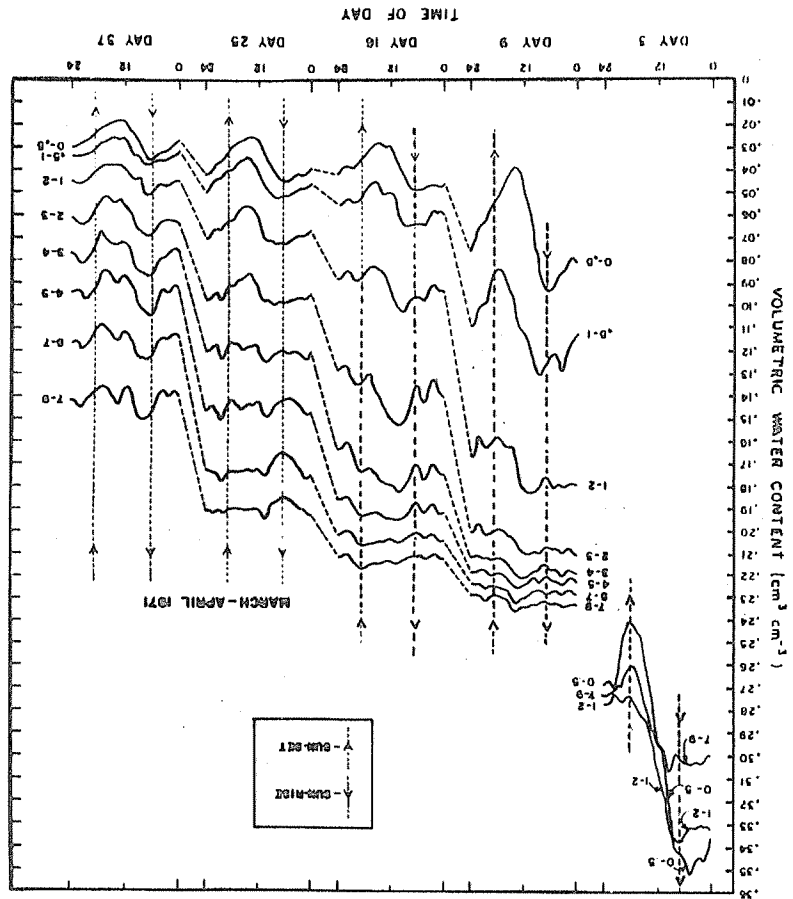


Figure 5. Volumetric water content in the 0-0.5 cm increment versus time for three days during March 1971. The solid line represents smoothed data and the symbols represent the measured values.

Figure 6. Volumetric water content versus time for several depths at 3, 9, 16, 23, and 37 days after irrigation.



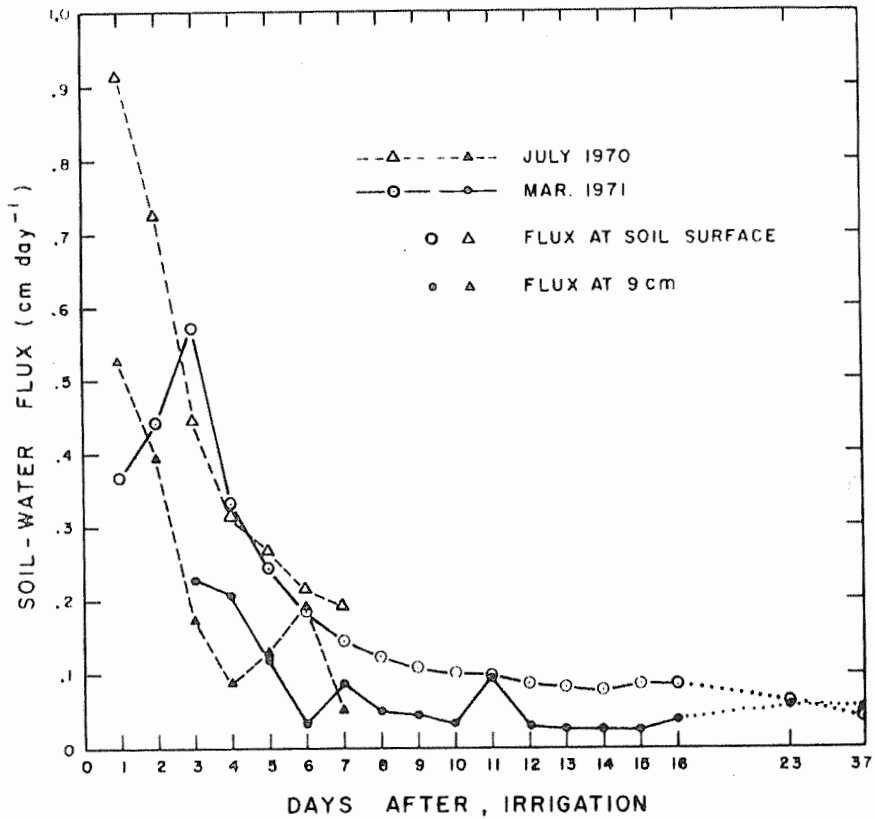


Figure 7. Daily evaporation at the soil surface and soil-water flux at 9 cm.

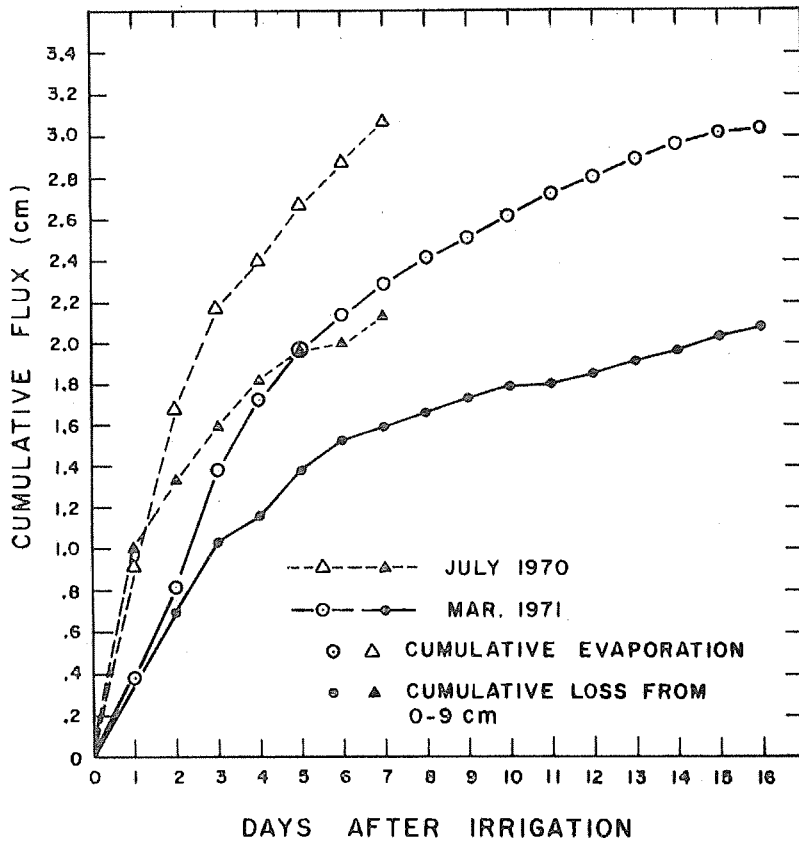


Figure 8. Cumulative evaporation and cumulative loss from the 0-9 cm profile.

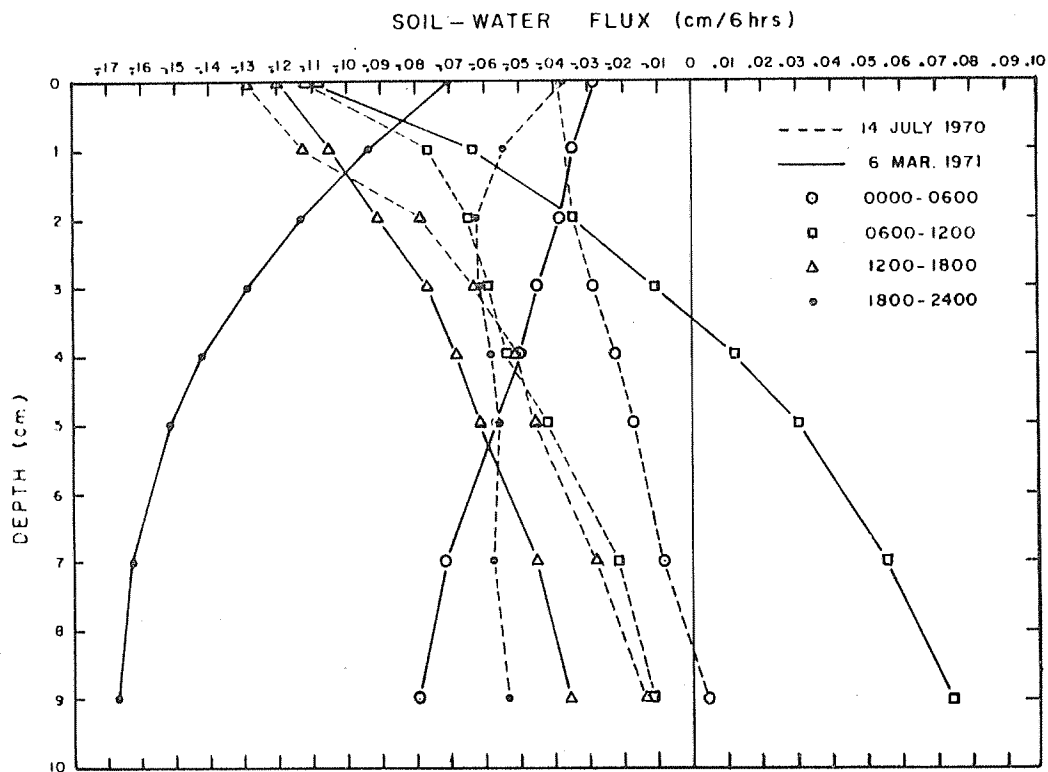


Figure 9. Soil-water flux profiles for four time periods for two days. The evaporation rate for the 24-hour period was nearly the same for the two days.

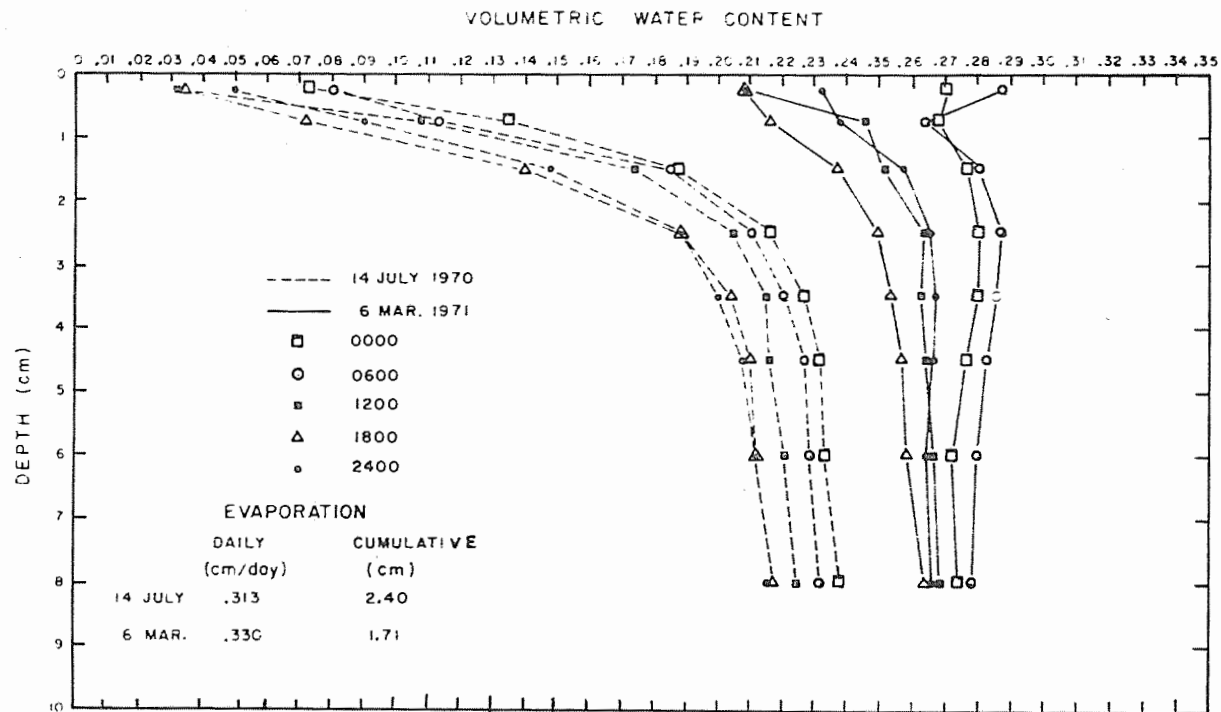


Figure 10. Volumetric water content profiles for five times for two days. The evaporation rate was nearly the same for the two days.

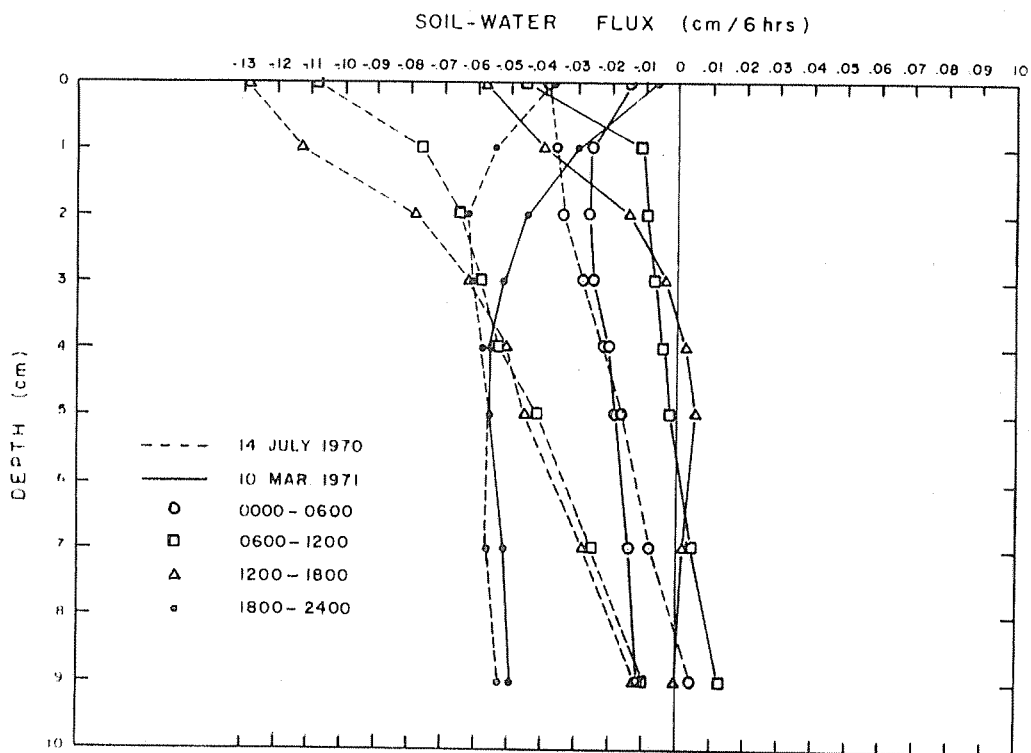


Figure 11. Soil-water flux profiles for four time periods for two days. The cumulative evaporation was nearly the same for the two days.

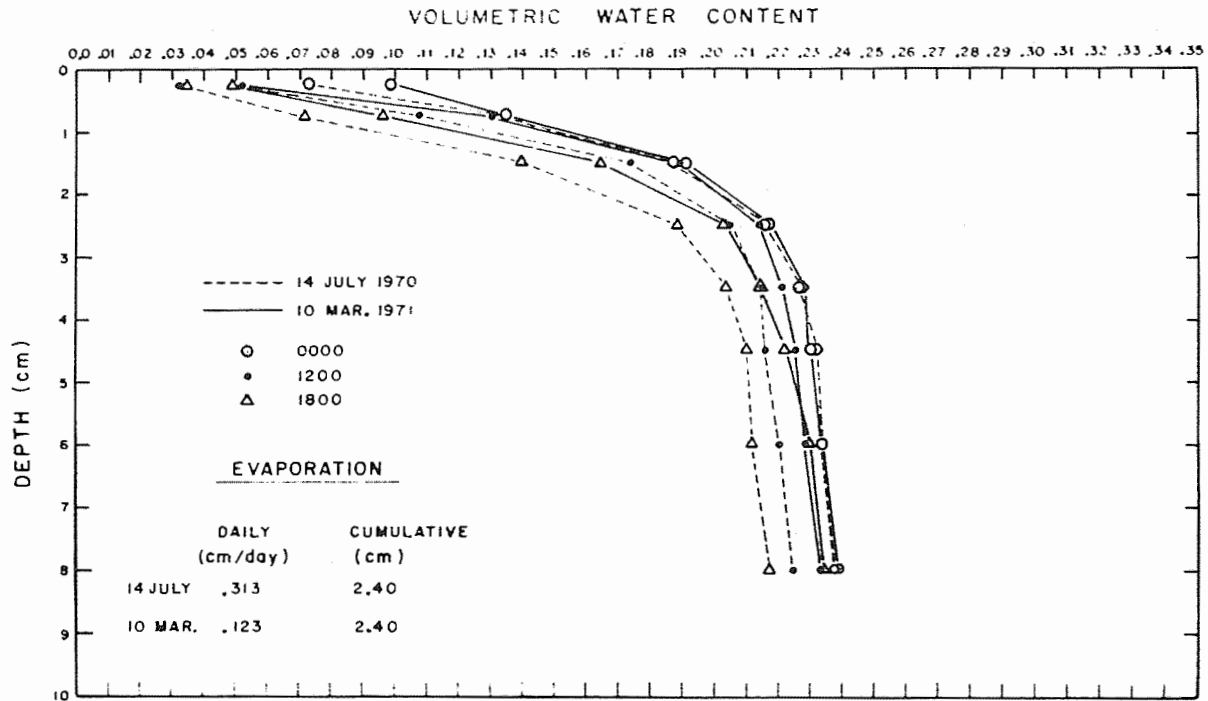


Figure 12. Volumetric water content profiles for three times for two days during which cumulative evaporation was nearly the same.

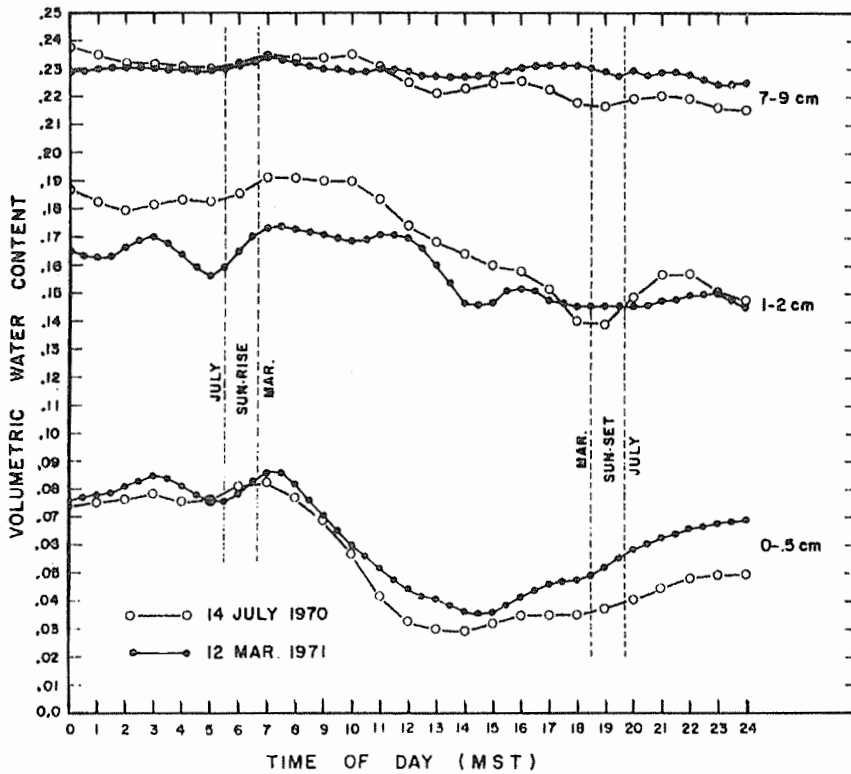


Figure 13. Volumetric water content versus time of day for three depths. Data are for 14 July 1970 and 12 March 1971, four and ten days after irrigation, respectively. The cumulative loss from the 0-9 cm profile was the same for the two days.

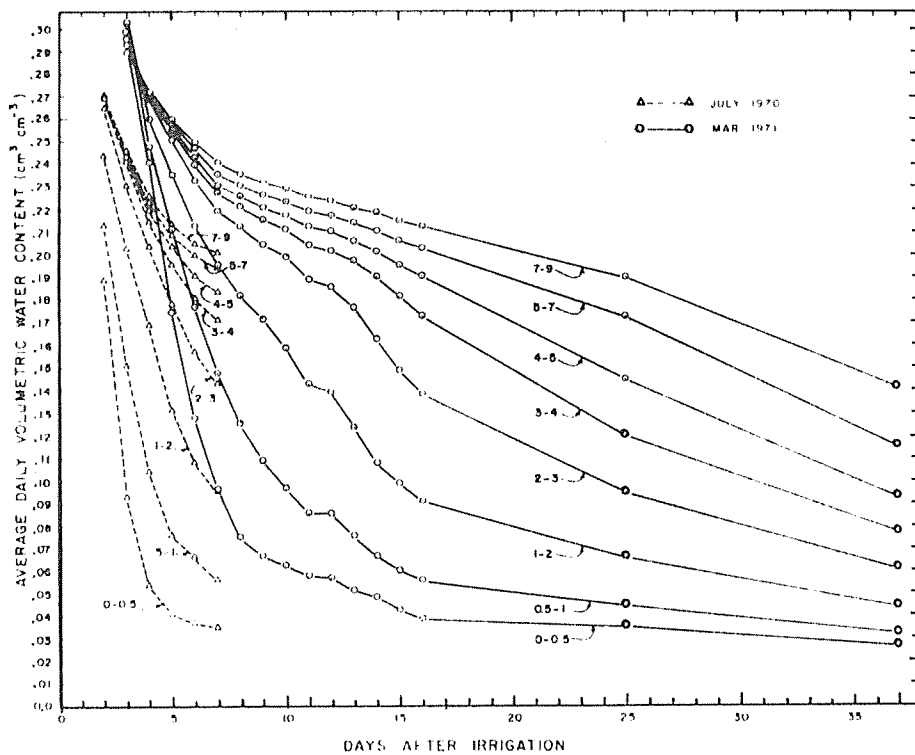


Figure 14. Average daily water contents versus days after irrigation for the July 1970 and March 1971 experiments.

TITLE: FABRICATED-IN-PLACE, REINFORCED LININGS AND  
GROUND COVERS

CRIS WORK UNIT: SWC-018-gG4

CODE NO.: Ariz.-WCL 68-2

INTRODUCTION:

New surface coating treatments for asphalt-fiberglass linings were evaluated using the pressure plate assembly to determine the maximum head of water the treatments are capable of supporting without leakage. New field installations consisted of an operational catchment on the San Carlos Indian Reservation and an operational catchment on Kukaiiau Ranch near Paauilo, Hawaii. Laboratory personnel assisted and instructed at the installation of an operational catchment installed by the Southwest Watershed Research Center, ARS, near Tombstone, Arizona. Studies were started in evaluating supported asphalt-fiberglass membranes for covers over water storages to reduce evaporation losses.

PROCEDURE:

Weathering of Surface Treatments for Asphalt-Fiberglass. The weathering performance of new surface coatings for asphalt-fiberglass membranes is being evaluated at the Granite Reef testing site using small soil trays covered with asphalt-fiberglass and treated with various surface coatings. Soil trays, 1 meter square and 6 cm deep, were filled and compacted with Granite Reef soil. Fiberglass matting (1 oz per ft<sup>2</sup>) was laid on the soil surface and treated with the basecoat asphalt emulsion. After the basecoat had cured, the surface treatments were applied. Observations of their weathering characteristics are being noted at periodic intervals.

RESULTS AND DISCUSSION:

PART I. OPERATIONAL FIELD CATCHMENTS

Turnbull Catchment: This is an operational water harvesting catchment on the San Carlos Indian Reservation. The catchment area of 10,000 ft<sup>2</sup> had previously been covered with one-half inch thick asphalt planking. Cracks had developed in the covering due to shrinkage of the planking sheets and wind eventually destroyed

approximately 50 percent of the covering. The remainder of the planking was removed and in July 1971 the catchment was covered with asphalt-fiberglass. The treatment of 1 oz per ft<sup>2</sup> fiberglass matting with one-half gal per yd<sup>2</sup> of SSKH asphalt emulsion was installed by 5 men in 5 hours. Air temperatures at time of installation exceeded 100 F in the shade. In October 1971, asphalt-clay emulsion was brushed on the catchment at a rate of one-third gal per yd<sup>2</sup> by 4 men in 3 hours.

Water from the catchment is stored in a 25,000 gal open top steel tank for use by cattle and wildlife. The water harvesting unit will be instrumented in 1972 to measure water collected, evaporation losses, and water use to determine the effectiveness of this type of catchment under operational conditions.

Coffee Pond Catchment: This catchment located at Kukaiau Ranch near Paauilo, Hawaii, had previously been covered with chlorinated polyethylene sheeting. A description of the catchment site is presented in previous annual reports titled "Materials and Methods for Water Harvesting and Water Storage in the State of Hawaii." The catchment was covered in June 1971 with 1 1/2 oz per ft<sup>2</sup> fiberglass matting and 0.6 gal per yd<sup>2</sup> RS-1 asphalt emulsion. The fiberglass was cut into strips 50 ft long and laid on the catchment surface. The asphalt emulsion was hand sprayed from an asphalt distributor truck. The total time of installation was 2.25 hours for 8 men, including the truck driver. Asphalt clay emulsion was brushed on 2 months later by personnel from Kukaiau Ranch.

Metate Catchment: A description of this catchment is presented in previous annual reports titled "Soil Treatment to Reduce Infiltration and Increase Precipitation Runoff." The asphalt-fiberglass was installed on the catchment in June 1968 and the asphalt clay emulsion applied in October 1969. The catchment was inspected in December 1971 and was considered in fair condition. The asphalt-fiberglass covering was brittle and showed evidence of the clay emulsion sealcoat "chipping off" the surface. This is the result

of oxidation of the basecoat asphalt during the time lag of 16 months between the original installation and application of the sealcoat. A poor bond was obtained between the sealcoat and the oxidized asphalt-fiberglass surface.

The asphalt-fiberglass pit lining was considered in fair condition. There was approximately one foot of water in the reservoir and several plants were growing through the lining near the water line. There is no evidence of any maintenance being performed on the catchment or reservoir lining since 1969.

Miscellaneous Field Installations: The asphalt-fiberglass catchment at the Maui test site was in excellent condition when inspected in June 1971. The asphalt-fiberglass ditch lining on Maui was damaged when inspected in June 1971. The lining was still present and in good condition but the growth of nutgrass through the membrane caused numerous small holes. The lining should still be reasonably effective in reducing seepage. The ditch is filled with water during about 11 months of the year. As a result, most of the growth through the lining is near the water line.

The three operational asphalt-fiberglass catchments installed in cooperation with the Bureau of Land Management in southeastern Arizona are reported to be in excellent condition. The ornamental fish pond in Phoenix, Arizona, and the small collection reservoir at Granite Reef are considered to be in excellent condition. Although asphalt-fiberglass linings installed more than 6 years ago are still in good condition, the asphalt-clay emulsion sealcoat becomes brittle with time. This can be a problem when the lining is installed over loose soil or sand and is subjected to animal traffic. There is an obvious need for a better sealcoat material.

Laboratory personnel assisted in the installation of a new operational, asphalt-fiberglass catchment built near Tombstone, Arizona, by the Southwest Watershed Research Center, ARS. This catchment was built in lieu of drilling a well to provide water for livestock.

## PART II. LABORATORY STUDIES

Pressure Plate Studies: Recent studies with the pressure plates have been concerned with evaluating various sprayable rubber and elastomeric materials as surface coatings on asphalt-fiberglass. Two sprayable butyl latex materials were able to withstand pressures equivalent to 30 feet of water before failure. The samples were checked, after failure had occurred, with a high frequency static electric generator. It was found that the coatings had developed several small pinholes at thin spots in the coating. The quantity of water which would be lost through these small holes is not presently known.

Weathering of Coatings: Weathering of various surface coatings on asphalt-fiberglass is being evaluated on the small soil trays at the Granite Reef testing site. Two butyl latex compounds developed minute craters or pinholes. It is not yet known if the pinholes will cause an increased deterioration rate. Other coatings have also shown these very small imperfections. These may result from application by brushing, and tests of brushing versus roller applications will be made.

Puncture Resistance: Puncture resistance tests were made on asphalt-fiberglass and on 30 mil nylon-reinforced butyl sheeting laid over loose sand. A sharp edged foot, one-inch square, was forced into the materials at a rate of one-fourth inch per minute. Increasing penetration to three-fourths inch, at an average maximum load of 300 lbs, cut the butyl. The asphalt-fiberglass was deformed but was not cut.

## PART III. EVAPORATION COVERS

A full scale test panel of a supported asphalt-fiberglass membrane for use in reducing evaporation from open water storage structures was constructed at the Granite Reef testing site. A small reservoir was constructed by excavating a hole 4 feet deep, 1:1 side slopes, and 20 feet square at the top. A drain line from

the reservoir bottom extends to a stilling well where the water level can be recorded. The reservoir was lined in October 1971 with 1 oz per ft<sup>2</sup> fiberglass matting and SSKH asphalt emulsion. Two weeks later a sealcoat of asphalt clay emulsion was applied by brushing. The cover consists of a 1 inch diameter pipe frame 21 × 23 feet. Woven wire fencing with rectangular grids approximately 6 × 4 inches was tied to the frame and 1 oz per ft<sup>2</sup> fiberglass matting laid on the wire. The fiberglass was then saturated with SSKH asphalt emulsion at a rate of one-half gallon per yd<sup>2</sup>. Two weeks later asphalt-clay emulsion was applied by brushing at a rate of one-fourth gal yd<sup>2</sup>. This was allowed to cure three weeks, then the entire cover was placed over the reservoir and the frame staked into place. Studies will be conducted in 1972 to determine the effectiveness of the cover for reducing evaporation.

#### SUMMARY AND CONCLUSIONS:

Two new operational water harvesting catchments were constructed in 1971. One unit on the San Carlos Indian Reservation will be instrumented to determine the effectiveness of these units under operational conditions. The second unit is located near Paauilo, Hawaii, and will be used to evaluate the performance of asphalt-fiberglass catchments in high rainfall climates. Observations of previous field installation has shown the need for periodic maintenance and a better sealcoat than asphalt-clay roofing emulsion. All field units are in good condition but do require maintenance to continue satisfactory performance.

Laboratory studies were conducted to evaluate sprayable new compounds for use as surface coatings to improve weathering characteristics and to obtain sealcoats capable of supporting pressures equivalent to 30 or more feet of water. Some of the compounds appear promising. Puncture resistance of asphalt-fiberglass linings was shown to be superior to 30 mil, nylon reinforced butyl rubber sheeting.

A field model of a supported asphalt-fiberglass membrane over open top water storages was constructed. The model will be used to

evaluate the feasibility and economics of covers of this type for reducing evaporation.

PERSONNEL: L. E. Myers and G. W. Frasier

CURRENT TERMINATION DATE: December 1973

TITLE: COLUMN STUDIES OF CHEMICAL, PHYSICAL, AND  
BIOLOGICAL PROCESSES OF WASTEWATER RENOVATION  
BY PERCOLATION THROUGH THE SOIL

CRIS WORK UNIT: SWC-018-gG-4 CODE NO.: Ariz.-WCL 68-3

PART I. CHEMICAL AND BIOLOGICAL PROCESSES DURING RENOVATION

INTRODUCTION:

Experiments on the renovation of secondary sewage effluent with soil columns were continued during 1971. It was hoped that these experiments would provide information on the feasibility of adding organic carbon sources to sewage water to promote nitrogen removal and on the capacity of the soil system to renovate wastewater which is lower in quality than the effluent produced by the Phoenix treatment plant. The organic carbon content of the secondary effluent was increased by adding methanol or dextrose with the following objectives:

- (1) To determine if nitrogen removal could be stimulated by additions of organic carbon before infiltration;
- (2) To study the removal of organic carbon by the soil system at various carbon levels; and
- (3) To determine the effect of increased organic carbon on clogging.

PROCEDURE:

Secondary sewage effluent was flowed through 8 polyvinyl chloride columns packed with soil taken from the Flushing Meadows groundwater recharge basins. The flow system was the same as reported in previous annual reports (Figure 1). Four levels of organic carbon were maintained by flooding 2 columns with secondary sewage effluent and three sets of 2 columns with different levels of organic carbon added in the chemical form. The organic carbon was mixed with sewage water in 5-gal jugs and the columns were flooded by using a Mariotte siphon. The jugs were replaced daily with a fresh supply of spiked sewage water. The organic

carbon was measured to approximate levels because the volumes of water handled, the variable infiltration rates during the flooding cycles, and the deterioration of the carbon source in the jug made highly accurate metering impractical.

The sewage water was sampled from the jug at the beginning of 24-hr periods, and from the column at the end of the 24 hrs, to determine the average organic carbon concentrations entering the columns. Methanol was first used as a carbon source until it was determined that the organic carbon analyzer did not recover all of the carbon from methanol. Dextrose was then used to supply carbon.

Sample ports were constructed by sealing ceramic into copper tubing and inserting the tubes at intervals along the columns. Serum caps were placed in the tubes, and samples for carbon and nitrogen analyses and fecal coliform counts were withdrawn with a hypodermic syringe. The ports were located at soil depths of 2, 5, 10, 20, 40, 80, 160, and 240 cm. Samples could also be taken from the head of water above the column and from the water flowing through the column outlet. The columns were also instrumented with oxidation-reduction electrodes at 2, 10, 20, and 40 cm depths, and with tensiometers in the head and at 2, 20, and 40 cm.

The columns were operated on cycles of 9-days flooding followed by 5-day dry periods. The column infiltration rates were determined by weighing the outflow daily, and gaseous output from columns was measured and analyzed as described in previous reports. The cumulative outflow from the columns was sampled periodically and analyzed for the various nitrogen components and organic carbon.

#### RESULTS AND DISCUSSION:

Nitrogen Removal. The percent nitrogen removal from sewage water was increased by about 12% by the addition of approximately

150 mg/l methanol. The addition of lower concentrations of methanol did not increase nitrogen removal and resulted in lower N removal during one cycle. The amount of nitrate leached out following the dry period must be reduced in order to substantially increase nitrogen removal. The nitrate peak was reduced by each increment of methanol added to the sewage water (Figure 2), but due to a corresponding increase in nitrite concentrations the total nitrogen content of these samples did not change (Figure 3). The increase in nitrite concentration could have been due to either incomplete nitrification or incomplete denitrification. The addition of high concentrations of methanol did stimulate an increase in the volume of gas expelled from the column, but the gas collected after the first day of flooding consisted of about 50% methane and only 40% nitrogen. Therefore, methanol appeared to stimulate denitrification only slightly. Data on nitrogen removal were collected for only 3 flooding cycles, however, and this might not have been sufficient time for the microbial population to adapt to methanol. It is also possible that the detention time in the columns might have been too short for complete denitrification with methanol. The carbon source was changed to dextrose after 3 cycles because the total carbon analyzer would not recover all of the methanol from samples.

The addition of dextrose to the sewage water resulted in progressively higher nitrogen removal with each increment of added carbon (Figure 4). Flooding with sewage water containing 150-ppm organic carbon resulted in almost complete nitrogen removal (91%). Denitrification appeared to be responsible for at least part of the increase in nitrogen removal. The gas collected from the columns flooded with sewage containing 150-ppm carbon accounted for an average of 245 grams per cycle more nitrogen than was present in the gas collected from the columns flooded with sewage water only (Table 1). However, the columns flooded

with the spiked sewage water removed about 450 grams per cycle more nitrogen than the columns flooded with sewage water only. Traces of  $N_2O$  were detected in the air space above the soil columns during the dry period, indicating that denitrification occurred during that time, also. Some nitrogen gas produced during the dry period could be lost from the column by diffusion. It is likely, however, that increasing the carbon content of the sewage water would result in an increase in the amount of nitrogen incorporated into microbial tissue. Later analysis of soil samples and/or leaching of the columns could clarify this point.

The difference in the reaction of the columns to the different carbon sources is difficult to explain. Since dextrose is more readily available to microorganisms than methanol, it may stimulate the nitrogen removal processes more readily.

The  $NH_4^+$  concentrations of samples taken at various depths in the columns are shown in Figure 5. The  $NH_4^+$  concentration actually increased between the 0- and 20-cm depths and then rapidly declined between the 20- and 40-cm depths. A similar increase in the organic carbon concentration occurred between 0-20 cm. These increases in  $NH_4^+$  and C are apparently due to the decomposition of organic materials which have accumulated in the column near the surface. The  $NH_4^+$  concentrations of samples taken after 8 days of flooding indicated that the soil was becoming saturated with  $NH_4^+$ .

Carbon Removal. The addition of organic carbon as methanol did not result in much increase in the organic carbon content of the water collected from the columns, except for the highest rate of carbon added (Figure 6). The organic C content of the sewage water spiked with methanol could not be accurately measured because analyses of methanol standards indicated that 15-25% of the carbon injected into the carbon analyzer as methanol passed through without being detected. The same was true of ethanol.

It is likely that a fraction of very volatile compounds may pass through the carbon analyzer furnace without being combusted. These data indicate that the addition of up to approximately 75-ppm C as methanol resulted in only a slight carbon increase in the water collected from the column, while the addition of approximately 150-ppm C substantially increased the C content of the reclaimed water.

The soil columns apparently did not remove as much organic carbon from the sewage water spiked with dextrose as they removed from the sewage water spiked with methanol. Most of the organic C was removed from the water when the average concentration entering the columns was 40 ppm, but a considerable amount of organic C passed through the columns when the average concentration entering was 80 ppm (Figure 7). About half of the organic C passed through the columns when the average organic C concentration entering the columns was 150 ppm. The columns flooded with water containing 150-ppm organic carbon did not remove much more total carbon than the columns flooded with water containing 80-ppm organic carbon.

The organic C content of the samples from the columns flooded with only sewage water actually increased as the water moved to the 40-cm depth, and then gradually declined. The samples from columns flooded with sewage water spiked with dextrose showed a sharp decline in organic carbon content as the water moved to the 40-cm depth, and then gradually declined. The sharp drop in the organic carbon content between the 240-cm depth and the column outlet at 250 cm may be due to some oxygen leaking into the columns at the lower end. It could also be due to the difference in the way the sample was taken since the 240-cm samples were taken from a ceramic sampling tube, while the 250-cm samples were withdrawn from water flowing freely through the outlet tube. Some colloidal

organic particles associated with the soil could be included with the sample taken from the soil with the ceramic sampler.

The Effect of Dissolved Organic Carbon on Soil Clogging. The addition of organic carbon as either methanol or dextrose did not affect the infiltration rates during the first flooding period, but the infiltration rates dropped sharply during the second flooding period in both cases (Table 2). Some time was apparently needed for the carbon addition to stimulate a buildup in the microbial population of the soil columns. Tensiometer data indicated that the decrease in infiltration rates was not due to clogging at the surface of the soil, as was reported previously when columns were flooded for long periods of time. The suspended solid content of the sewage water increased substantially during the fourth flooding period due to technical problems at the activated sludge plant in Phoenix. The infiltration rates of the check columns which received only sewage water declined sharply during this cycle, and the tensiometer data indicated that the decline was due to clogging at the soil surface. The infiltration rates of the check columns were about the same as the carbon-treated columns after several flooding cycles with water high in suspended solids. This indicates that the effects of the suspended solids and the organic carbon were not additive. Surface clogging was not indicated by the tensiometers in the carbon-treated columns even after flooding with water high in suspended solids. There appeared to be no differences in the infiltration rate reduction among the different levels of carbon treatment.

Gas production in the columns treated with carbon could have been responsible for some clogging, although gas was not emitted from the columns after the first day of the flooding cycle except in the case of the highest methanol treatment.

Fecal Coliform Removal. The addition of dextrose to the sewage water resulted in a tremendous growth of fecal coliform

bacteria within 24 hrs. The average number of fecal coliforms in the sewage water was  $4.2 \times 10^5/100$  ml, and this increased to an average of  $3.3 \times 10^7/100$  ml within 24 hrs after the carbon addition. The number of bacteria taken at different levels in the profile was quite erratic (Figure 8). However, it was discovered that a ceramic sampler screened out half of the fecal coliforms when sewage was drawn through it. Some of the samplers may have been clogged more than others, resulting in erratic counts. The samples taken from the head of water above the columns and the outlet tube at the lower end of the columns were not pulled through ceramic. When lines were drawn through these two points for the sewage water and the sewage water plus dextrose, it appeared that the rate of reduction of coliforms with column depth was the same for the two treatments (Figure 8). More coliforms passed through the columns flooded with sewage plus dextrose because more entered the columns at the top. The ceramic samplers were obviously not suitable for taking samples for bacterial counts, even though the pore size was 25-30  $\mu$ .

The Comparison of COD and Organic Carbon Analyses. The chemical oxygen demand (COD) was plotted vs. organic carbon for samples from groundwater (reclaimed) secondary sewage effluent and reclaimed sewage water ponds (Figure 9). The scatter of points was similar to that reported by other workers, and the correlation coefficient was 0.83. The average mean value for COD/organic carbon was  $3.46 \pm 1.22$ .

## PART II. REDOX POTENTIAL MEASUREMENTS

### INTRODUCTION:

In a recent article Bailey and Beauchamp (1) investigated the differences in redox potential measurements due to leaving the electrodes in place versus taking them out of the soil after every reading. They used bright platinum electrodes in saturated soil, even though they acknowledged that Quispel (2) had found better

results for well-aerated soils with platinum-blackened platinum electrodes. They found that "permanently" placed electrodes poised at -200 mv in a saturated soil system to which  $\text{NO}_3^-$  had been added, but that "temporarily" placed electrodes poised at +200 mv when the  $\text{NO}_3^-$  was added to the system.

In previous work with soil columns intermittently flooded with sewage effluent, it had been our practice to use "permanently" placed, blacked platinum electrodes (see 1969 and 1970 Annual Reports for details). While changes in the readings did occur during a flooding cycle, the data did not indicate whether or not the electrodes may have been malfunctioning.

The present study was designed to see if the permanently placed electrodes would function properly over a long period of time and several flooding and draining cycles. The study also tested the effect of added carbon in the sewage effluent water on the pH and redox potential of the soil-water system.

#### PROCEDURE:

The schematic diagram of the system was given in the earlier section as Figure 1. Samples were taken from the sampling ports during one of the infiltration cycles to determine the pH profile of the soil-water system. Since the pH of the sewage effluent changes very little, one sampling was thought to be sufficient.

Blacked platinum electrodes were inserted into each of the eight columns at 2-, 10-, 20-, and 40-cm depth below the soil surface. Column 8 had a double set of these electrodes 2 cm apart horizontally. From past experience it appeared that this zone would undergo the widest redox potential changes, and if the probes were going to be poised at some negative value, it should show up here. It would be very inconvenient and give doubtful results to change the redox probes after every reading like Bailey and Beauchamp. The air introduced into the soil when the probes were inserted and withdrawn would certainly affect the redox reading.

If the probes were inserted through a membrane or rubber serum cap, it would probably take off a lot of the platinum black and again the readings would be suspect.

The electrodes were checked in a pH 7 buffer solution before insertion into the column and again after being taken out of the column. The probes were allowed to stand in this buffer for 2 or 3 days to equilibrate with the buffered solution, both before and after the experiments. The redox readings were taken with a calomel electrode to complete the circuit, but were corrected to a hydrogen electrode basis by adding 240 to each reading.

Columns 1 and 2 had no added carbon. Columns 3 and 4 had carbon added to attain an average concentration of 40 ppm. Columns 5 and 6 had carbon added to attain an average concentration of 80 ppm. Columns 7 and 8 had carbon added to attain an average concentration of 150 ppm. All carbon was added as dextrose.

#### RESULTS AND DISCUSSION:

The pH profiles are shown in Figure 10. The effluent-only columns (1 and 2) did not show much of a pH change down the columns, except at 20 cm. The high-carbon treatment (7 and 8), however, had a distinct pH profile. Thus, correcting the redox readings for pH as has been done previously might be meaningless where carbon has been added to the system.

Before the redox probes were installed in the columns, the redox value in a pH 7 buffer was  $592 \pm 34$  mv. After the probes were removed, after 6 months' usage, the redox readings on all probes were  $477 \pm 276$  mv. Out of the 36 probes, 9 seemed to be giving faulty readings, as judged by low readings both in the column and in the buffer solution. In addition, two other probes appeared to have been damaged when removing them from the columns. The remaining 25 probes (or 70%) had a standard reading of  $543 \pm 123$  mv in the pH 7 buffer. While this is not as good as might be hoped for, it indicates the probes were not permanently poised at

some low reading. The wide variation in the final test readings is probably not too bad for probes in such a system for 6 months.

Figure 11 shows the redox potentials as a function of time for the two control or straight-effluent inundated columns (1 and 2). Each curve is the average of the two columns. As can be seen, the redox values cycled with every infiltration (I on the time scale) and drainage (D on the time scale) period with the same amplitude. It also is apparent that the probes were not permanently poised by this system. While there is scatter with position, it appears that about the end of the infiltration period (14 days) some denitrification could have taken place (i.e.,  $E_h = 200$  mv) if nitrate had been present.

Figure 12 shows the redox potential as a function of time for columns 7 and 8 with water containing 150-ppm organic C. Each curve is the average of 3 values. Here the changes in the redox values are much wider than in columns 1 and 2. The values indicate, however, that the probes were not poised at the low negative levels reached during the infiltration cycle. The recovery of the redox value seemed to be a function of depth; i.e., the lower probes (40 cm) were slowest to register an increase in potential after the start of the drainage period. The other carbon-treated columns acted much the same as columns 7 and 8, except the redox value was not quite as low at the end of the infiltration period.

In order to check the redox reading as a function of depth, two sets of probes were installed in column 8. Figure 13 shows the readings of the two probes at 2 cm, as well as their average over the same time period. While there is scatter between the two probes, they did seem, for the most part, to be in phase with one another. Figures 14, 15, and 16 show the readings and average values for probes at 10, 20, and 40 cm. While there is some scatter at each depth, it appears to decrease with depth. Thus, the scatter between probes may be real in that the microenvironment around the probes may be different close to

the soil surface where cracks and uneven soil surfaces play an important part, but deeper in the soil profile the redox potential in a plane is fairly uniform.

#### SUMMARY AND CONCLUSIONS:

Soil columns filled with material from the Flushing Meadows recharge basins were flooded with sewage water and sewage water spiked with organic carbon as methanol or dextrose to provide organic carbon levels of 15, 40, 80, and 150 ppm. Carbon levels in water spiked with methanol were approximate because the total organic carbon analyzer did not recover all of the methanol. All carbon concentrations entering the columns are reported as average concentrations because of deterioration in the containers before entering the columns.

The addition of methanol increased nitrogen removal only slightly. The high-nitrate peak occurring after the dry period was eliminated, but it was replaced by a high-nitrate peak. The nitrite peak was due to inhibition of either nitrification or denitrification.

The addition of dextrose to the sewage resulted in an increase in nitrogen removal with each increment of added carbon, and more than 90% of the nitrogen was removed from the sewage water containing 150-ppm organic carbon. An increase in the volume of gas collected from the columns indicated that denitrification was stimulated, but some nitrogen could also have been incorporated into microbial cells.

A high concentration of organic carbon remained in the water collected from the columns when the organic carbon content of the sewage water was increased to 150 ppm with either carbon source. Increasing the carbon concentration of the sewage water to 80 ppm by adding dextrose also increased the carbon concentration of the water collected from the columns. Most of the organic carbon was removed from sewage water containing 40- or 80-ppm organic carbon as methanol and from water containing 40-ppm organic carbon as dextrose.

The maximum concentration of dissolved organic carbon that could be removed from the sewage water by predominantly anaerobic reactions in this high-rate flow system (1-2 ft infiltration/day) appeared to be between 40 and 80 ppm.

Infiltration rates were reduced by about 30% on the average by the addition of dissolved organic carbon to the sewage water. Organic sediments appeared to cause more clogging than was developed by the addition of dissolved organic carbon. The clogging due to organic sediments developed at the surface, while the clogging caused by dissolved organic carbon developed internally.

The addition of dextrose to the sewage water stimulated the growth of fecal coliform bacteria in the jugs of sewage. The rate of reduction of fecal coliforms with column depth seemed to be about equal for the columns flooded with sewage only and the columns flooded with sewage containing 150-ppm organic carbon. More fecal coliforms were present in the water collected from columns flooded with the sewage water spiked with dextrose because more fecal coliforms were present in the water applied to those columns.

The blacked platinum electrodes appear to be satisfactory in measuring the redox potential in a soil column treated with sewage effluent, with or without added carbon. These probes appear to function properly for the most part, even when they were left in place for 6 months. This was inferred from the fact that the probes cycled with the same amplitude for several infiltration and drainage cycles and did not become permanently poised at some low value. The redox potential close to the soil surface undergoes the widest changes and most rapid changes with infiltration and drainage periods. The deeper parts of the profile appear to lag behind the surface in rate of change if not in magnitude. The redox potential in a plane of soil appears to become more constant with depth than at the soil surface where microrelief plays an important part. Adding carbon

to the sewage effluent used to inundate the columns lowered the redox potential attained during the infiltration period.

REFERENCES:

1. Bailey, L. D., and Beauchamp, E. G. Nitrate reduction, and redox potentials measured with permanently and temporarily placed platinum electrodes in saturated soils. Canadian J. Soil Sci. 51:51-58. 1971.
2. Quispel, A. Measurements of the oxidation-reduction potentials of normal and inundated soils. Soil Sci. 63:265-275. 1946.

PERSONNEL: J. C. Lance, F. D. Whisler, and R. S. Linebarger.

CURRENT TERMINATION DATE: 1971

Table 1. Volumes of gas collected from soil columns flooded with secondary sewage effluent supplemented with dextrose during cycles of 9-days flooding and 5-days drying.

Cycle	Sewage Only	Sewage + Dextrose	Difference
	ml	ml	ml
1	1930	1990	60
2	1965	2143	178
3	1833	2112	279
4	1834	2264	430
5	<u>1528</u>	<u>1805</u>	<u>277</u>
Average	1818	2063	245

Table 2. Infiltration rates (ft/day) of soil columns intermittently flooded with secondary sewage effluent spiked with different levels of organic carbon.

Cycle no.	Organic carbon level (average)			
	15 (sewage only)	50	80	150
	Base period (no C added)			
1	1.9	1.6	1.6	1.7
2	1.8	1.6	1.6	1.7
	Methanol added*			
1	2.0	1.7	1.6	2.3
2	2.0	1.3	1.0	1.3
3	1.9	1.5	1.2	1.3
	Dextrose added			
1	2.0	1.7	1.6	2.0
2	1.6	1.1	0.9	1.3
3	1.8	1.2	0.9	1.5
4**	1.2	0.9	0.8	1.0
5	1.3	0.8	0.7	1.2
6	1.1	1.1	0.6	0.9
7	1.0	1.1	0.6	0.9

\*Carbon values are approximate because analyzer was not accurate for methanol analysis.

\*\*The suspended solid content increased substantially during cycles 4-7 due to problems in the city sewage plant.

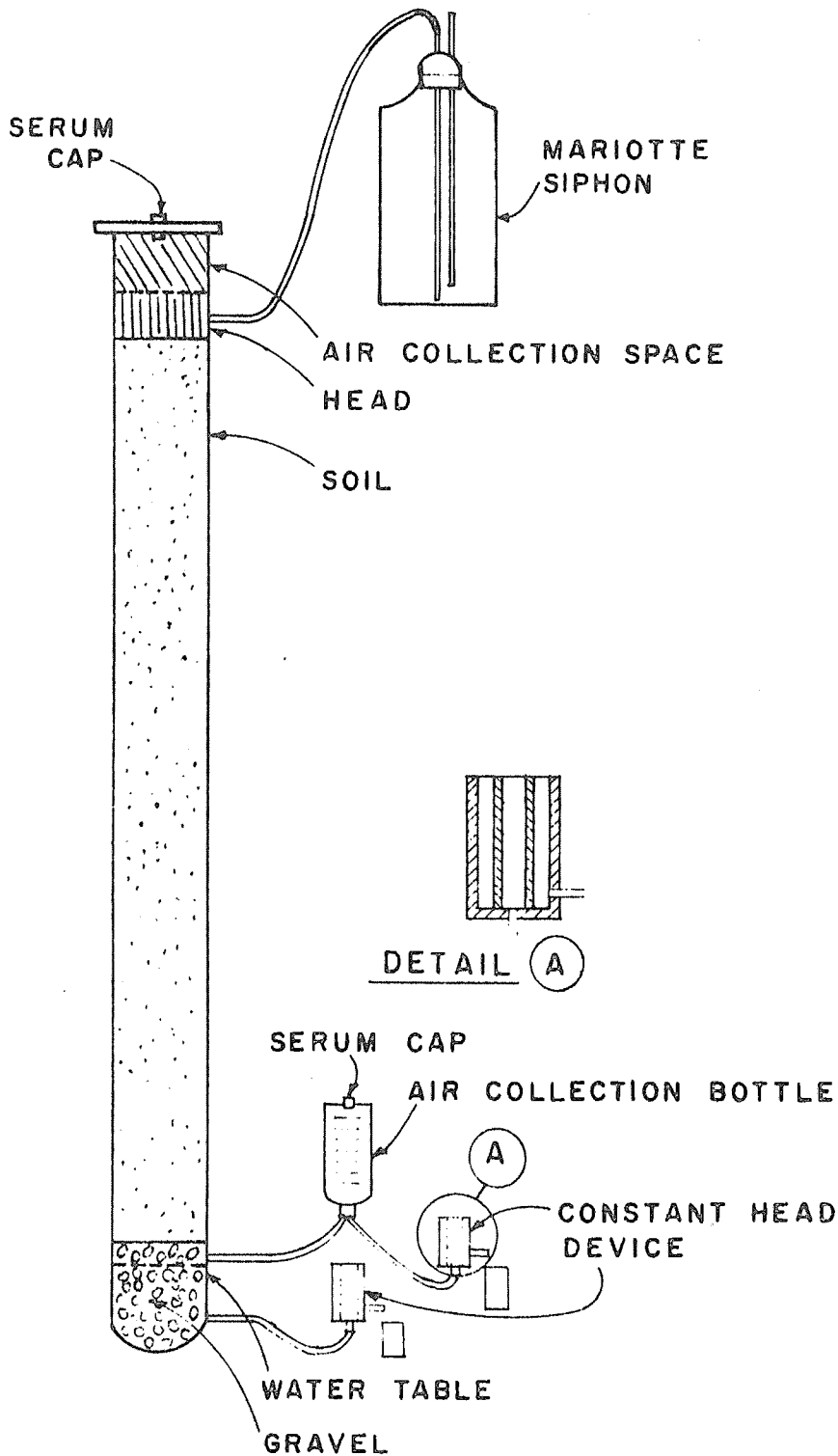


Figure 1. Soil column for wastewater renovation studies. Ceramic samplers were located at soil depths of 2, 5, 10, 20, 40, 80, 160, and 240 cm. Tensiometers were located in the head and at 2, 20, and 40 cm. Oxidation-reduction electrodes were located at 2, 10, 20, and 40 cm.

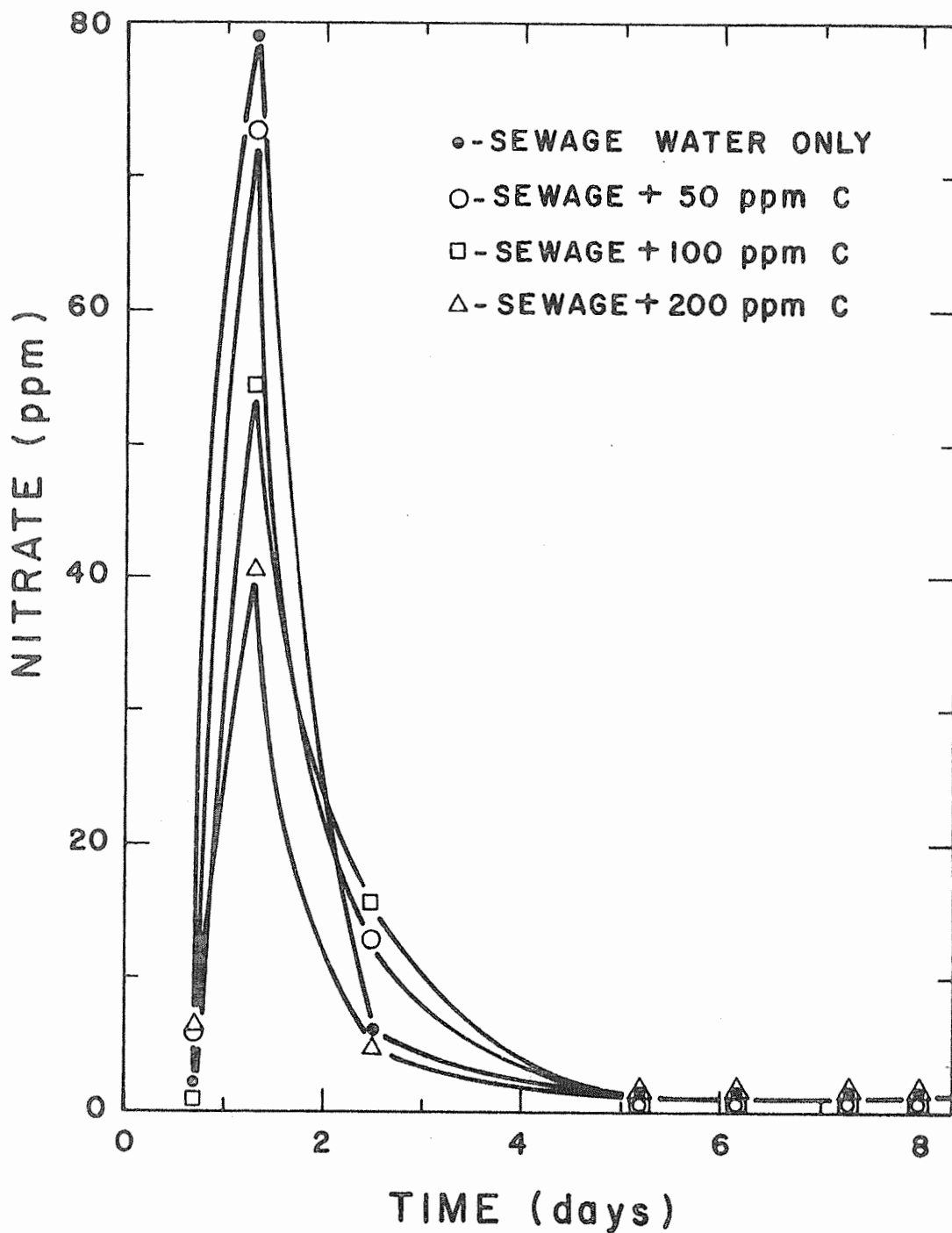


Figure 2. The effect of organic carbon as methanol on the nitrate content of water collected from soil columns flooded on cycles of 9 days flooding and 5 days dry. (C concentrations entering the columns were less than the concentrations added to the sewage because of deterioration in the container.)

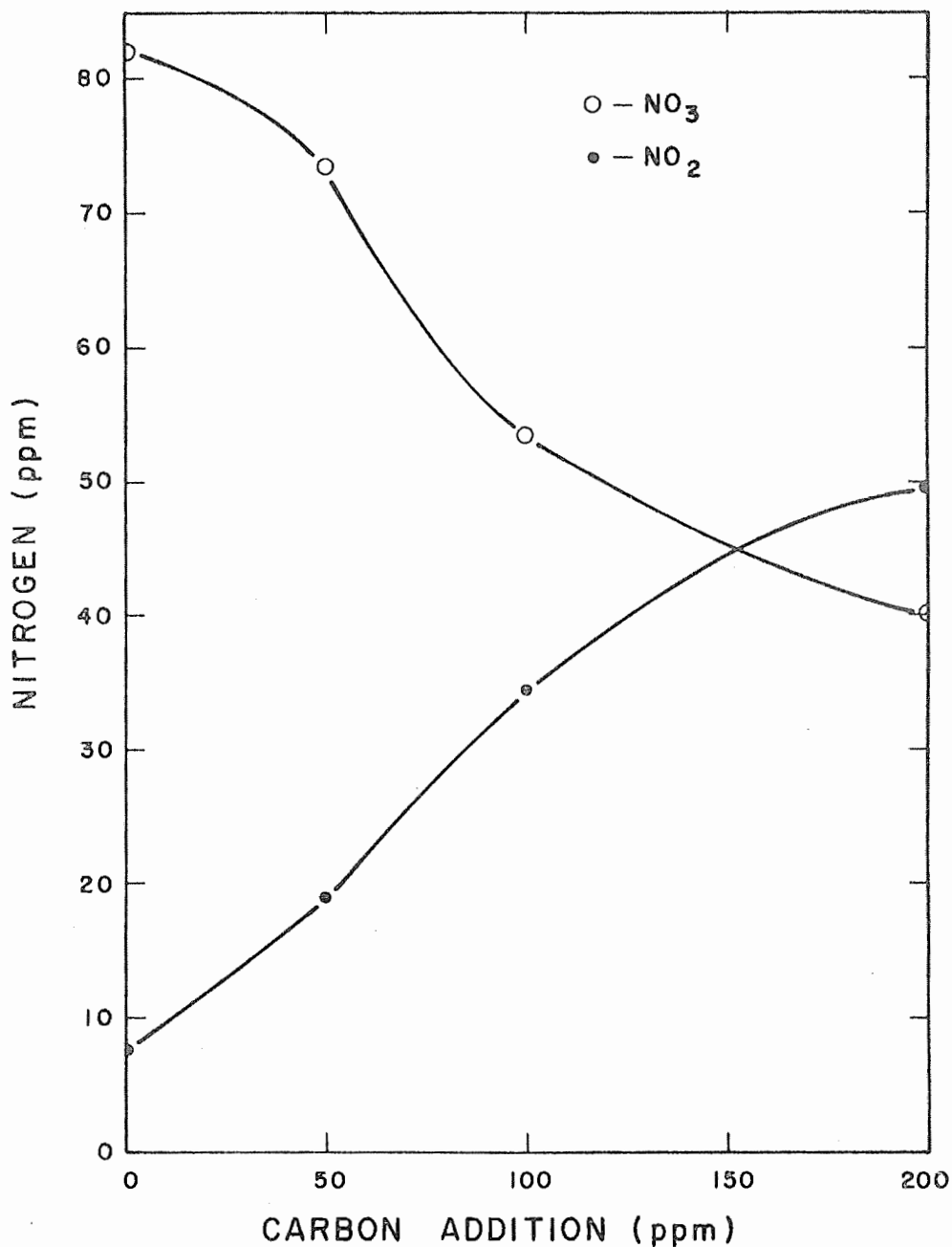


Figure 3. The nitrate and nitrite concentrations in water from soil columns flooded with sewage water containing different levels of organic carbon. (C concentrations entering the columns were less than the concentrations added to the sewage water due to deterioration in the containers.)

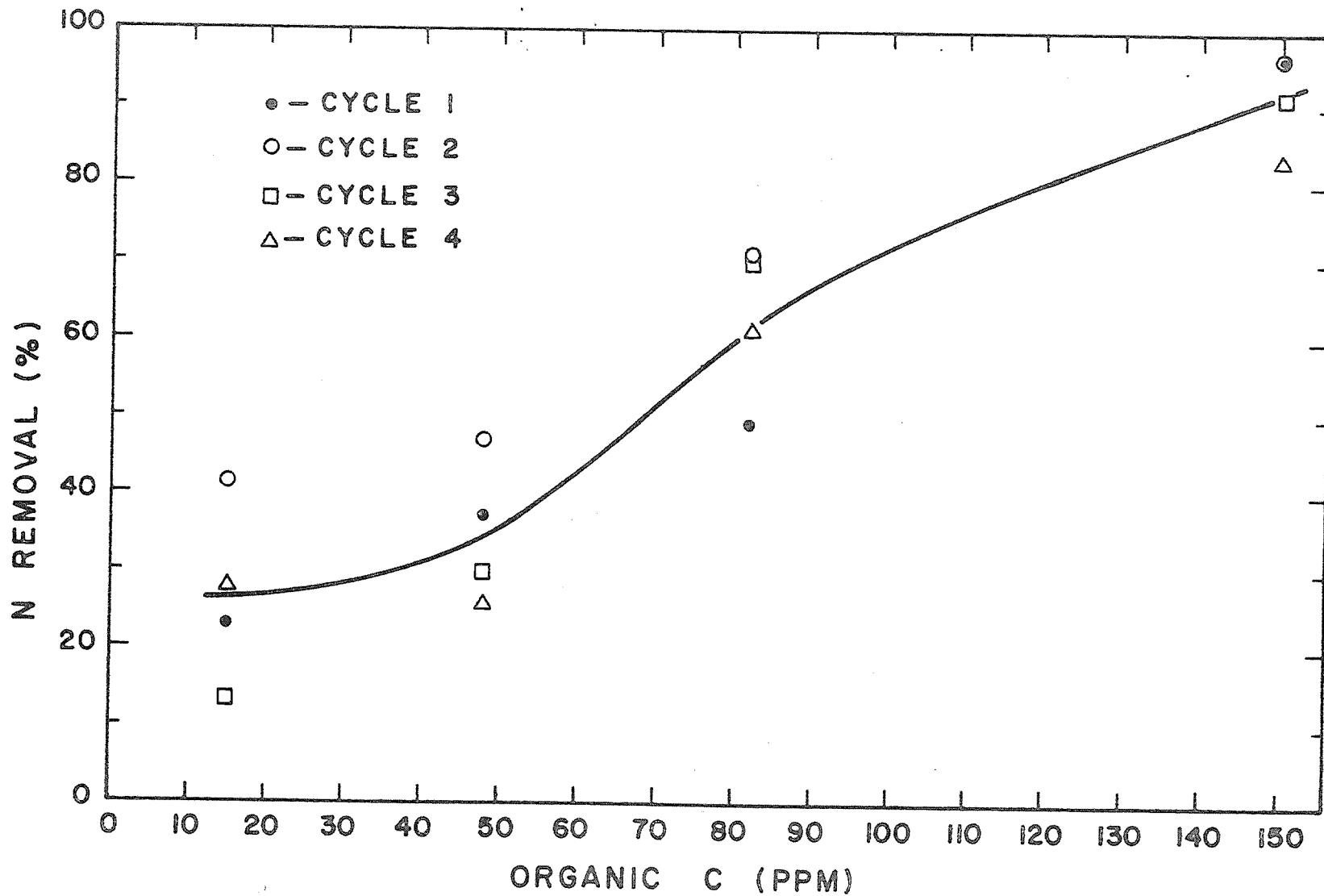


Figure 4. The effect of the organic carbon content of secondary sewage effluent on percent nitrogen removal from the sewage by soil columns flooded on cycles of 9 day flooding and 5 day drying. The sewage was supplemented with dextrose to provide levels of organic C.

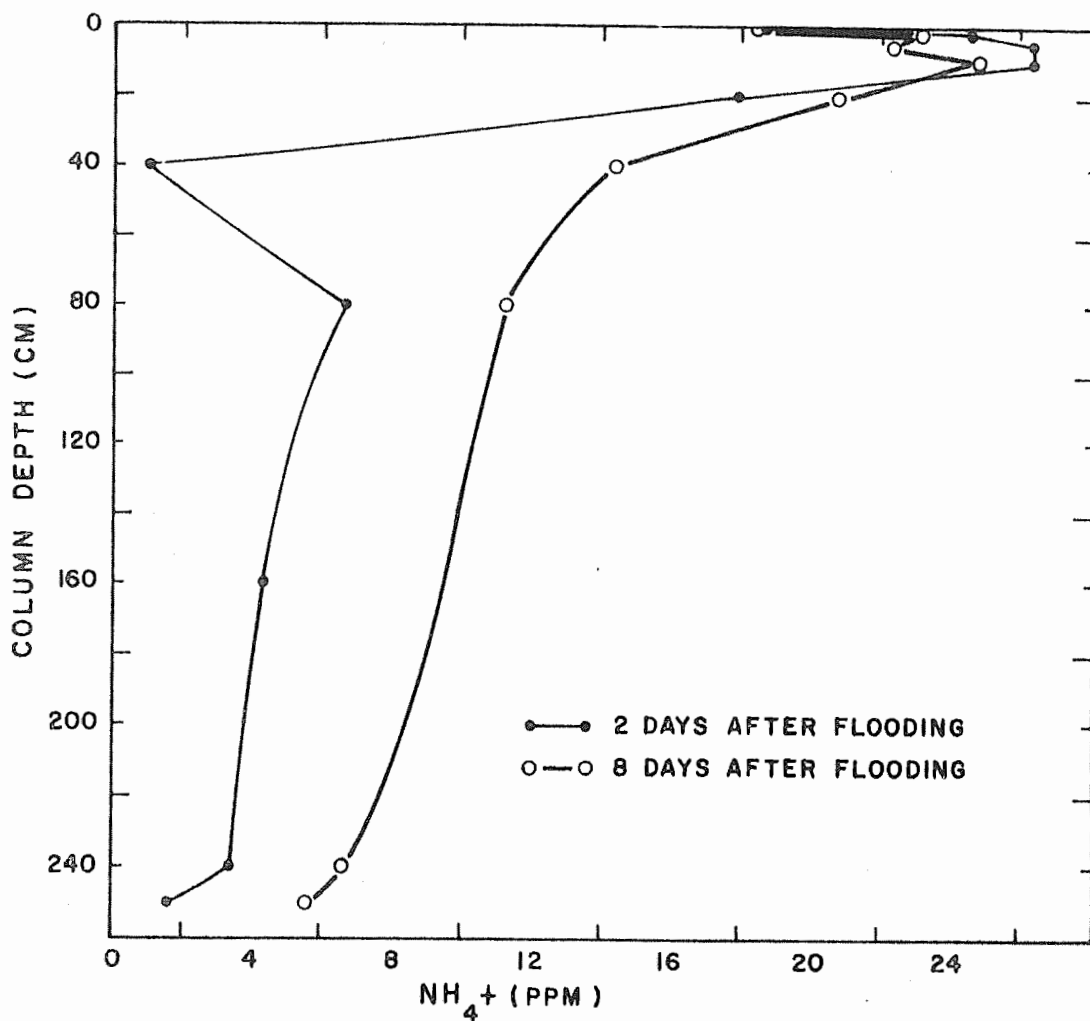


Figure 5.  $\text{NH}_4^+$  concentrations of samples from various depths along soil columns flooded with secondary sewage effluent.

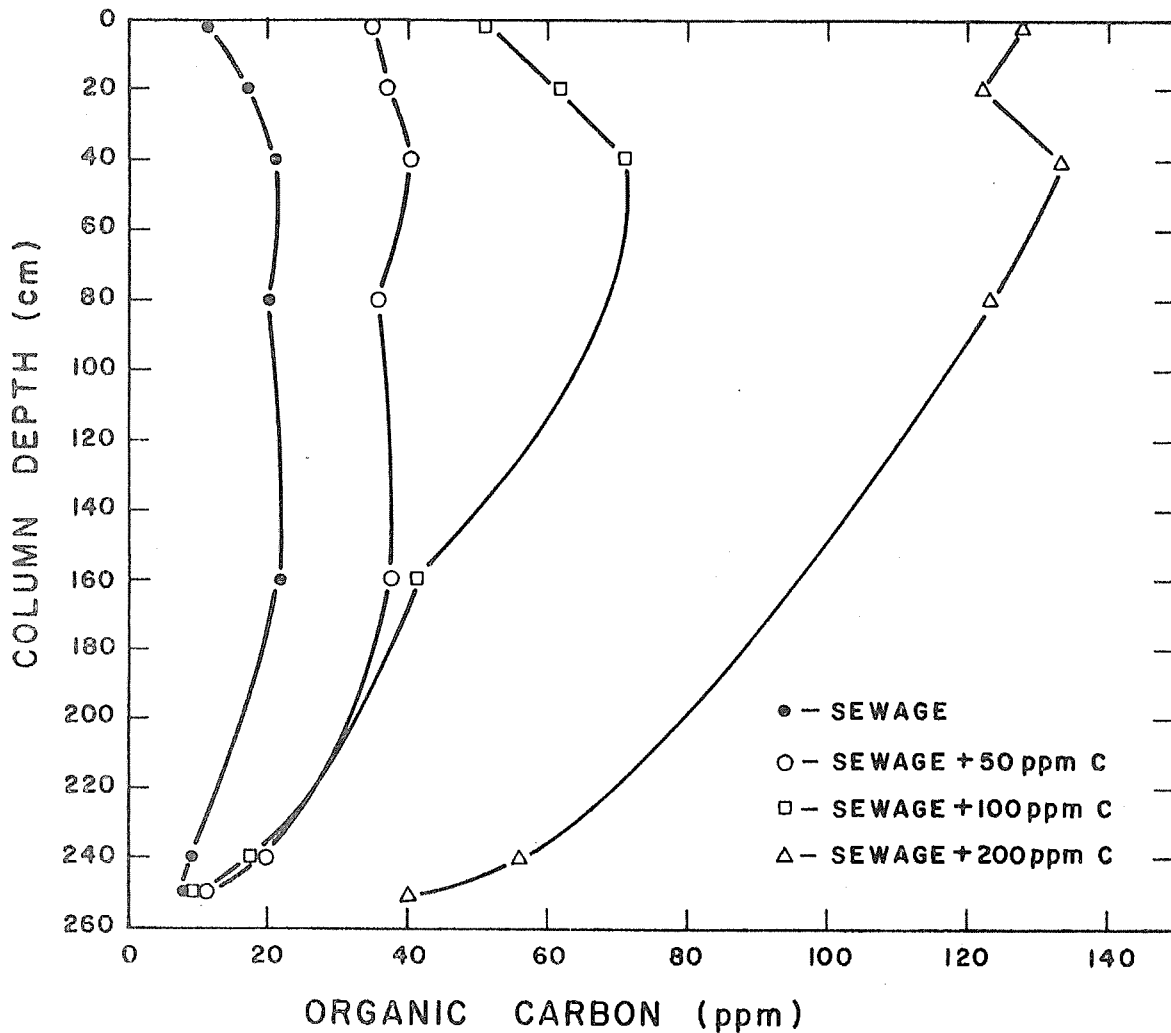


Figure 6. The organic carbon concentration of samples from different depths along soil columns flooded with sewage water supplemented with various levels of organic carbon as methanol. (C concentrations entering the columns were less than the concentrations added to the sewage water due to deterioration in the containers.)

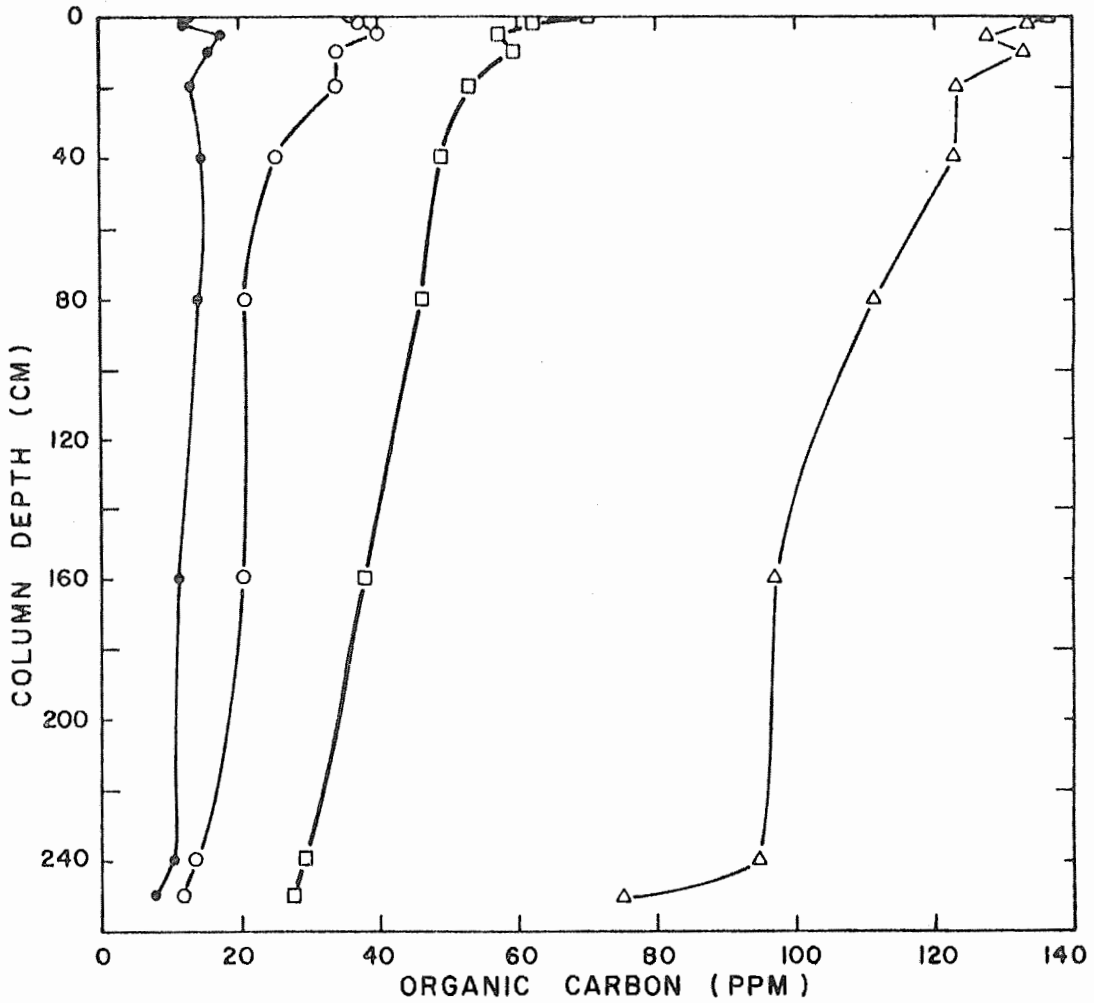


Figure 7. Organic carbon concentrations of samples from various depths along soil columns flooded with secondary sewage effluent supplemented with different levels of organic carbon as dextrose. (Average organic C concentrations entering the columns were 15, 40, 80, and 150 ppm.)

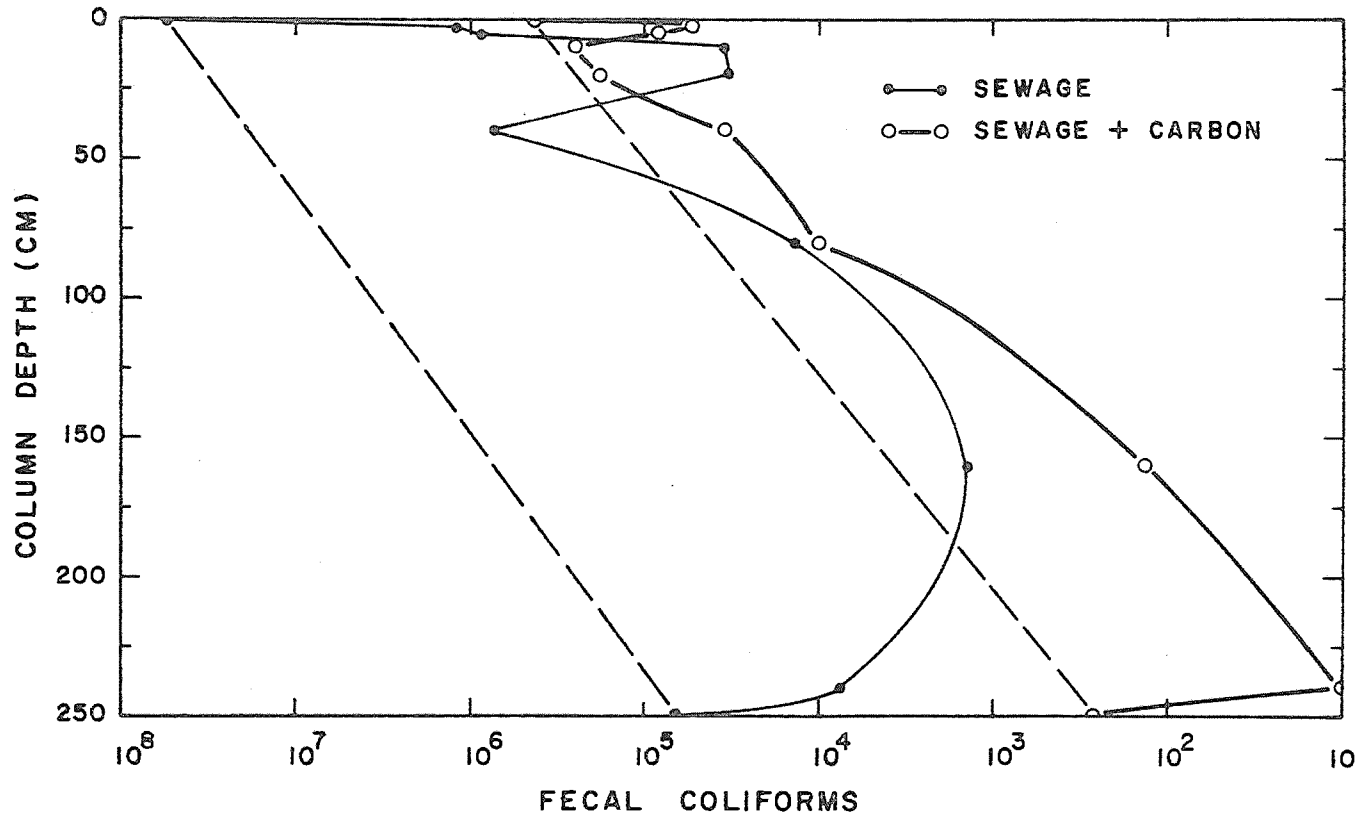


Figure 8. Fecal coliform counts of samples from various depths along soil columns flooded with secondary sewage effluent supplemented with organic carbon as dextrose.

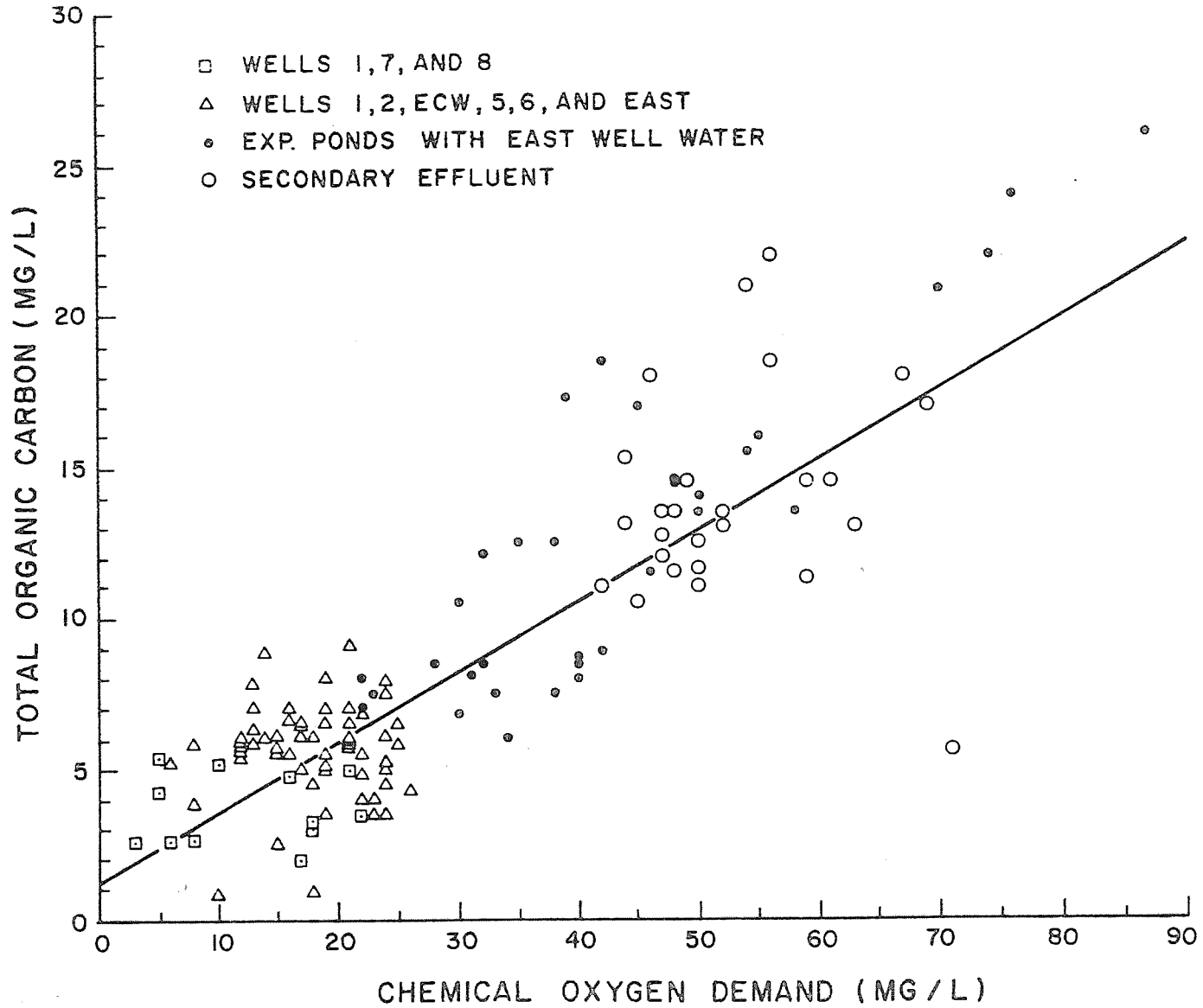


Figure 9. Relation between TOC and COD for various waters.  
Annual Report of the U.S. Water Conservation Laboratory

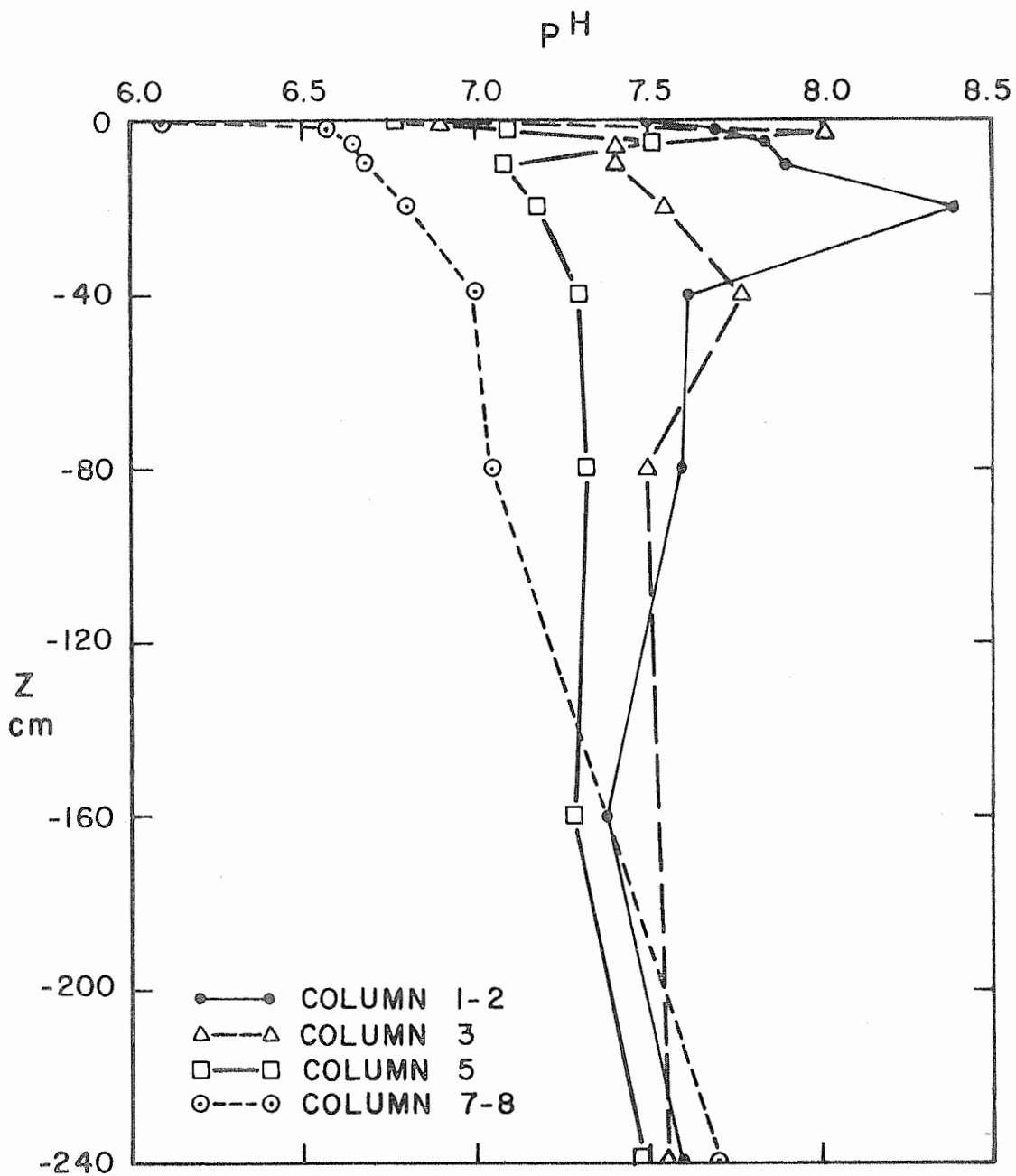


Figure 10. Profiles of pH for soil columns flooded with secondary sewage effluent. Columns 1-2 had sewage water only (15-ppm organic carbon); column 3 had 50-ppm organic carbon; column 5, 100-ppm organic carbon; and columns 7-8, 150-ppm organic carbon.

9-26

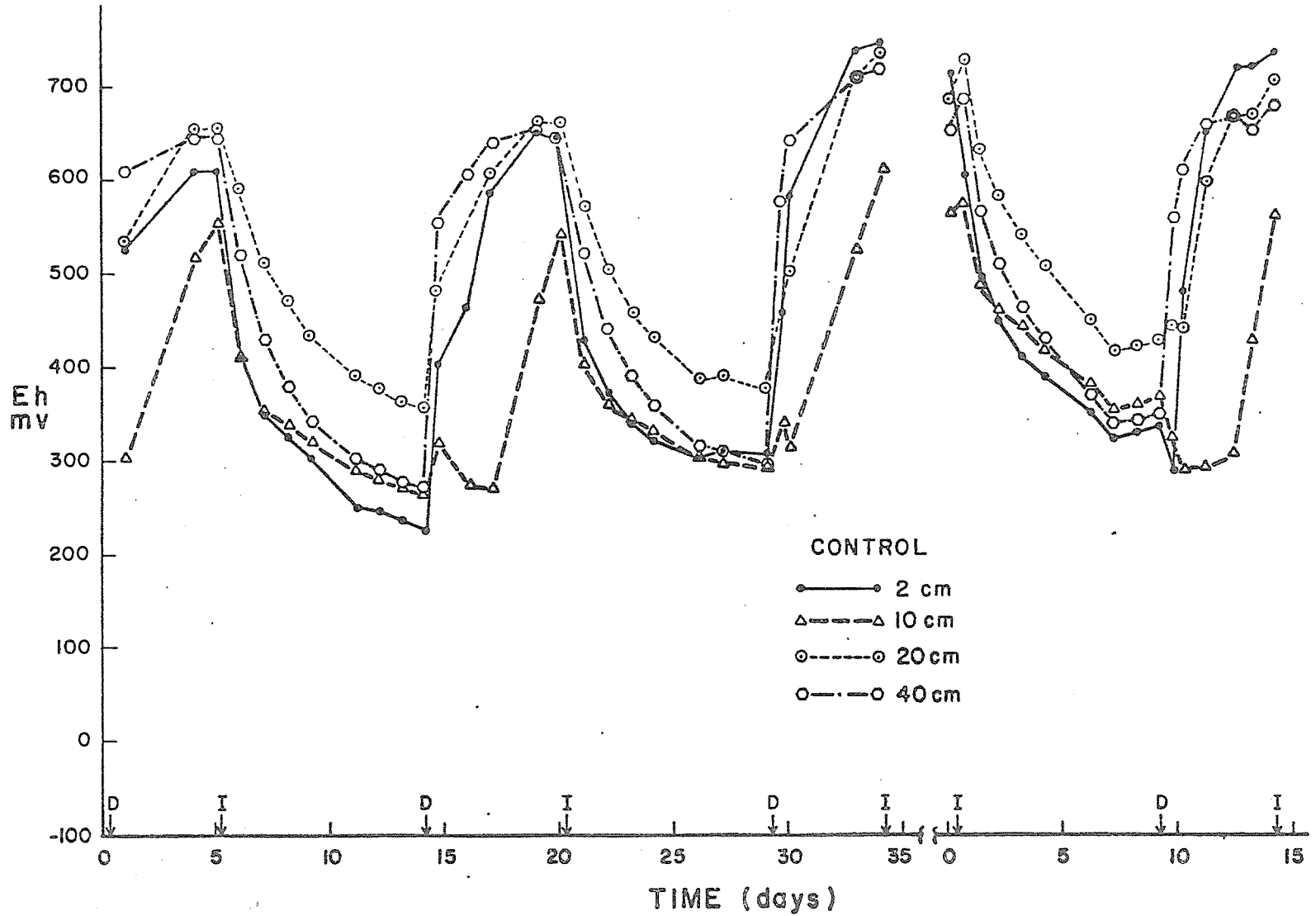


Figure 11. Redox potential as a function of time and depth for soil columns flooded with secondary sewage effluent. I and D on the time scale are the starting times for infiltration and drainage, respectively.

9-27

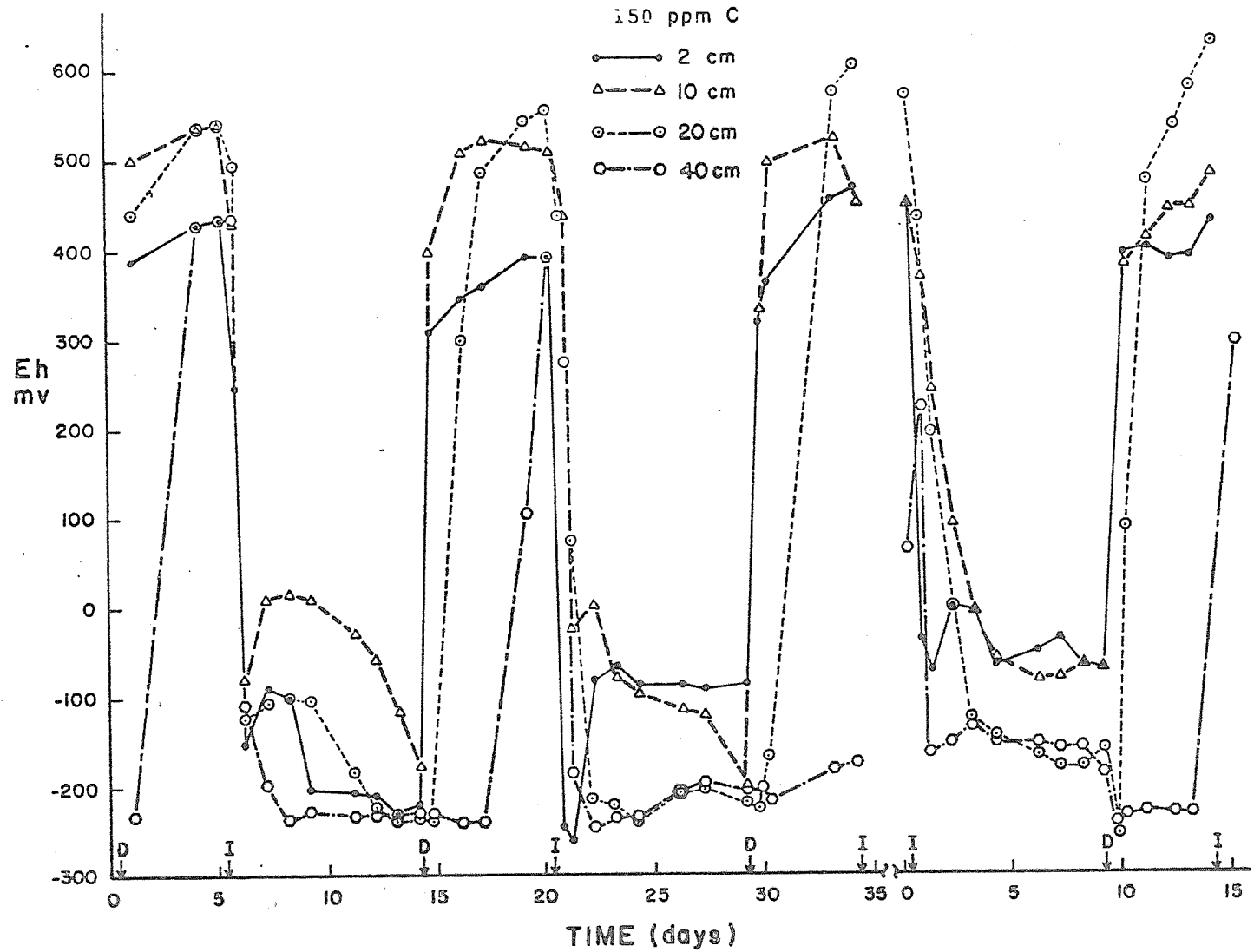


Figure 12. Redox potential as a function of time and depth for soil columns flooded with secondary sewage effluent containing 150-ppm added carbon.

9-28

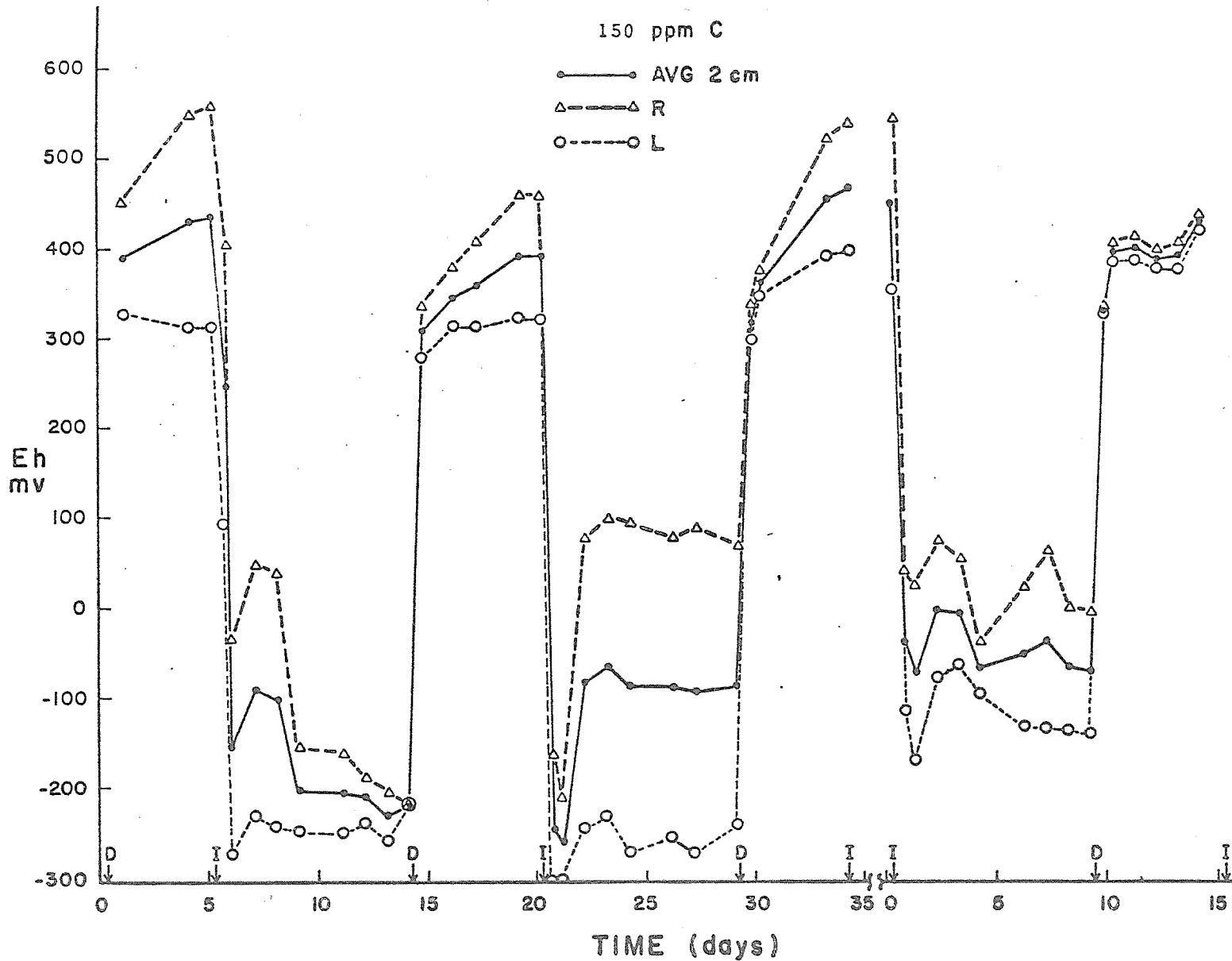


Figure 13. Redox potential as a function of time for two probes at 2-cm depth in a soil column flooded with secondary sewage effluent containing 150-ppm added carbon.

9-29

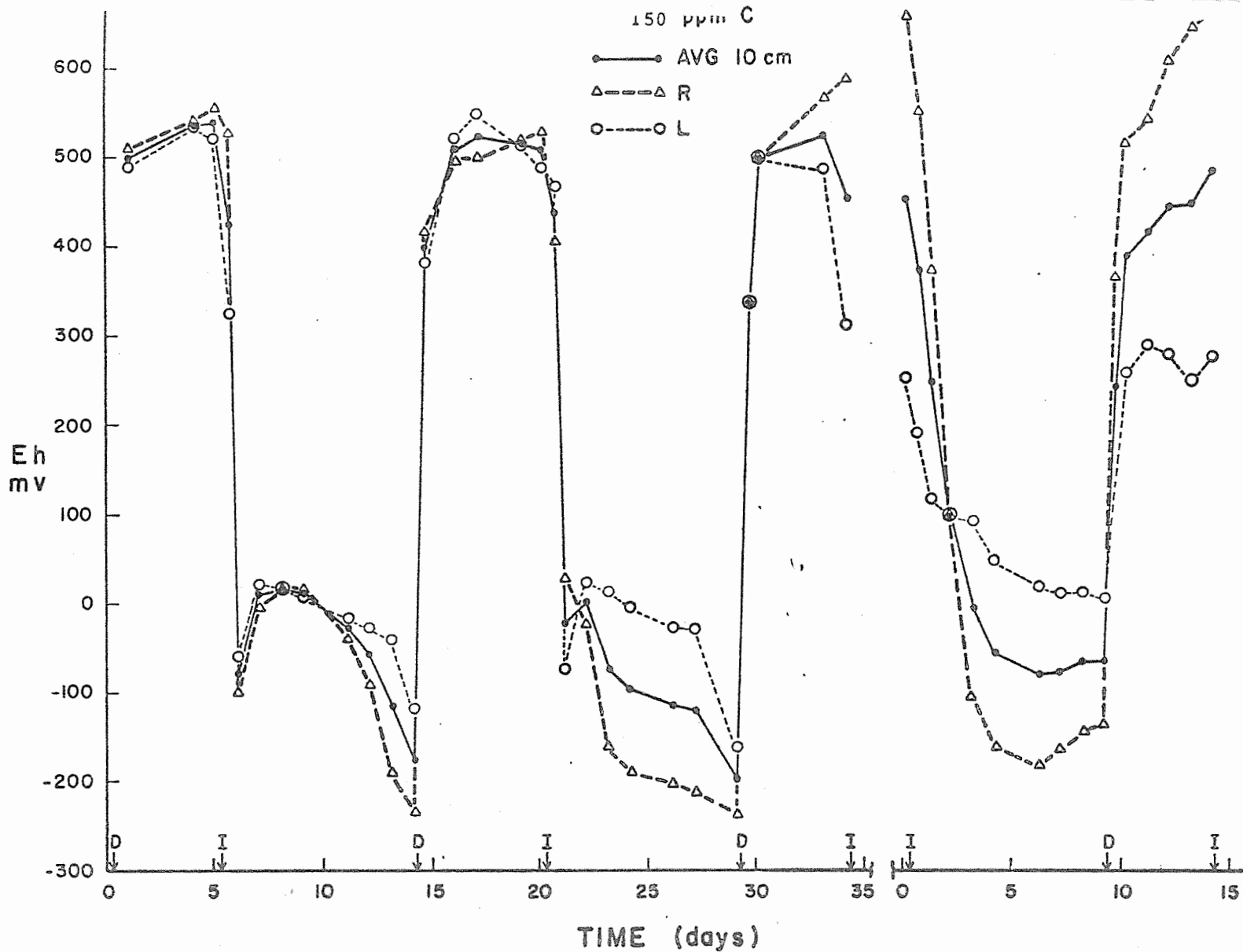


Figure 14. Redox potential as a function of time for two probes at 10-cm depth in a soil column flooded with secondary sewage effluent containing 150-ppm added carbon.

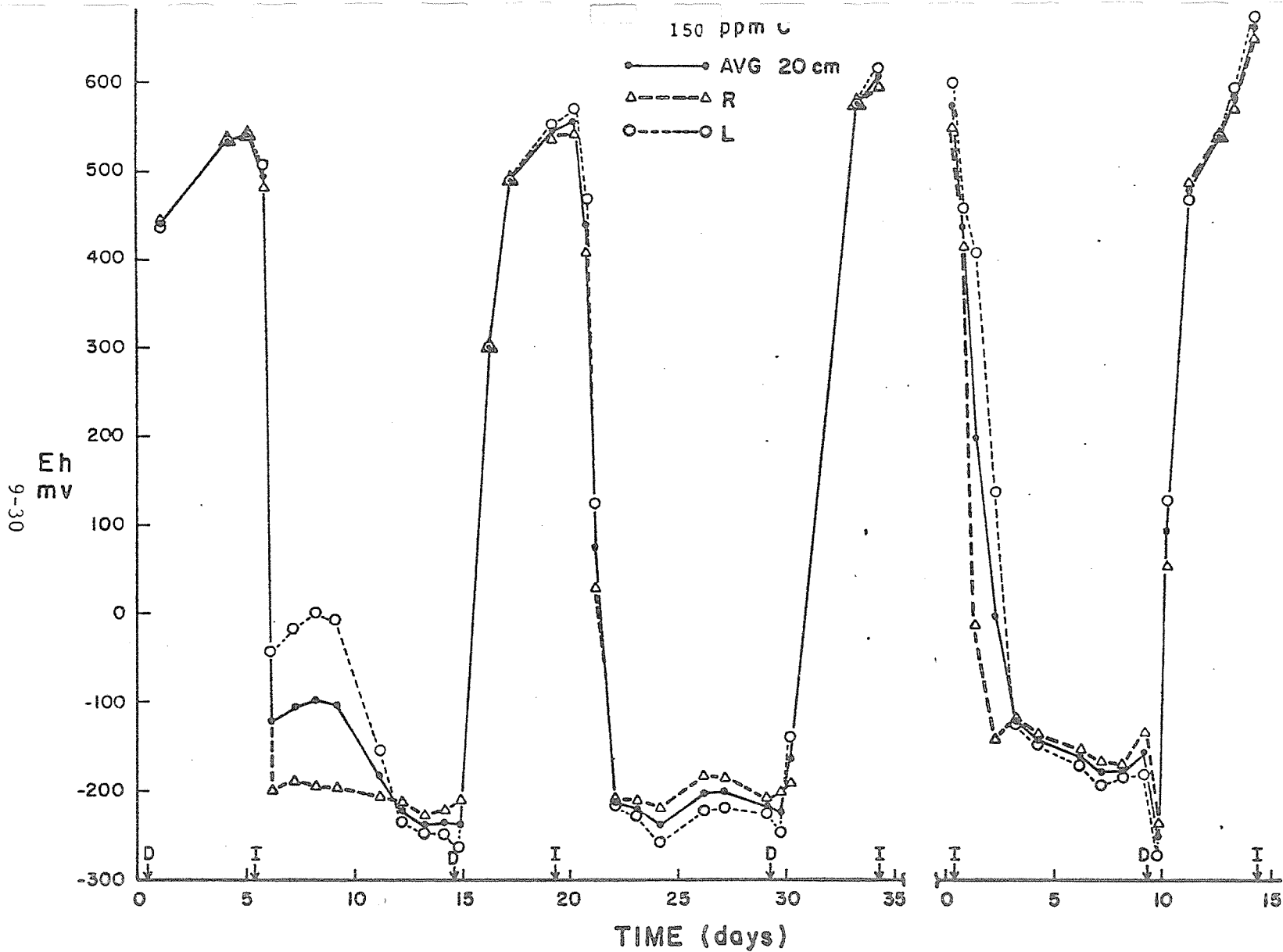


Figure 15. Redox potential as a function of time for two probes at 20-cm depth in a soil column flooded with secondary sewage effluent containing 150-ppm added carbon.

9-31

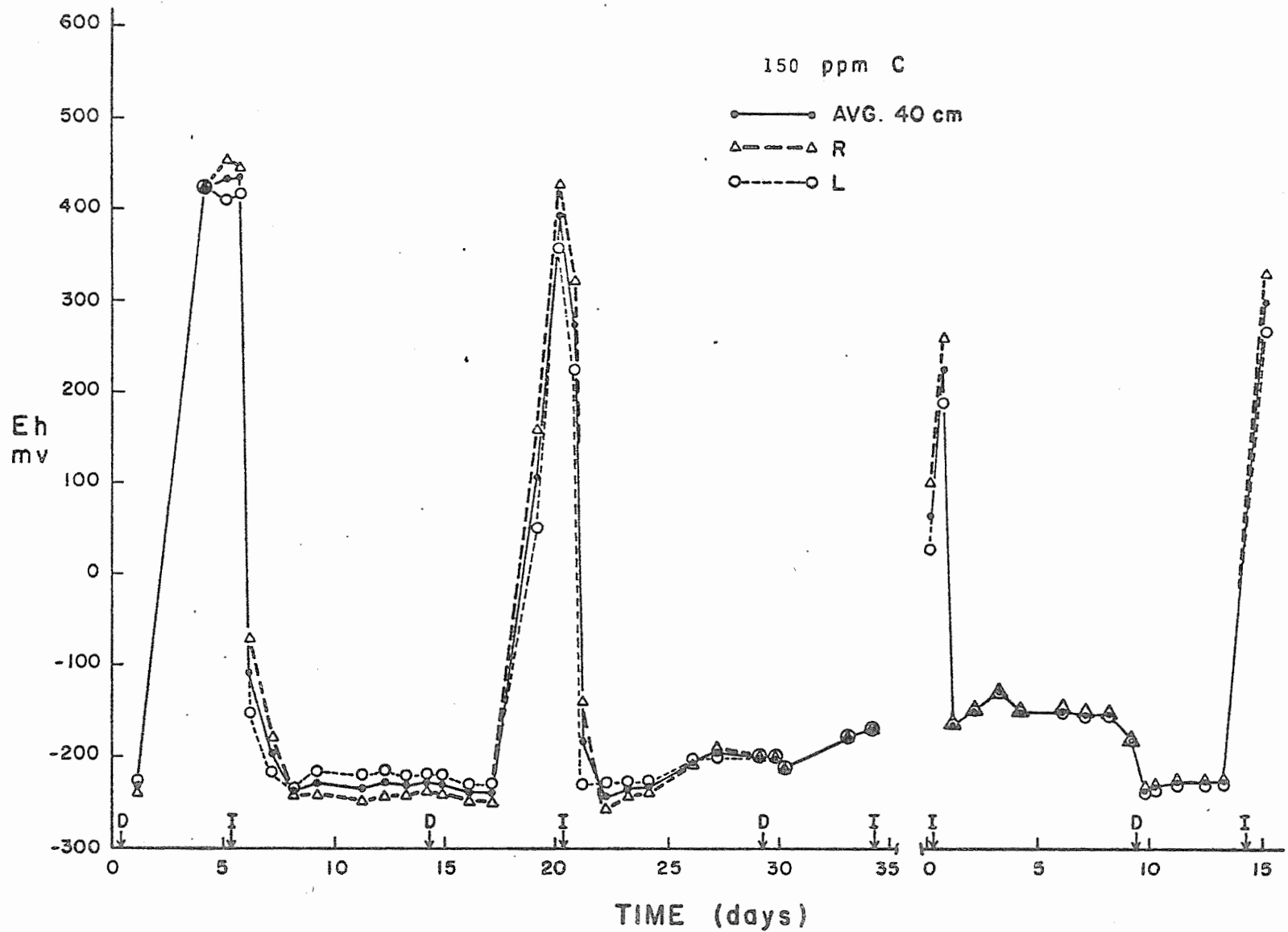


Figure 16. Redox potential as a function of time for two probes at 40-cm depth in a soil column flooded with secondary sewage effluent containing 150-ppm added carbon.

TITLE: ASSESSING THE ENERGY ENVIRONMENT OF PLANTS

CRIS WORK UNIT: SWC-018-gG-4

CODE NO.: Ariz.-WCL-68-5

INTRODUCTION:

Outside of a short period spent in summarizing the results of the previous two years' solar radiation-air pollution studies, work this year dealt rather exclusively with the hemispherical radiometer developed in 1970. It was tested against the Funk technique of transformation, vastly simplified, and used in two field studies.

PROCEDURES AND RESULTS:

A comparison of four Fritschen net radiometers and two Funk net radiometers converted to hemispherical operation by the procedures of Idso and Funk, respectively, was made in a large, open, bare field over a period of 17 consecutive days. Data were collected every half-hour during this period. Under both clear and cloudy conditions, the mean 24-hour energy totals received by each instrument type differed by only 2.3%. The Idso technique generally gave the higher results throughout the entire 24-hour period, and agreed almost exactly with the combination of measured solar and calculated clear sky atmospheric thermal radiation utilizing the Idso-Jackson formula. If the Swinbank formula had been used, however, the theoretical results would have been about 2% lower and thus closer to the Funk results. Since there is no basis for choosing between these two formulas in the air temperature range of this study, both instrument transformation techniques were concluded to be equally valid.

The Idso transformation technique was subsequently simplified as follows: instead of constructing a second set of polyethylene domes and sandwiching three fine thermocouples between the bottom pair and spraying the outer surface with black and then white paint, the paint was applied directly to the lower dome without its dismantlement and a thermocouple subsequently taped to the painted surface. During an extended field comparison of the two procedures for a period of 19 days, there was essentially no difference

between the 24-hour totals of the two techniques. Even instantaneous midnight and solar noon values differed by less than 1%.

Following these tests, the Idso technique was used to measure incoming atmospheric thermal radiation in two field studies. In the first, four replicated measurements of atmospheric thermal radiation were obtained every half-hour of seven clear days during February. All indicated the existence of systematic deviations from the predictions of empirical formulae. By invoking an explanation for the existence of such deviations recently given by Paltridge, however, the times of occurrence of these deviations could be predicted quite accurately.

The second study concerned the comparative solar and long-wave energy fluxes during a dust storm under cloudless skies as opposed to non-dust storm conditions. The results indicated that increased atmospheric thermal radiation under the dust storm conditions more than compensated for the reduced reception of solar radiation. Consequently, it was concluded that increasing the dust content of the earth's atmosphere may not necessarily tend to cool the earth, as most atmospheric scientists have supposed, but may possibly cause it to warm up somewhat.

#### SUMMARY AND CONCLUSIONS:

A field comparison of the Funk and Idso techniques for transforming net radiometers into hemispherical radiometers indicated that both procedures were equally valid. A test of a simplified version of the Idso technique also proved valid. The basic technique was used to detect some systematic deviations in atmospheric thermal radiation from predictions of empirical formulae and to characterize radiative regimes of both the clear and dusty atmosphere.

PERSONNEL: S. B. Idso

OUTLINE TERMINATED: Sept. 1971

TITLE: DESIGN AND PERFORMANCE OF TRICKLE IRRIGATION SYSTEMS  
CRIS WORK UNIT: SWC-018-gG4 CODE NO.: Ariz.-WCL 70-3

The need and objectives for this study are given in the 1970 Annual Report. A method for improving uniformity of discharge from orifices along a low-pressure trickle irrigation lateral was developed in 1971. This proposal is described in Part I. In addition, a field experiment using trickle irrigation for cotton production was completed and is reported in Part II.

#### PART I. IMPROVED PRINCIPLES AND METHODS FOR DESIGNING TRICKLE IRRIGATION SYSTEMS.

##### INTRODUCTION:

Trickle irrigation systems, at present, do not apply water with perfect uniformity along the crop row. Some of the variability is caused by manufacturing imperfections in the applicators and by applicator clogging. These problems can be corrected by improved manufacturing processes, water filtration, and management techniques to avoid salt precipitation. The major problem in system design is the friction-induced pressure drop in the direction of flow within the applicator pipe. High pressure, high head loss applicator systems have offered the best opportunity for uniform applicator discharge up to the present time. Previously designed low-pressure systems have suffered from non-uniform applicator discharge because the pressure changes along the pipe represent a relatively high percentage of the total pressure. Low-pressure systems could have several advantages over high-pressure systems in terms of lower manufacturing and operating costs, larger orifices to reduce clogging, and simple pressure and flow regulation devices. An alternative for improving uniformity from low-pressure systems is to use simple orifices with diameters varied to compensate for pressure changes along the pipe.

## RESULTS AND DISCUSSION:

Arithmetic calculations to characterize flow in a pipe with a large number of outlets are time-consuming, so a computer model providing for different orifice sizes along the pipe was developed. This model calculated effects of friction, velocity, and elevation from the Bernoulli energy equation, while applicator flow interference was ignored. The computer calculations are quite precise. Such precision may not be necessary, however, because deviations from design assumptions will inevitably occur in the actual system. Simplified calculations and graphical methods offer reasonable solutions for trickle system design.

The graphical procedure was used to show the validity of changing orifice sizes. The theoretical performance of a system using five orifice sizes in a 250-ft lateral was compared with a system that was identical except that a single intermediate-size orifice was used. Initial line pressure was 2 psi, orifices were spaced 2 ft apart, and orifice design discharge was 1.5 gph. Maximum deviations from design discharge were +21.0% to -7.4% for the single size system vs  $\pm$  3.3% for the multiple-size system.

A comparable multiple-size system was constructed and field tested. The hand-made orifices were not identical and mean deviation of discharge from orifices of the same diameter ranged from 1.7% to 3.3% when operated at the same pressure. Also, a proper range of orifice sizes were not available. Despite this handicap, maximum deviations from design discharge were +5.2% to -6.6%. HCl was initially used to insure that orifices were clean before checking discharge rates. Later, the 250-ft lateral was placed on a single-row cotton bed and performed satisfactorily for a single growing season. Some orifice plugging due to salt precipitation was especially noticed in the field where applicators were exposed to sunlight.

## SUMMARY AND CONCLUSIONS:

Application uniformity from low-pressure trickle irrigation systems can be greatly improved by varying outlet sizes to compensate for friction-induced pressure changes in the lateral pipe. Low-pressure systems using single applicator sizes suffer from non-uniform applicator discharge because friction-induced pressure changes are a large percentage of total pressure. High-pressure trickle systems alleviate this problem by using high head loss applicators. Low-pressure systems, using simple orifices, can have several advantages over high-pressure systems in reduced manufacturing and operating costs, larger orifices to reduce clogging, and simpler flow control devices. Comparable application uniformity can be obtained by varying orifice sizes in the low-pressure systems. Procedures for designing low-pressure, multiple orifice size trickle systems by computer or by a simplified computation and graphic method were developed. Theoretical computations and the performance of an actual system showed a marked advantage for a multiple orifice size system over a single-size system.

## PART II. TRICKLE IRRIGATION MANAGEMENT FOR COTTON PRODUCTION

### INTRODUCTION:

Alleged advantages of trickle irrigation over other irrigation methods include higher crop yields and use of less water. These advantages, however, have not been proven. To acquire practical knowledge in trickle irrigation management, an experiment on cotton was initiated in 1971. Cotton was not chosen because it would be economical to raise cotton with trickle, but because it is an excellent "indicator" crop of moisture stress. The objective of the field experiment was to develop criteria for managing trickle irrigation for increased water-use efficiency and improved crop production.

### PROCEDURE:

The experiment was located on 16 rows on the west side of Field C-1 at the University of Arizona Cotton Research Center, Phoenix,

Arizona. Prior history of the field included barley for one year and cotton for three years prior to barley. After cotton stalks from the 1969 season were plowed under and fertilizer applied (150 lb/acre of 21-53-0), Arivat barley was planted. Barley was then harvested on 24 June 1970; urea applied to the field (250 lb/acre); Arivat barley once again planted on 30 September 1970; urea applied to the field (170 lb/acre); and the second barley crop was plowed under as green manure on 12 January 1971. Residual effects were now eliminated from the field, and it was readied for cotton production. On 5 April, the field was furrowed out into 40-inch furrows, and Deltapine-16 cotton was planted on 16 rows plus 2 buffer rows. Gravity irrigations were given on 6 and 10 April for germination; 36 individual plots (20 ft long and 4 rows wide) were laid out; and the plots were thinned on 10 May to a population of 20,000 plants per acre.

The trickle irrigation system used for the experiment was Chapin's "Twin-Wall" irrigation hose, with an 8-inch spacing of outside holes and a 32-inch spacing of inside holes. A manifold system was designed to supply and measure water applications to the individual plots. Time of application was controlled by electric time clocks and solenoid valves, and water application was measured with a turbine vane, household-type water meter.

Management criteria for trickle irrigation was investigated by applying three irrigation quantities, based on ratios of the plant's consumptive use estimate, at three irrigation frequencies. The quantities were 1.0, 0.8, and 0.6 ratios of the consumptive use estimate for cotton on a standard furrow irrigation practice. Seasonal use for cotton is estimated to be 41.2 inches, as determined from eight years of gravimetric soil moisture measurements at the Cotton Research Center. Seasonal use of 41.2 was taken to represent the 1.0 consumptive use estimate. The three quantities were applied at frequencies of every 3, 6 and 12 days; thus, prescribed quantities were applied at set dates according to estimated consumptive uses.

These nine treatment combinations were subsequently randomized in a split-plot design and replicated four times.

#### RESULTS AND DISCUSSION:

A good stand was obtained, with temperatures slightly below normal in April and early May, and above normal during the last half of May. Trickle irrigations were started on 17 May for all treatments. Precise quantities of water were applied at each quantity ratio and frequency until 1 October. For irrigation frequencies of 3, 6 and 12 days, the total number of trickle irrigations were 44, 22, and 11, respectively. Rainfall on all plots from 1 April to 1 November amounted to 2.6 inches. From moisture sampling on 19 May, before starting trickle irrigations, the water stored for later consumptive use was estimated to be 6.5 inches. Table 1 shows the available moisture for consumptive use to include rainfall, and gravity and trickle irrigations, resulting in adjusted 1.06, 0.90, and 0.72 ratios of the consumptive use estimate (41.2 inches).

Insect populations were low in the early season, with minimum lygus and leaf perforator damage, and the pink bollworm damage late in the season was also small, because of an excellent insecticide control program. The field was defoliated twice, on 18 and 26 October. These defoliations were assumed to be late enough so that overall yield was not greatly affected. However, an early frost on 26 October undoubtedly reduced late-season boll size and overall yield.

Hand-picked yield and boll-count measurements were made on 30 ft of the two inside rows for the 4-row plots on 1 September, 8 October, and 20 November. Table 2 shows the accumulated cotton production for the season at the adjusted quantities for each irrigation frequency in terms of mean seed weight, weight per boll, lint percentages and lint weight, from four replications. Analysis of variance for boll size showed that differences for the season were non-significant at the 10% level, although trends were evident. Boll sizes tended to become smaller with longer irrigation frequencies at the adjusted

1.06 and 0.90 consumptive use, and boll size tended to be smaller for all frequencies at the adjusted 0.72 consumptive use, as compared to 1.06 and 0.90 ratios. Mean lint percentages for the entire season showed no significant difference. Lint weight in bales per acre was exceptionally good this year, for all trickle irrigation plots. Analysis of variance on yield data showed no significant difference among the three frequencies for each of the three irrigation quantities, but there was a significant 18% yield reduction for the adjusted 0.72 consumptive use as compared to 0.90 and 1.06 ratios.

Table 2 also shows calculated water-use efficiencies in lint production per acre-inch of water (based on adjusted available moisture figures for consumptive use) for the nine treatment combinations. The adjusted 0.72 consumptive use obtained a slightly greater mean water-use efficiency, although there was an 18% reduction in yield. Nevertheless, with an additional 7 inches of available moisture and a small mean reduction in water-use efficiency of 1.7%, the adjusted 0.90 consumptive use provided a significant increase in yield of 0.5 bales per acre.

#### SUMMARY AND CONCLUSIONS:

Trickle irrigation management for increased water-use efficiency and improved crop production was investigated, using cotton as the "indicator" crop. Irrigations consisted of three quantities, based on ratios of the plant's consumptive use estimate, applied at three frequencies. The three adjusted quantities, to include rainfall, gravity irrigations for germination, and trickle irrigations, were ratios 1.06, 0.90, and 0.72 times the seasonal consumptive use estimate of 41.2 inches. The three frequencies were every 3, 6 and 12 days. Cotton yield response showed no difference between irrigation frequencies and an 18% reduction in yield for the 0.72 consumptive use as compared to the 0.90 and 1.06 quantities. The mean cotton yield for 1.06 and 0.90 quantities was 3 bales/acre. A slightly greater water-use efficiency resulted from the 0.72

consumptive use, along with a significant reduction in yield, whereas the 0.90 consumptive use provided nearly as high a water-use efficiency. This study would suggest that plant needs for maximum production with trickle irrigation on cotton are nearly the same as present consumptive use estimates for furrow irrigation.

PERSONNEL: Dale A. Bucks, Leonard J. Erie, Lloyd E. Myers, and  
O. F. French.

CURRENT TERMINATION DATE: October 1973.

<u>Quantity of Irrigations</u>	<u>Frequency of Irrigations (days)</u>	<u>Rainfall on All Plots (inches)</u>	<u>Gravity Irrigation April 6 &amp; 10 Water Stored (inches)</u>	<u>Trickle Irrigation May 17 thru Oct 1 Water Applied (inches)</u>	<u>Available Moisture for Consumptive Use (inches)</u>	<u>Adjusted<sup>a</sup> Quantity of Irrigations</u>
1.0	3	2.6	6.5	34.5	43.6	1.06
Consumptive use	6	2.6	6.5	34.7	43.8	Consumptive use
	12	2.6	6.5	35.0	44.1	
0.8	3	2.6	6.5	27.4	36.5	0.90
Consumptive use	6	2.6	6.5	27.4	36.5	Consumptive use
	12	2.6	6.5	29.0	38.1	
0.6	3	2.6	6.5	20.5	29.6	0.72
Consumptive use	6	2.6	6.5	20.4	29.5	Consumptive use
	12	2.6	6.5	21.8	30.9	

<sup>a</sup> Mean of 3 frequencies; 1.0 consumptive use = 41.2 inches.

TABLE 2. COTTON PRODUCTION WITH TRICKLE IRRIGATION, 1971.  
(DPL-16, 20,000 plants per acre).

<u>Adjusted Quantity of Irrigations</u>	<u>Frequency of Irrigations</u> (days)	<u>Seed</u> <sup>a</sup> (gms/plot)	<u>Wt/boll</u> <sup>b</sup> (gms)	<u>Lint</u> <sup>c</sup> (%)	<u>Lint</u> <sup>d</sup> (bales/acre)	<u>Water-use</u> <sup>a</sup> <u>Efficiency</u> (lbs/acre-in of water)
1.06 Consumptive use	3	4237	4.08	35.9	2.92	33.5
	6	4432	4.02	36.3	3.09	35.3
	12	4467	3.99	35.7	3.06	34.7
0.90 Consumptive use	3	4285	4.12	36.1	2.97	40.7
	6	4299	4.09	36.4	3.00	41.2
	12	4267	3.88	36.8	3.02	39.5
0.72 Consumptive use	3	3643	3.90	36.3	2.54 **	42.9
	6	3361	3.82	36.6	2.36 **	40.0
	12	3561	3.90	36.9	2.52 **	40.7

<sup>a</sup> Mean, four replications.

<sup>b</sup> Mean, four replications, ns between frequency or quantity.

<sup>c</sup> Mean, four replications, ns between frequency or quantity.

<sup>d</sup> Mean, four replications, ns between frequency, .72 cu highly sig. from 1.06 and .90 cu.

\*\* Sig. at .01 level.

6-11

TITLE: RELATIVE CHANGES IN TRANSPIRATION AND PHOTOSYNTHESIS INDUCED BY SOIL WATER DEPLETION IN A CONSTANT ENVIRONMENT.

CRIS WORK UNIT: SWC-018-gG-4 CODE NO.: Ariz.-WCL-71-1

INTRODUCTION:

Much research has been done on transpiration, both in the laboratory and the field. Likewise, there has been an abundance of photosynthesis research, although most of it emphasizing laboratory studies. However, relatively few investigations have dealt with both processes simultaneously as they are affected by soil water depletion. Yet, such studies are necessary because they hold promise of improving a plant's water-use efficiency (WUE) and thus decreasing the tremendous amount of water that crops use in competition with increasingly important urban demands. A crop with a high WUE is defined as one with a low transpiration ratio (TR), which, in turn, is defined as the number of units of water transpired per unit gain in dry weight or per unit of photosynthesis.

The objective of the present research is to find ecologically important species differences in the TR by surveying widely different plant species, as characterized by their short-term responses to drought imposed in a controlled environment. This report deals with the facilities and instrumentation that have been assembled for studying WUE in the Controlled Environment Room.

PROCEDURE:

When the equipment has been fully tested, well known agricultural crops such as cotton and sorghum will be studied at first. Later it is planned to extend the research to succulents and perhaps some other desert species. The technique will consist of greenhouse culture of the plant until several mature leaves are present, followed by short-term measurements of both transpiration and photosynthesis in the Controlled Environment Room.

The measurements will be made in either a small chamber designed for an intact leaf or a large chamber accommodating a whole

intact plant.

Continued transpiration will be permitted to deplete the soil water content from the initial fully irrigated value to a lesser amount low enough to induce at least partial stomatal closure due to leaf dehydration.

During the test the following environmental factors will be kept constant: air temperature, vapor pressure, light (after a "sunrise," windspeed, and CO<sub>2</sub> content of the air.

Theory. Calculation of the TR requires data for the following equation:

$$TR = \frac{T}{P} = \frac{\frac{\Delta C}{R_A + R_L}}{\frac{\Delta' C}{R'_A + R'_L + R'_M}} \quad (1)$$

where T = transpiration, in g cm<sup>-2</sup> sec<sup>-1</sup>, P = photosynthesis, in g cm<sup>-2</sup> sec<sup>-1</sup>, ΔC = the difference in concentration of water vapor between the leaf and ambient air in g cm<sup>-3</sup>, R<sub>A</sub> = the leaf boundary layer resistance, in sec cm<sup>-1</sup>, R<sub>L</sub> = the leaf resistance, also in sec cm<sup>-1</sup>; Δ'C = the difference between the concentration of CO<sub>2</sub> in the ambient air and the leaf chloroplasts, in g cm<sup>-3</sup>, and R'<sub>A</sub> and R'<sub>L</sub> are the respective resistances due to the boundary layer and the stomates to the entrance of CO<sub>2</sub> in the leaf, both in sec cm<sup>-1</sup>. Finally, R'<sub>M</sub>, the so-called "mesophyll resistance," can be obtained as the only unknown in equation (1), and expressed in sec cm<sup>-1</sup>.

Of all the foregoing terms in equation (1) probably the most important are R'<sub>L</sub> and R'<sub>M</sub>. This is because they are involved in the two mechanisms that have been proposed to explain the drought-induced lowering of photosynthesis: (1) stomatal closure, which increases leaf resistance to CO<sub>2</sub>, (R'<sub>L</sub>) and thereby reduces the supply of CO<sub>2</sub>, a raw material for photosynthesis, and (2) an increase in R'<sub>M</sub> due to desiccation of the chlorophyll. The ability

to distinguish between these two mechanisms would be a key to lowering TR. It would be desirable for a plant to maintain a low value of  $R'_M$  as  $R'_L$  was increased by drought.

The numerator on the right side of equation (1) can be partitioned as follows:

$$\Delta C = C_L - C_O \quad (2)$$

where  $C_L$  = the water vapor concentration, in  $g\ cm^{-3}$ , in the sub-stomatal cavities of the leaf, estimated by assuming there is saturation vapor pressure at a given leaf temperature. Leaf temperature is measured with micro-thermojunctions inserted in the leaf midrib.  $C_O$  = the water vapor concentration of the air surrounding the leaf, also in  $g\ cm^{-3}$ .

$R_A$  can be determined by measuring the evaporation rate from a simulated plant with leaves made of green blotter paper, and knowledge of the wet blotter temperature and ambient vapor pressure.  $R_L$  can be measured directly with a resistance meter if a large plant chamber is used, or calculated according to a rearrangement of the numerator on the right side of equation (1) as follows:

$$R_L = \frac{\Delta C}{T} - R_A \quad (3)$$

where T, in turn, is defined as:

$$T = \frac{(C_I - C_O)F}{A} \quad (4)$$

where C is the water vapor concentration, in  $g\ cm^{-3}$ , and the subscripts I and O refer to inlet and outlet air streams, respectively; F = the flow rate, in  $cm^3\ sec^{-1}$ , precisely regulated and then measured with a flow meter or manometer, and A = the leaf area, in  $cm^2$ .  $(C_I - C_O)$  may be calculated from a measurement of the differential vapor pressure,  $\Delta e$ , obtained from measurements with a

differential micro-psychrometer in the air stream through the chamber, as follows:

$$\Delta e = \gamma(T_{WA} - T_{WB}) + e_{WA} - e_{WB} \quad (5)$$

where  $\gamma$  = the psychrometric constant,  $0.667 \text{ mb } (^{\circ}\text{C})^{-1}$ ,  $T_{WA}$  = the wet bulb temperature after the air stream has passed over the leaf,  $T_{WB}$  = the wet bulb temperature of the entering air, and  $e_{WA}$  and  $e_{WB}$  are the corresponding saturation vapor pressures at the wet bulb temperatures. When  $R_A$  is already known, Equations (2), (3), (4) and (5) take care of the right side of Equation (1).

In regard to the denominator of Equation (1),  $P$  is obtained from another equation:

$$P = \frac{(C'_I - C'_O)F}{A} \quad (6)$$

where  $C'_I$  = the  $\text{CO}_2$  concentration at the inlet of the chamber, in  $\text{g cm}^{-3}$ , given by the reading of the absolute IRGA in the Controlled Environment Room,  $C'_O$  = the  $\text{CO}_2$  concentration at the outlet, also in  $\text{g cm}^{-3}$ , which is obtained by subtracting the reading of the differential IRGA (connected across inlet and outlet tubes) from the absolute  $\text{CO}_2$  level. The values for  $F$  and  $A$  are as defined earlier.

$\Delta'_C$  of Equation (1) can be partitioned as follows:

$$\Delta'_C = C'_O - C'_C \quad (7)$$

where  $C'_O$ , defined above, provides the ambient  $\text{CO}_2$  level for the leaf, provided there is vigorous mixing of the air;  $C'_C$  is the  $\text{CO}_2$  level at the chloroplasts, the ultimate destination of the  $\text{CO}_2$  molecule.  $C'_C$  can be estimated by measuring the  $\text{CO}_2$  compensation point.

$R'_A$  can be obtained by multiplying the value of  $R_A$  by 1.35, to account for the difference in the coefficients of diffusion between  $CO_2$  and water vapor. Similarly,  $R'_L$  is obtained by multiplying the value of  $R_L$  by 1.56.

Finally,  $R'_M$  is solved for as the only unknown in Equation (1), after finding  $R_A$  and applying Equations (2) through (7).

#### CONTROLLED FACTORS:

Air Temperature. Precision control and recording of air temperature can be achieved by the recorder-controller for the Controlled Environment Room, to  $\pm 0.2$  C. Within the experimental chambers located in this room additional temperature measurements can be taken with thermocouples. Cool water circulation through water jackets on upper and lower leaf surfaces prevent the leaf chamber from overheating in intense radiation.

For the large chamber a differential filter will be placed between the overhead battery of lights and the transparent polyvinyl chloride chamber. It has been found that a 2-cm layer of water between two 6.3-mm thicknesses of lucite removes 45% of the heat load, but only 5% of the visible light. The heat load inside the chamber will be dissipated by vigorous air flow over chilled water coils. The vigorous air flow will serve also to maintain a low  $R_A$  value in the chamber.

Light. Up to 120, 400-watt mercury vapor lamps can be turned on at one time in the experimental room. A satisfactory illuminance can be developed with 88 lamps, which provide 100 kilolux ( $1.0 \text{ ly min}^{-1}$ ) 1.5 m away from the lamps, i.e. at the usual working level. A card programmer can be used to raise the light level gradually over a variable length of time to simulate a sunrise. With this high a light level, a fully hydrated plant can be expected to have  $R_L$  readings as low as those in the field,  $1.0 \text{ sec cm}^{-1}$ .

Air Flow. A compressor supplies air to the small leaf chamber at a pressure of 2-3 PSIG. Flow is regulated by needle valves and measured by a precision flow meter. However, even when the maximum

air volume of  $1.42 \text{ l min}^{-1}$  is flowing, the cross-sectional area of the leaf chamber is so small ( $31 \text{ cm}^2$ ) that the equivalent air speed is much too low to produce a low  $R_A$ . Therefore, a small propeller blade is spun, with a 3-volt motor and belt, near each leaf surface to induce turbulent air flow and thus to produce a low  $R_A$ . This value was found experimentally to be  $0.08 \text{ sec cm}^{-1}$ . This is suitably low to permit changes in  $R_L$  due to soil water depletion to be reflected in different transpiration rates.

The large chamber achieves the same objective by having vigorous mixing and return flow of air through a heat exchanger.

Carbon Dioxide. No direct control of  $\text{CO}_2$  is available for either the small or the large chamber. However, the Controlled Environment Room can be maintained to within  $\pm 10$  ppm of the normal atmospheric level of 350 ppm  $\text{CO}_2$  by requiring use of gas masks by all personnel entering the room. The air inlets of both chambers admit room air at an initial  $\text{CO}_2$  concentration indicated by the absolute reading of the infrared gas analyzer (IRGA) reserved just for that purpose, with a scale permitting absolute readings from 0 to 500 ppm  $\text{CO}_2$  by volume. A differential IRGA is used to measure the change between inlet and outlet air streams (and to determine by subtraction the amount in the outlet stream). The differential IRGA has a range of 0-50 ppm  $\text{CO}_2$  by volume, readable to 0.5 ppm.

Vapor Pressure (e). Air from the compressor is forced over a saturated salt solution held at a specified temperature to control  $e$  at a prescribed level. This value is the reference, or air inlet vapor pressure. For the large chamber the room air serves the same purpose, being precisely controlled by a vapor pressure controller to within  $\pm 0.3$  mb of the set point, by injection of steam.

The measurement of  $e$  as the air passes over the leaf or whole plant is done with a micro-psychrometer developed specifically for this purpose and usable with either the large or small chamber. The psychrometer can measure the correct wet bulb depression at quite low wind velocities. For example, at 30 C, whereas a

standard psychrometer (Assmann type) requires an air velocity over the wet bulb of at least  $2 \text{ m sec}^{-1}$  to give the correct reading, the micro-psychrometer needs only  $0.12 \text{ m sec}^{-1}$  to do so at a relative humidity (RH) of 33% ( $e = 14.0 \text{ mb}$ ), and no more than  $0.30 \text{ m sec}^{-1}$  at the very low RH of 7% ( $e = 3.0 \text{ mb}$ ). Such a reduction in the ventilation requirement is due to the minute dimensions of the wet bulb, which has a copper constantan thermojunction as the temperature sensor. The wire diameter is 0.05 mm. Since the two wires are butt-welded, the overall diameter of the junction still is only slightly more than 0.05 mm. When the junction is placed between two strands of fine cotton thread (0.15 mm diameter) that has been untwisted and then retwisted, the final diameter of the miniature wet bulb is only 0.20 mm.

The reduced requirement for ventilation speed for the micro-psychrometer permitted a lower air flow over the enclosed leaf and thereby increased the  $\Delta e$  across the leaf due to transpiration. This increase in  $e$  made possible a measurement that may have been impossible, or at best unreliable at higher flow rates. Also, the lower flow rates permitted the use of a flow meter with excellent precision ( $\pm 2\%$  of the reading), but limited volume ( $1416 \text{ cm}^3 \text{ min}^{-1}$  maximum rate).

#### VARIABLE FACTORS:

Soil Water Potential. ( $\psi_T$ ). When the standard soil mixture is at "pot capacity," the soil water content by volume ( $\theta_V$ ) is 0.390. The corresponding soil matric potential ( $\psi_M$ ) is -0.02 bar. When half-strength Hoagland nutrient solution has been used to saturate the soil initially, the soil osmotic potential ( $\psi_\pi$ ) at pot capacity (achieved by a standard period of vacuum filtration) then is -0.56 bar, resulting in a  $\psi_T$  value of -0.58 bar. By continued transpiration under a precisely controlled evaporative demand in the Controlled Environment Room,  $\psi_T$  will decrease gradually. Eventually, the decline in  $\psi_T$  will induce plant dehydration as water absorption becomes less than transpiration. Leaf dehydration will result in

decreases in transpiration and photosynthesis.

It is planned to measure  $\psi_{\pi}$  with in-place soil salinity sensors and  $\psi_M$  with fast-response tensiometers employing pressure transducers. Summing up the readings from these two types of sensors will yield the equivalent  $\psi_T$  value.

Plant Water Potential. As  $\psi_T$  decreases, eventually plant water content also will diminish. A beta ray gauge will be used to monitor changes in leaf thickness due to changes in leaf water content. Later, a calibration will be made between leaf water content and leaf water potential by means of a thermocouple psychrometer making use of leaf discs. Such a calibration should permit the characterization of plant dehydration in terms of leaf water potential. In turn, decreases in leaf water potential can be related to the lowered rates of transpiration and photosynthesis as stomatal closure affects  $R_L$  and  $R'_L$ . Alternatively, it may turn out that in some species photosynthesis can be lowered directly by decreased tissue hydration, if  $R'_M$  increases without a significant increase in  $R'_L$ .

#### RESULTS AND DISCUSSION:

Testing of a small leaf chamber has established that the fans give an adequately low  $R_A$  value. Other developmental research has come up with a satisfactory control of vapor pressure at two levels, 14 mb and the very low level of 3 mb, both controlled with a precision of  $\pm 0.5$  mb. These two levels will permit step-changes in the transpiration rate to be induced merely by moving a plastic tube from one cylinder to another.

Adequate temperature control in the leaf chamber has been accomplished, even at the high irradiance of  $1 \text{ ly min}^{-1}$  (illuminance 100 kilolux), by supplementing the water-cooled jackets surrounding the chamber with a stream of cool air directed on the outside walls.

One major difficulty with the small chamber has been the inability to obtain consistently an air-tight seal of the leaf without injury. For this reason no usable data have been collected. A

large fraction of time has been spent in developing and refining the micro-psychrometer to its present status as a working, reliable apparatus.

It is planned to shift attention to the large chamber which accommodates whole plants, and to report the resulting data next year.

#### SUMMARY AND CONCLUSIONS:

Equipment has been assembled and apparatus has been built to carry out research on the effect of soil water depletion on the relative reduction in transpiration and photosynthesis. Precise control has been achieved for air temperature, light, air flow, CO<sub>2</sub>, and vapor pressure. A micro-psychrometer has been built especially for measuring differential vapor pressure at very low air flows across the chamber enclosing an intact leaf. A differential infrared analyzer measures the change in CO<sub>2</sub> across the chamber.

However, testing has shown that the difficulty in consistently obtaining an airtight seal of the leaf in the chamber is so great as to have prevented collection of reliable data for the research project. For this reason emphasis will be shifted toward use of the large chamber accommodating a whole plant.

PERSONNEL: W. L. Ehrler, B. A. Kimball, and S. T. Mitchell

CURRENT TERMINATION DATE: 1975

TITLE: THE EFFECT OF IRRIGATION REGIMES AND EARLY CUT-OFF  
OF IRRIGATION WATER ON THE YIELD OF HIGH POPULATION  
COTTON

CRIS WORK UNIT: SWC-018-gG4 CODE NO.: Ariz.-WCL 71-2

INTRODUCTION:

High pink bollworm populations, especially late in the season, government acreage limitations and payment regulations, and need for reduction in production costs have incited interest in producing short-season, high-population cotton. Astonishingly, during the last two years, cotton pickers have been designed and are available to harvest high-population cotton at a higher efficiency than the standard pickers.

It is argued that by increasing plant populations and discontinuing irrigations early, the savings in water, labor, and insect control will offset possible reductions in yield.

Early harvest would make possible earlier plow-under, which will help control future pink bollworm infestations. There is also the possibility that an extra-early plow-under will be initiated into law, which would mean that only short-season production is possible, whether or not it is economically feasible. At present, Arizona laws are still such that a full growing season can be utilized. In certain areas of California, plow-under dates have been set by law that make a full growing season impossible.

There are many unanswered questions as to methods for managing this type of production, especially with respect to water. Studies on high-population cotton are very limited, and the majority of these are of an extension type. The themes of most cotton meetings in the last six months have been oriented toward high-population cotton. Many success stories have been reported, but certain tests repudiate these stories. It is questionable that the feasibility of short-season, high-population cotton would be the same for the Southwest as for the High Plains of Texas, or other areas having cooler

and shorter growing seasons.

It is recognized by all plant breeders and growers that we probably do not have the ideal variety of cotton for high-population production -- but neither is there an ideal variety for standard production. Plant breeders will continue to improve varieties and growers will use the variety that is best adapted to their areas.

Studies to date seem to indicate that fertilizer needs for high-population cotton are similar to standard 40-inch row cotton production. However, with high populations and early irrigation cut-off, many investigators feel that it is important to keep plants short and not overly vegetative by judicious use of fertilizer.

In order to evaluate the economic potential of this new trend toward high populations, we must understand the effect of various irrigation regimes on cotton production, including cut-off of irrigation water. Results from this study will be applicable to arid, high-production areas having high temperatures and long growing seasons.

#### OBJECTIVES:

1. To evaluate the effects of various irrigation regimes on recommended varieties of high-population cotton.
2. To determine the effect of an early cut-off of irrigation water on the yield of high-population cotton.

#### PROCEDURE:

The experiment is located on Field C-1 at the University of Arizona Cotton Research Center, Phoenix, Arizona. The field had been in cotton in 1969, and in December of 1969, Arivat barley was planted. The barley was harvested in June 1970, and the field lay fallow until September when 250 lbs/acre of urea was applied and plowed under. The field was fitted and again planted to Arivat barley on 30 September 1970.

On 12 January 1971, 170 lbs/acre of urea was applied and plowed down, along with the barley. The field was furrowed out

into 40-inch furrows and a pre-plant irrigation given.

A weed-control mixture of Treflan and Karmex was incorporated into the furrows with a "Lilliston" as soon as the field was dry enough to accommodate machinery.

Two-thirds of the furrows were shaped into beds with a "Sidewinder" and bed-shaper for the 40,000 and 80,000 plant populations, as per plot design. Each bed contained two rows to accommodate the high plant populations. The remaining one-third of the furrows contained single rows of normal planting, or 20,000 plants/acre.

Three varieties of cotton, Deltapine 16, Stoneville 213, and Pima S-4, were planted on 3 and 5 April, in a random split-plot design (See Fig. 1). Irrigations for germination were given on 6 and 10 April.

Rows were thinned to their respective plant populations around 10 May. At the same time, tagging areas were marked off and the proper number of plants were counted and maintained within these respective areas. Each tagging area consisted of two rows or beds, each 6 ft long.

Timing of irrigations was based on soil moisture samples along with visual plant symptoms on the medium and wet treatments. The dry treatment was irrigated according to calendar schedule.

Within each plot, two 20-ft lengths of row or bed were marked off for yield measurements. Generally this was the inner two rows, or beds, of 4-row, or 4-bed, plots. In a few bed plots, stands were not ideal on the inner two beds and buffer rows were substituted to obtain the designated yield area.

A border dike was constructed across the middle of the field perpendicular to the flow of irrigation water, around the first of August. This was to facilitate an early-season cutoff of irrigation water to the lower half of the field.

## RESULTS AND DISCUSSION:

In nearly all plots, a good stand was obtained. However, growth was slow, as temperatures remained below normal from the middle of April to the middle of June.

Tagging commenced on 20 June and continued through 18 September. Several days of tagging information were lost during the season, due to insecticide regulations barring entry to the field. However, most of the days lost were during the normal cut-out period when a minimum number of blossoms were involved.

On the medium and wet treatments, irrigations were given during the major blossoming period at somewhat drier conditions than originally set up. For the wet treatment, the average soil moisture depletion in the top 3 ft of soil before irrigation was 69%. For the medium treatment, depletion was 83%.

Several hard-soil spots were noted in the field, and lighter than desired applications of water were given. These hard spots caused uneven distribution of water. The upper wet treatment was given 8 irrigations, and the lower wet, 6; the upper medium, 6, and the lower medium, 4; the upper dry, 4, and the lower dry, 3. The last irrigation on the lower wet treatment was given on 28 July; the last to the lower medium on 20 July; and the last to the lower dry on 21 July. Lower plots were beginning to desiccate by mid-August.

A build-up of pink bollworms was noted in the last week in June. Insecticide applications began immediately, and excellent control was attained throughout the season. Two defoliations were given on 18 and 26 October. An early frost occurred on 29 October and, together with the defoliations, affected the late-season boll size, the color, and probably all quality measurements.

Table 1 shows the seed weight of Deltapine 16 for the three irrigation treatments and three populations. Differences between both irrigation and population treatments are large enough to be statistically significant. The significance is between the 20,000

population, dry treatment, and the other treatments. The 40,000 and 80,000 populations are 25.1% higher in weight than the 20,000 population, when the two wetter treatments are considered. Yields for the dry treatment are 14.9% less than for the wetter treatments.

Yield differences for the Stoneville-213 are not large enough to show significance in the moisture levels, but definite trends exist as yields are reduced by decreased moisture. The differences in yield between populations are significant at the 1% level, between the 20,000 population and the others. The production of seed cotton for both the 40,000 and 80,000 populations was 18% higher than for the 20,000 population.

In Table 3, 82% of the total Deltapine yield was developed from blossoms opening before 15 August. For the Stoneville-213, 87% was developed before this date.

On the Deltapine variety, all blossoms for all treatments were tagged throughout the flowering period, beginning 20 June and extending through 18 September. Table 4 shows a significant increase in blossoms as populations are increased, up to 80,000 plants per acre. When all irrigation treatments are averaged, the total number of blossoms were increased 34% and 43% respectively for the 40,000 and 80,000 over the 20,000 populations. This increase in blossoms occurred principally before 17 July. There is no advantage for one population over the other after this date. When the dry treatment is compared to the two wetter treatments, regardless of plant population, a 6% decrease in blossoms is noted.

The number of bolls was increased by doubling the population from 20,000 to 40,000 for both Deltapine and Stoneville, but no significant increase was measured between the 40,000 and 80,000 populations. (Table 5). For all irrigation treatments, the average of the higher populations (40,000 and 80,000) showed an increase in bolls of over 25% for the Deltapine. The data for Stoneville showed an average 20% boll increase. Of the total bolls, 77% of the Delta-

pine and 85% of the Stoneville were from blossoms which opened before 15 August.

Table 6 shows that boll size decreased for populations over 40,000. The boll size for the 80,000 population was decreased enough to offset the increase in blossoms that the 80,000 population had over the 40,000 population. The bolls for the last week of the flowering season were very small, partially because of the early frost. Thus, total yield and boll size were affected.

Lower-half yields were so variable that a true analysis is questionable. Variability is partly due to residual moisture associated with hard soil, or high spots, and probably would be typical of a farm operation. If a legitimate trend does exist, it would be reflected as a yield reduction between upper and lower halves because of moisture differences. Also, a trend within the lower half showed reduced production with decreased number of irrigations. Since the greatest increase in blossoms because of increased plant populations occurred before 17 July, it would be logical to assume that a greater number of bolls would mature with high populations, if an early irrigation cut-off program were practiced. This is what happened, as the number of bolls and yield of seed cotton increased as plant populations increased.

Figures 2, 3, and 4 show the pattern of events for blossom and boll production for the wet treatment. Other moisture treatments followed the same trend. There was no indication that any one population gained any earlier production advantage. (June production). It should be noted that any unusually good or bad efficiency periods followed the same trend; i.e., the peak blossom and boll producing period was mid-July. Poor efficiency of bolls from blossoms also occurred on similar dates; for example, the last two weeks of July, and another period just before the beginning of the increase which reached peak production. The efficiency of bolls from blossoms for the 20,000 population was higher during the period just before the

peak, but considerably less blossoms were involved and thus the number of bolls were essentially the same.

**SUMMARY AND CONCLUSIONS:**

Three irrigation regimes and an early irrigation cut-off, using three plant populations and three varieties, were investigated.

When water was applied for a full growing season where populations were increased from the standard 20,000 to 40,000 plants per acre, production of seed cotton was increased more than 25%. This increase in yield was due to more flowers and bolls. However, yield was not greater for the 80,000 population over the 40,000. Although flowering was greater for 80,000 plants per acre, a decrease in boll size nullified any production advantage over the 40,000 population. Increases in blossoms due to higher populations occurred during the first month of flowering, which was before 17 July in 1971. There was no hastening of the pattern of events for blossom and boll production due to varied populations, nor any major changes in the trend of events associated with peaks or efficiency of bolls from blossoms. Of the seed cotton production, 82% of the Deltapine and 87% of the Stoneville-213 were produced from flowers opening before 15 August. Of the total number of bolls, 77% of the Deltapine and 85% of the Stoneville were from blossoms which opened before 15 August.

When irrigations were cut off in late July, the number of flowers and bolls and the quantity of yield of seed cotton increased as plant populations were increased.

**PERSONNEL:** Leonard J. Erie, Dale A. Bucks, and Orrin F. French.

**CURRENT TERMINATION DATE:** December 1973.



Blossoms and bolls per day

13-9

Blossoms  
 Bolls

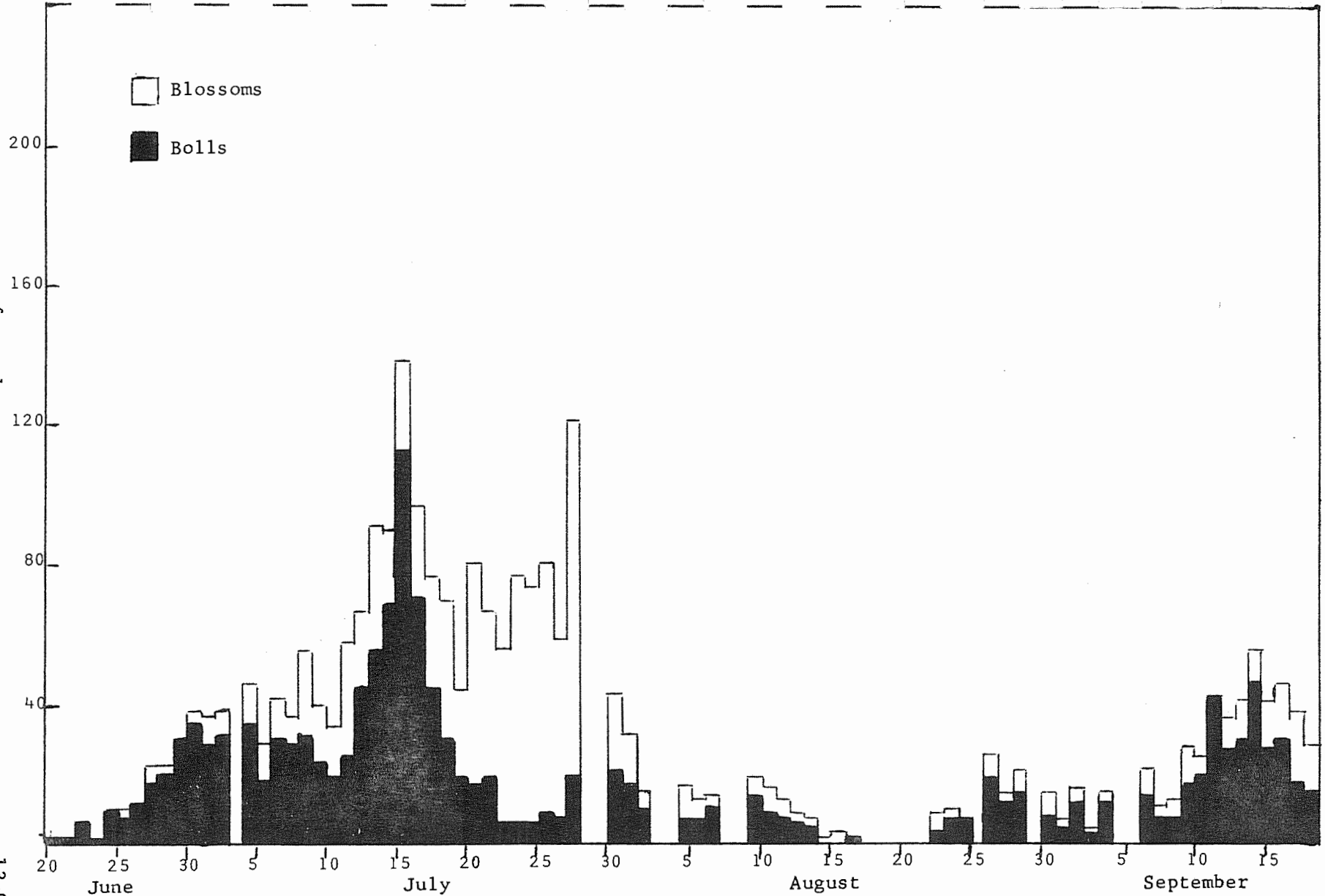


Figure 2. Blossom and boll count, Deltapine-16, wet treatment (20,000), University of Arizona Cotton Research Center, Phoenix, 1971.

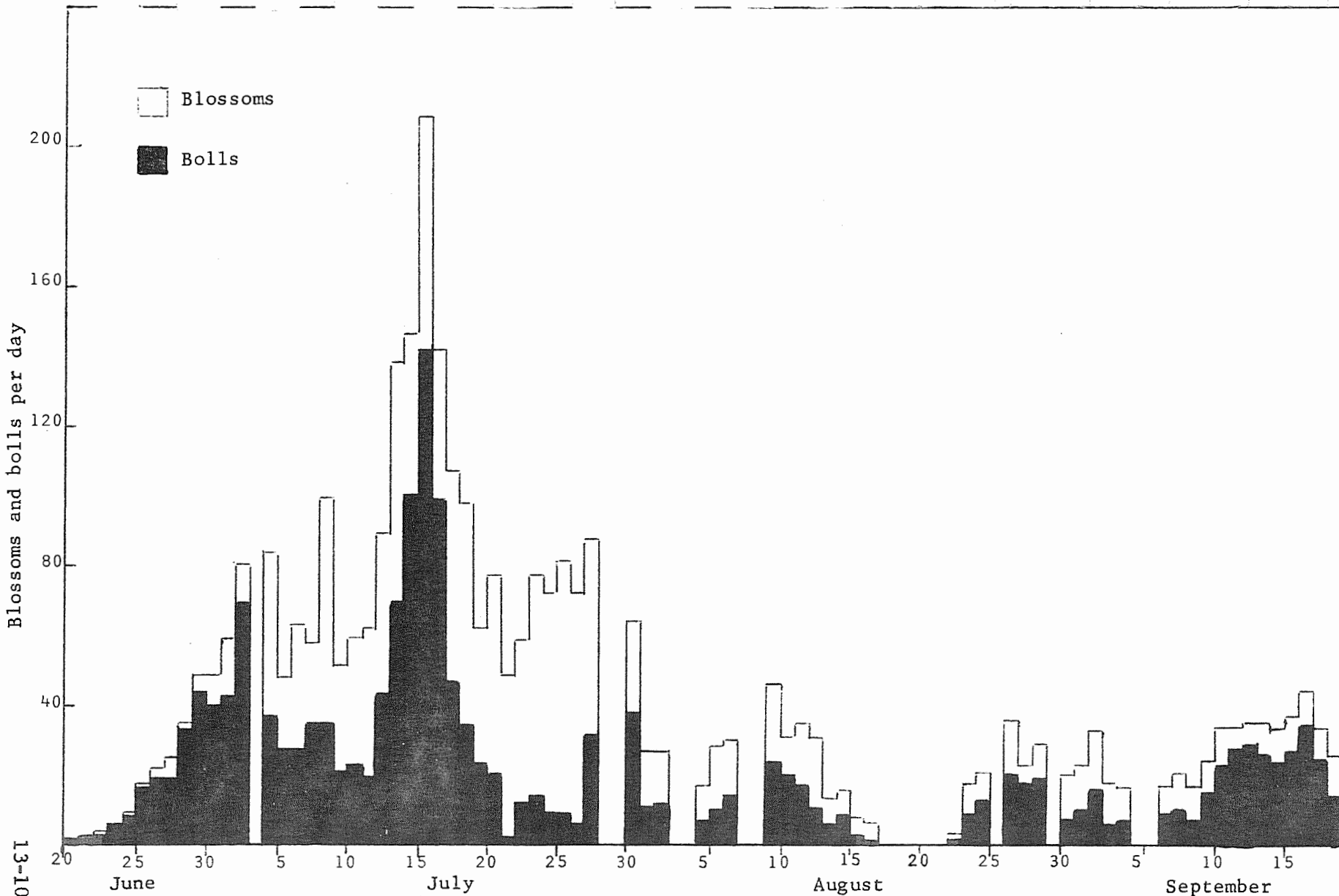


Figure 3. Blossom and boll count, Deltapine-16, wet treatment (40,000), University of Arizona Cotton Research Center, Phoenix, 1971.

11-11  
Blossoms and bolls per day

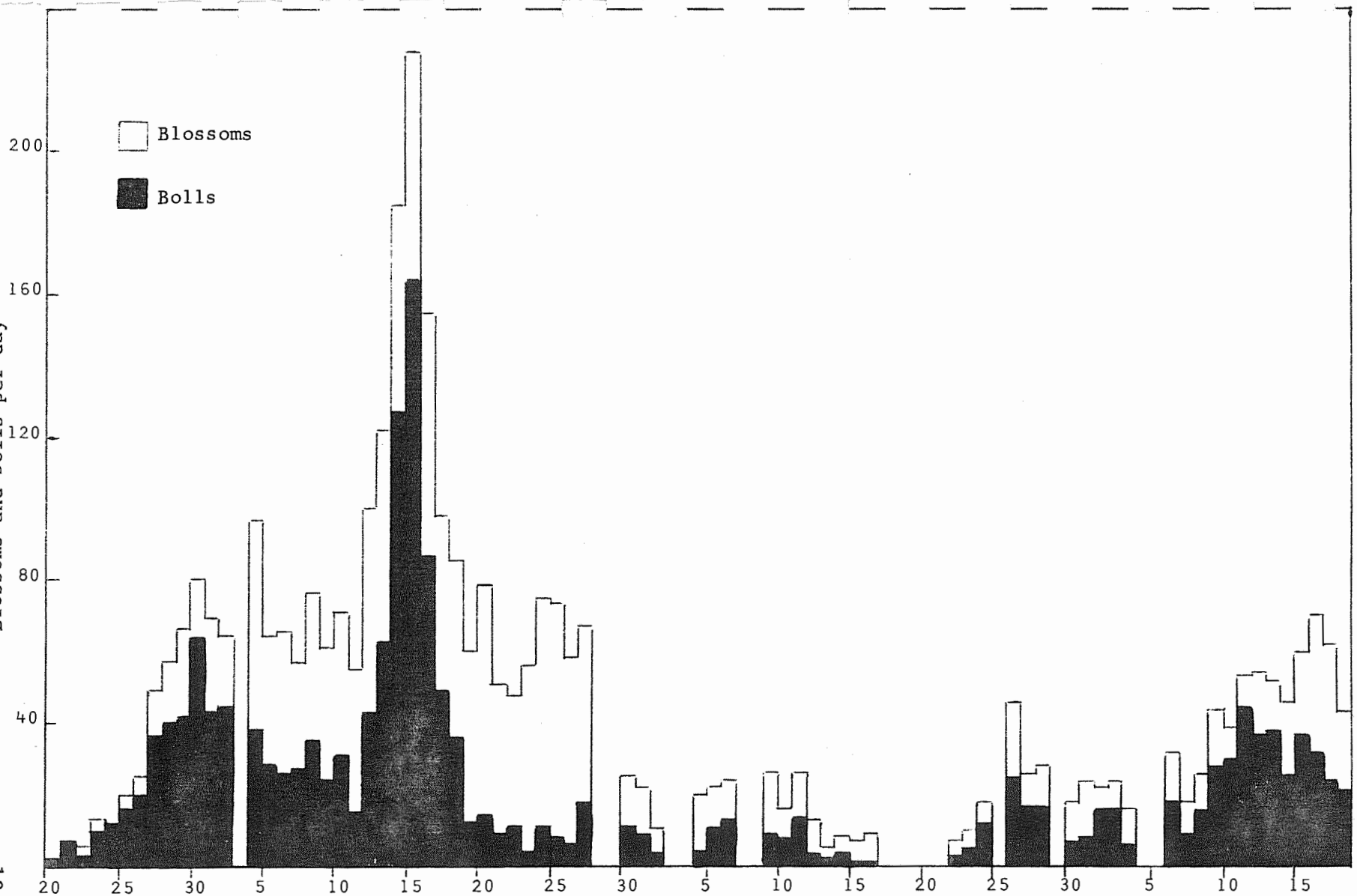


Table 1. Seed cotton weight in grams, per plot of Deltapine-16 for three irrigation treatments and three populations.

Irrigation	Population	Replications				Mean
		1	2	3	4	
Wet	20,000	1828.0	1481.6	1627.8	1785.8	1680.8
	40,000	2082.4	2087.3	1994.8	2180.6	2086.3
	80,000	1785.6	2133.4	1692.2	1974.0	1896.3
Med.	20,000	1860.2	1536.5	1323.4	1362.4	1520.6
	40,000	2013.5	1974.2	2405.1	1724.5	2029.3
	80,000	2449.8	2410.3	1795.6	1842.7	2124.6
Dry	20,000	1414.4	1349.3	1455.2	1537.6	1439.1
	40,000	1413.7	2246.9	1541.5	1562.9	1691.3
	80,000	2030.3	1654.3	1568.4	1526.2	1694.8

Irrigation -- sig. 5%                      LSD 230.7

Population -- sig. 1%                      LSD 419.7

Table 2. Seed cotton weight in grams, per plot of Stoneville-213 for three irrigation treatments and three populations.

Irrigation	Population	Replications				Mean
		1	2	3	4	
Wet	20,000	1620.4	1806.2	1678.6	1628.6	1683.5
	40,000	2085.8	2028.9	1747.6	2131.2	1998.4
	80,000	1932.3	2068.7	2018.6	1866.7	1971.6
Med.	20,000	1837.1	1574.0	1669.8	1370.3	1612.8
	40,000	2043.3	1792.7	1833.8	1910.5	1895.1
	80,000	1914.4	1882.1	2337.1	1697.3	1957.5
Dry	20,000	1697.8	1679.7	1509.8	1026.9	1478.6
	40,000	1899.6	1708.9	1764.7	1878.7	1813.0
	80,000	2092.7	1745.2	1621.1	1608.1	1766.8

Irrigation -- no sig.

Population -- sig. 1%      LSD    294.5

Table 3. Weight of seed cotton, and that portion of total weight which was from blossoms that opened before 15 August.

Irrigation	Population	Deltapine		Stoneville	
		Total	Opened by 15 August	Total	Opened by 15 August
		gms	%	gms	%
Wet	20,000	6723.2	80	6733.8	86
	40,000	8345.0	82	7993.5	82
	80,000	7585.2	80	7886.3	83
Med.	20,000	6082.5	83	6451.2	89
	40,000	8117.3	82	7580.3	89
	80,000	8498.4	79	7830.9	84
Dry	20,000	5756.5	87	5914.2	92
	40,000	6765.0	86	7251.9	89
	80,000	6779.2	80	7067.1	88

Table 4. Number of blossoms, and percent of total opened by specific dates, for Deltapine-16 variety.

Irrigation	Population	Total No. Blossoms	Blossoms Opened by 17 July		Blossoms Opened by 15 Aug
		Season	No.	%	%
Wet	20,000	2597	1108	43	78
	40,000	3463	1714	49	81
	80,000	3627	1899	52	76
Med.	20,000	2583	1110	43	82
	40,000	3583	1746	49	81
	80,000	3851	1892	49	78
Dry	20,000	2491	944	38	84
	40,000	3228	1341	42	83
	80,000	3485	1589	46	77

Table 5. Number of bolls, and percent of total from blossoms that opened on specific dates.

Irrigation	Population	Deltapine			Stoneville	
		Total	Open by 17 July %	Open by 15 Aug %	Total	Open by 15 Aug %
Wet	20,000	1655	55	72	1726	85
	40,000	2034	58	77	2029	81
	80,000	2034	61	73	2038	82
Med.	20,000	1489	53	78	1642	86
	40,000	2037	56	76	1919	88
	80,000	2218	56	73	2039	83
Dry	20,000	1426	48	82	1566	91
	40,000	1731	50	83	1848	87
	80,000	1817	51	76	1891	87

Table 6. Average boll weights, in grams, for the season, and for blossoms opened before and after 15 August.

Irrigation	Population	Deltapine			Stoneville		
		Seasonal	Before 15 Aug	After 15 Aug	Seasonal	Before 15 Aug	After 15 Aug
Wet	20,000	4.05	4.47	2.96	3.90	3.97	3.62
	40,000	4.10	4.37	3.24	3.94	3.99	3.73
	80,000	3.73	4.06	2.83	3.87	3.91	3.65
Med.	20,000	4.08	4.37	3.08	3.92	4.03	3.31
	40,000	3.98	4.31	2.95	3.95	3.99	3.62
	80,000	3.84	4.10	3.11	3.84	3.89	3.63
Dry	20,000	4.04	4.24	3.07	3.97	4.01	3.56
	40,000	3.91	4.07	3.13	3.92	3.99	3.49
	80,000	3.73	3.94	3.08	3.74	3.80	3.34

13-17

TITLE: HEAT AND LIGHT TRANSFER IN PONDS

CRIS WORK UNIT: SWC-018-gG-4

CODE NO.: Ariz.-WCL-71-3

INTRODUCTION:

As part of a comprehensive cooperative effort to characterize the biological, chemical, and physical factors relating to the growth of phytoplankton, zooplankton, and fish in an aquatic ecosystem of ponded tertiary treated sewage water, a program of intensive measurement of several physical factors was begun and made operational by mid-May 1971. Parameters measured were air temperatures at +10 and +60 cm, water temperatures at the surface, -15, -60, and -110 cm, incoming solar radiation, reflected solar radiation, solar radiation transmitted to -20 cm depth, incoming atmospheric thermal radiation, and evaporation. Data on these factors have been collected continuously every half-hour since the experiment's initiation, except during periods of instrument or recorder failure.

RESULTS AND DISCUSSION:

So far, data for four and one-half months have been reduced and summarized. They indicate that total water body heating from above is almost solely due to the internal absorption of solar radiation, with all of the energy exchanges at the surface being between the surface and the air above, rather than the water beneath. This observation led to the development of an evaporation equation that could be tested over other bodies of water in an attempt to delineate its realm of validity as a function of water surface exposure. With greater surface areas and exposure to wind, the equation would be postulated to be less accurate, but to what degree remains to be determined experimentally.

Forelian and Birgean heat budget calculations were both utilized in several situations, with the Birgean technique generally giving the more reasonable results. Both techniques plus a complete energy balance approach led to the discovery that sediment heat exchanges played a commanding role in the over-all transfer

of energy within the water. Not only did they control the efficiency of night-time energy removal by surface generated convection currents, but they appeared to be responsible for a possible bottom-generated convection regime. This latter phenomenon, however, should not be construed to be firmly established at this stage, but only conjectured. Its reality remains to be determined by more intensive experimentation with either tracer techniques or more thermocouples more closely spaced near the pond bottom.

Finally, another interesting phenomenon indicated by the data was that the concentration of phytoplankton may have a significant effect upon the depth of penetration of the surface-generated convection currents. When phytoplankton concentrations were high and down-welling solar radiation was extinguished rapidly in the upper water layers, the convection currents only penetrated about two-thirds of the way to the pond bottom, whereas under lower concentrations they reached the bottom regularly. This phenomenon too, however, must remain somewhat tenuous as regards a cause and effect relation until more data are available for more seasons.

#### SUMMARY AND CONCLUSIONS:

An intensive study of light and heat transfer in a small man-made pond was initiated in mid-May 1971. As a result, a new evaporation equation was developed for small sheltered bodies of water, and some intriguing patterns of convection were postulated. One involved the possibility of a bottom-generated convection regime extending upwards into the water from below, and another involved the possible control of depth of penetration of surface-generated convection currents by the presence of phytoplankton. Lastly, heat exchange at the sediments was shown to be the dominant factor in determining the efficiency of energy removal from the water by convective transport to the surface.

PERSONNEL: S. B. Idso

CURRENT TERMINATION DATE: May 1973

TITLE: MEASUREMENT AND PREDICTION OF THE SOLUBILITY  
BEHAVIOR OF THE CALCIUM MINERAL CONSTITUENTS  
OF SOILS.

CRIS WORK UNIT: SWC-018-gG-4

CODE NO.: Ariz.-WCL 71-4

INTRODUCTION:

The calcium ion,  $\text{Ca}^{2+}$ , aids in promoting good soil structure. Conditions in the arid Southwest are such that the effectiveness of the  $\text{Ca}^{2+}$  in the soil system is drastically reduced by its precipitating or its complexing through chemical interactions with other dissolved constituents. The basic processes that occur, however, are not clearly understood, and consequently the behavior of the various calcium compounds in different kinds of solution systems must be followed.

The solubility product principle is used extensively in this type of investigation. By suitable theoretical and experimental development not considered previously, a simple and straightforward determination of the solubility product of  $\text{CaCO}_3$  can be made.

THEORY:

The first and second dissociation constants of carbonic acid and the ionic activity solubility product of  $\text{CaCO}_3$  are defined, respectively, as

$$K_1 = \frac{(\text{H}^+) (\text{HCO}_3^-)}{(\text{H}_2\text{CO}_3)} = \frac{(\text{H}^+) (\text{HCO}_3^-)}{(kP_{\text{CO}_2})} \quad (1)$$

$$K_2 = \frac{(\text{H}^+) (\text{CO}_3^{2-})}{(\text{HCO}_3^-)} \quad (2)$$

$$K_{\text{sp}} = (\text{Ca}^{2+}) (\text{CO}_3^{2-}) \quad (3)$$

where the parenthesis ( ) is the activity,  $k$  is Henry's law constant for  $\text{CO}_2$  solubility, and  $P_{\text{CO}_2}$  is the partial pressure of  $\text{CO}_2$ . Solving equations (1) and (2) in terms of  $(\text{CO}_3^{2-})$  and substituting it into equation (3) yields

$$K_{\text{sp}} = \frac{(\text{Ca}^{2+})K_1K_2kP_{\text{CO}_2}}{(\text{H}^+)^2} \quad (4)$$

Since existing analytical techniques allow the measurement of  $(\text{Ca}^{2+})$ ,  $(\text{H}^+)$ , and  $P_{\text{CO}_2}$ , and the values for the rest of the components in equation (4) are available from the literature,  $K_{\text{sp}}$  is directly calculable.

#### PROCEDURE:

Various concentrations of  $\text{CO}_2$  gas (0.54 to 99.98%) were bubbled through saturated  $\text{CaCO}_3$  solutions (Nakayama, 3). The gases were premoistened in bubbling towers prior to passage through the samples. The pH was determined with a glass electrode previously calibrated in NBS standard buffers. Calcium activities were measured with the membrane electrode which was standardized in  $\text{CaCl}_2$  solutions. Experiments were conducted at  $25 \pm 0.5$  C.

#### RESULTS AND DISCUSSION:

The various constants were obtained from the literature, where  $k = 0.0344$  (Harned and Davis, 1),  $K_1 = 4.41 \times 10^{-7}$  and  $K_2 = 4.65 \times 10^{-11}$  (Nakayama, 4).

The  $K_{\text{sp}}$ 's computed from equation (4) and listed in Table 1 should give the most direct estimate of the activity products of Ca and  $\text{CO}_3$  as defined in equation (3), and their reliability is dependent primarily upon the accuracy of the activity measurements of the H- and Ca-electrodes. We are quite confident of the hydrogen glass electrode, and somewhat less so with the Ca-electrode since the Ca-electrode used was one of the very earliest available. The  $K_{\text{sp}}$  value appears to be pH-related, and this should be further checked out. Langmuir (2) from a detailed literature survey and analysis

of  $\text{CaCO}_3$  solubility data reported by other investigators concluded that a value of  $4.00 \times 10^{-9}$  is the best estimate of  $K_{sp}$ , as compared to a mean of  $3.25 \times 10^{-9}$  obtained in this discussion.

SUMMARY:

The theoretical and experimental treatment presented here appears to be the most direct method developed for getting the thermodynamically defined  $K_{sp}$ . It avoids the need to know the dissociation constants of any other Ca-associated species if present, and does not require the total Ca and carbonate analyses usually obtained from titration measurements. Furthermore, the  $K_{sp}$  for other sparingly soluble metallic carbonate salts (viz.  $\text{MgCO}_3$ ,  $\text{BaCO}_3$ ,  $\text{SrCO}_3$ ,  $\text{ZnCO}_3$  ...) could be determined similarly, provided that the activity of the metallic constituents can be determined.

REFERENCES:

1. Harned, H. S. and Davis, R., Jr. The ionization constant of carbonic acid in water and the solubility of carbon dioxide in water and aqueous salt solutions from 0 to 50°. J. Amer. Chem. Soc. 65:2030-2037. 1943.
2. Langmuir, D. Stability of calcite based on aqueous solubility measurements. Geochim. Cosmochim. Acta 32:835-851. 1968.
3. Nakayama, F. S. Calcium activity, complex and ion-pair in saturated  $\text{CaCO}_3$  solutions. Soil Sci. 104:429-434. 1968.
4. Nakayama, F. S. Sodium bicarbonate and carbonate ion-pairs and their relation to the estimation of the first and second dissociation constants of carbonic acid. J. Phys. Chem. 74:2726-2728. 1970.

PERSONNEL: F. S. Nakayama and B. A. Rasnick

CURRENT TERMINATION DATE: December 1972

Table 1. Ion-activity solubility product constant of  $\text{CaCO}_3$   
 at 25 C obtained from H- and Ca-activity measurements.

$(\text{Ca}^{2+}) \times 10^3$	pH	$P_{\text{CO}_2}$ , atm.	$K_{\text{sp}} \times 10^9$
4.24	6.005	$9.266 \times 10^{-1}$	2.84
3.81	6.110	$7.058 \times 10^{-1}$	3.15
3.48	6.212	$4.902 \times 10^{-1}$	3.19
2.69	6.474	$1.884 \times 10^{-1}$	3.17
1.82	6.867	$4.735 \times 10^{-2}$	3.30
1.38	7.130	$1.951 \times 10^{-2}$	3.46
0.94	7.521	$5.013 \times 10^{-3}$	3.66

TITLE: WATER VAPOR MOVEMENT THROUGH MULCHES UNDER  
FIELD CONDITIONS

CRIS WORK UNIT: SWC-018-gG-4 CODE NO.: Ariz.-WCL-71-5

INTRODUCTION:

This project was initiated to evaluate the relative contributions of molecular diffusion and mass flow to water vapor movement through mulches under field conditions. Generally, water vapor has been regarded as moving only by molecular diffusion through porous materials. In recent years, however, evidence has appeared which suggests that air turbulence may cause an increase in the rate of movement, particularly in coarse textured materials. By using a variety of waterproofed (to prevent movement of liquid water) porous materials as mulches over moist soil, the influence of air turbulence on water vapor movement has been investigated.

METHODS AND MATERIALS:

The method of investigation has been to apply mulches to three weighing lysimeters and then obtain the rates of water loss through the mulches. Concurrent measurements of air temperature, air vapor pressure, wind velocity and soil temperature at the soil-mulch interface permit the amount of water vapor loss attributable to mass flow processes to be calculated.

Table 1 lists the mulches which were used and some of their physical properties. The glass beads were purchased from a manufacturing company. The soil aggregates were sieved from Adelanto loam. The glass bead aggregates were made by first heating layers of 0.047-0.084 mm diameter glass beads in a pan slowly in a muffle furnace up to 605 C to form porous "cakes" as the beads fused together. After slowly cooling, the cakes were broken into smaller chunks with a meat tenderizer, and then they were further reduced in size by grinding in a Wylie mill. The 0.84-1.65 mm diameter aggregates were sieved out using a mechanical shaker. The air permeabilities were determined by measuring the air pressure drop (with a sensitive capacitance-type differential pressure transducer)

and the flow rate (with a stop watch to time a soap film passing through a glass cylinder) as air was passed through a column of each mulch. All of the mulches were treated with a water-repellent material, trichlorosilane, so that they would not conduct liquid water from the moist soil beneath them to their upper surface.

Table 2 lists the experiments which were conducted, the dates for each, the depths of mulch, and the particular mulch materials used on each lysimeter. The skies were generally clear during all the experiments, and there were no interruptions due to rain. The soil in the field around the lysimeters was bare and dry, having not been irrigated for three months prior to the experiments.

The rates of water vapor loss through the mulches were obtained from measurements obtained with the lysimeters described in the 1960 Annual Report. Air temperatures were measured with an aspirated, radiation-shielded thermocouple, air vapor pressures with a radiation-shielded dew probe, and wind velocities with a cup anemometer. All of the above-ground measurements were taken at the 50 cm height a few meters from the lysimeters. Soil temperatures at the soil-mulch interfaces were measured with three thermocouples in each lysimeter. The voltages or counts from the instruments were scanned and punched on paper tape at half-hour intervals with a data acquisition system. Lysimeter data for half-hour intervals tends to be noisy, so all of the lysimeter data and also the data from the other instruments were smoothed using a 1, 4, 6, 4, 1 running weighted average. A programmable calculator equipped with a paper tape reader is being used to perform the not yet completed analysis of the data.

The data are being analyzed as follows. An effective diffusion coefficient,  $D_e$ , for water vapor under field conditions is being calculated for each of the mulches using the following equation

$$D_e = \frac{38.5 E}{(e_s - e_o)/\Delta x} \quad (1)$$

where  $D_e$  = effective diffusion coefficient ( $\text{cm}^2/\text{sec}$ )  
 $E$  = water vapor flux or evaporation rate (mm/hr)  
 $e_s$  = saturation vapor pressure at the mulch-soil interface (mb)  
 $e_o$  = vapor pressure at upper surface of mulch (mb)  
 $\Delta x$  = depth of mulch (cm)

The evaporation rate is calculated from the lysimeter measurements. The water vapor concentration at the mulch-soil interface is obtained from the soil temperature measurements assuming that the vapor pressure was at saturation at the interface. This is a safe assumption because the soil in the lysimeters was freshly irrigated before the mulches were spread evenly over the surfaces of the lysimeters at the beginning of each experiment, and because the soil was still moist to the touch at the end of each experiment. The vapor pressure at the upper surface of the mulch is calculated from the air vapor pressure at 50 cm using the following equation

$$e_o = e_a + \frac{38.5 E}{h} \quad (2)$$

where  $e_a$  = air vapor pressure (mb)  
and  $h$  = transfer coefficient from the upper surface of the mulch to a height of 50 cm (cm/sec).

The transfer coefficient,  $h$ , is assumed to have a maximum of infinity or is calculated from the log wind profile equation.

$$h = v \left[ \frac{0.4}{\ln(z/z_o)} \right]^2 \quad (3)$$

where

$v$  = wind velocity at 50 cm (cm/sec)

$z$  = height (50 cm)

$z_o$  = roughness height (cm)

For comparison purposes the molecular diffusion coefficient,  $D$ , must also be known and it is calculated from the following

equation derived from the work of previous investigators.

$$D = (0.27)(0.239) \left[ \frac{T_s + 273.16}{281.16} \right]^{1.75} \quad (4)$$

#### RESULTS AND DISCUSSION:

The analysis of the data is far from complete; however, the data from 26 May 1971 for the 5 mm depth of 2 mm diameter beads has been analyzed, and the results for the daylight hours are shown in Figure 1.

The effective diffusion coefficients for the nighttime hours are not shown because they are unreliable. They are unreliable because both the numerator and the denominator of Equation 1 could not be accurately determined. The nighttime evaporation rates in the numerator were very low and at the limit of the resolution of the lysimeters. The vapor pressure at the soil-mulch interface was also low and approximately equal to  $e_a$  and  $e_o$ , so the accuracy of the nighttime  $D_e$ 's was further impaired by having to take the difference between two numbers of equal magnitude. Thus, only those data where  $e_s$  was considerably bigger than  $e_a$  are presented in Figure 1.

The lowest curve of  $D_e/D$  marked " $h = \infty$ " in Figure 1 is the ratio of the effective diffusion coefficient to the molecular diffusion coefficient calculated by assuming  $h = \infty$  in Equation 2. This assumption implies infinite mixing in the air above the mulch so that the vapor pressure at the mulch surface equaled the air vapor pressure measured at a height of 50 cm. The vapor pressure difference across the mulch could have been no larger, so the  $D_e$ 's calculated by this procedure represent minimums; the true  $D_e/D$  ratio cannot lie below the curve for  $h = \infty$  in Figure 1. Thus, it appears that mass flow processes have caused the water vapor loss through this 2 mm dia. glass bead mulch to be generally at least 5 to 15%

higher than the loss attributable solely to molecular diffusion.

The other two curves of  $D_e/D$  in Figure 1 were calculated using  $z_o = 0.1$  cm or  $z_o = 0.01$  cm in Equation 3. Many wind profiles obtained under neutral conditions over the same bare soil field in March of 1971 showed that the roughness height generally was between 0.1 and 0.01 cm. Since thermally induced mixing during the sunny daylight hours should have caused the vapor pressures at the mulch surface to be closer to the vapor pressures at 50 cm than an adiabatic wind profile would predict, the upper curve for  $z_o = 0.01$  cm represents a reasonable maximum curve, and the curve for  $z_o = 0.1$  cm is probably close to the true curve. Thus, mass flow processes have caused the water vapor loss through this mulch to be generally no more than 30-70% higher than the loss attributable to molecular diffusion. It appears from the middle  $D_e/D$  curve that mass flow processes may typically cause the loss to be generally about 15-35% higher.

Inspection of Figure 1 reveals no correlation between the peaks in the wind velocity curve and the peaks in the  $D_e/D$  curves. This is somewhat surprising since mass flow processes appear to have made a significant contribution to water loss, and one would expect the magnitude of the contribution to increase with increasing wind velocity. However, the wind velocities plotted in Figure 1 are quite steady so perhaps there simply wasn't enough range in wind velocity on this particular day. The analysis of the data obtained for other days, other mulch materials, and other depths of mulch may reveal different magnitudes of mass flow processes to water vapor loss, and may reveal whether any correlations with wind velocity exist.

#### SUMMARY:

This study was initiated to evaluate the relative contributions of mass flow and molecular diffusion to water vapor movement through mulches and other porous materials under field conditions. A variety of mulch materials were waterproofed to assure that all

water moved in the vapor phase. These mulches were spread in 5, 10, and 20 mm layers over lysimeters and concurrent measurements were made of evaporation rates, temperatures at the moist soil-mulch interfaces, air vapor pressures, air temperatures, and wind velocities. By assuming that the air was saturated at the moist soil-mulch interfaces, effective diffusion coefficients for field conditions were calculated.

The analysis of the data is far from complete. However, the data for the daylight hours of one day with a 5 mm depth of a 2 mm dia glass bead mulch indicate that mass flow processes increased the water vapor loss more than generally 5-15%, and less than generally 30-70% of the loss attributable to molecular diffusion. No obvious correlations of the mass flow contribution with wind velocity were present on this particular day.

PERSONNEL: B. A. Kimball

CURRENT TERMINATION DATE: 1973

Table 1. Properties of the mulch materials.

Mulch Material	Approx. mean diameter (mm)	Particle diameter range (mm)	Porosity	Air perme- ability ( $\mu^2$ )
1 glass beads	2	1.65-2.37	0.38	3350
2 glass beads	1	0.84-1.65	0.39	903
3 glass beads	0.5	0.41-0.84	0.41	356
4 glass bead aggregates	1	0.84-1.65	0.66	1570
5 glass beads*	0.06	0.044-0.074	0.47	2.12
6 soil aggregates	1	0.84-1.65	0.63	740
7 soil aggregates	0.5	0.41-0.84	0.63	169
8 Adelanto loam			0.52	54.5

\*These beads were used to make the glass bead aggregates.  
They were not used as a mulch.

Table 2. List of materials used for each experiment.

Experi- ment no.	Date 1971	Mulch depth (mm)	Mulch material		
			Lysimeter 1	Lysimeter 2	Lysimeter 3
Ia	25 May-28 May	5	2 mm glass beads	0.5 mm glass beads	1 mm glass beads
Ib	28 May- 4 Jun	10	"	"	"
Ic	4 Jun-16 Jun	20	"	"	"
IIa	18 Jun-22 Jun	5	1 mm glass beads	1 mm glass bead aggregates	1 mm soil aggregates
IIb	22 Jun-29 Jun	10	"	"	"
IIc	29 Jun- 9 Jul	20	"	"	"
IIIa	9 Jul-13 Jul	5	Adelanto loam	0.5 mm soil aggregates	1 mm soil aggregates
IIIb	12 Jul-19 Jul	10	"	"	"
IIIc	19 Jul- 2 Aug	20	"	"	"

8-9t

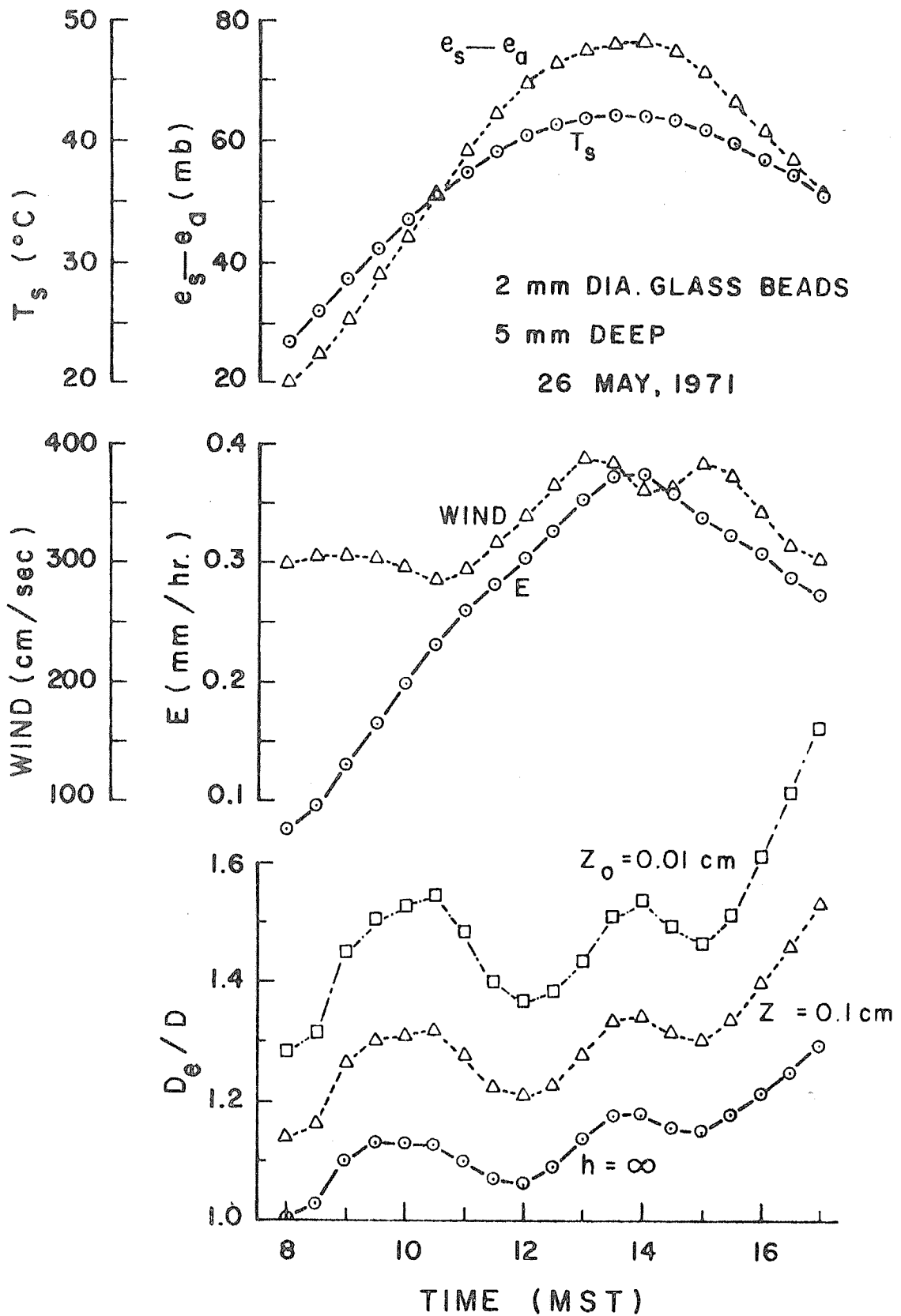


Figure 1. A plot of ratio of the effective diffusion coefficient to the molecular diffusion coefficient against time of day for three methods of calculation. Evaporation rate, wind velocity, soil interface temperature, and soil interface to air vapor pressure difference are also shown.

TITLE: USE OF FLOATING MATERIALS TO REDUCE EVAPORATION FROM WATER SURFACES

CRIS WORK UNIT: SWC-018-gG4

CODE No.: Ariz.-WCL 71-6

INTRODUCTION:

Two floating materials that appeared promising in previous tests were evaluated at the Granite Reef test site to determine long range durability and efficiency. These materials, which were observed from June 1970 to December 1971, consisted of wax blocks and treated perlite ore.

Evaluated at the Laboratory site between May and December 1971 on insulated evaporation tanks were commercial samples of foamed butyl rubber in a sheet, and small plastic pieces. A sample of treated perlite ore was also tested during this period.

In order to properly evaluate the results of evaporation reduction experiments, the relationship between evaporation rates of evaporation pans, tanks and ponds before treatment must be established. It takes considerable time to establish this type of relationship since the energy balance of the evaporating bodies changes throughout the year, and from year to year, because of differences in the weather. Data from 1969, 1970 and 1971 were used to determine evaporation relationships between two Young pans, six stock tanks, and a lined pond at the Granite Reef test site.

PROCEDURE:

The evaporation reduction experiment at Granite Reef was conducted from June 1970 to December 1971 on three stock tanks. The treated perlite was placed on one tank, the wax blocks on another, and the third was used as a standard. The perlite was treated with a mixture of 2 percent DuPont PVA 72-60 and 4 percent Dow 772 silicone repellent. Sufficient perlite was then placed on the tank to just cover the entire water surface one layer thick. The wax blocks averaged about 12 cm in diameter and covered about 60 to 70 percent of the surface area. Point gage readings of the water depth were

recorded periodically throughout the study period to determine evaporation rates.

The experiment at the Laboratory site was conducted on four insulated evaporation tanks. A sheet of commercially available, cream colored, foamed butyl rubber supplied by Segmented Swimming Pools Ltd. was placed on one tank. On another was a one layer cover of a commercial plastic material called mini-vaps. This material is in the shape of a plus sign, each of the four legs being about 2 cm long, 1 cm wide, and 1/2 cm thick. The third cover was a layer of perlite ore treated with a 3 percent solution of Dow 772 silicone repellent. The fourth tank was used as a standard and evaporation was determined from point gage readings.

Evaporation from the two standard Young pans was determined from point gage readings. The same procedure was used on the six stock tanks which are 2.7 meters in diameter and 0.9 meters deep. A water stage recorder was used to give a continuous record of water level in the pond, from which evaporation could be determined. Once evaporation was known, it was possible to determine pan coefficients between the pans and the pond, and also between the pans and each tank. Regression analysis also provided correlation coefficients in each case.

#### RESULTS AND DISCUSSION:

The evaporation reduction efficiency of the treated perlite at Granite Reef averaged 10 percent over the study period as shown in Table 1. The efficiency was generally higher than 10 percent except for the last five months when the treatment apparently deteriorated and coverage was less than 100 percent. Wind storms during June and September 1970 also caused a reduction in efficiency when a large portion of the perlite was blown off the water surface, requiring a retreatment in each case. The reduction in efficiency during the winter months was also observed on the wax covered tank and was due to a change in the energy balance of the tanks. It appears from

this and previous perlite studies that the water repellent treatments used have deteriorated after exposure of from 6 to 8 months, thus requiring complete retreatment to maintain an acceptable efficiency.

The efficiency of the 60 to 70 percent cover of wax blocks has remained essentially the same over the 19 month study period. The efficiency is somewhat higher during the hot season and lower during the cold season with an overall average of 37 percent.

Evaporation reduction efficiency of the Segmented Swimming Pools foamed cover on the insulated tank averaged 67 percent with about 80 percent of the surface covered. This is a reduction in efficiency of 7 percent from last year and may be due to weathering of the butyl or to a change in the surface color as the cover collects dust during exposure, thus reflecting less of the incoming radiation.

The commercial mini-vaps reduced evaporation by 27 percent over the study period with essentially a complete cover. There was an increase in efficiency with time as shown in Table 2, however, this may be due to seasonal cooling, which additional data will bear out.

Also shown in Table 2 are results of the water repellent perlite ore treatment. The original perlite reduced evaporation 24 percent at the beginning, but dropped off to 6 percent in the third period. A new layer of perlite was then added and efficiency increased to 38 percent during the last period. Some of the original perlite was blown from the tank during a thunderstorm the latter part of the second period and caused the rapid decrease in efficiency. There was no evidence of the treated perlite sinking, which has been a problem in the past. The overall efficiency was 20 percent which compared with previous studies where a full cover was maintained most of the time.

Evaporation records for the six stock tanks at Granite Reef without covers indicated considerable variation in evaporation. The four end tanks evaporated essentially the same ( $\pm$  2 percent), but the two inner tanks evaporated 5 to 8 percent less because of the

moisture gradient change, or more likely, the shading of the tank walls by the outer tanks. The evaporation factors for the initial calibration periods are shown in the upper portion of Table 2 with tank #2 being used as a standard. Subsequent factors are also shown in the lower part of Table 3 for tanks 3 and 4 when covers were not present. Although the factors varied somewhat during the year, the average value remained about the same. These factors can be used to adjust evaporation readings to account for the natural variation and therefore better evaluate the effectiveness of covers, although except for the two inner tanks, the factors are small enough to ignore.

The pan coefficients for Young pans are generally thought to approach unity. However, the coefficients between the Granite Reef pond and the two Young pans were found to average 0.73 and 0.77 for the south and north pans, respectively. These coefficients were calculated on a monthly basis and compared to both water depth in the pond and time of year. The depth of water in the pond had no apparent effect on the coefficient, but there was a slight tendency for the coefficient to be higher than average in the summer and lower in the winter.

The correlation coefficients between the evaporation from the pond and that from the pans was 0.98 for both pans. These correlation coefficients are surprisingly high considering the errors involved in determining evaporation from the pond water stage chart, since water is pumped in and out of the pond for other uses.

Pan coefficients for both Young pans and the six stock tanks are shown in the upper portion of Table 4. These coefficients show that tank evaporation is from 6 to 21 percent higher than pan evaporation, which is within the normal range of exposed wall tanks. The coefficients also indicate that the inner tanks evaporate 5 to 10 percent less than the outer tanks as previously indicated in Table 3.

The lower portion of Table 4 shows the correlation coefficients between pan and tank evaporation. In all cases the correlation is

very good, indicating that evaluation of the effectiveness of floating covers would be quite adequate.

In addition to the pan coefficients developed during the initial calibration period as shown in Table 4, the coefficient for tank #2 is presented in Table 5 by months for portions of 1969, 1970, and all of 1971. Although more data will be needed to establish good average monthly coefficients, the available data does show differences from year to year and also trends. For example, there is a tendency for the coefficients to be higher than average in the spring, and lower in the late fall.

The ratio of evaporation between the north and south Young pans varied from 0.87 to 1.04 over the 24 months that data have been collected, with an overall average of 0.95. The correlation coefficient between the two pans was 0.99, showing good correlation. The differences in evaporation must be due to exposure or a combination of prevailing winds and location of the pan with respect to the pond, thus setting up a different moisture gradient between the two pans.

#### SUMMARY AND CONCLUSIONS:

The evaporation reduction efficiency of treated perlite ore in two experiments decreased from initial values of about 25 to 30 percent to essentially zero after exposure of 6 to 8 months, indicating a breakdown of the silicone treatments. The efficiency of wax blocks remained about the same over a 19 month study period and averaged 37 percent with 60 to 70 percent of the surface covered. The efficiency of a complete cover of a commercial plastic material called "mini-vaps" increased during a six month study from 18 to 31 percent with an average of 27 percent. A foamed butyl cover that reduced evaporation 74 percent with 80 percent coverage a year ago reduced evaporation 67 percent this year. The decrease in efficiency was probably due to weathering of the material or to a build-up of dust on the surface, thus reducing the amount of incoming radiation reflected.

Pan coefficients were established between two Young pans, six stock tanks 2.7 meters in diameter and 0.9 meter deep, and a lined pond with a surface of 12 × 27 meters and 2 meters deep. The pan to pond coefficients were 0.73 and 0.77 for the south and north pans, respectively. Coefficients for the stock tanks varied from 1.06 to 1.21 with the two inner tanks having the lowest coefficients due to shading from the outer tanks. Monthly tank coefficients were found to be higher than average in the spring and lower in the late fall.

Regression analysis between the pans and pond, the pans and tanks, and between the two pans produced correlation coefficients of 0.98 or greater in all cases. Because of the good correlations, evaporation reduction experiments on the tanks and pond should provide accurate information concerning the efficiency of cover materials.

PERSONNEL: Keith R. Cooley

CURRENT TERMINATION DATE: 31 December 1972

Table 1. Evaporation reduction efficiency of perlite and wax blocks  
(evaporation in cm)

MONTH	Evaporation Open	Evaporation Perlite	Efficiency Perlite	Evaporation Wax	Efficiency Wax
Jun 70	36.93	37.36	-1	25.14	32
Jul	41.82	34.19	18	27.37	35
Aug	34.96	28.89	17	21.33	39
Sep	23.62	21.74	8	15.07	36
Oct	21.18	15.81	25	13.33	37
Nov	10.72	9.87	8	7.13	33
Dec	10.00	9.90	1	7.44	26
Jan	9.48	8.10	14	6.72	29
Feb	15.02	13.84	7	10.01	33
Mar	20.93	19.02	8	13.52	35
Apr	24.94	21.46	13	15.34	40
May	37.30	27.75	25	21.39	43
Jun	41.91	35.11	15	23.77	43
Jul	44.50	39.80	10	24.61	45
Aug	29.70	28.62	3	18.31	38
Sep	32.08	30.74	3	20.64	36
Oct	8.24	9.06	-11	5.43	34
Nov	15.79	16.39	-11	11.48	27
Dec	8.06	8.74	-5	6.83	14
Avg.	467.18	420.04	10	294.84	37

Table 2. Evaporation reduction efficiency of mini-vaps foamed butyl and perlite (evaporation in cm).

PERIOD	Evap. Open	Evap. Mini- Vaps	Effic. Mini- Vaps	Evap. Butyl	Effic. Butyl	Evap. Perlite	Effic. Perlite
25 May - 29 Jun	25.15	20.61	18	8.07	68	19.10	24
29 Jun - 3 Aug	26.18	20.51	22	9.11	65	21.41	18
17 Sep - 27 Oct	14.98	10.55	30	5.05	66	14.15	6
27 Oct - 6 Dec	8.59	5.89	31	2.60	70	5.36	38
Average	74.90	54.56	27	24.83	67	60.02	20

Table 3. Granite Reef stock tank coefficients (Tank #2 used as a standard).

	Tank #1	Tank #2	Tank #3	Tank #4	Tank #5	Tank #6
<u>1969 - All Tanks Open</u>						
8 May - 8 Aug	.99	1.00	.94	-	-	-
8 May - 8 Sep	-	-	-	.93	.98	1.01
<u>1971 - Tanks 2, 3, &amp; 4 Open</u>						
Jan		1.00	-	.86		
Feb		1.00	.86	.92		
Mar		1.00	.93	.89		
Apr		1.00	.93	.94		
May		1.00	.94	-		
Jun		1.00	.92	-		
Jul		1.00	.93	-		
Aug		1.00	.94	-		
Sep		1.00	.93	-		
Oct		1.00	.97	-		
Nov		1.00	1.00	-		
Dec		1.00	1.07	-		
Avg.		1.00	.94	.91		

Table 4. Granite Reef pan to tank coefficients and correlation coefficients.

	Tank #1	Tank #2	Tank #3	Tank #4	Tank #5	Tank #6
<u>Pan to Tank Coefficients</u>						
South Pan	1.14	1.15	1.07	1.06	1.12	1.16
North Pan	1.18	1.19	1.13	1.11	1.17	1.21
<u>Pan to Tank Correlation Coefficients</u>						
South Pan	.993	.994	.994	.987	.993	.994
North Pan	.996	.993	.997	.983	.985	.989

Table 5. Monthly pan coefficients for Granite Reef stock tank #2

Month	1969		1970		1971	
	North	South	North	South	North	South
Jan					1.16	1.09
Feb					1.22	1.15
Mar					1.28	1.16
Apr					1.24	1.15
May	1.21	1.14			1.20	1.13
Jun	1.20	1.15	1.18	1.17	1.25	1.14
Jul	1.20	1.16	1.09	1.05	1.24	1.10
Aug	1.12	1.15	1.12	1.08	1.15	1.10
Sep			1.02	1.05	1.26	1.18
Oct			1.08	1.05	1.12	1.13
Nov			1.09	1.05	1.15	1.10
Dec			1.03	0.98	1.01	1.01
Avg.	1.18	1.15	1.09	1.06	1.19	1.12

TITLE: WATER ADSORPTION PROPERTIES OF SOIL SURFACES  
COATED WITH ORGANIC COMPOUNDS.

CRIS WORK UNIT: SWC-018-gG-4 CODE NO. Ariz.-WCL 71-7

INTRODUCTION:

Soils may be made water-repellent by coating the particulates with monomolecular films of low surface-energy organic additives. Such water-repellent soils have been shown to exhibit a contact angle with water of greater than  $90^{\circ}$ , and to effectively resist the movement of liquid water through the soil pore structure, so long as the pressure head of the water does not exceed the break-through pressure of the soil.

Preliminary experimentation also showed that the water-vapor adsorptive properties of soils could be altered by coating the soils with organic films. Related work in other fields suggested that such adsorption studies could be used to characterize certain physical-chemical phenomena and interrelationships at the soil-organic-water interfaces. The present study was initiated to evaluate these phenomena and interrelationships in soils.

PROCEDURE:

The adsorption isotherm apparatus used in the first phase of this work was described in the 1969 Annual Report. It consists of a Cahn electrobalance for measuring adsorption, and a chromatographic gas flow system using  $N_2$  as the carrier for control of the relative vapor pressure. Only one soil has been tested extensively to date — this, a red, acid Lloyd soil from the southeast United States.

The soil ( $< 50\mu$ ) was dried in the adsorption apparatus at 20 C by continuously passing  $N_2$  gas past the sample. A water vapor adsorption isotherm was run on the sample, and the sample then redried.

Methyltrichlorosilane vapor then was introduced into the flow system to react with the soil, after which the excess chlorosilane was removed with straight carrier gas. Water vapor adsorption

isotherms at three temperatures (6, 20 and 30 C) then were run on the treated soil sample.

#### RESULTS AND DISCUSSION:

It was found that the adsorption isotherm for water on the untreated soil fit the Type-II classification (Figure 1). This is normal for a hydrophilic soil which does not contain excessive amounts of 2:1 type, expanding clay minerals.

The soil irreversibly bound 6.3% by weight of the chlorosilane to its surfaces. The amount of chlorosilane is presupposed to be chemically adsorbed by the soil, since it could not be displaced by the normal evaporative process. This chemisorbed chlorosilane also is assumed to have reacted with the exposed hydroxyl sites on the soil to form stable coordinate bonds.

The treated soil adsorbed less water than the untreated over the vapor pressure ranges tested (Figure 1), suggesting that the chemisorbed silicone with its exposed methyl groups has lowered the surface energy of the soil. However, since the isotherms for the treated soil retain their Type-II sigmoidal shape, it must be concluded that the soil surface has retained some of its hydrophilic sites, i.e., the methyl groups are not close packed so as to completely exclude water from the soil surface.

The *c*-value from the BET equation provides some measure of the bond energy between the water adsorbate and the soil surface — the higher the *c*-value, the tighter the bond. The *c*-values for water on this soil were: untreated, 20 C (*c* = 10.5); treated, 6 C (*c* = 5.3); 20 C (*c* = 6.9); 30 C (*c* = 6.8). Thus the methyltrichlorosilane treatment has lowered the soil surface energy, but apparently has not rendered it completely hydrophobic, since the *c*-value for a completely hydrophobic surface should be only 2 or less. Contact angle data on this treated soil is needed to determine if the roughness contribution factors have increased the apparent contact angle beyond 90° to render the soil hydrophobic to liquid water.

It was observed that the treated soil adsorbed less water vapor at 6 C than at the two higher temperatures. This is contrary to normal expectation where physisorption is inversely proportional to the kinetic energy of the system. There are systems, however, which do exhibit this reversal. The surface area of such a system is predominantly hydrophobic, but has some isolated, scattered hydrophilic sites which tend to serve as nucleating centers for the water vapor to condense on; and the higher the temperature, the more active these sites become. Silver iodide and certain hydrophobed silicas are examples.

#### SUMMARY AND CONCLUSIONS:

Changes in the surface chemistry of a soil, brought about by coating it with a thin, molecular film of the organic methyltrichlorosilane, were observed using the adsorption of water vapor. Adsorption isotherms were run on the untreated soil (20 C only), and at three different temperatures (6, 20, 30 C) on the sample after coating it with the chlorosilane. It was found that the soil (an acid, sesquioxide rich Lloyd soil from the southeastern United States) reacted chemically with the chlorosilane to permanently bond 6.3% by weight of the organic. The coated soil adsorbed appreciably less water vapor than the untreated over the vapor pressure range tested (up to 80%). Nevertheless, residual hydrophilic sites apparently remained after the organic treatment — this adjudged from the general shape of the isotherms and from the BET c-values which retained values greater than 2, i. e., the maximum value for a completely water-repellent surface. It was also observed that the treated soil adsorbed more water at the higher temperatures than for the 6 C isotherm. This was contrary to normal expectation, but in accord with certain hydrophobic materials which have isolated, scattered hydrophilic sites.

PERSONNEL: D. H. Fink.

CURRENT TERMINATION DATE: December 1973.

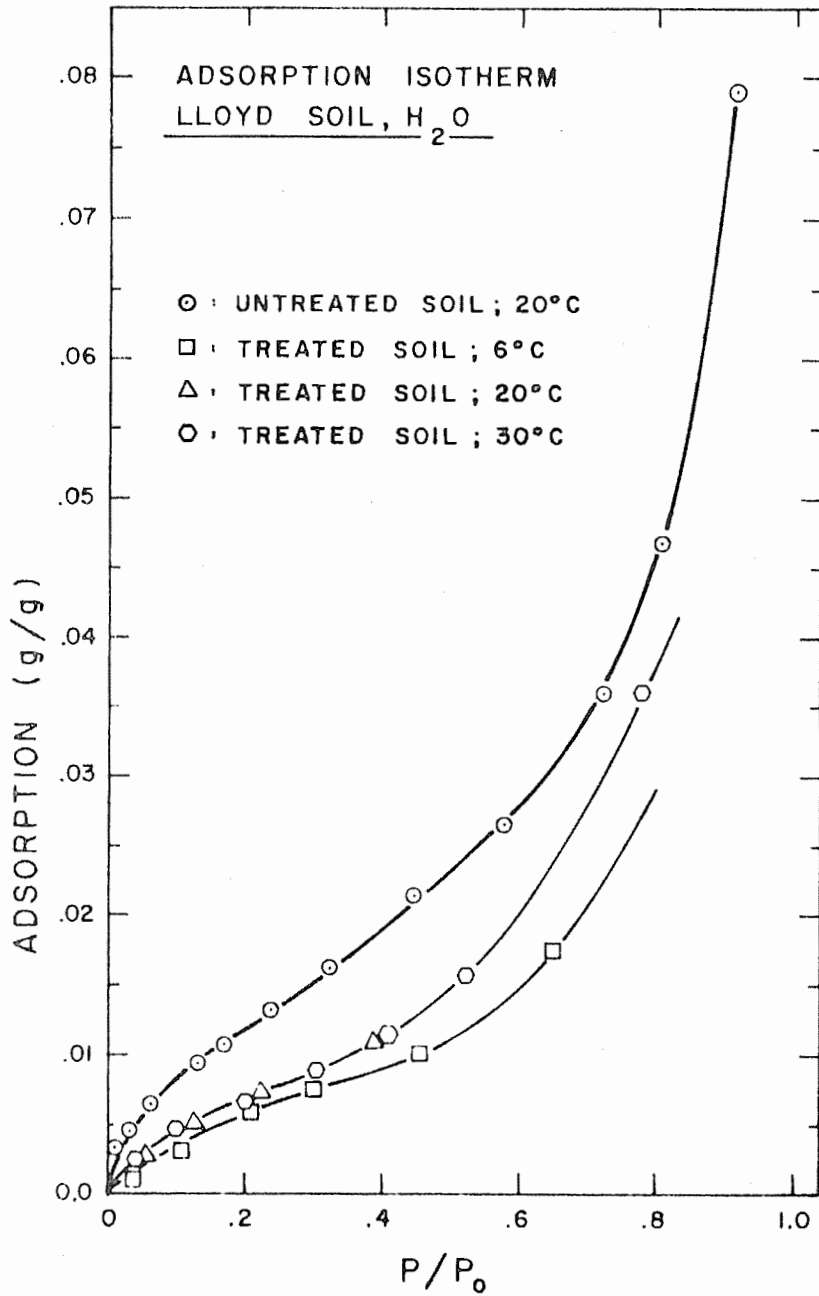


Figure 1. Adsorption isotherms of water on Lloyd soil before and after treatment with methyltrichlorosilane.

TITLE: THE EFFECT OF AIR ENTRAPMENT ON WATER MOVEMENT  
IN SOILS

CRIS WORK UNIT: SWC-018-gG-4 CODE NO.: Ariz.-WCL 71-8

INTRODUCTION:

With border irrigation projects, wastewater renovation by basin spreading and groundwater recharge, large areas of soil are intermittently inundated with water. Especially in the latter two projects any restriction in flow due to air entrapment could have serious economic implications, especially if flow is stopped as Adrian and Franzini (1) reported.

The effect of entrapped air on soil-water flow has long been recognized (Slater and Byers, 7). Peck (4, 5) and co-workers (Youngs and Peck, 11) studied the amounts of air flow and pressure buildup in columns of uniform material. Wilson and Luthin (10) used, in addition, layered systems in their studies. None of these authors, however, used a water table as the lower boundary condition as would occur in a wastewater renovation system or groundwater recharge system. Adrian and Franzini (1) used either an open or a closed bottom in their studies. They found for some materials, even though the bottom end was closed, water still infiltrated. Bianchi and Haskell (2) studied the effects of air in soil below a 2-acre square plot, but did not measure the air pressure directly. R. M. Dixon (personal communication) has developed a method of measuring the air pressure buildup in agricultural fields flooded for irrigation, but has not been studying the effect of depth of ponding, water table depression, etc.

Much of the problem has been due to a lack of reliable measurements of the soil parameters affecting air movement. The development of theoretical studies is somewhat limited. Youngs and Peck (11) point out the movement of air through the wetted zone introduced hysteresis into the flow study, but they used some simplifying assumptions to avoid considering it further. Phuc and

Morel-Seytoux (6) reported on some numerical studies that they had made for two-phase flow, but they did not have any experimental verification. Whisler and Watson (9) have developed a numerical analysis program that takes into account hysteresis, and have verified (Whisler and Watson, 8) that it basically predicts experimental conditions quite well where air is not restricted.

Experimental laboratory and numerical analysis work to date has involved essentially one-dimensional models. The actual field problem is three-dimensional, but can be reasonably approximated with two-dimensional models. Solution of problems associated with restricted soil-air movement beneath flooded soil areas requires: (1) a better understanding of the physical processes involved, and (2) the development of models that reasonably approximate the actual two-dimensional case.

#### PROCEDURE:

Three soil columns have been constructed from 4-inch I.D. PVC irrigation pipe to study the amount of air pressure buildup and its effect on infiltration rate, amounts and drainage (Figure 1). Since most of the air pressure changes occur quite rapidly, the air pressure changes have been monitored by pressure transducers connected directly to the air access ports. The output of these transducers is recorded on an electronic data acquisition system. Restricted air venting from the sides and bottom of these columns can be utilized to approximate lateral escape of air which might occur under field conditions. The columns were packed with air-dry material, starting with coarse gravel at the bottom, 62 cm of coarse sand and gravel, and then 72 cm of loamy sand from the Flushing Meadows area. An air vent and transducer were placed in both the upper and lower layers of each column. For the studies reported here, a water table was maintained at the bottom of the column 10 cm above the coarse gravel, and during infiltration a constant head of water of 1.5 cm was maintained on the soil surface

from a measuring supply system. For those studies where the lateral restriction of air movement was removed, vents were drilled into the sides of the columns every 10 cm.

#### RESULTS AND DISCUSSION:

The accumulated infiltration is shown in Figures 2-4 for each of the three columns as a function of time. Each curve on the graphs is the average of two or four infiltrations, depending upon whether the vents were closed or open. As can be seen, the open air vents did make a difference. The three columns behaved differently, probably due to nonuniform packing.

The infiltration rates can be determined by three ways. They could be measured by the supply system, but this was erratic due to bubbling in the burettes used to hold the water. They could be estimated from the slopes of the straight line portion of the curves in Figures 2-4. They could also be estimated from the out-flow rates after a steady state had been reached. The results of the latter two methods are shown in Table 1. This also shows the percentage decrease in infiltration rates due to closing the vents. The two methods of calculating the infiltration rate gave similar results. A nonvented system could decrease the infiltration rate as much as 12%. Thus, if the cost of renovating wastewater as is done by the Flushing Meadows project (Bouwer and Lance, 3) is \$5/acre-ft, and if the reduction in infiltration rate is carried over into a similar percentage in infiltration amount, the restricted flow is costing about \$0.60/acre-ft of water. If, on the other hand, by venting the soil-water system the flow is not restricted, an economic benefit is achieved if the cost of venting is less than the value of the increased amount of reclaimed water.

The amount of air pressure buildup during an infiltration is shown for column 2 in Figure 5 for both closed and vented systems in both the upper and lower layers. The dots represent the actual data for an individual run, while the solid or dashed curves are

averages for 2 or 4 runs. Venting did not cause much change in the amount of air pressure in the top layer, but did change the rate. This may have been due to "fingering" around the opening into the transducer port. Of course this may happen in the field, also. The air pressure buildup in the bottom layer was prevented by venting.

The amounts of accumulated drainage as a function of time for column 2 are shown in Figure 6. Each curve is an average of two runs. For a closed infiltration there was less water in the column and, therefore, less to drain. For an open infiltration and closed drainage, the drainage rate was slower than for a completely open or vented system. Thus, venting affects both the infiltration and drainage of a soil profile.

The air pressure change in soil column 2 during drainage is shown in Figure 7. The top of the column had an unusual but characteristic behavior. When the air pressure dropped to zero, it "overshot" and then returned back to zero. This may be due to pores in the soil being open and then closing due to Haines' drainage of surrounding pores, and then opening again. When the air vents were always open, the bottom transducer showed no pressure change. When the air vents were always closed, the bottom air pressure gradually declined to zero pressure with drainage. When, however, the air vents were sealed during drainage but had been open during infiltration, the air pressure in the bottom became negative and remained that way until the next infiltration. Probably what happened was that the bottom layer drained faster than the top layer, creating some tension in the air phase; then when the top layer stopped draining, the interface remained almost saturated, allowing very little air pressure relief to the bottom layer.

#### SUMMARY AND CONCLUSIONS:

The results of these experiments show that entrapped air may build up air pressures in the soil of 50-60 cm and may retard the infiltration rate as much as 12% in layered soil systems. Venting of the soil system overcomes much of the problems of entrapped air and may be of an economic benefit in groundwater recharge and renovation systems.

#### REFERENCES:

1. Adrian, D. D., and Franzini, J. B. Impedance to infiltration by pressure buildup ahead of the wetting front. *J. Geophys. Res.* 71:5857-5862. 1966.
2. Bianchi, W. C., and Haskell, E. E., Jr. Air in the vadose zone as it affects water movements beneath a recharge basin. *Water Resources Res.* 2:315-322. 1966.
3. Bouwer, H., and Lance, J. C. Reclaiming municipal waste water by groundwater recharge. Proc., AAAS Symposium on Urbanization of Arid Lands, Chicago, Illinois, December 1970.
4. Peck, A. J. Moisture profile development and air compression during water uptake by bounded porous bodies: 2. Horizontal columns. *Soil Sci.* 99:327-334. 1965.
5. Peck, A. J. Moisture profile development and air compression during water uptake by bounded porous bodies: 3. Vertical columns. *Soil Sci.* 100:44-51. 1965.
6. Phuc, Le Van, and Morel-Seytoux, H. J. Effect of air flow on infiltration rates. Presentation, SSSA meetings, Tucson, Arizona, August 1970.
7. Slater, C. S., and Byers, H. G. A laboratory study of the field percolation rates of soils. U.S. Dept. Agri. Tech. Bull. 232. 1931.
8. Whisler, F. D., and Watson, K. K. One-dimensional gravity drainage of uniform columns of porous material. *J. of Hydrol.* 6:277-296. 1968.
9. Whisler, F. D., and Watson, K. K. Analysis of infiltration into draining porous media. *ASCE J. of Irrig. and Drain. Div.* 95:481-491. 1969.

10. Wilson, L. G., and Luthin, J. N. Effect of air flow ahead of the wetting front on infiltration. Soil Sci. 96:136-143. 1963.
11. Youngs, E. G., and Peck, A. V. Moisture profile development and air compression during water uptake by bounded porous bodies: Theoretical introduction. Soil Sci. 98:209-294. 1964.

PERSONNEL: Frank D. Whisler

CURRENT TERMINATION DATE: 1975

Table 1. Infiltration rates ( $\text{cm}/\text{min} \times 10^{-2}$ ) calculated from the slopes of the accumulated infiltration curves or the volume outflow method. The values are shown for both open and closed air vents.

Column	S l o p e			O u t f l o w		
	Open	Closed	% Decrease	Open	Closed	% Decrease
1	-2.28*	-2.00	-12	-2.15	-1.90	-12
2	-1.51	-1.38	-9	-1.27	-1.20	-6
3	-1.23	-1.18	-4	-1.01	-0.98	-3

\*The more negative (larger in magnitude) the number, the higher the flow rate.

# SCHEMATIC DIAGRAM OF SOIL COLUMNS

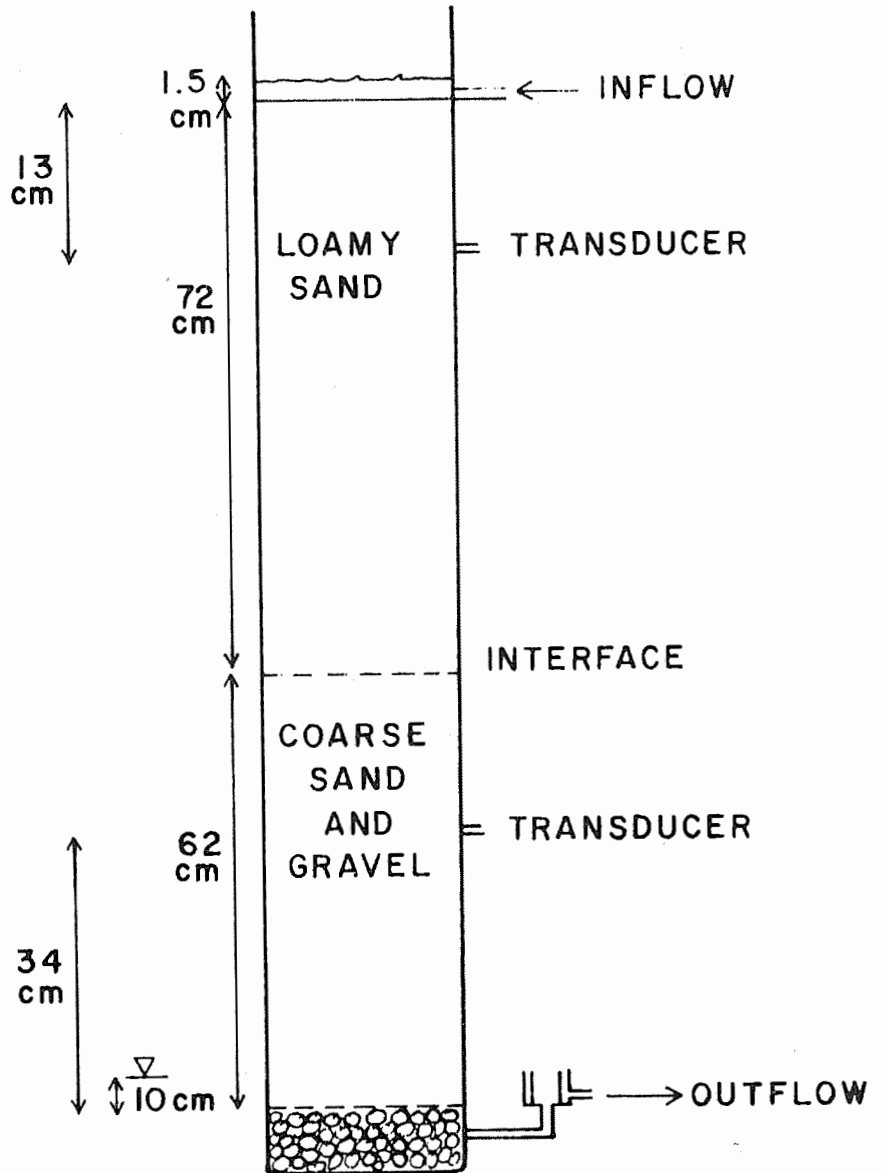


Figure 1. A schematic diagram of the flow system.

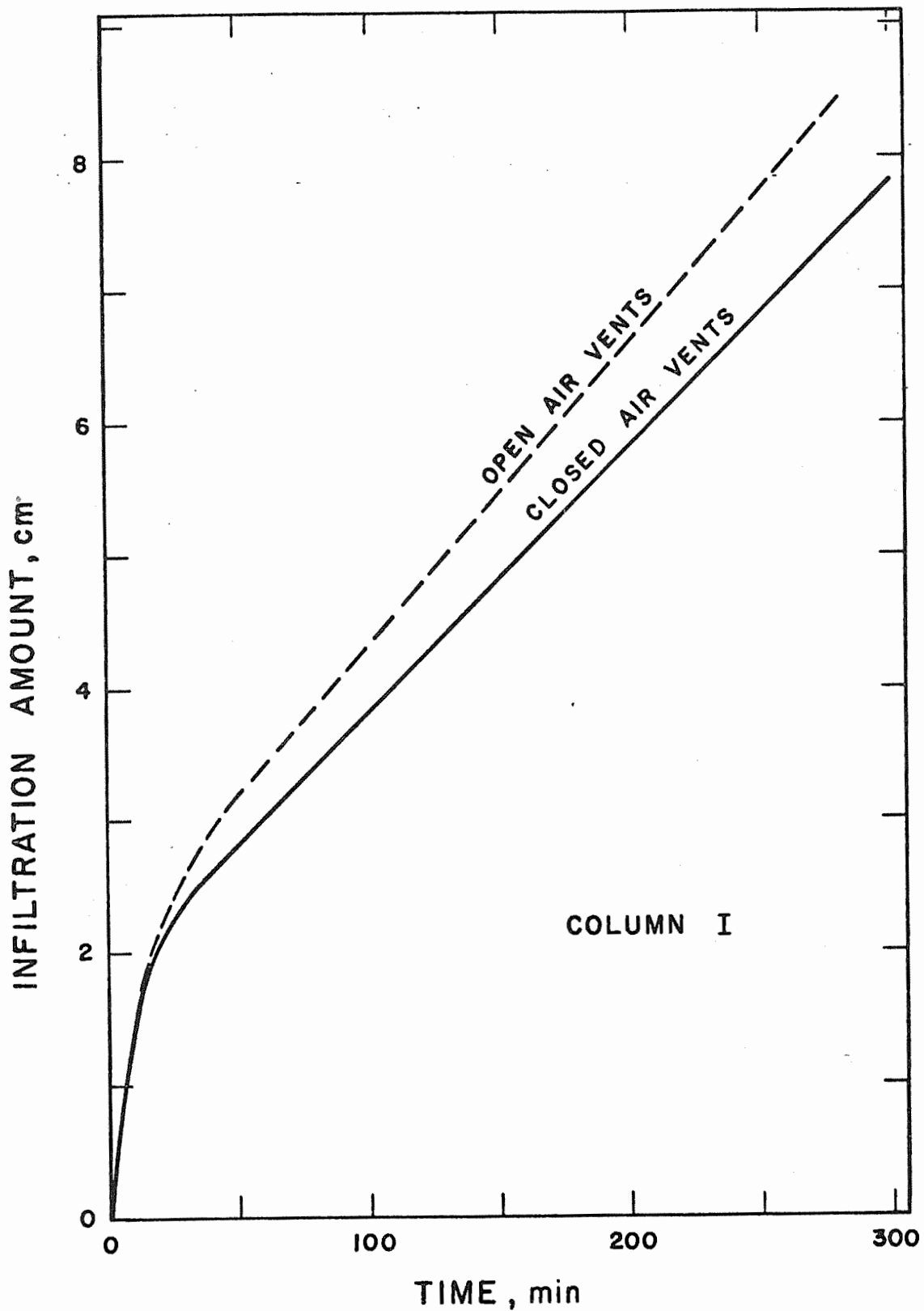


Figure 2. Accumulated infiltration versus time for column 1. The curves are the averages for two runs for closed air vents and four runs for open air vents.

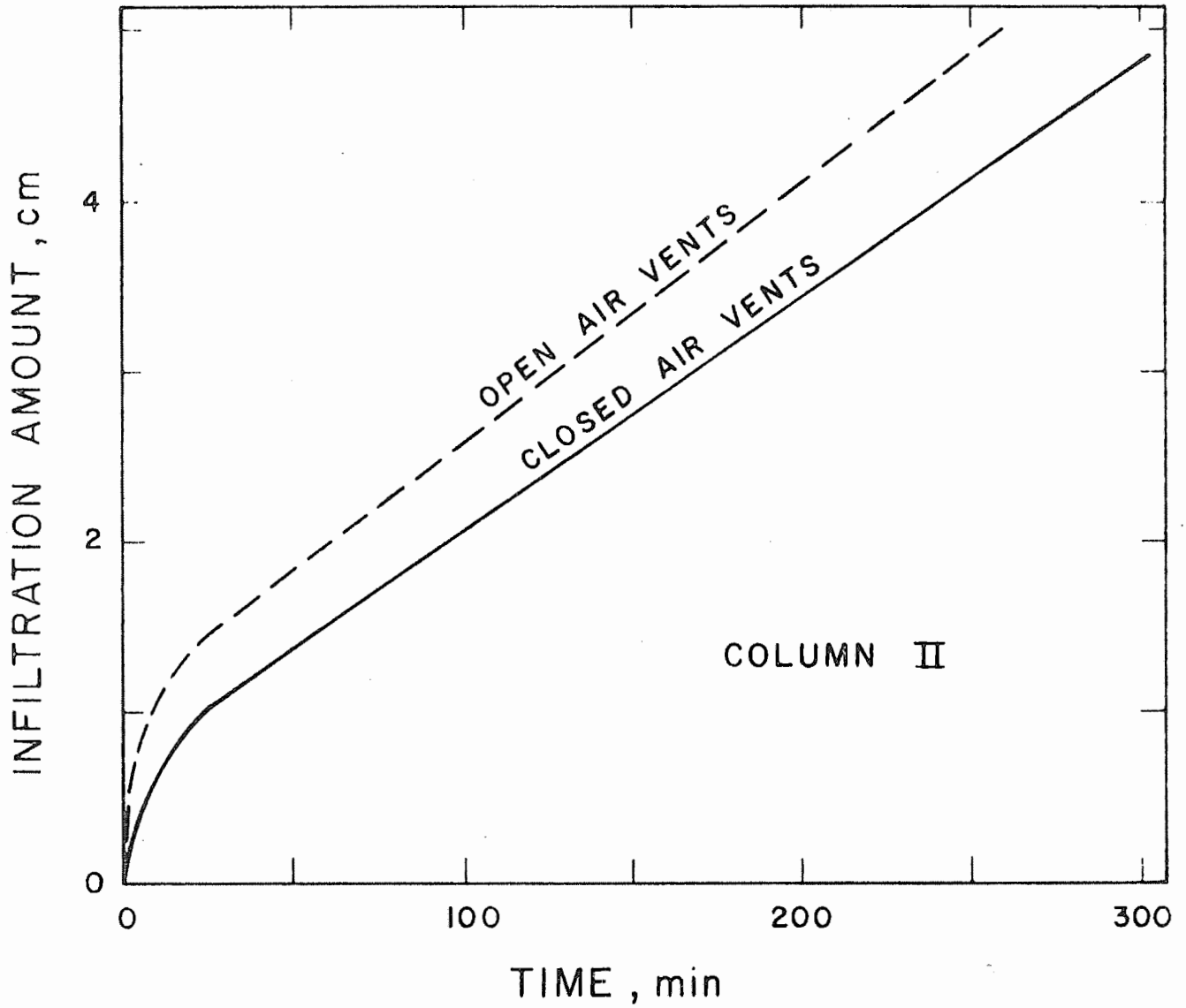


Figure 3. Accumulated infiltration versus time for column 2.

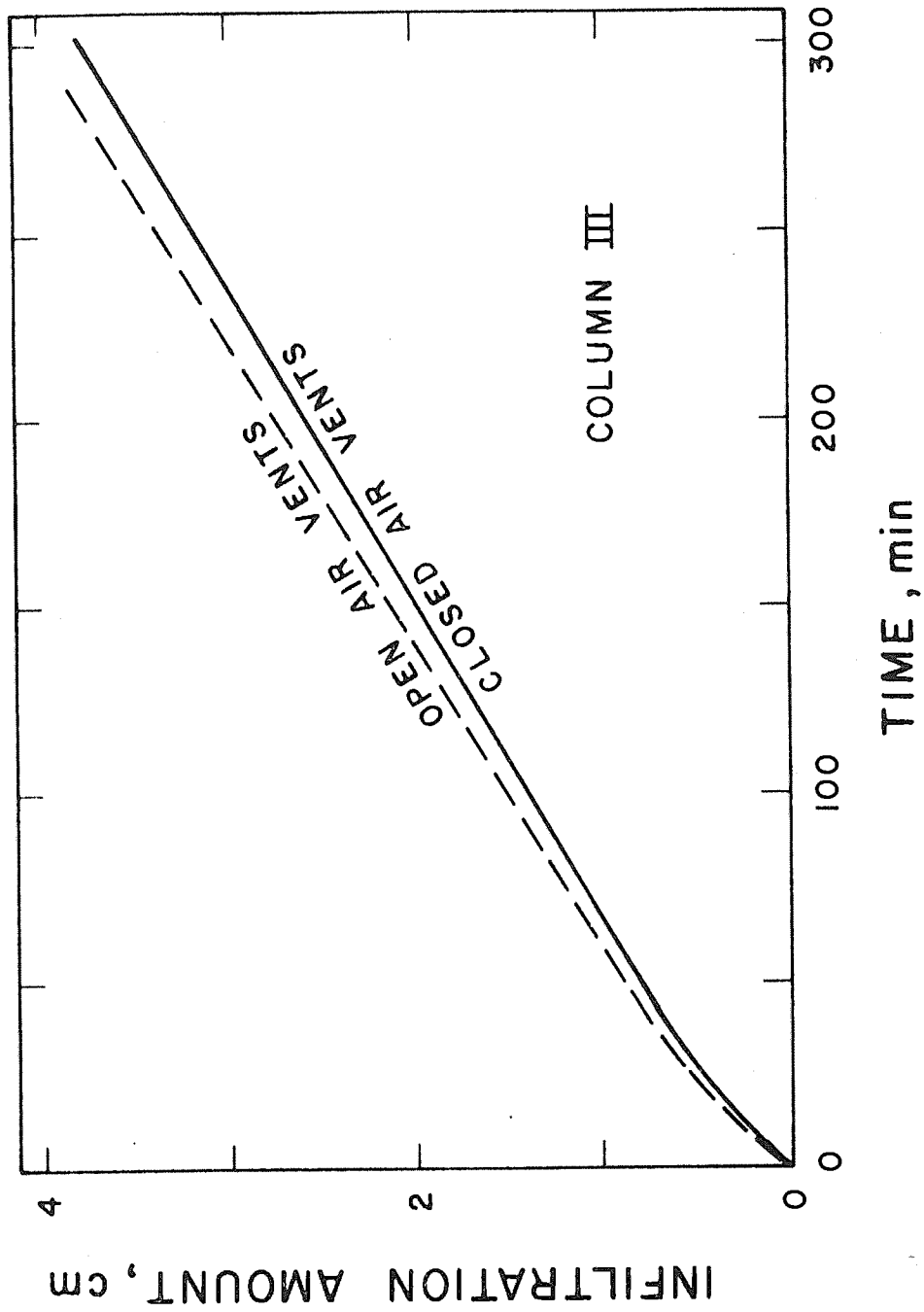


Figure 4. Accumulated infiltration versus time for column 3.

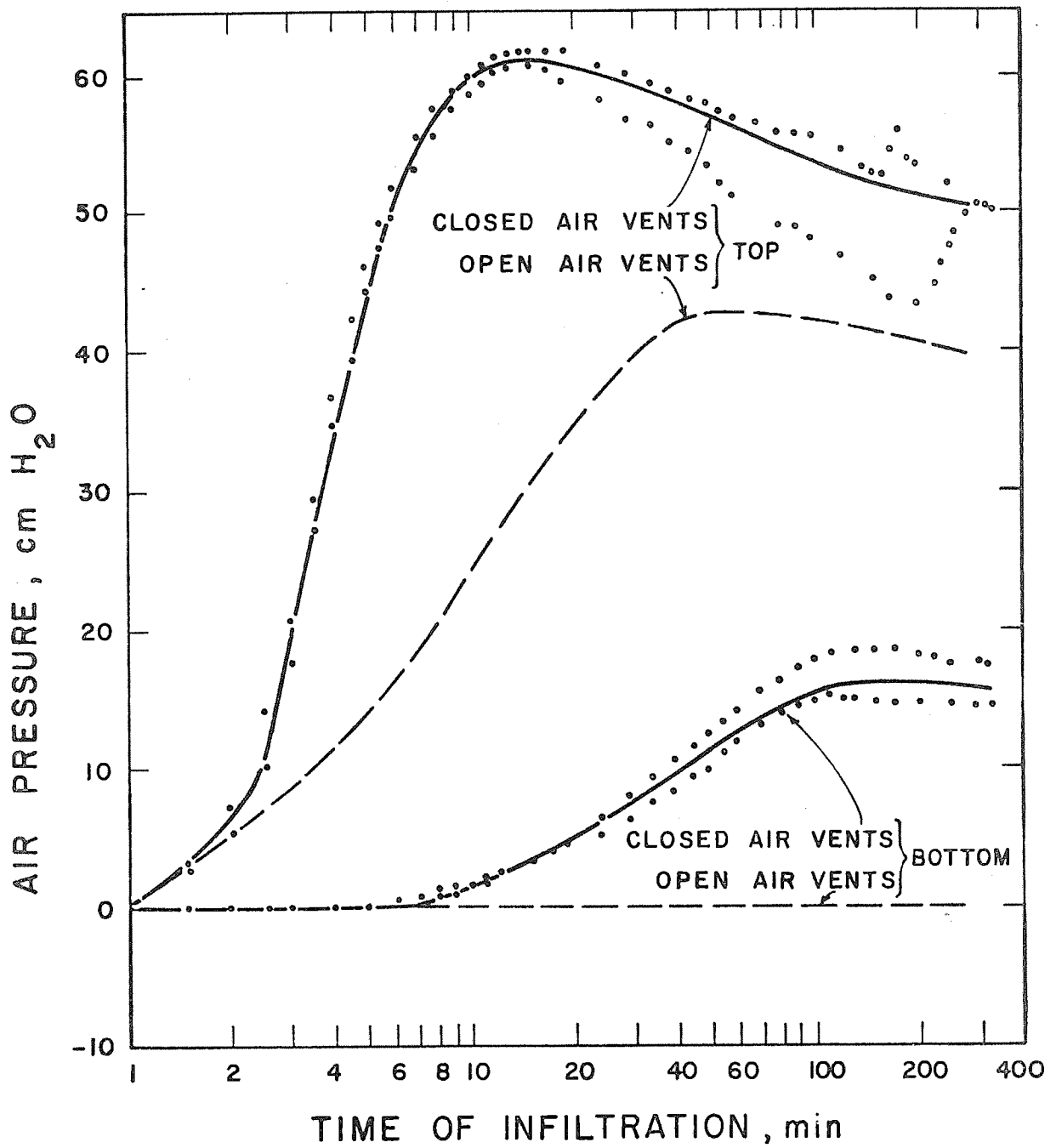


Figure 5. Air pressure buildup with time for infiltration into column 2.

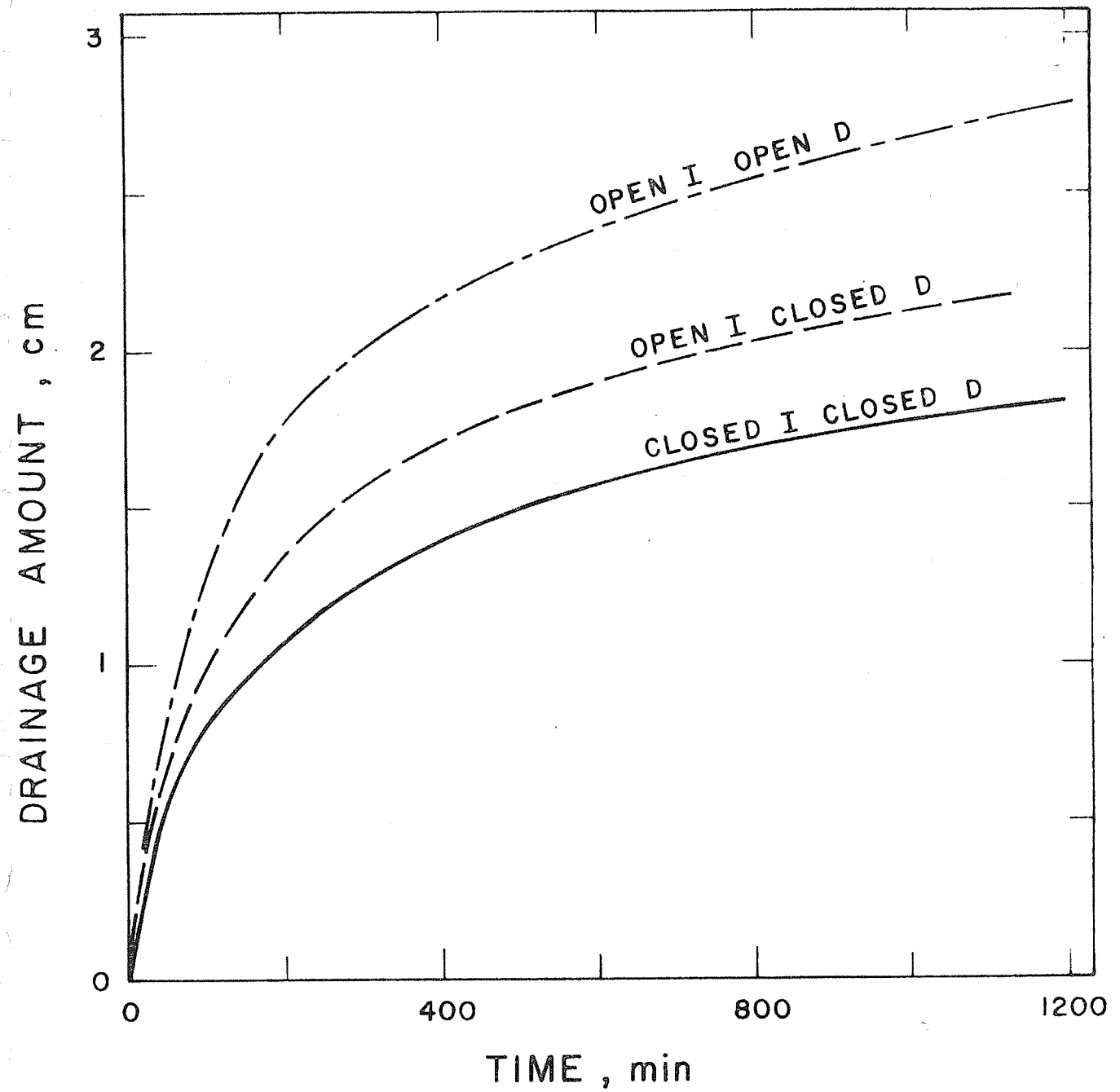


Figure 6. Accumulated drainage versus time for column 2.

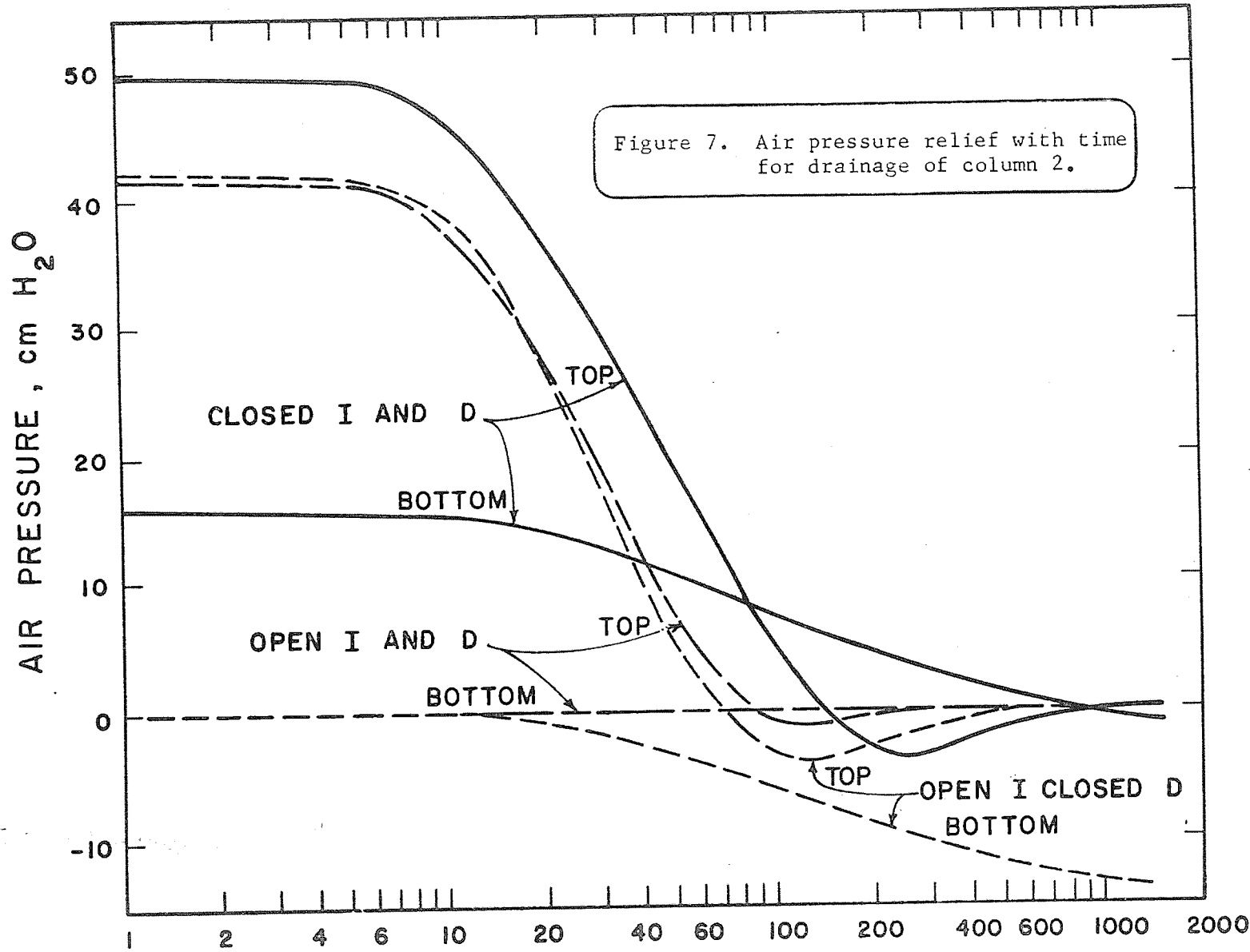


Figure 7. Air pressure relief with time for drainage of column 2.

TITLE: ONE-DIMENSIONAL FLOW IN SCALED HETEROGENEOUS  
POROUS MEDIA

CRIS WORK UNIT: SWC-018-gG-4

CODE NO.: Ariz.-WCL 71-9

INTRODUCTION:

Models have been developed for predicting the movement of water into and through homogeneous soil profiles. Poor correlation between predicted and actual field results has often been encountered because the field soils were not in fact homogeneous or composed of homogeneous layers. A predictive model for heterogeneous soils is needed. Such a model would be useful to both research and operational personnel. Two areas of application are, for example, the design of more efficient irrigation systems and the management of watersheds to retain precipitation in the soil. Soil profiles are usually heterogeneous, and that fact must be recognized in developing realistic and useful models for predicting water movement in such profiles.

PROCEDURE:

A convenient and systematic method of studying heterogeneous porous media is to make use of the concept of scale heterogeneity in conjunction with some prescribed spatial variation of a characteristic parameter. By using several different sources of hydrologic data of similar porous media, it can be shown that

$$K_{sat} h_{AEV}^2 = \Omega \approx 1850 \text{ cm}^3/\text{min} \quad (1)$$

where  $K_{sat}$  is the saturated hydraulic conductivity and  $h_{AEV}$  is the air-entry value of a particular medium. In this study the heterogeneity down the profile is defined in terms of a linear variation of the saturated hydraulic conductivity from  $K_t$  at  $z = 0$  to  $K_b$  at  $z = -L$ , where  $z$  is the depth below the soil surface and positive in the upward direction.

A finite differential form of the soil water flow equation is solved using as initial and boundary conditions, either drainage

of a soil column to a water table, or infiltration into a soil column of an initially constant, but low, water content. The soil parameters are described as empirical, functional relationships between the pressure head, water content, and hydraulic conductivity. This was done to save computer space and is satisfactory for the present study. Average values from available data were used for the constants in the empirical equations, but hysteresis was taken into account. A column length of 200 cm was assumed.

Drainage. The drainage case reported here is:

$$\begin{array}{ll} \text{Case I} & K_t = 1.0 \text{ cm/min} \\ & K_b = 0.1 \text{ cm/min} \\ & \theta_{\text{sat}} = 0.35 \text{ cc/cc} \end{array}$$

where  $K_t = K_{\text{sat}}(0)$

$K_b = K_{\text{sat}}(-L)$

Infiltration. The infiltration cases reported here are:

$$\begin{array}{ll} \text{Case I} & K_t = 0.5 \text{ cm/min} \\ & K_b = 0.05 \text{ cm/min} \\ \text{Case II} & K_t = 0.05 \text{ cm/min} \\ & K_b = 0.5 \text{ cm/min} \\ & \theta_{\text{rs}} = 0.30 \text{ cc/cc} \end{array}$$

where  $K_t = K_{\text{rs}}(0)$

$K_b = K_{\text{rs}}(-L)$

The ponding depth,  $h_t$ , was 3 cm of water.

Case I for drainage and case I for infiltration are for the same soil material, with hysteresis taken into account.

## RESULTS AND DISCUSSION:

Drainage. The pressure head profile for case I of drainage is shown in Figure 1. In this profile a zone of positive pressure is maintained in the column for a considerable length of time during drainage. Another characteristic feature of the profile is the development during drainage of a more negative pressure head in the vicinity of the drainage front than at the surface. A similar effect has been noticed in the drainage of layered profiles at the interface region.

The numerical solution was not continued sufficiently long for equilibrium to be reached throughout the entire profile. This procedure was adopted because complete equilibrium would only occur at very long time due to the low hydraulic conductivity applicable at that time in the upper region of the column. The lower part of the profile had, however, reached equilibrium at 4,999 min. It took longer for other cases examined.

The equilibrium water content profile as well as the transient profiles is given in Figure 2. As might be expected, these profiles do not show any unusual characteristics, although the manner in which the profiles are developed reflect the distribution of the air-entry value.

Infiltration. The calculated infiltration, pressure head profiles for case I are given in Figure 3. Sometime between 40 and 50 min the characteristic bulge begins to form in the pressure head profile in the middle of the column. The reason that this shape occurs is that the soil above any plane in this column is coarser than that below, thus the potential flux of water into that plane is always greater than will move on downward through that plane. Figure 4 shows the water content profiles corresponding to the pressure heads in Figure 3. Here again, since the material above any plane across the column is always coarser than that below, the pores quickly fill (if air is free to escape as is

normally assumed), and one gets a step-like function for the water content profiles.

The pressure head profiles for case II are shown in Figure 5. Here several differences are noted between this case and case I. The initial pressure head ( $t = 0$ ) is more negative toward the top of the column and not the bottom. After about 80 min the pressure head around -55 cm remains the same, and its value is close to the water entry value. The only positive pressure head values are right at the soil surface. The water content profiles corresponding to these pressure head profiles are shown in Figure 6. Here it is observed that up to about 80 min the shapes of the water content curves are the same as in Figure 4, but lag behind in position. After 80 min the profiles are different in shape. Below -68 cm the water content did not reach  $\theta_{rs} = 0.3$ . What seems to be happening is that above any plane across the profile the material is finer and restricts the flow such that the soil can only supply water fast enough to resaturate the zone above -68 cm.

The analogous drainage case for case II of infiltration is basically an unstable one since the initial pressure head values over much of the column are more negative than the air-entry values at those points. Physically, the  $K_t < K_b$  case only has reasonable meaning in drainage if air entry were permitted solely through the surface layer. For such a boundary condition the most restrictive pores to air entry would be at the surface, and the access of air to the draining system could not be neglected as is done in this analysis.

Assume that one had tensiometers in a soil profile at -20, -60, -120, and -200 cm and was calculating the pressure head changes with time during a drainage or infiltration experiment. If one assumed that the soil profile was uniform but in reality it was like case I, the high positive readings in the lower part of the

profile would be most puzzling. One might assume erroneously that there were leaks around the tensiometers which allowed the positive pressure to build up. Such an assumption would also account for the faster-than-normal advance of the wetting front for infiltration.

On the other hand, assume the soil was in reality like case II during an infiltration. One might assume erroneously that the -60 cm tensiometer was not functioning properly when, in fact, it was working. In all cases one would suspect the initial profile readings, but might erroneously assume that the tensiometers were not in equilibrium with the soil.

If at the same time the experimenter were measuring the water content in a profile like case II at the same depths as the tensiometers, he would wonder about the readings at -120 cm. He would wonder why after 120-150 min these readings were less than at the higher elevations as might be expected.

#### SUMMARY AND CONCLUSIONS:

It appears that a heterogeneous soil or porous media may behave quite differently than a homogeneous one in terms of pressure head and water content profiles. It should be noted that the choice of a variation of saturated or resaturated hydraulic conductivity down the profile as the means of defining a heterogeneous medium was made with possible field applications in mind. By using one of the available experimental methods for determining  $K_{sat}$  in the field at different depths, it is possible to check the homogeneity of the profile. If heterogeneity is found and if the scale heterogeneity assumption is considered reasonable for the material in question, it would be possible to predict at least approximately the drainage and infiltration behavior using a numerical solution.

PERSONNEL: Frank D. Whisler

CURRENT TERMINATION DATE: 1972

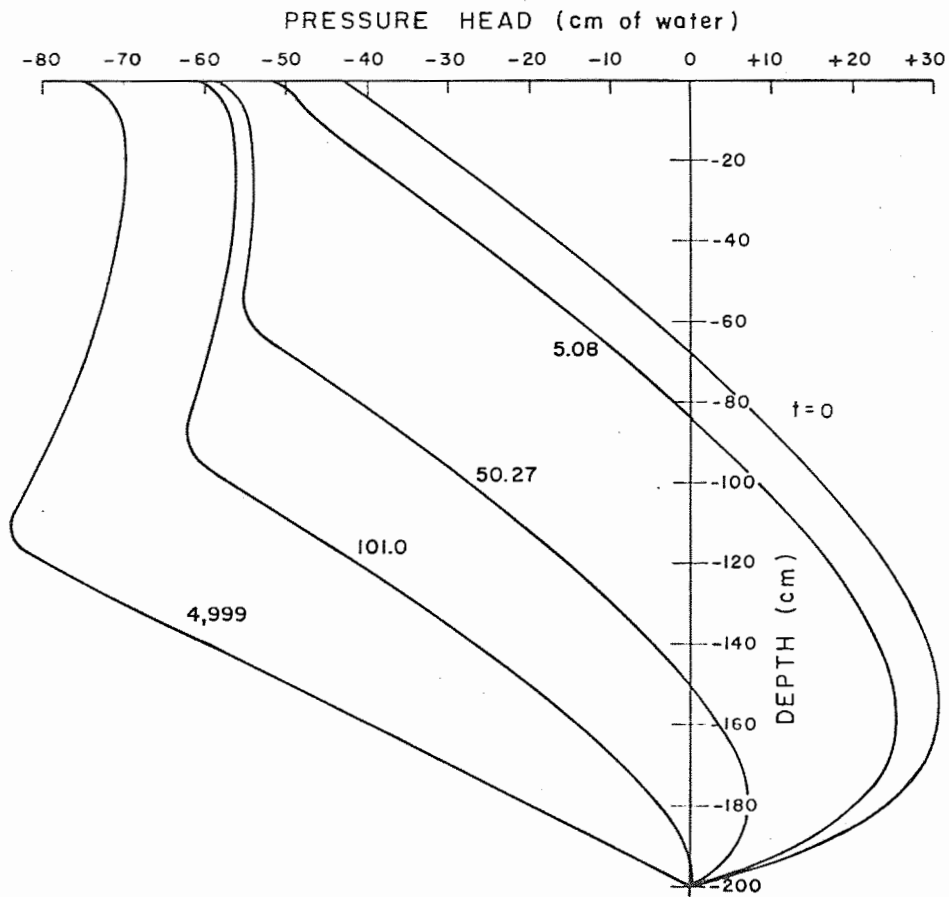


Figure 1. Pressure head profiles during drainage case I ( $K_t = 1.0$  cm/min,  $K_b = 0.1$  cm/min). The times on the profiles are given in minutes.

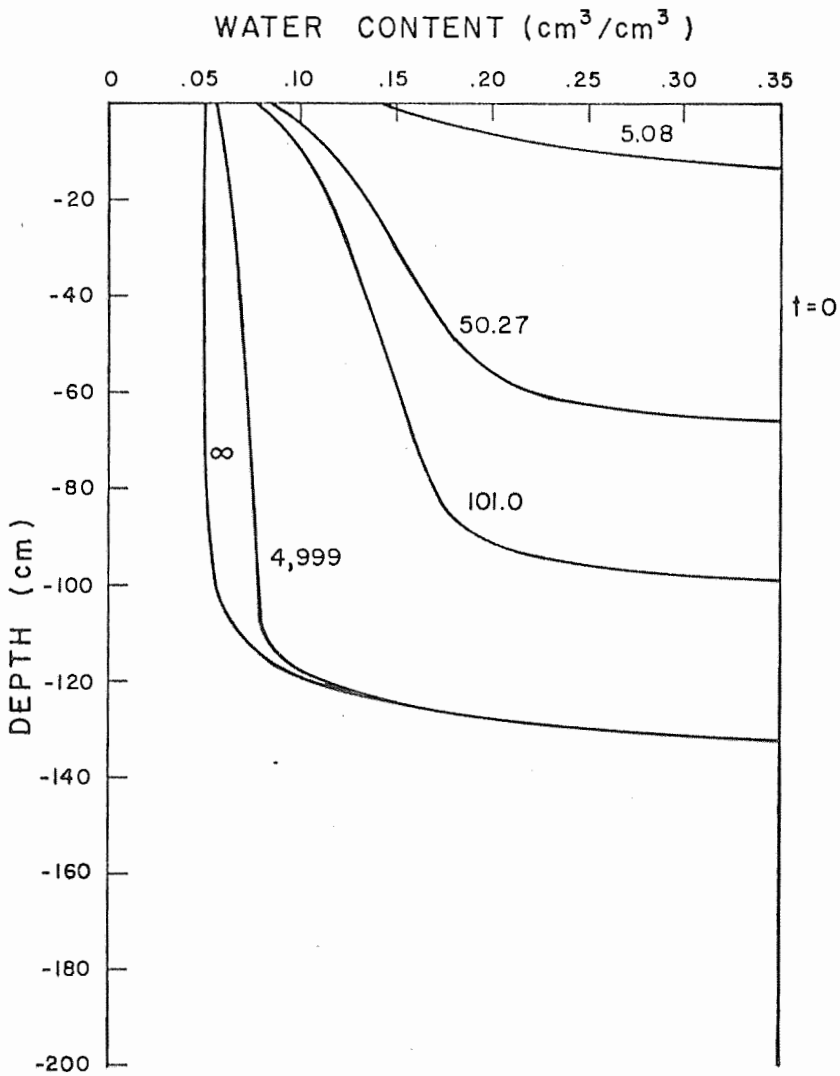


Figure 2. Water content profiles for drainage case I.

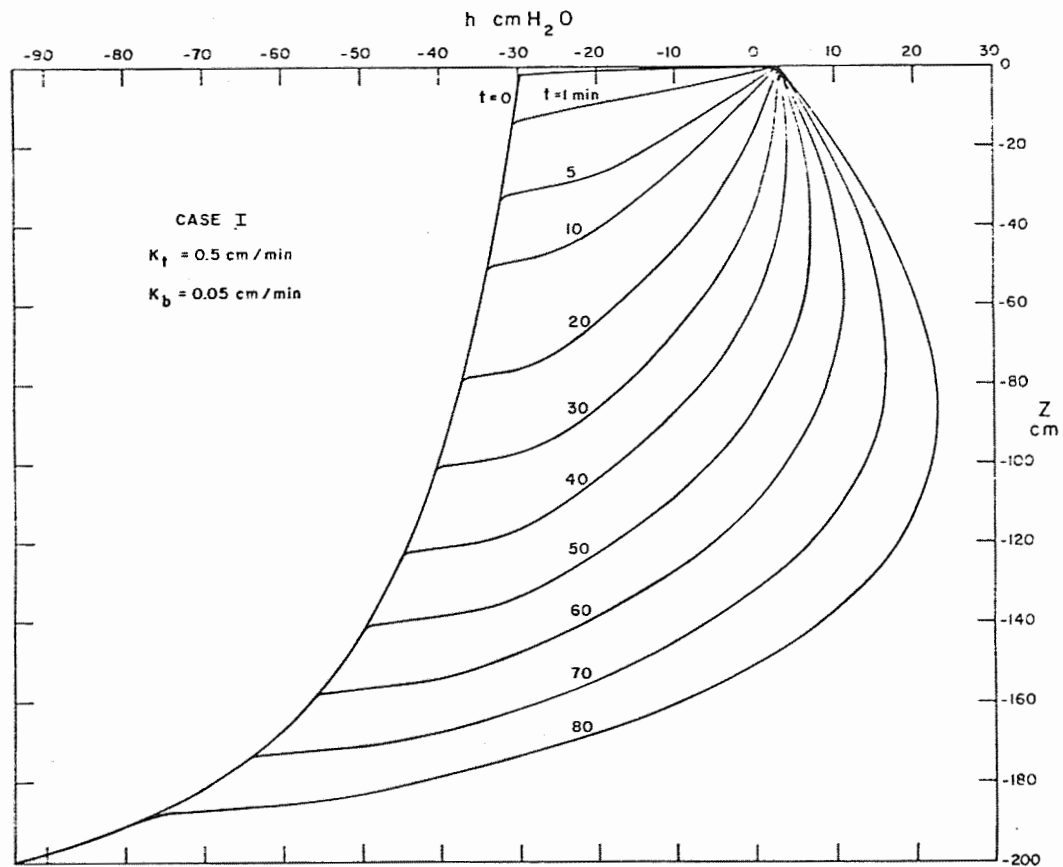


Figure 3. Pressure head profiles for infiltration case I.

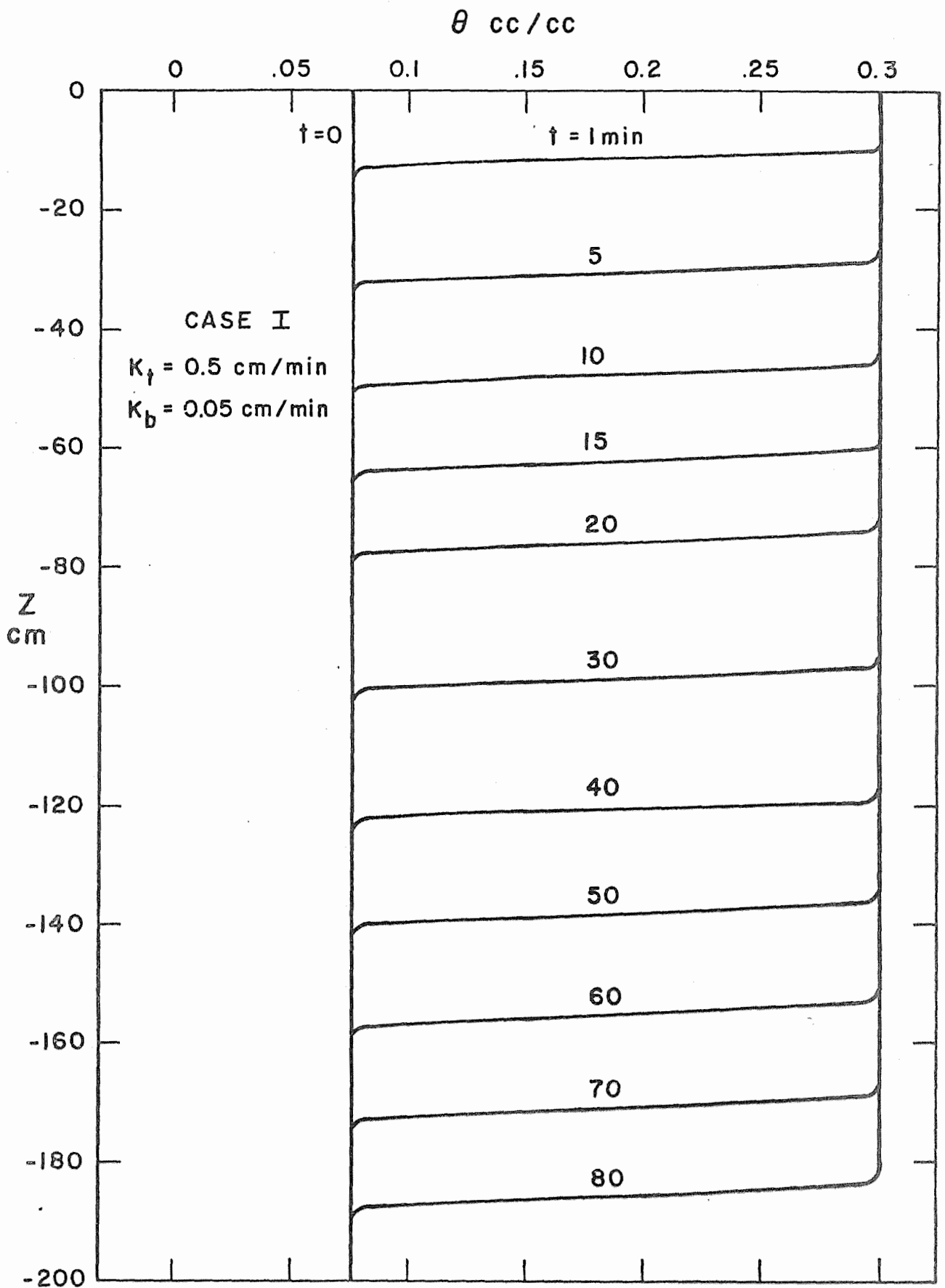
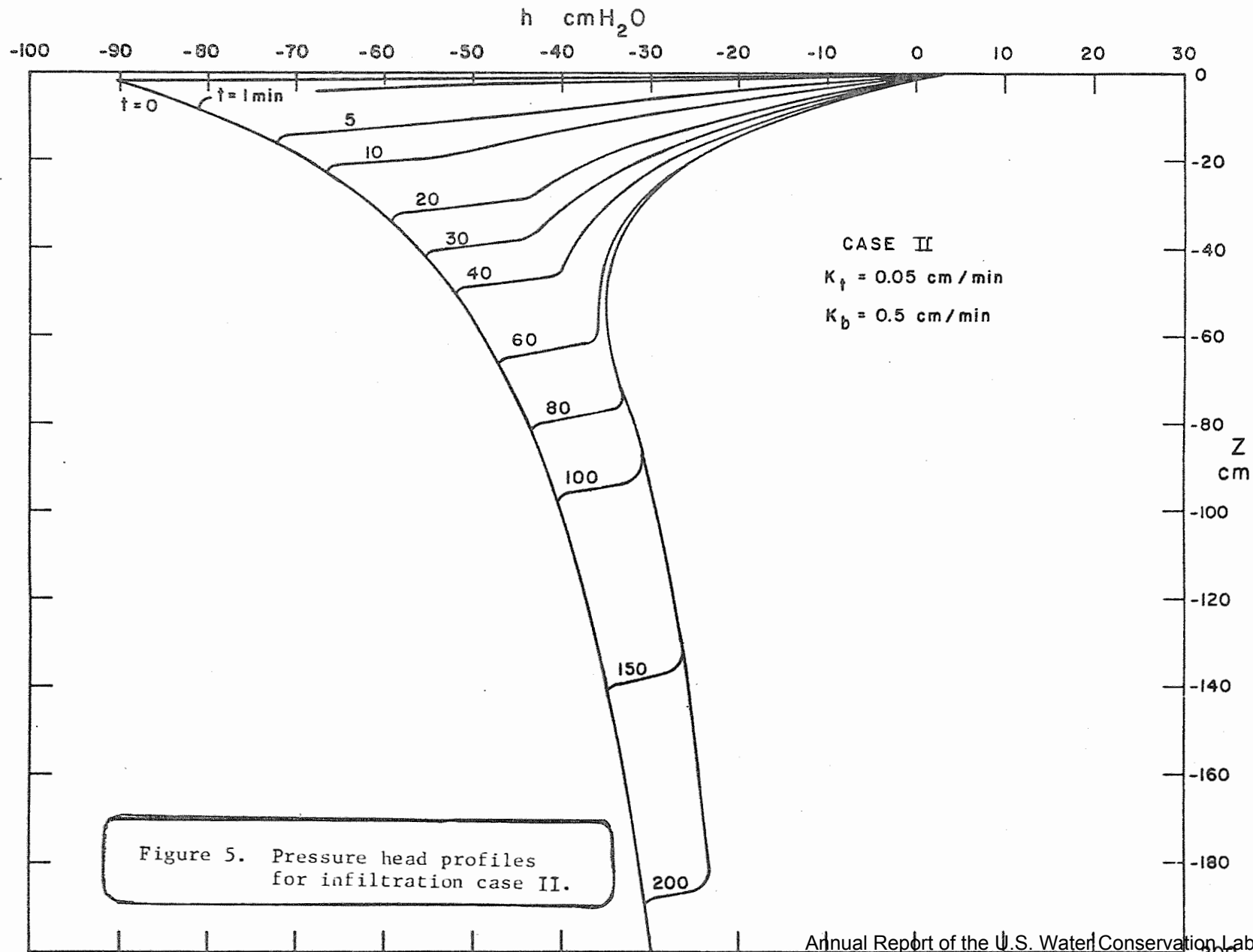


Figure 4. Water content profiles for infiltration case I.



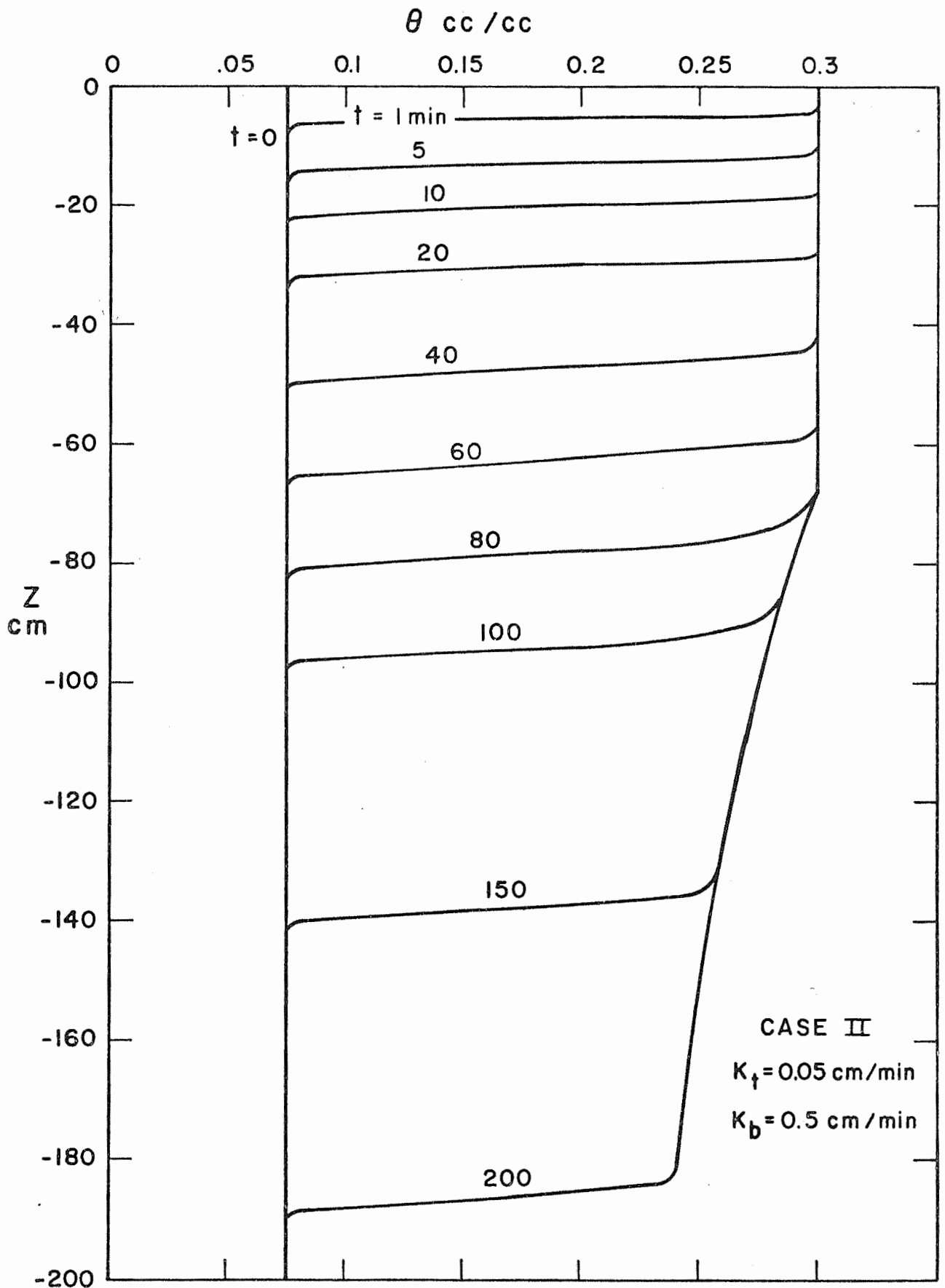


Figure 6. Water content profiles for infiltration case II.  
 Annual Report of the U.S. Water Conservation Laboratory  
 20-11

TITLE: ASSESSMENT OF BIOSTIMULATION AND EUTROPHICATION OF RECLAIMED WASTE WATER.

CRIS WORK UNIT: SWC 018-gG-4 CODE NO.: Ariz.-WCL-71-10

INTRODUCTION:

Field studies on ponds (approximately 40 ft long x 30 ft wide x 5 ft deep) at Flushing Meadows were initiated to determine the biological productivity, utilization and recycling of inorganic and organic nutrients, and modifications brought about by aquatic life in reclaimed sewage water. The first objective was to determine the biological, chemical, and physical factors that contribute to the growth of phyto- and zooplankton and fish in ponded renovated sewage water. Secondly, the aquatic ecosystem that establishes in ponded renovated sewage water will be characterized. Lastly, management practices for reducing problems created by biological activity in ponded renovated sewage water in an arid environment will be developed. The results obtained will aid in the development and establishment of the "Rio Salado Project" in the Salt River bed. This project will be designed to use renovated sewage water from Phoenix and the surrounding communities for recreational ponds and lakes, impoundments for endangered aquatic wildlife, for production of food and sports fish and for unrestricted irrigation and industrial use.

PROCEDURES:

An interdisciplinary approach was taken so a comprehensive physical-chemical-biological study of ponded reclaimed sewage water could be made. Numerous factors were evaluated simultaneously so that cause-and-effect relationships relative to the growth of micro- and macro-organisms in an aquatic ecosystem could be established.

I. General Information:

The ponds, West Lined Pond (WLP) and East Lined Pond (ELP), were filled in early May 1971 and will be studied for a period of one year until May 1972. Since the ponds have an asphalt-fiberglass lining, seepage is minimal and water loss from the ponds is essentially from surface evaporation. The ponds were replenished with

reclaimed water from the "Ease well" every few days to compensate for evaporative and minor seepage losses, and thus are kept at reasonably constant levels. The East well is located about 50 ft east of the end of basins 3 and 4 at Flushing Meadows and was perforated from 15 to 30 ft to increase its water supplying capacity. When make-up water was required, the chemical and biological quality of the water was determined.

## II. Analysis of Biological Factors:

1. Plankton populations - The phytoplankton population was analyzed qualitatively and quantitatively with Sedgewick-Rafter counting chambers. Zooplankton populations were analyzed in a similar manner. The water samples were concentrated 10-fold by centrifugation.

2. Bacterial populations - The standard dilution plate technique was used to analyze water samples for total bacteria using plate count agar. Millipore filter techniques were used for fecal coliform analysis.

3. Chlorophyll pigment analysis - Water samples were filtrated with fiberglass filters (Whatman GF/C 4.25 cm filters) and 5 cc of 95% acetone were used for extraction of the filtered algae. Chlorophyll a was analyzed with optical density (OD) measurements at 6630 Å using a Bausch & Lomb Spectronic "20."

4. Carotenoid pigment analysis - These animal and plant pigments were analyzed in a similar manner as chlorophyll, only the OD was measured at 5100 Å and 4800 Å, respectively.

5. Dissolved oxygen (DO) and primary productivity - A Beckman oxygen analyzer was used to measure the dissolved oxygen, while gross primary productivity was determined by the conventional light and dark bottle method. Incubation periods were generally for one to two hours between 1000 and 1400 hours.

## III. Analysis of Chemical Factors:

1. Nitrogen - Organic and inorganic forms of nitrogen

were analyzed with a Technicon automatic analyzer.

2. Phosphorus - Standard colorimetric procedures for ortho-phosphate analysis were followed. In the future, however, the automatic analyzer will be used.

3. Carbon - Organic and inorganic carbon were analyzed with a Beckman carbon analyzer.

4. Dissolved carbon dioxide -  $\text{CO}_2$  was calculated from a standard equation derived from the association of pH and total alkalinity.

5. Alkalinity - Phenolphthalein alkalinity was determined by acid titration when the pH was above 8.2. Total alkalinity was determined by acid titration ( $0.02 \text{ N H}_2\text{SO}_4$ ) to the end point of bromo-cresol-green and methyl-red mixed indicator.

6. Total dissolved salts (TDS) - A conductivity meter was used to measure the electrical conductance of the water, which is related directly to the TDS.

#### IV. Analysis of Physical Factors:

1. Light - Solar and thermal radiation were measured with a net radiometer and an Eppley pyranometer. A multichannel recorder located between the ponds recorded the readings continuously at one-half hour intervals.

2. Temperature - Air and water temperature profiles were measured with thermocouples. Air temperatures were taken at 10 cm and 60 cm above the water surface. Water temperatures were measured at the surface, -15 cm, -60 cm, and -110 cm. A multichannel recorder was also used to record these readings continuously at one-half hour intervals.

3. Water visibility - A Secchi disc was used to measure the depth of water visibility.

4. Water turbidity - A HACH turbidometer was used to measure turbidity in Jackson turbidity units.

V. Treatments:

1. Physical treatment - Black plastic tarps (50 x 40 ft, 20 mil) were used to cover both ponds from 2000 hr on 20 July to 2000 hr on 23 July. The purpose was to exclude light and deplete the DO in the water until anaerobic conditions were established.

2. Biological treatment - In mid-October catfish (12) were added to the WLP only. The growth of these fish will be monitored for approximately 6 months. Fish size, length and weight, will be determined periodically by trapping the fish.

VI. Methods of Sampling Water:

Since many variables were monitored simultaneously, it was important to establish reliable methods for routine water sampling from these small ponds. A plexiglass tube was constructed and used to obtain most of the water samples. The tube was gently lowered vertically into the pond until it touched bottom. The top was stoppered, the column of water raised, and the bottom stoppered just under the water surface. After the tube sampler was removed from the pond, the column of water was held vertically and samples were collected by removing the top stopper and successively collecting 30 cm sections of water from each side port. Water samples were usually taken at about 1000 hr of each study day. Sampling at the same time each day minimized the effect of diurnal changes.

Two types of plexiglass sampling tubes were used. They will be termed: (1) the profile tube sampler, and (2) the primary productivity or plankton tube sampler. The profile tube sampler was 3.0 cm in diameter (I.D.) and contained side ports (0.6 cm I.D.) at 30 cm intervals. The individual water profile samples were collected from the side ports in two 125-ml plastic bottles. Approximately 250 ml of water were collected from each interval and used for analysis of biological and chemical factors previously

described. The profile tube sampler was also used to obtain a composite water sample from each pond, which consisted of a complete column of water mixed and subsampled for later analysis.

The primary productivity or plankton tube sampler was 7.0 cm I.D. and contained side ports (0.6 cm I.D.) at 50 cm intervals. The volume in each 50-cm section was approximately 2 liters. Primary productivity was determined in the water from 0- to 50-cm depths and the 50- to 100-cm depths. A manifold containing 3 ports (0.6 cm I.D.) was attached to the side port. The initial, light and dark BOD bottles used for primary productivity measurements were filled simultaneously with the manifold and allowed to overflow expelling air bubbles containing oxygen. This tube and the profile tube sampler were also used to obtain water samples for zooplankton analysis. The water samples obtained were poured into a plankton net. The net was washed with distilled water, and a small vial attached to the net collected the plankton.

#### RESULTS AND DISCUSSION:

Pond Studies: The initial phase of the pond studies on eutrophication and biological productivity in reclaimed sewage water began in early May of 1971 and will be continued through May of 1972, so that a yearly cycle of data is obtained for all the factors monitored. Therefore, since the work is still in progress, a detailed report and analysis of data will be prepared at a later date. However, during the summer months some ecological relationships between phyto- and zooplankton were observed that will be summarized in the next section.

Evaluation of Water Sampling Methods: Collecting water samples for analysis can be accomplished in many ways. But since no analytical results can be any better than the sample it represents, it is important to use an accurate and standardized water sampling method. In preliminary work it was found that the standard types of water samples, the Kremmerer-type (vertical) and the Van Dorn-type

(horizontal), were not satisfactory for use in small ponds. Each pond has only one site equipped with a small platform for sampling. When repeated samples were needed, it was important that the sampler did not disturb the pond stratification when the first sample was taken. The standard water samplers are large and require the use of a messenger weight that trips the sampler when positioned. The messenger hitting and traveling in the water as well as the tripping disturbs the pond stratification which makes it essentially impossible to obtain a second valid sample from that site. Therefore, a new tube-type sampler was designed and constructed of plexiglass tubing. Analytical data of water samples collected with the three types of samplers were compared, so that the accuracy of the new tube-type sampler could be evaluated.

The use of the tube-type sampler was first evaluated directly by measuring the DO in the ponds and then measuring the DO of representative water samples obtained with the profile tube sampler. The results were essentially identical regardless of whether the DO profiles were measured directly with the oxygen probe in the ponds or indirectly in water samples collected with the profile tube sampler (Table 1).

Considerable effort was made to compare the results from water samples taken with the Kremmerer- and Van Dorn-type samplers with the tube-type sampler. The Kremmerer sampler obtains a vertical column of water about 46 cm in length, 9 cm in diameter, and 2.1 liters. The Van Dorn sampler obtains a horizontal section of water from any desired depth that is approximately the same size as the sample collected with the Kremmerer sampler. Water samples from each pond taken with the profile tube sampler were compared with profile samples obtained with the Van Dorn. Similar analyses were made to compare the primary productivity tube sampler with the Kremmerer sampler.

Profile analyses of the two ponds for dissolved oxygen, carbon dioxide, pH, alkalinity, turbidity, and bacterial numbers comparing the tube- and Van Dorn-type samplers were essentially identical (Table 2). Water samples were obtained on three occasions from both ponds with the tube and Kremmerer sampler. The analytical results comparing DO and primary productivity showed that the initial DO concentration did not vary more than 0.8 ppm, and the primary productivity, which was low because of the winter temperatures, was very similar (Table 3). Chemical analyses of these unfiltered and fiberglass filtered water samples were also very similar (Table 4). From these results it was concluded that the new tube-type sampler was more than satisfactory, since the data were as accurate as those obtained with other types of water samplers. Also, with the tube-type sampler the pond stratification was only slightly disturbed, samples were obtained rapidly, and several samples could be taken easily from approximately the same site in the pond.

It was also of interest to determine the degree of mixing that occurred during the collection of water from the side ports of the tube-type sampler. Laboratory experiments were designed using dye-salt solutions to measure the distribution and mixing of water flowing from the side port. The bottom section of water contained the dye-salt solution. This solution was poured into the column until it was at the level of the side port. Then a small ice cylinder of the same diameter as the tube sampler was positioned at the surface of the dye-salt solution. Distilled water was then poured into the tube sampler to the desired height. The ice was allowed to melt and the water column equilibrated for about 1 hour. A sharp interface between the distilled water and the dye-salt solution was established. The side port was opened and the distilled water collected.

During the collection of the sample, the flow pattern and the disturbance of the dye-salt interface were observed. The first result observed was that the sharp interface between the two solutions was maintained. After the distilled water was collected, the interface was positioned below the side port. Therefore, the measurement of the clear distilled water layer remaining was assumed to be equal to the amount of dye-salt solution that was collected and mixed with the sample.

The height of the remaining layer of distilled water was termed the "mixing zone." The "%-mixing" between adjacent samples was determined by dividing the height of the mixing zone by the height of the section of water collected. In this manner the influence of column diameter, port size and flow rate, and water head level on the %-mixing was determined. As column diameter increased, the mixing zone and %-mixing increased slightly (Table 5). Port size and flow rate had the greatest influence on the %-mixing. The slower the rate of flow, the less the %-mixing, and no detectable mixing occurred with a port size of 0.1 mm I.D. (Table 6). Water head levels from 30 to 90 cm did not alter the mixing zone markedly, but the %-mixing decreased as the water head level increased, simply because more water is collected as the water head level increased (Table 7).

It was further determined by visual evaluation of the dye intensity in the collected water sample that mixing occurs during the initial period of flow. Once the flow pattern is established, then laminar flow occurs with very little mixing. This probably results from the decrease in rate of flow as the water head decreases. Thus, there is very little dye-salt solution in the last portion of the sample collected.

From these results it was concluded that a port-size to tube-diameter ratio of 1:10 is recommended for tube-type samplers. This size tube will minimize the height of the mixing zone and the

%-mixing. Also, this size tube will deliver the water sample sufficiently fast for ease of handling and rapidity of analysis.

#### SUMMARY AND CONCLUSIONS:

The assessment of biostimulation and eutrophication in reclaimed waste water was begun on two small fiberglass-asphalt-lined ponds (40 ft long x 30 ft wide x 5 ft deep) at the Flushing Meadows project west of Phoenix, Arizona. The first phase of the work, which is still in progress, was to monitor several biological, chemical, and physical factors that contributed to the growth of phytoplankton, zooplankton, and fish in reclaimed sewage water. Since the Flushing Meadows Project has a field laboratory and electric power, many of the factors monitored were measured at the site. Multichannel recorders were set up to measure at half-hour intervals for 24 hours temperature profiles in the ponds, solar and thermal radiation, and surface evaporation. Water visibility was also measured with a Secchi disc, and the necessary fill-up water from the East well was added to the ponds to maintain a constant water level. Water samples were immediately analyzed in the field laboratory for dissolved oxygen, pH, phenolphthalein, and total alkalinity and turbidity. (Carbon dioxide was later calculated from the relationships of pH and alkalinity.) Primary productivity was determined at two levels, 30-cm and 60-cm depths. Similar water samples were filtered and later analyzed for chlorophyll content photometrically.

Other water samples from each pond were stored in the refrigerator prior to chemical analysis for total dissolved salts, carbon, nitrogen, phosphorus, and other minor nutrient elements. Water samples were also concentrated (10-fold), preserved (formalin), and stored (4 C), until they could be analyzed for phyto- and zooplankton populations.

The total bacteria population was analyzed immediately after

returning to the research laboratory. Also, fecal coliform bacteria were assayed weekly with the millipore filter method.

In July both ponds were covered with a black plastic tarp for 3 days for the purpose of excluding light and producing anaerobic conditions in the ponds. Also, in October small channel catfish were introduced into only one pond. The rate of fish production will be determined by trapping and making length and weight measurements.

Therefore, a physical-chemical-biological study of ponded reclaimed sewage water from the Flushing Meadows Project is being conducted. Pertinent factors are being simultaneously evaluated to establish cause-and-effect relationships in the growth of micro- and macro-organisms in an aquatic ecosystem.

A detailed interpretation and analysis of the results obtained will be made in a later report, since the ponds are still being monitored for a one-year period ending in May 1972. However, certain observations and general results could be noted at this time. During the time prior to covering the ponds with black plastic, cycles of zoo- and phytoplankton activity occurred. Dense rotifer populations grazed heavily on unicellular planktonic green algae. During these grazing periods chlorophyll content, primary productivity, dissolved oxygen concentrations were decreased, and light penetration was increased, until the Secchi disc was visible at the bottom of the ponds. After the ponds were covered and subjected to anaerobic conditions, these cycles did not occur again, and within a few weeks a prominent algal bloom of a blue-green filamentous-type algae, *Oscillatoria*, was present, and this algal bloom has continued to persist. Also, the zooplankton populations were altered and rotifer populations have decreased greatly. The succession of phyto- and zooplankton development in these ponds is being studied in detail.

A new tube-type water sampler was designed for use in small shallow bodies of water. A plexiglass tube was constructed with side ports at 30-cm intervals. The tube was gently lowered vertically into the pond until it touched bottom. The top was stoppered, the column of water raised, and the bottom stoppered just under the water surface. While holding the tube vertically, the profile samples were taken by removing the top stopper and successively collecting from each side port 30 cm of water. Chemical and biological analyses of water samples taken with the tube-type sampler were compared with two other types of water samplers. The results showed that the tube-type sampler was as accurate as the other samplers and, because of its simplicity, was more satisfactory for use in the ponds. Also, the degree of mixing that occurred in the tube samplers while the water sample was being collected from the side port was determined. The results indicated that a tube-diameter and port-diameter ratio of 10:1 would minimize the mixing and increase the accuracy of the tube-type sampler.

PERSONNEL: R. G. Gilbert, J. C. Lance, J. B. Miller, S. B. Idso;  
and Gerald Cole and Joyce Foster, Arizona State  
University, Zoology Department.

CURRENT TERMINATION DATE: December 1975

Table 1. Dissolved oxygen profiles of two ponds comparing two methods of measuring DO, either directly in the pond or in samples taken with the tube-type water samples.

Pond	Depth cm	Method of Measuring DO	
		Pond Analysis <u>1/</u> ppm	Sample Analysis <u>2/</u> ppm
West Lined Pond	30	6.2	6.2
	60	6.1	6.0
	90	6.0	6.0
	120	6.3	6.8
	150	6.2	6.4
East Lined Pond	30	11.2	10.8
	60	11.0	10.8
	90	11.2	11.2
	120	11.6	11.8
	150	11.6	11.2

1/ Oxygen probe was placed directly into pond at desired depth for DO measurement.

2/ Oxygen probe was placed in 125-ml plastic bottle containing water samples collected with the profile tube sampler.

Table 2. Profile analysis of two ponds for DO, CO<sub>2</sub>, pH, alkalinity, turbidity, and bacteria comparing the tube-type (T) and Van Dorn (V) water sampler.

Depth cm	DO - ppm		CO <sub>2</sub> - ppm		pH		Alkalinity		Turbidity		Bacteria/ml × 10 <sup>3</sup>	
	T	V	T	V	T	V	T	V	T	V	T	V
<u>West Lined Pond</u>												
0-30	10.8	11.6	.09	.07	9.50	9.55	220	212	17	17	104	173
30-60	10.0	10.8	-	-	9.50	9.50	-	-	17	17	-	-
60-90	9.6	10.4	.10	.11	9.45	9.45	208	216	17	17	152	150
90-120	9.2	10.0	-	-	9.45	9.50	-	-	18	18	-	-
120-150	9.4	9.6	.12	.12	9.40	9.40	212	216	21	27	161	159
Average	9.8	10.5	.10	.10	9.46	9.48	213	215	18	19	142	161
<u>East Lined Pond</u>												
0-30	11.2	11.6	.13	.11	9.50	9.55	296	300	13	14	126	172
30-60	10.8	10.8	-	-	9.45	9.55	-	-	13	13	-	-
60-90	10.4	10.4	.15	.11	9.45	9.55	304	304	14	13	220	170
90-120	10.0	10.4	-	-	9.50	9.55	-	-	14	14	-	-
120-150	10.0	10.4	.11	.13	9.55	9.50	292	296	17	15	137	185
Average	10.5	10.7	.13	.12	9.49	9.54	297	300	14	14	161	176

21-13

Table 3. Primary productivity and dissolved oxygen in two ponds comparing the tube-type and Kremmerer-type water samplers.

Date	Dissolved oxygen (ppm)		Primary productivity (ppm O <sub>2</sub> /hr)	
	Tube	Kremmerer	Tube	Kremmerer
<u>West Lined Pond</u>				
11 NOV 71	11.2	12.0	0.40	0.40
16 NOV 71	12.4	12.0	1.20	1.03
20 DEC 71	14.4	15.2	0.91	0.91
<u>East Lined Pond</u>				
11 NOV 71	12.0	12.0	0.00	0.40
16 NOV 71	12.4	12.8	1.48	1.11
20 DEC 71	16.8	16.4	0.76	0.76

Table 4. Chemical data of unfiltered (U) and fiberglass filtered (F) water samples from ponds comparing the tube-type and Kremmerer-type water samplers.

Water sampler	Treatment	Carbon			Nitrogen			P ppm	TDS ppm
		Total ppm	Organic ppm	Inorganic ppm	Ammonium ppm	Nitrite ppm	Nitrate ppm		
<u>W e s t L i n e d P o n d</u>									
Tube	U	102.7	49.7	53.0	1.2	0.0	0.1	1.2	1696
	F	74.8	25.0	49.8	0.7	0.0	0.1	0.3	-
Kremmerer	U	108.9	48.7	59.1	1.3	0.0	0.1	1.4	1696
	F	75.1	23.8	51.3	0.8	0.0	0.1	0.3	-
<u>E a s t L i n e d P o n d</u>									
Tube	U	134.6	79.7	54.9	0.4	0.0	0.0	0.9	1696
	F	76.7	26.5	50.2	0.3	0.0	0.0	0.5	-
Kremmerer	U	137.2	75.9	61.3	1.0	0.0	0.1	0.7	1696
	F	79.0	25.3	53.7	0.7	0.0	0.1	0.4	-

21-15

Table 5. Influence of column diameter on %-mixing of water samples taken from side port (0.6 I.D.) of tube-type water samplers. Water head level was 90 cm (3460 ml).

Column Diameter cm	Mixing Zone cm	%-Mixing
7.0	4.1	4.6
4.5	4.8	5.3
3.0	5.5	6.1

Table 6. Influence of port size on flow rate and time and %-mixing of water samples taken from tube-type water sampler 4.5 cm ID. Water-head level was 30 cm (478 ml).

Port Size cm	Flow Rate ml/min	Flow Time min	Mixing Zone cm	%-Mixing
0.6	2,516	0.19	4.2	14.0
0.3	655	0.73	1.6	5.3
0.2	228	2.10	1.1	3.6
0.1	14	35.00	0.0	0.0

Table 7. Influence of water-head level on %-mixing of water samples taken from side port (0.6-cm ID) of tube-type water sampler.

Water-head level cm	Mixing zone cm	%-mixing
	<u>4.5-cm ID tube sampler</u>	
90	4.8	5.3
30	4.2	14.0
	<u>3.0-cm ID tube sampler</u>	
90	5.5	6.1
30	5.0	15.0

TITLE: CHEMICAL TREATMENT OF IRRIGATION WATER FOR THE  
PREVENTION OF CLOGGING AND THE REMOVAL OF FLOW  
OBSTRUCTIONS IN TRICKLE IRRIGATION SYSTEMS

CRIS WORK UNIT: SWC-018-gG-4 CODE NO.: Ariz.-WCL 71-11

INTRODUCTION:

A major problem encountered with some types of trickle irrigation system under intermittent application is the eventual clogging of the orifices. The water quality is a main cause of this difficulty. Suspended particles originally present in the water can be physically filtered to prevent clogging, but the precipitates formed chemically and/or biologically in the water after passing the filter cannot. These precipitates tend to form around the narrow outlets and reduce or stop water flow, and cannot be removed by ordinary means.

The objective of the study is to develop chemical treatment techniques both from the standpoint of unplugging clogged orifices and of preventing the clogging of orifices. The investigation will also cover the chemical reactions involved in the plugging process and, consequently, classifying irrigation waters in terms of the problems they cause and methods of avoiding them in trickle irrigation systems.

PROCEDURE:

Irrigation waters used in the trickle system were sampled and analyzed for the various constituents.

Trickle orifices that plugged were removed and investigated in the laboratory to find the cause of the clogging. Preliminary attempt was made in the field to remove the clogging by injecting  $\text{CO}_2$  gas into the irrigation water. This involved the bubbling of pure  $\text{CO}_2$  gas into a 50-gallon reservoir tank of irrigation water and subsequently passing the treated water into a section of the trickle system.

The effects of different acids on the dissolution of calcium salts were determined for possible selection of the one most

suited for dissolving the pore obstructions. The acids included  $\text{HNO}_3$ ,  $\text{HCl}$ ,  $\text{HClO}_4$ ,  $\text{H}_2\text{SO}_4$ , and  $\text{HAc}$ .

Investigations were also started using chemicals to prevent the precipitation of Ca-salts or to modify the precipitate and/or its attachment to the trickle orifice so that it could be readily removed by water flow alone. In the first series the chemicals selected were limited to sodium hexametaphosphate, sodium ethylenediamine tetra acetic acid (EDTA), and polyvinyl alcohol (PVA).

#### RESULTS AND DISCUSSION:

The analysis of irrigation water is listed in Table 1. The pH of the water is unusually high. This and also the high soluble silica indicate possible dissolution of the concrete conveyance system by the water. The positive saturation indices (Bower et al., 1) for both waters would predict a high tendency for carbonates to precipitate out from solution onto the trickler irrigation pipe.

Microscopic examination of the plugged orifices showed that 0.0762 mm (0.003 inch) particles were cemented by crystalline material in the 0.762 mm (0.030 inch) pores.

Even though the pore was ten times greater than the individual particles, clogging occurred. A combination of biological and chemical activities which caused the buildup and cementation of the suspended materials is possible. An immediate solution to this problem is to remove these particles by filtering the original water, if they are indeed present as a suspended material, before entering the trickle system.

The exact composition of the crystalline material is not known at present, but based on the water analysis it appears to be a combination of Ca and Mg carbonate, sulfate, and silicate.

When the irrigation water was evaporated on the pore in the laboratory, crystal growth occurred which eventually covered the opening.

The injection of pure  $\text{CO}_2$  in the irrigation water did not aid in removing the orifice obstructions, even though the solution pH was lowered to approximately 5.7. The lowest pH achieved under laboratory conditions was 5.5. The treatment was made on systems that had some completely and very strongly obstructed orifices. One of the problems encountered in this type of treatment was the need to flush out the residual untreated water from the trickle system. In addition, treated water was lost from the system through the unplugged orifices. The rate of reaction between the precipitated material and the chemical also appears to be an important factor.

The effect of other acids on the irrigation water was also determined. The water used at the Cotton Research Center field was titrated with  $\text{HNO}_3$ ,  $\text{HCl}$ ,  $\text{H}_2\text{SO}_4$ , and  $\text{HAc}$ . As evidenced by Figure 1, all these acids affected the water equally well down to a pH of approximately 5.7. Beyond this the acetic acid could not reduce the pH of the water below 4 up to 20 me/l. If it is a matter of removing  $\text{CaCO}_3$ , any of these acids would work equally well, and the additional questions that need to be considered are the cost, ease of application, and residual effects on the plant and soil.

The dissolution in mineral acids of calcium sulfate, the other possible precipitate and cementing agent, is presented in Figure 2. The solubility of gypsum in the various acids is quite different. Dissolution was limited in  $\text{H}_2\text{SO}_4$  due to common-ion effect and in  $\text{HAc}$  due to limited dissociation of the  $\text{HAc}$  molecule. An attempt was made to predict the solubility of gypsum in  $\text{HClO}_4$ ,  $\text{HCl}$ , and  $\text{HNO}_3$ . The theoretical curve for  $\text{HClO}_4$  based on results obtained for  $\text{CaSO}_4 \cdot 2\text{H}_2\text{O}$  solubility in the Na-salts (Nakayama, 2) shown in the graph was higher than the experimental values. A theoretical treatment of the acid systems is being developed, but, for the present, empirical equations relating gypsum solubility up to 1 molar in the three acids are as follows:

$$S_{\text{HNO}_3} = 1.50 \times 10^{-2} + 0.225 c + 0.268 c^2 + 0.151 c^3$$

$$S_{\text{HCl}} = 1.50 \times 10^{-2} + 0.224 c - 0.296 c^2 + 0.171 c^3$$

$$S_{\text{HClO}_4} = 1.50 \times 10^{-2} + 0.209 c - 0.292 c^2 + 0.158 c^3$$

where S is the solubility in m/l, and c is the acid concentration, m/l.

A 15 ppm concentration of Na-hexametaphosphate was able to prevent the precipitation of  $\text{CaSO}_4$  from a solution of  $5.0 \times 10^{-2}$  m/l  $\text{CaCl}_2$  and  $\text{Na}_2\text{SO}_4$  mixture. At lower concentrations of 1 to 10 ppm, precipitation occurred after approximately 3 weeks of standing. Concentrations of up to 230 ppm EDTA and PVA were not able to prevent the precipitation of  $\text{CaSO}_4$ . However, less solids were formed in the EDTA-treated than untreated samples, and with the PVA treatment, the precipitates were fluffed up instead of being compacted as with the check sample. Further study is being conducted to analyze both the solution and solid phases of the chemically treated materials.

#### SUMMARY:

The plugging of trickle orifices was found to consist of particles cemented together at and around the opening. The use of finer filter systems could in part alleviate this problem. When the cementing agent consists primarily of  $\text{CaCO}_3$ , acids such as HCl,  $\text{HNO}_3$ , and  $\text{H}_2\text{SO}_4$  can dissolve the precipitate. If, on the other hand, scale formation is caused by  $\text{CaSO}_4$ , HCl or  $\text{HNO}_3$  must be used, and, even then, if large quantities of precipitates are present, the amount and rate of dissolution may be too small to alleviate the problem. The best solution appears to be one of prevention, either with the acids or with Ca complexing chemicals such as sodium hexametaphosphate.

REFERENCES:

1. Bower, C. A., et al. An index for the tendency of  $\text{CaCO}_3$  to precipitate from irrigation waters. Soil Sci. Soc. Amer. Proc. 29:91-94. 1965.
2. Nakayama, F. S. Calcium complexing and the enhanced solubility of gypsum ( $\text{CaSO}_4 \cdot 2\text{H}_2\text{O}$ ) in concentrated sodium salt solutions. Soil Sci. Soc. Amer. Proc. (In press) 1972.

PERSONNEL: F. S. Nakayama and B. A. Rasnick

CURRENT TERMINATION DATE: December 1973

Table 1. Analysis of water used in trickle irrigation.

Cotton Research Center

pH	= 8.31	Cl	= 8.50 me/l
Ca	= 3.64 me/l	SO <sub>4</sub>	= 1.80 me/l
Mg	= 2.32 me/l	HCO <sub>3</sub>	= 3.40 me/l
Na	= 6.85 me/l	CO <sub>3</sub>	= 0.41 me/l
Total salt	= 900 ppm	SiO <sub>2</sub>	= 15.6 ppm

Saturation Index = +0.9

Mesa Agricultural Experiment Station

pH	= 8.31	Cl	= 7.82 me/l
Ca	= 3.23 me/l	SO <sub>4</sub>	= 1.00 me/l
Mg	= 2.22 me/l	HCO <sub>3</sub>	= 3.12 me/l
Na	= 6.04 me/l	CO <sub>3</sub>	= 0.34 me/l
Total salt	= 800 ppm	SiO <sub>2</sub>	= 25 ppm

Saturation Index = +1.0

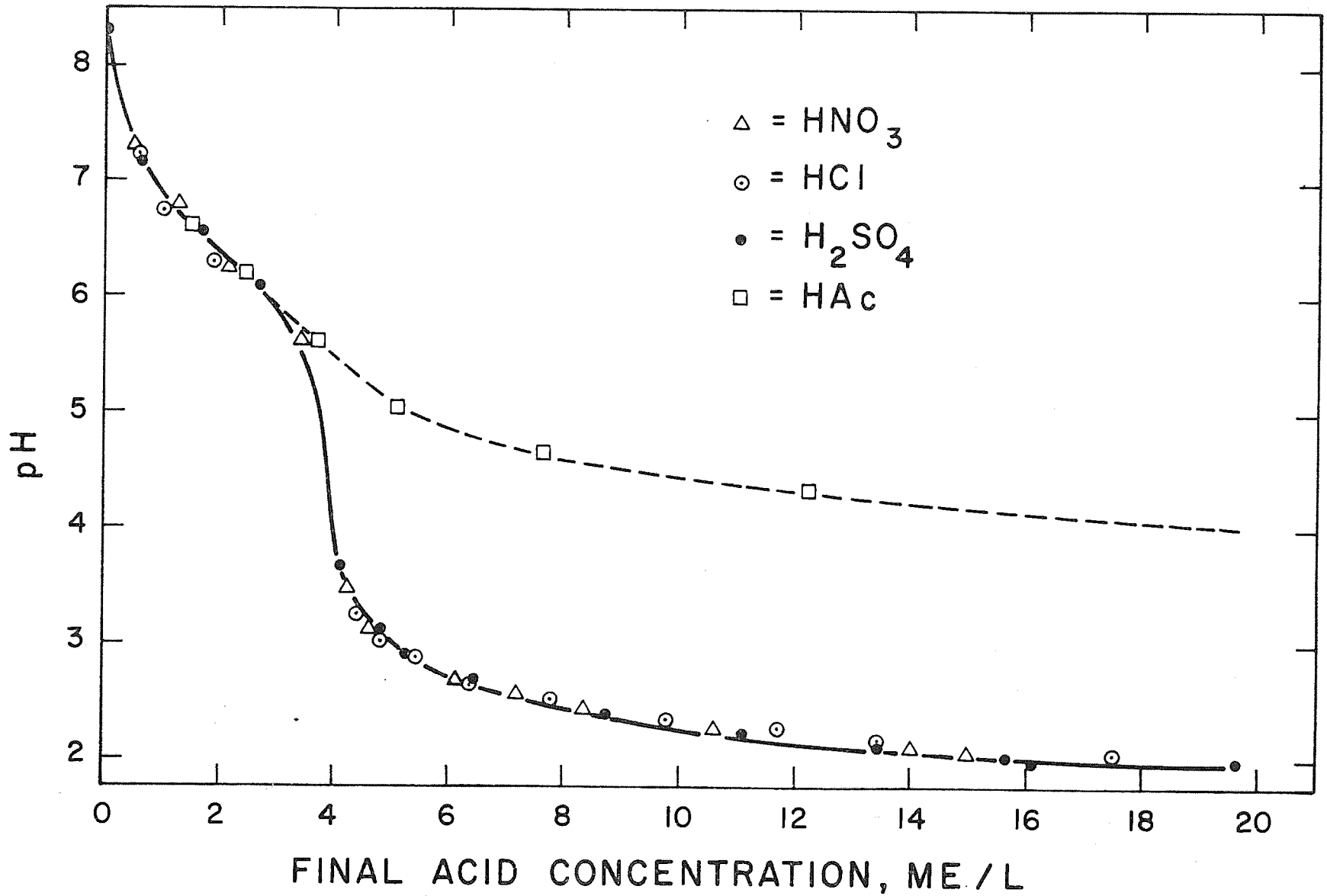


Figure 1. Titration of irrigation water with various acids.

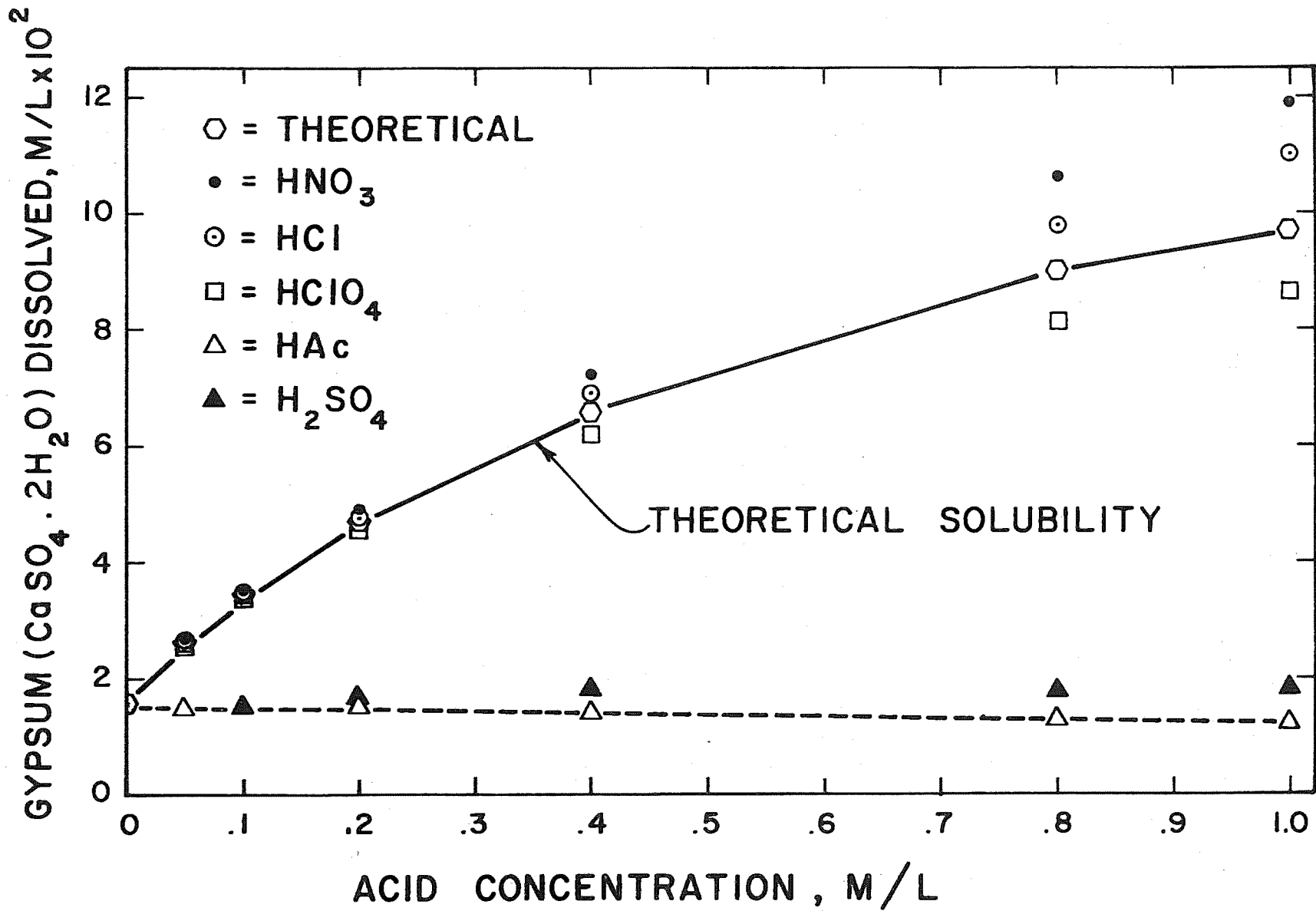


Figure 2. Dissolution of gypsum in different acids.

TITLE: LOWER COST WATER HARVESTING SYSTEMS

CRIS WORK UNIT: SWC-018-gG-4 CODE NO.: Ariz.-WCL 71-12

INTRODUCTION:

This project is a continuation and extension of the previous research conducted under the outline titled "Soil Treatment to Reduce Infiltration and Increase Precipitation Runoff." Previous investigations have reduced the cost of catchment materials by more than one-half, but additional cost reduction is required before broad-scale water harvesting is feasible. Attention must also be paid to lower cost facilities for storing harvested precipitation. The problem must now be approached by considering the total water harvesting system rather than concentrating on any single component. Where past emphasis has been on livestock water supplies, future work will include problems related to obtaining water for farmstead, rural, domestic, and supplemental irrigation uses.

Measurements of rainfall and runoff were continued on the large watersheds at the Monument Tank testing site, on the plots at the Granite Reef test site, and at the Seneca catchment. Laboratory studies were concerned with the continued evaluation of low-cost soil stabilizer, water repellent treatments. Small test plots at Granite Reef of different treatments were continued to evaluate weathering characteristics.

Major progress has been made in analyzing rainfall and runoff data collected since 1961. Most of the effort has been devoted to converting raingage and water stage recorder charts to digital tabulations. The work has been greatly facilitated by combined use of a chart reader with paper tape output and a Wang calculator with a tape reader and a plotter. The chart reader was obtained in 1970 and the Wang was purchased in June 1971. Adequate facilities for data processing were not previously available. Analysis of some data is complicated by daily volumetric measurement of runoff which allows a single runoff measurement to contain runoff from more than

one storm. From 27 July 1961 to 1 January 1971 at Granite Reef there were 244 runoff measurements from 457 individual storms. Analysis of rainfall-runoff relationships requires elimination of runoff measurements involving more than one storm. Similarly, occasional malfunctioning of remotely located recording raingages and water stage recorders on measuring flumes creates difficulty in matching rainfall and runoff events. Problems have been encountered with the chart reader and the Wang so that considerable cross-checking and recalculation has been required. Progress has also been delayed several months by emergency work for the Hawaii program. Nevertheless, data processing is now essentially up to date and analysis and interpretation has begun.

#### PART I. RAINFALL CHARACTERISTICS, GRANITE REEF

Preliminary data analysis has shown that storm sizes and rainfall intensity are much lower than originally assumed. Distribution of rainfall quantity by storm size for individual years 1961 through 1970 is shown in Table 1. During most years, 50% or more of the rainfall has occurred in storms of less than 10 mm. The variation in storm size distribution can be highly variable among years. In 1962, 79% of the total rain fell in storms of less than 10 mm while in 1967, only 26% of the storms were less than 10 mm.

Average rainfall intensity at Granite Reef was found to be very low as shown in Table 2. Average intensity of 94% of the storms during 1961 through 1970 was less than 5 mm per hour. Almost 80% of the total quantity of rainfall fell in storms of less than 5 mm per hour average intensity. Data in Tables 1 and 2 indicate that most of the rainfall at Granite Reef occurs in small showers of low intensity. Under these conditions the performance of our baresoil catchments has been remarkably good.

## PART II. GRANITE REEF TESTING SITE

Rainfall during 1971 totaled only 144 mm. Twenty-two runoff events were measured and nineteen of these resulted from rainfall of less than 10 mm. As a result, runoff from all plots at Granite Reef was low.

Paved or Covered Plots. The treatments applied to the plots are listed in Table 3 and the runoff results in Table 4.

Runoff from the three plots covered with thin films, L-1 (30-mil chlorinated polyethylene), L-4 (15-mil butyl), and L-7 (1-mil aluminum foil) averaged 87.2%, 63.6%, and 78.9%, respectively for the year. The physical appearance of the aluminum foil and chlorinated polyethylene has not changed in the past year, and they are still in excellent condition. The 15-mil butyl has severely deteriorated the past year and has essentially failed. Numerous holes have developed in the sheeting and the tear resistance of the material is very low.

The two-phase asphalt treatments on plots L-5 and L-6 averaged 79.3% and 93.8%, respectively, for the past year. The reduced runoff from L-5 is a result of cracks which have developed in the pavement.

The vinyl-coated asphalt-fiberglass plot A-1 averaged 87.7% runoff. This again was lower than previous years. Plots A-2 (standard gravel roofing) and A-5 (concrete) averaged 67.2 and 56.0%, respectively. The roofing plot shows no sign of deterioration. There are two large transverse cracks on the concrete which allow losses of water from the upper half of the plot.

Bare Soil Plots. The bare soil plots are all treatments where the soil is not completely covered or paved. The treatments are listed in Table 5, and the runoff results presented in Table 6.

Rainfall runoff occurred only four times from the uncleared watershed W-1 and only three times from uncleared watershed W-2 and cleared watershed W-3. Total runoff averages were 9.2%, 4.6%, and 14.9% for W-1, W-2, and W-3, respectively.

Runoff from the smoothed, untreated plots L-2, A-3, and A-4a was also infrequent for the year. Plots L-2 and A-3 averaged 14.3% and 17.8% runoff for the year. Plot A-4a averaged 22.8% runoff for the period 1 January through 24 October 1971.

The three untreated ridge and furrow plots R-1, R-2, and R-3 averaged 24.2%, 21.0%, and 19.9% rainfall runoff for the year. Plots R-1 and R-3 have 20% sideslope and R-2 has 10% sideslope. There were no significant differences in runoff with respect to plot slope.

### PART III. STABILIZED HYDROPHOBIC SOILS

Runoff from bare soil catchments treated with hydrophobic chemicals was reasonably good in spite of the low rainfall during 1971. Plot R-4, a 200 m<sup>2</sup> ridge and furrow catchment treated in November 1970 with a soil stabilizer and a water repellent, produced 70% runoff. Plot L-3, a 200 m<sup>2</sup> rectangular catchment treated in November 1969 with water repellent alone, produced 50% runoff. Plot L-2, similar to L-3 except that it is untreated, produced only 14% runoff. Plot A-4, a 200 m<sup>2</sup> rectangular plot, treated with soil stabilizer and water repellent in November 1971, produced 73% runoff of the 15.7-mm rainfall for the remainder of the year. Comparable runoff for the other plots during this period was: L-2, 0%; L-3, 9%; R-4, 36%.

The effectiveness of hydrophobic soil catchments declines with time, as the above information indicates. This results in part from deterioration of the hydrophobic chemical. We had been told that sodium methyl silicate (SMS) did not degrade in sunlight, but field observations indicated otherwise. In February 1971 triplicated soil samples treated with SMS and four different soil stabilizers, plus three disks of smooth concrete treated with SMS alone, were exposed to sunlight on the laboratory roof. Air-water-solid contact angles were measured prior to exposure and once a month during exposure. Initial contact angles ranged from 120° to 140°, indicating excellent water repellency on all samples.

After four months exposure, contact angles on all samples had decreased to less than  $90^{\circ}$ , indicating that none of them were water repellent. This means that the surface of bare soil catchments treated with SMS will become wettable about three months after treatment.

Erosion resistance of  $1 \text{ m}^2$  natural soil plots treated with SMS and various soil stabilizers, as reported in 1970, was continued in 1971. Ten treatments were applied in July 1970. One failed in 3 months, one in 6 months, two in 1 year, and six are still in excellent condition. Six additional materials were applied in 1970 and 1971 and four of these are still in excellent condition. An "excellent" rating means no erosion after 1,000 drops, 5 mm dia., falling from a height of 2 meters. The untreated soil begins to erode immediately after the first few drops. Although the surface of the treated plots is wettable, soil immediately under the surface remains hydrophobic and there is little or no infiltration.

#### PART IV. MONUMENT TANK TESTING SITE

Analysis of the rainfall data recorded by the mechanical weather stations by individual storm event has been started. Preliminary indications are that the majority of the storms occur as small showers of less than 10 mm. Precipitation intensities average less than 5 mm per hour. Larger size storms with higher intensities do occur but at much less frequency than originally assumed.

Total rainfall for the past year (16 Dec 1970 through 4 Jan 1972) as measured with the 13-raingage network was as follows: Area 1 - 365.5 mm, Area 2 - 346.2 mm, Area 3 - 387.8 mm, and Area 4 - 376.2 mm. Approximately 100 mm of this rainfall occurred in a series of 5 storms the later part of September 1971. These storms had relatively high intensities ( $>200 \text{ mm/hour}$ ) and caused major erosion on the slopes of the test watersheds. The eroded

material was deposited in the channels, collection ditches, and measuring flumes causing a loss of runoff data for this period. This has initiated a re-evaluation and design of the critical-depth flumes to allow measurements of flows carrying large quantities of suspended sediment and bed load material.

Prior to plugging of the flumes, runoff from the watersheds was less than 1% of the total precipitation. Complete analysis of rainfall vs runoff has not been completed.

#### PART V. OPERATIONAL FIELD CATCHMENTS

Runoff from the Seneca catchment continued to be very low for the first half of 1971. In April 1971 a butane burner was used to burn all grass from the plot. In early August 1971 the plot was scraped smooth, removing all vegetation, and treated with polyborchlorate soil sterilant. Runoff since clearing has been higher, but may in part be a result of the type of storms since that time. This will be evaluated when analysis of runoff vs individual rainfall events is completed.

#### SUMMARY AND CONCLUSIONS:

This project is a continuation and extension of the previous research conducted under outline titled "Soil Treatment to Reduce Infiltration and Increase Precipitation Runoff." Past research has reduced the cost of water harvesting structures. Future work will be concerned with evaluating the total water harvesting system. Major progress has been made in analyzing rainfall and runoff data collected since 1961.

Preliminary data analysis has shown that storm sizes and rainfall intensities at Granite Reef and Monument Tank are much lower than originally assumed. At Granite Reef for the period of 1961 through 1970, average intensity of 94% of the storms was less than 5 mm per hour. Almost 80% of the total quantity of precipitation fell in storms averaging less than 5 mm per hour intensity. Approximately 50% of the rainfall quantity has occurred in storms of less than 10 mm.

Rainfall for 22 runoff events at Granite Reef during 1971 totaled 144 mm. Nineteen of these storms produced less than 10 mm of precipitation. As a result, total runoff from the plots was low. Runoff of rainfall from 200 m<sup>2</sup> covered plots was: chlorinated polyethylene - 87%, butyl - 64%, and aluminum foil - 79%. The 15-mil butyl has severely deteriorated the past year and has essentially failed. Runoff from the two asphalt pavement plots and the asphalt-fiberglass plot ranged from 80 to 90%. The concrete and roofing plots averaged 56 and 67%, respectively. Less than five runoff events occurred from the watersheds, smoothed untreated plots, and untreated ridge and furrow plots.

Runoff from bare soil treatments treated with hydrophobic chemicals was reasonably good. A 200 m<sup>2</sup> ridge and furrow plot treated in November 1970 with soil stabilizer and water repellent averaged 70% runoff. A plot treated with water repellent alone in 1969 produced 50% runoff. The effectiveness of hydrophobic soil catchments declines with time, partly because of a deterioration of the hydrophobic chemical. Laboratory tests indicate the surface soil loses water repellancy within 4 months. Although the surface becomes wettable, the soil below remains hydrophobic.

Rainfall at the Monument Tank testing site was approximately 350 mm for 1971. The majority of the storms produce less than 1% runoff. A series of 5 high-volume, high-intensity storms in September 1971 caused major erosion on the watersheds. The eroded material was deposited in the measuring flumes resulting in a loss of actual runoff which occurred. This has initiated a re-evaluation and design of the flumes to permit measurement of flows carrying a high volume of sediment.

Runoff from Seneca was also low. The plot has been cleared and smoothed to determine the feasibility of this method for increasing runoff.

PERSONNEL: L. E. Myers, G. W. Frasier

CURRENT TERMINATION DATE: 1974

Table 1. Percent total annual rainfall occurring in storms of various sizes at Granite Reef test site.

Storm size	Year									
	1961 <sup>1/</sup>	1962	1963	1964	1965	1966	1967	1968	1969	1970
mm	%	%	%	%	%	%	%	%	%	%
0-2	20	19	9	9	11	12	9	10	17	9
2-4	22	27	12	13	13	12	10	11	19	15
4-6	36	7	3	3	9	10	7	10	5	6
6-8	22	12	23	7	17	6	0	6	9	4
8-10	0	14	20	5	17	12	0	9	12	16
10-12	0	8	6	17	4	5	8	5	5	0
12-15	0	0	0	0	0	0	5	7	0	17
15-20	0	13	0	8	15	0	25	18	24	11
> 20	0	0	27	38	14	43	36	24	9	22
Total rain mm	68	133	182	201	320	219	274	196	215	163

<sup>1/</sup> Beginning 28 July 1961

Table 2. Distribution by average intensity of rainfall at Granite Reef test site during years 1961 through 1970.<sup>1/</sup>

Average Intensity mm/hr	Event Distribution		Quantity Distribution	
	No. Storms	% Total	Quantity mm	% Total
0-1	206	45.1	307.6	15.6
1-2	124	27.1	428.9	21.7
2-3	65	14.2	481.3	24.4
3-4	23	5.0	238.1	12.1
4-5	13	2.8	108.3	5.5
5-6	8	1.8	131.6	6.7
6-7	5	1.1	44.7	2.2
7-8	4	0.9	46.8	2.4
8-9	3	0.7	31.5	1.6
9-10	1	0.2	9.0	0.4
10-12	0	0	0	0
12-15	0	0	0	0
15-20	2	0.4	23.3	1.2
> 20	3	0.7	121.5	6.2
Total	457	100	1972.6	100

<sup>1/</sup> 1961 data began 28 July

Table 3. Treatments on paved or covered plots at Granite Reef.

Plot	Treatment Date	Treatment
L-1	8 Aug 1967	Basecoat. MC-250 at 1.5 kg asphalt m <sup>-2</sup>
	22 Aug 1967	Topcoat. RSK asphalt emulsion at 0.7 kg asphalt m <sup>-2</sup>
	20 May 1968	Top Sheeting. 30-mil chlorinated black polyethylene
L-4	30 Nov 1961	Butyl Rubber Sheeting. 15-mil
L-5	18 Sep 1962	Basecoat. S-1 at 1.04 kg asphalt m <sup>-2</sup>
	16 Mar 1966	Topcoat. RSK asphalt emulsion at 0.6 kg asphalt m <sup>-2</sup>
	22 Apr 1970	Sealcoat. Modified SSKH asphalt emulsion at 0.6 kg asphalt m <sup>-2</sup>
L-6	19 Apr 1963	Basecoat. RC-special at 1.5 kg asphalt m <sup>-2</sup>
	8 May 1963	Topcoat South Half. S-2 asphalt emulsion at 0.65 kg asphalt m <sup>-2</sup> with 3% butyl latex
	9 Jul 1963	Topcoat North Half. S-1 at 0.5 kg asphalt m <sup>-2</sup> with 3% butyl latex
	22 Apr 1970	Sealcoat. Modified SSKH asphalt emulsion at 0.6 kg asphalt m <sup>-2</sup>
L-7	3 Aug 1967	Basecoat. MC-250 at 1.5 kg asphalt m <sup>-2</sup>
	22 Aug 1967	Top Sheeting. 1-mil aluminum foil bonded with RSK asphalt emulsion at 0.7 kg asphalt m <sup>-2</sup>
A-1	3 Aug 1967	Basecoat. MC-250 at 1.5 kg asphalt m <sup>-2</sup>
	22 Aug 1967	Top Sheeting. 3/4-oz chopped fiberglass matting bonded with RSK asphalt emulsion at 1.4 kg asphalt m <sup>-2</sup>
	Jan 1968	Top Spray. Vinyl aluminum coating at 0.1 gal yd <sup>-2</sup>

Table 3. Treatments on paved or covered plots at Granite Reef  
(continued).

Plot	Treatment Date	Treatment
A-2	3 Aug 1967	Basecoat. MC-250 at 1.5 kg asphalt m <sup>-2</sup>
	12 Sep 1967	Top Sheeting. Standard rag felt-rock roofing treatment
A-5	Sep 1968	Concrete Slab.

Table 4. Rainfall and runoff for paved or covered plots at Granite Reef.

Date	Total Rainfall	L-1 Runoff		L-4 Runoff		L-7 Runoff	
	mm	mm	%	mm	%	mm	%
1971	mm	mm	%	mm	%	mm	%
2 Jan	6.2	5.9	95.2	4.6	74.2	5.0	80.7
17 Feb	7.7	7.1	92.2	6.4	83.1	6.0	77.9
15 Apr	8.3	6.8	81.9	5.7	68.7	5.4	65.1
3 Aug	5.1	4.5	88.2	3.7	72.5	3.5	68.6
6 Aug	4.5	4.0	88.9	3.0	66.7	2.9	64.4
10 Aug	1.2	0.6	50.0	0.4	33.3	0.2	16.7
12 Aug	13.5	6.9	51.1	13.1	97.0	13.2	97.8
14 Aug	6.2	5.4	87.1	4.6	74.3	4.8	77.4
25 Aug	4.3	3.7	86.0	3.4	79.1	3.6	83.7
8 Sep	6.2	5.8	93.5	4.4	71.0	4.6	74.2
29 Sep	24.5	24.4	99.6	16.4	66.9	22.6	91.1
29-30 Sep	3.8	2.7	71.0	1.1	28.9	2.5	65.8
30 Sep	3.0	2.4	80.0	0.9	10.0	2.3	76.7
30 Sep	9.5	9.7	102.1	7.3	76.8	9.0	94.7
16-17 Oct	16.4	15.2	92.7	6.8	41.5	12.5	76.2
18 Oct	2.4	2.1	87.5	0.9	37.5	1.5	62.5
24 Oct	5.5	4.7	85.5	2.3	41.8	3.8	69.1
15 Nov	1.7	1.5	88.2	0.6	35.3	1.1	64.7
21 Nov	1.5	1.0	66.0	0.1	6.7	0.6	40.0
7 Dec	2.8	2.7	96.4	1.3	46.4	1.9	67.9
13 Dec	6.3	5.8	92.1	3.2	50.8	4.2	66.6
28 Dec	3.4	2.6	76.5	1.4	14.2	2.4	70.6
Total	144.0	125.5	87.2	91.6	63.6	113.6	78.9

Table 4. Rainfall and runoff for paved or covered plots at Granite Reef (continued).

Date	Total Rainfall	L-5 Runoff		L-6 Runoff		A-1 Runoff	
	mm	mm	%	mm	%	mm	%
1971							
2 Jan	6.2	5.5	88.6	5.9	95.2	5.2	83.4
17 Feb	7.7	6.2	80.5	7.1	92.2	6.8	88.3
15 Apr	8.3	4.6	55.4	6.6	79.5	6.6	80.0
3 Aug	5.1	3.5	68.6	4.4	86.3	4.6	90.1
6 Aug	4.5	3.1	68.8	3.6	80.0	4.0	88.9
10 Aug	1.2	0.4	33.3	0.4	33.3	0.6	50.0
12 Aug	13.5	13.8	102.2	17.6	130.4	13.2	97.8
14 Aug	6.2	5.2	83.9	5.7	91.9	5.7	91.9
25 Aug	4.3	3.3	76.7	3.5	81.4	3.6	83.7
8 Sep	6.2	5.3	85.5	5.3	85.5	5.2	83.9
29 Sep	24.5	24.2	98.8	27.5	112.2	24.4	99.6
29-30 Sep	3.8	2.3	60.5	} 5.3	77.9	2.9	76.3
30 Sep	3.0	2.1	70.0			2.7	90.0
30 Sep	9.5	9.9	104.2	11.3	118.9	9.3	97.9
16-17 Oct	16.4	12.5	76.2	13.9	84.8	14.8	90.2
18 Oct	2.4	1.5	62.5	1.7	70.8	1.8	75.0
24 Oct	5.5	3.5	63.6	4.5	81.8	4.7	85.5
15 Nov	1.7	0.9	52.9	1.1	64.7	1.4	82.4
21 Nov	1.5	0.4	26.7	0.7	46.7	1.0	66.7
7 Dec	2.8	1.5	53.6	2.1	75.0	2.7	96.4
13 Dec	6.3	3.3	52.4	4.7	74.6	1.9	30.1
28 Dec	3.4	1.3	38.2	2.2	64.7	3.2	94.1
Total	144.0	114.3	79.3	135.1	93.8	126.3	87.7

Table 4. Rainfall and runoff for paved or covered plots at Granite Reef (continued).

Date	Total Rainfall	A-2 Runoff		A-5 Runoff	
	mm	mm	%	mm	%
1971	mm	mm	%	mm	%
2 Jan	6.2	4.1	66.1	2.5	40.3
17 Feb	7.7	5.0	64.9	4.6	59.7
15 Apr	8.3	5.2	62.7	3.8	45.8
3 Aug	5.1	3.0	58.8	2.8	54.9
6 Aug	4.5	2.7	60.0	2.0	44.4
10 Aug	1.2	0	0	0	0
12 Aug	13.5	10.1	74.8	8.0	59.2
14 Aug	6.2	4.5	72.6	3.8	61.3
25 Aug	4.3	2.6	60.5	2.6	60.5
8 Sep	6.2	4.3	69.3	3.7	59.7
29 Sep	24.5	22.9	93.4	19.7	80.4
29-30 Sep	3.8	2.2	57.9	1.6	42.1
30 Sep	3.0	2.0	66.7	2.1	70.2
30 Sep	9.5	9.5	100.0	8.1	85.3
16-17 Oct	16.4	12.3	75.0	8.1	49.4
18 Oct	2.4	0.9	37.5	1.1	45.8
24 Oct	5.5	2.4	43.6	2.1	38.1
15 Nov	1.7	0	0	0.5	29.4
21 Nov	1.5	0	0	0	0
7 Dec	2.8	0.6	21.4	1.1	39.2
13 Dec	6.3	1.9	30.2	1.7	26.9
28 Dec	3.4	0.6	17.6	0.8	23.5
Total	144.0	96.8	67.2	80.7	56.0

Table 5. Treatments of bare soil plots at Granite Reef.

Plot	Treatment Date	Treatment
L-2	30 Nov 1961	Smoothed soil, 14.14 m X 14.14 m plot
L-3	4 Aug 1965	Smoothed soil, 14.14 m X 14.14 M plot treated with R-9 at $0.057 \text{ kg m}^{-2}$
	6 Nov 1969	Retreated with R-9 at $0.04 \text{ kg m}^{-2}$
R-1	1 Mar 1965	Ridge and furrow, 20% sideslope
R-2	1 Mar 1965	Ridge and furrow, 10% sideslope
R-3	1 Mar 1965	Ridge and furrow, 20% sideslope
R-4	13 May 1966	Ridge and furrow, 10% sideslope, treated with $44.9 \text{ g m}^{-2}$ sodium carbonate
	3 Nov 1970	Treated with 3% silicone water repellent and 2% soil stabilizer - 1.2 liters of solution $\text{m}^2$
A-3	1 Aug 1967	Smoothed soil, 6 m X 30 m plot
A-4a	1 Aug 1967	Smoothed soil, 6 m X 30 m plot
A-4b	10 Nov 1971	Smoothed soil treated with 3% silicone water repellent and 2% soil stabilizer - 1.2 liters of solution $\text{m}^{-2}$
W-1	1 Dec 1963	Uncleared watershed
W-2	1 Dec 1963	Uncleared watershed
W-3	1 Dec 1963	Cleared watershed

Table 6. Rainfall and runoff for bare soil plots at Granite Reef.

Date	Total Rainfall	W-1 Runoff		W-2 Runoff		W-3 Runoff	
1971	mm	mm	%	mm	%	mm	%
2 Jan	6.2	0	0	0	0	0	0
17 Feb	7.7	0	0	0	0	0	0
15 Apr	8.3	0	0	0	0	0	0
3 Aug	5.1	0	0	0	0	0	0
6 Aug	4.5	0	0	0	0	0	0
10 Aug	1.2	0	0	0	0	0	0
12 Aug	13.5	0.5	3.0	3.5	25.9	10.7	79.3
14 Aug	6.2	0	0	0	0	0	0
25 Aug	4.3	0	0	0	0	0	0
8 Sep	6.2	0	0	0	0	0	0
29 Sep	24.5	6.5	26.5	1.5	6.0	3.8	15.5
29-30 Sep	3.8	0	0	0	0	0	0
30 Sep	3.0	0	0	0	0	0	0
30 Sep	9.5	5.4	56.8	1.6	16.8	6.9	72.6
16-17 Oct	16.4	1.5	9.2	0	0	0	0
18 Oct	2.4	0	0	0	0	0	0
24 Oct	5.5	0	0	0	0	0	0
15 Nov	1.7	0	0	0	0	0	0
21 Nov	1.5	0	0	0	0	0	0
7 Dec	2.8	0	0	0	0	0	0
13 Dec	6.3	0	0	0	0	0	0
28 Dec	3.4	0	0	0	0	0	0
<b>Total</b>	<b>144.0</b>	<b>13.9</b>	<b>9.7</b>	<b>6.6</b>	<b>4.6</b>	<b>21.4</b>	<b>14.9</b>

Table 6. Rainfall and runoff for bare soil plots at Granite Reef  
(continued).

Date	Total Rainfall	L-2 Runoff		A-4a Runoff		A-4b Runoff	
		mm	mm	%	mm	%	mm
1971	mm	mm	%	mm	%	mm	%
2 Jan	6.2	0	0	1.2	19.3		
17 Feb	7.7	0	0	0.5	0.6		
15 Apr	8.3	0	0	0	0		
3 Aug	5.1	0	0	0	0		
6 Aug	4.5	0	0	0	0		
10 Aug	1.2	0	0	0	0		
12 Aug	13.5	2.3	17.0	8.1	60.0		
14 Aug	6.2	0	0	0	0		
25 Aug	4.3	0	0	0.6	13.9		
8 Sep	6.2	1.1	17.7	0.8	12.9		
29 Sep	24.5	10.3	42.0	10.6	43.2		
29-30 Sep	3.8	0	0	0	0		
30 Sep	3.0	0	0	0	0		
30 Sep	9.5	6.9	72.6	7.4	77.9		
16-17 Oct	16.4	0	0	0	0		
18 Oct	2.4	0	0	0	0		
24 Oct	5.5	0	0	0	0		
15 Nov	1.7	0	0			0.9	52.9
21 Nov	1.5	0	0			0.8	53.3
7 Dec	2.8	0	0			2.2	78.6
13 Dec	6.3	0	0			5.4	85.7
28 Dec	3.4	0	0			2.2	64.7
Total	144.0	20.6	14.3	29.2	22.8	11.5	73.2

Table 6. Rainfall and runoff for bare soil plots at Granite Reef  
(continued).

Date	Total Rainfall	A-3 Runoff		L-3 Runoff		R-1 Runoff	
1971	mm	mm	%	mm	%	mm	%
2 Jan	6.2	0	0	0.6	9.7	0.6	9.7
17 Feb	7.7	0	0	4.4	57.1	0.8	10.3
15 Apr	8.3	0	0	4.0	48.2	0.2	2.4
3 Aug	5.1	0	0	1.3	25.4	0	0
6 Aug	4.5	0	0	1.0	22.2	0	0
10 Aug	1.2	0	0	0	0	0	0
12 Aug	13.5	5.9	43.9	9.1	67.4	9.4	70.0
14 Aug	6.2	0	0	3.0	48.4	0.9	14.5
25 Aug	4.3	0.8	18.6	2.4	55.8	1.0	23.2
8 Sep	6.2	1.4	22.5	3.6	58.1	1.5	24.2
29 Sep	24.5	10.4	22.4	20.1	82.0	11.3	46.1
29-30 Sep	3.8	0	0	1.3	34.2	0	0
30 Sep	3.0	0	0	0.3	10.0	0.2	6.7
30 Sep	9.5	7.1	74.7	8.3	87.4	7.7	81.1
16-17 Oct	16.4	0	0	8.0	48.8	1.3	8.0
18 Oct	2.4	0	0	0.8	33.3	0	0
24 Oct	5.5	0	0	2.4	43.6	0	0
15 Nov	1.7	0	0	0	0	0	0
21 Nov	1.5	0	0	0	0	0	0
7 Dec	2.8	0	0	0	0	0	0
13 Dec	6.3	0	0	1.3	20.6	0	0
28 Dec	3.4	0	0	0.1	2.9	0	0
<b>Total</b>	<b>144.0</b>	<b>25.6</b>	<b>17.8</b>	<b>72.0</b>	<b>50.0</b>	<b>34.9</b>	<b>24.2</b>

Table 6. Rainfall and runoff for bare soil plots at Granite Reef  
(continued).

Date	Total Rainfall	R-2 Runoff		R-3 Runoff		R-4 Runoff	
		mm	%	mm	%	mm	%
1971	mm	mm	%	mm	%	mm	%
2 Jan	6.2	0	0	0	0	4.4	71.0
17 Feb	7.7	0	0	0	0	5.5	71.4
15 Apr	8.3	0	0	0	0	5.7	68.7
3 Aug	5.1	0	0	0	0	2.9	57.0
6 Aug	4.5	0	0	0	0	2.7	60.0
10 Aug	1.2	0	0	0	0	0	0
12 Aug	13.5	9.7	71.9	9.8	72.7	12.7	94.1
14 Aug	6.2	0	0	0	0	4.7	75.8
25 Aug	4.3	0.9	20.9	0.6	14.0	2.6	41.9
8 Sep	6.2	1.5	24.3	1.3	21.0	4.6	74.2
29 Sep	24.5	10.4	42.4	9.7	40.0	20.9	85.3
29-30 Sep	3.8	0	0	0	0	} 2.9	42.6
30 Sep	3.0	0	0	0.1	3.3		
30 Sep	9.5	7.2	75.8	7.0	73.7	9.6	101.1
16-17 Oct	16.4	0.6	3.7	0.2	1.2	11.1	67.7
18 Oct	2.4	0	0	0	0	1.4	58.3
24 Oct	5.5	0	0	0	0	3.4	61.8
15 Nov	1.7	0	0	0	0	0.5	29.4
21 Nov	1.5	0	0	0	0	0.1	6.7
7 Dec	2.8	0	0	0	0	1.1	39.2
13 Dec	6.3	0	0	0	0	3.0	47.6
28 Dec	3.4	0	0	0	0	1.0	29.4
Total	144.0	30.3	21.0	28.7	19.9	100.8	70.0

TITLE: SOIL CLOGGING DURING INTERMITTENT INFILTRATION WITH  
SECONDARY SEWAGE EFFLUENT

CRIS WORK UNIT: SWC-018-gG-4

CODE NO.: Ariz.-WCL 71-15

INTRODUCTION:

Laboratory studies were continued to investigate the soil clogging process when using secondary sewage effluent. (See Annual Report 1969-1970, Section WCL 67-4.)

PROCEDURE:

Soil columns 61 cm in length and 10 cm in diameter were filled with soil. Tensiometers were installed at 1, 4, 10, and 30 cm below the soil surface. Two soils, a loamy sand and a coarse sand, were used. Sewage effluent with different suspended solids concentrations was applied to the soil columns. Algal growth on the soil surface was prevented in most instances by excluding light from the columns. Infiltration was continued until a clogged surface layer was formed. The effect of algal growth on infiltration was studied on two occasions when algae was permitted to grow on the soil surface on 3 columns containing loamy sand. No algal growth was permitted on 3 other columns.

RESULTS AND DISCUSSION:

The relationship between hydraulic impedance of the clogged surface layer and the total solids load is shown in Figure 1 for loamy sand. The curve for unit hydraulic gradient is average of a series of 6 different runs representing suspended solids concentration from 1.8 to 108 mg per liter. Each run is an average of 6 columns. The dashed lines represent the scatter of the points. It takes about the same total solids load for an equal impedance change irrespective of the suspended solids concentration of the effluent. The clogging rate is dependent on the total solids deposited on the soil surface. Reductions in infiltration rate then will be faster as the suspended solids concentration is increased.

The total solids load - impedance relationship for the coarse sand is shown in Figure 2 for gradients of 0.1, 0.2 - 0.6, and 1.

Each curve is the average of 10 to 18 columns. Clogging occurred at a faster rate as the gradient became smaller. The opposite occurred with the loamy sand (Figure 1). One explanation for the different behavior of the two soil materials is that in the coarse sand the solids are able to move into the larger pores. At higher gradients the solids move further into the pores because of the higher seepage forces. This distributes the solids over a larger volume of soil and consequently results in a lower impedance than if the solids were deposited only at the soil surface. The depth of solids penetration would be less than 1 cm because the pressure head at that depth was always negative after clogging started. The infiltration rates at 0.1 gradient was sufficiently high, resulting in a compact clogged layer rather than a loose layer that was observed with 0.2 gradient in the loamy sand. In the loamy sand, the pore size was such that little suspended solids moved past the surface. The higher seepage force at unit gradient resulted in a more compact clogged layer. At lower gradients the solids were less compact, forming a more permeable layer.

The effect of algal growth on infiltration is shown in Figure 3. The unit gradient columns were run in July and the 0.6 gradient columns were run in October. The suspended solids concentrations were 15 and 66 mg per liter for the 0.6 gradient and unit gradient columns, respectively. The infiltration rates in the covered and uncovered columns were initially the same and decreased evenly for the first few days. Algal growth was observed 2 days after the start of infiltration in the July test and 7 days after infiltration started in the October test. The infiltration rate increased to a level equal to or greater than the original infiltration rate a few days after the detection of the algal growth. In the covered columns, infiltration rate decreased to about 0.01 cm per min. and leveled off. As algae grew on the soil surface, gas bubbles were produced in the algae mat causing the mat to break loose from the soil surface. In some columns

the mat floated to the water surface while in other columns the mat only separated from the surface. In either case, the soil surface was free of any clogging materials resulting in increased infiltration rates.

**SUMMARY AND CONCLUSIONS:**

Soil clogging process during infiltration using sewage effluent was studied in soil columns. The rate of soil clogging for an initial hydraulic gradient of 1 was dependent on the total solids load, regardless of the suspended solids concentration of the effluent. For a given total solids load in a coarse sand material, the impedance increased with decreasing gradient. The opposite occurs when using a loamy sand soil. Algal growth on the loamy sand was found to increase the infiltration rate over columns where no algae was allowed to grow. The algae mat grows on the soil surface and separates as gas bubbles form in the mat. Consequently, a clean soil surface is exposed.

**PERSONNEL:** Robert C. Rice

**CURRENT TERMINATION DATE:** 31 December 1972

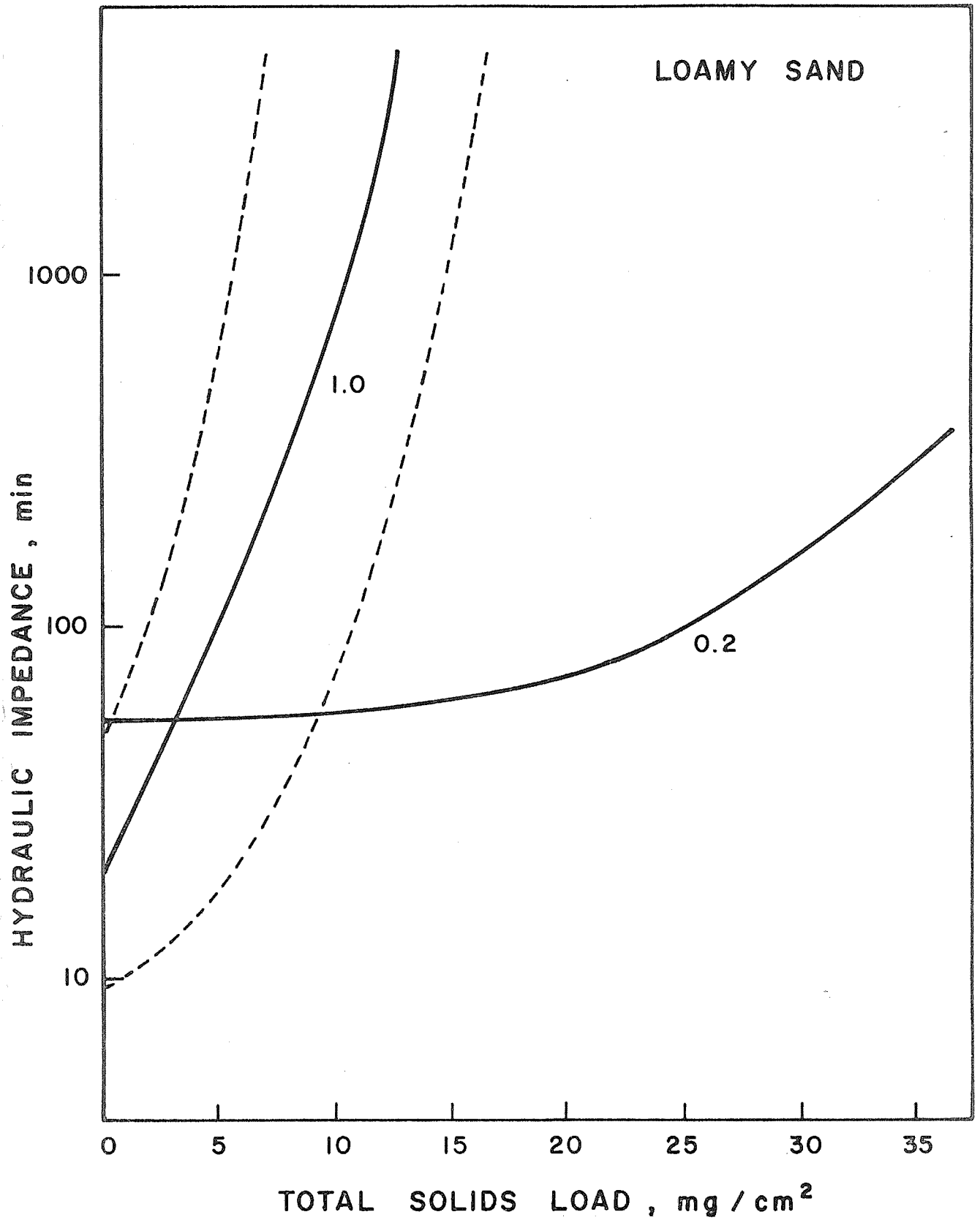


Figure 1. Hydraulic impedance in relation to total-solids load and hydraulic gradient (on the curves) for loamy sand.

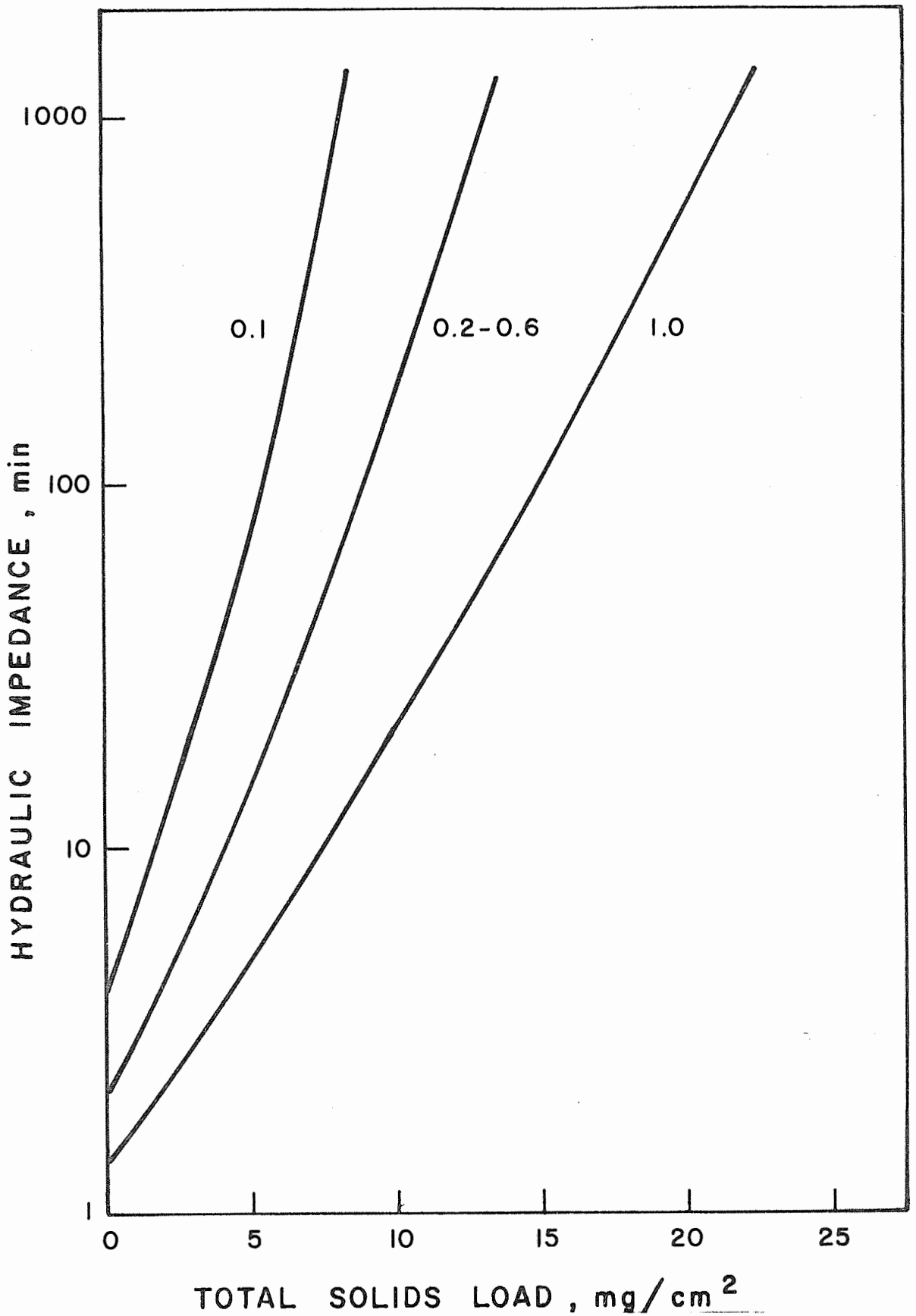


Figure 2. Hydraulic impedance in relation to total-solids load and hydraulic gradient. (Annual Report of the U.S. Water Conservation Laboratory)

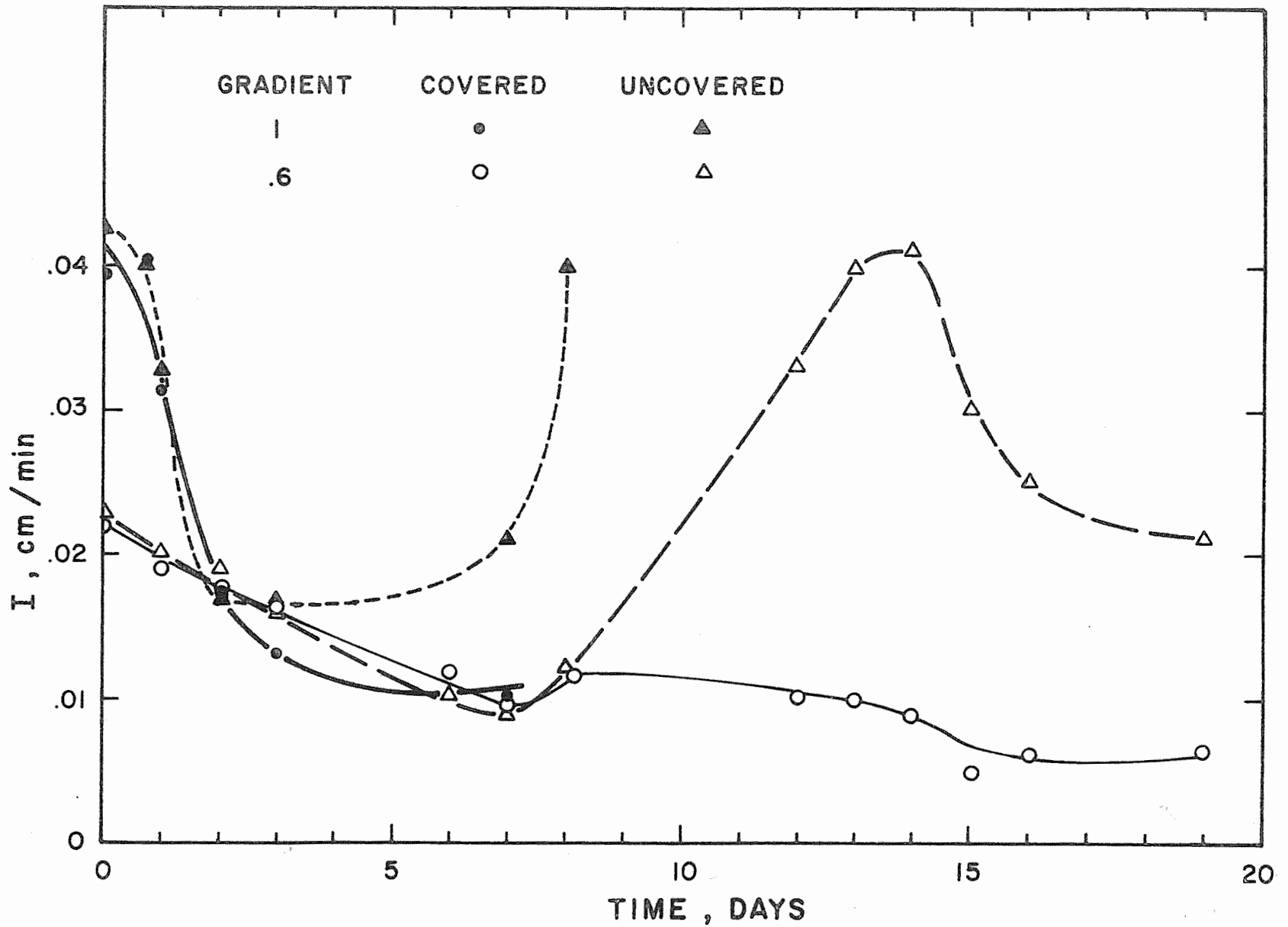


Figure 3. Infiltration rate with time for covered and uncovered columns. Annual Report of the U.S. Water Conservation Laboratory

## APPENDIX I

### SUMMATION OF IMPORTANT FINDINGS

#### SWC-018-gG-4 INCREASING AND CONSERVING AGRICULTURAL AND RURAL WATER SUPPLIES

Flow metering flumes can be constructed in lined channels with a contraction on only one side of the channel. They perform as well as the more conventional flumes where symmetry is maintained with identical contractions on either channel wall. The design details and hydraulic characteristics of this single side-wall sill are accurately predicted by computer techniques for a given flow situation using energy considerations and boundary layer development in the flume. This is an extension of the previous work wherein flows through symmetrically constructed flumes with trapezoidal, triangular and rectangular throat shapes were predicted to an accuracy of  $\pm 2\%$ . The side-wall sill always parallels the general flow direction but may or may not tilt to match the side-wall slope of the channel. Capability to design single-sided flumes for lined channels saves about 50% in materials, and can substantially reduce installation time. (WCL 67-1)

Fluctuation in the fecal coliform density in the ground water below recharge basins intermittently inundated with secondary sewage effluent could be traced directly to the flooding cycles. When a new flooding period was started, fecal coliform bacteria were able to penetrate the soil and cause densities of 100 to 500 per 100 milliliters in the ground water at 30-ft depths. With continued flooding, however, fecal coliform densities at this depth went down to zero in a few weeks, probably because clogging of the soil surface in the basins yielded better filtration and the continued supply of nutrients and resulting increase in microorganisms caused a more competitive environment in the soil.

Almost all the fecal coliform organisms were removed in the first 2 feet of the soil (WCL 67-4)

Removal of 90% of the nitrogen content of secondary sewage effluent was achieved when soil columns were intermittently flooded with sewage water which had been supplemented with dextrose to maintain an average organic carbon concentration of 150 ppm. The addition of 3 levels of dextrose resulted in an increase in the percentage nitrogen removal with each increment of additional organic carbon. The volume of gas collected from the columns increased, indicating that denitrification was stimulated by the addition of organic carbon. These results indicate that the denitrification rate in soils intermittently flooded with sewage water is limited by the amount of available organic carbon. The addition of organic carbon may prove useful in the management of a land filtration system for wastewater renovation. (WCL 68-3)

The organic carbon content of water collected from soil columns intermittently flooded with secondary sewage effluent was only slightly increased when the organic carbon concentration of the sewage water entering the columns was adjusted to 40 ppm by the addition of dextrose. Flooding with sewage water containing 80 or 150-ppm organic carbon resulted in a substantial increase in the organic carbon content of water collected from the columns. The infiltration rate was reduced by about 30% by the addition of organic carbon due to internal clogging, while flooding with sewage water high in suspended solids resulted in a 50% reduction in infiltration rates due to a surface clogging. A high-rate soil filtration system (1-2 ft/day) can remove 40-80 ppm dissolved organic carbon by predominantly anaerobic reaction, and organic sediments appear to be more of a problem in soil clogging than dissolved organics. This shows that a good quality secondary effluent is needed to maintain an efficient high-rate soil filtration system for wastewater reclamation. (WCL 68-3)

Platinum-blackened platinum redox electrodes can be left in soil columns for as long as 6 months and still cycle with infiltration and drainage with the same amplitudes. This is true even where the soil columns are flooded with secondary sewage effluent which contains as much as 150-ppm organic carbon. The added carbon increases the amplitude of the redox cycle and the rate of change of the redox potential. (WCL 68-3)

Application uniformity from low-pressure trickle irrigation systems can be greatly improved by varying outlet sizes to compensate for friction-induced pressure changes in the lateral pipe. Low-pressure systems using single applicator sizes suffer from non-uniform applicator discharge because pressure changes are a large percentage of total pressure. High-pressure trickle systems alleviate this problem by using high head loss applicators. Low-pressure systems, using simple orifices, can have several advantages over high-pressure systems in reduced manufacturing and operating costs, larger orifices to reduce clogging, and simpler flow-control devices. A graphical procedure was introduced to show the ease at which a multiple-size system can be designed and to verify the validity of changing orifice sizes. Theoretical maximum deviations from design discharge were + 21% to -7.4% for the single-size system, and  $\pm$  3.3% for the multiple-size system in a 250-ft lateral, 2-ft orifice spacing. A comparable multiple-size system using hand-made orifices was field tested, and maximum deviations from design discharge of + 5.2% to -6.6% resulted. Improved application uniformity can be obtained by varying orifice sizes. (WCL 70-3)

The soil moisture used for high cotton production with trickle irrigation on replicated plots was found to be nearly the same as present consumptive-use estimates for furrow irrigation. Irrigations consisted of three quantities, based on ratios of the plant's consumptive-use estimate, applied at three frequencies,

using cotton as the "indicator" crop. The three adjusted quantities, to include rainfall, gravity irrigations for germination, and trickle irrigations, were ratios 1.06, 0.90, and 0.72 times the seasonal consumptive-use estimate of 41.2 inches. The three frequencies were every 3, 6, and 12 days. Cotton yield response showed no difference between irrigation frequencies, and an 18% reduction in yield for the 0.72 consumptive use, as compared to the 0.90 and 1.06 quantities. The mean cotton yield for 1.06 and 0.90 quantities was 3 bales/acre. This study suggests that plant needs for maximum production when using trickle irrigation are no different than when other irrigation methods are used. (WCL 70-3)

Transpiration research has led to improved equipment for measuring the relative humidity (RH) of air at low wind speeds. At 30 C a micro-psychrometer shows an accurate wet bulb depression at a wind speed of only  $0.12 \text{ m sec}^{-1}$  when RH is 33% and requires no more than  $0.30 \text{ m sec}^{-1}$  at the low RH of 7%, in contrast to the minimum ventilation rate of  $2 \text{ m sec}^{-1}$  needed for standard psychrometers. The reductions in air flow requirement are due to the minute size of the wet bulb and the consequent minimizing of several errors common to all wet bulbs, which are compensated by ventilation. Size reduction comes about by use of a thermo-junction as the temperature sensor, made of 0.05 mm copper constantan wire wrapped in 0.15 mm cotton thread, resulting in an overall diameter of only 0.20 mm. An additional feature of the psychrometer is that force feeding of water to the wick permits adequate wetting even under the demanding conditions of very low RH. (WCL 71-1)

Where irrigations were applied for a full growing season and populations were increased from the standard 20,000 to 40,000 plants per acre, production of seed cotton was improved more than 25%; however, no yield increase was recorded for an 80,000 population over 40,000. For irrigation regimes, the difference in

yield from the dry treatment over the two wetter treatments was large enough to be statistically significant. A yield reduction of 14.9% for Deltapine-16 and 9% for Stoneville-213 was measured for the dry regime. For these varieties, 15% of the seed cotton was produced from flowers opening after 15 August. Any increases in flowers associated with high-population benefits occurred before 17 July in 1971. There was no hastening of the pattern of events for blossom and boll production for the varied populations, nor any major changes in the trend of events associated with peaks, or efficiency of bolls from blossom. When irrigations were cut off in late July, the numbers of flowers and bolls, and the yield of seed cotton, increased as plant populations were increased. This information is needed to enlighten cotton growers, State regulatory organizations, economists, and others involved with production of high-population cotton, early cut-off irrigation water, acreage limitations, early plow-under dates, and general control of pink bollworms. These findings will assist in more logical and economical decision-making for cotton production. (WCL 71-2)

A theoretical method was developed and was tested experimentally for determining the thermodynamic solubility product of calcium carbonate. The method involves the direct measurement of the activity of ions in equilibrium with the solid using recently developed selective ion electrodes. It is simple, and with proper modification can be used for studying solubility of other slightly soluble carbonate systems of magnesium, barium and strontium. The solubility product ( $3.25 \times 10^{-9}$ ) was comparable with those reported using other techniques, but was derived with less experimental complications. (WCL 71-4)

Ponded infiltration into three, layered soil columns shows that entrapped air may build up air pressures in the soil of 50-60 cm and may retard the infiltration rates as much as 12%.

Venting of the soil-air system overcomes much of the problem of entrapped air. If the total amount of infiltration is decreased by the same percentage as the infiltration rate, then venting will provide an economic benefit if its cost is less than the additional water produced in a groundwater recharge and renovation system. (WCL 71-8)

Numerical analysis studies have shown that heterogeneous soil or porous media behave quite differently than a homogeneous one in terms of pressure head and water content profiles during infiltration or drainage. A linear variation of saturated or resaturated hydraulic conductivity down the profile was chosen as the means of defining the scale heterogeneous porous media, and this was chosen with possible field applications in mind. By using one of the available experimental methods for determining  $K_{sat}$  in the field at different depths, it is possible to check the homogeneity of the profile. If heterogeneity is found and if the scale heterogeneity assumption is considered reasonable for the material in question, it would be possible to predict at least approximately the drainage and infiltration behavior using a numerical solution. Also, this concept of scale heterogeneity and method of studying it can be applied to the many soil-water flow models currently under investigation. (WCL 71-9)

Particles less than one-tenth the size of the trickle orifice were found to plug the orifice openings. The exact nature of this is not known, but use of better filtering systems can help to alleviate some of the plugging problem. Cementation by precipitating minerals appears to cause the buildup of the obstruction. If the cementing agent consists of  $CaCO_3$ , then acids such as  $HCl$ ,  $HNO_3$ , and  $H_2SO_4$  can be used to dissolve the precipitate. If it is  $CaSO_4$ , the  $HCl$  and  $HNO_3$  acids are preferable. The best solution is the prevention of orifice plugging either by the removal of suspended material, use of acids and Ca-complexing chemicals, or combinations of these treatments. (WCL 71-11)

APPENDIX II

LIST OF PUBLICATIONS PUBLISHED AND  
MANUSCRIPTS PREPARED IN 1971

	<u>MS No.</u>
SWC-018-gG4 Increasing and conserving agricultural and rural water supplies.	
Published: <u>Bouwer, Herman.</u> Digest: Planning and interpreting soil permeability measurements. Trans., Amer. Soc. Civil Engin. 135:1014-1016. 1970.	313
<u>Bouwer, Herman.</u> Digest: Salt balance, irrigation efficiency, and drainage design. Trans., Amer. Soc. Civil Engin. 135:995-996. 1970.	317
<u>Bouwer, Herman.</u> Waste water purification. Chap. in McGraw-Hill Yearbook of Science and Technology, 1971. Pp. 434-436.	324
<u>Bouwer, Herman.</u> Digest: Groundwater recharge design for renovating wastewater. Trans., Amer. Soc. Civil Engin. 136:468-469. 1971.	333
<u>Bouwer, Herman, Lance, J.C., and Rice, R.C.</u> Land disposal of sewage effluents. Proc., Symp. on Nitrogen in Soil and Water, Univ. of Guelph, Guelph, Ontario, Canada, March 30-31, 1971. Pp. 110-134.	353
<u>Bouwer, Herman, Lance, J.C., and Rice, R.C.</u> Renovating sewage effluent by groundwater recharge. In Hydrology and Water Resources of Arizona and the Southwest, Vol. I. Pp. 225-244. (Univ. of Arizona Press, 1971).	357
<u>Bouwer, Herman, and Rice, R. C.</u> Digest: Salt penetration technique for seepage measurements. Trans., Amer. Soc. Civil Engin. 135: 912-913. 1970.	315

	<u>MS No.</u>
<u>Cooley, Keith R., and Idso, S.B.</u> Atmospheric thermal radiation: An isolated anomaly. Bul. Amer. Meteorol. Soc. 52(6): 464-465. June 1971.	326
<u>Cooley, Keith R., and Idso, S. B.</u> A comparison of energy balance methods for estimating atmospheric thermal radiation. Water Resources Res. 7(1):39-45. Feb 1971.	329
<u>Erie, Leonard J.</u> Digest: Management; A key to irrigation efficiency. Trans., Amer. Soc. Civil Engin. 135:555-556. 1970.	286
<u>Fink, D. H., Nakayama, F. S., and McNeal, B. L.</u> Demixing of exchangeable cations in free-swelling bentonite clay. Soil Sci. Soc. Amer. Proc. 35(4):552-555. July-Aug 1971.	350
<u>Frasier, Gary W.</u> Optimum design of water harvesting structures by computer. USDA-ARS 41-175. March 1971.	330
<u>Idso, Sherwood B.</u> A simple technique for the calibration of long-wave radiation probes. Agric. Meteorol. 8(3):235-243. May 1971.	307
<u>Idso, Sherwood B.</u> Relations between net and solar radiation. Jour. Meteorol. Soc. Japan 49(1):1-12. 1971.	322
<u>Idso, Sherwood B.</u> Transformation of a net radiometer into a hemispherical radiometer. Agric. Meteorol. 9(2):109-121. 1971/1972.	323
<u>Idso, Sherwood B.</u> The utility of diffuse skylight measurements in characterizing low levels of particulate air pollution. Atmos. Environ. 5(8):599-604. Aug 1971.	338
<u>Idso, Sherwood B.</u> Evaporation suppression by solar radiation reflection. Jour. of Geophys. Res. 76(12):2900. Apr 20, 1971.	340

- Idso, Sherwood B., and Blad, Blaine L.  
The effect of air temperature upon net and  
solar radiation. Jour. Appl. Meteorol.  
10(3):604-605. June 1971. 344
- Idso, Sherwood B., Fuchs, M., and  
Tanner, C. B. Comments on "Errors in  
Infrared Thermometry and Radiometry".  
Jour. Appl. Meteorol. 10(5):1041. 1971. 354
- Jensen, Marvin, and Erie, Leonard J.  
Irrigation and water management.  
Chap. 8 in "Advances in Sugar Beet  
Production: Principles and Practices."  
Ortho Div., Chevron Chem. Co. Pp. 189-221. 319
- Kimball, Bruce A., and Jackson, R. D.  
Seasonal effects on soil drying after  
irrigation. In Hydrology and Water  
Resources of Arizona and the Southwest,  
Vol. I. Pp. 85-98. (Univ. of Arizona  
Press, 1971). 367
- Kimball, Bruce A., and Lemon, E. R.  
Air turbulence effects upon soil gas  
exchange. Soil Sci. Soc. Amer. Proc.  
35(1):16-20. Jan-Feb 1971. 320
- Myers, Lloyd E. Water conservation for  
food and fiber production in arid lands.  
Chap. in "Food, Fiber and the Arid Lands",  
Edited by Wm. G. McGinnies, B. J. Goldman,  
and Patricia Paylore. Pp. 301-309.  
(Univ. of Arizona Press, 1971). 300
- Myers, Lloyd E. Digest: Opportunities for  
water salvage. Trans., Amer. Soc. Civil  
Engin. 136:19-21. 1971. 311
- Myers, Lloyd E. Environmental fact and  
fancy. In Internatl. Comm. Irrig. and  
Drain. Newsletter No. 15, Pp. 5-6.  
Dec 1970. 365

- Myers, Lloyd E., and Frasier, Gary W.  
Digest: Creating hydrophobic soil for water harvesting. Trans., Amer. Soc. Civil Engin. 135:956. 1970. 297
- Myers, Lloyd E., and Frasier, Gary W.  
Digest: Evaporation reduction with floating granular materials. Trans., Amer. Soc. Civil Engin. 136:1272-1273. 1971. 369
- Myers, Lloyd E., Frasier, Gary W., and Griggs, John R. Digest: Sprayed asphalt pavements for water harvesting. Trans., Amer. Soc. Civil Engin. 135:187-188. 1970. 289
- Nakayama, F. S. Magnesium complex and ion-pair in the  $MgCO_3$ - $CO_2$  solution system. Jour. Chem. and Engin. Data 16:178-181. 1971. 262
- Nakayama, F. S. Thermodynamic functions for the dissociation of  $NaHCO_3^O$ ,  $NaCO_3^-$ ,  $H_2CO_3$ , and  $HCO_3^-$ . Jour. Inorg. and Nucl. Chem. 33(5):1287-1291. May 1971. 309
- Nakayama, F. S. Problems associated with the determination and application of the solubility product constant. Soil Sci. Soc. Amer. Proc. 35(3):442-445. May-June 1971. 341
- Nakayama, F. S. Calcium complexing and the enhanced solubility of gypsum in concentrated sodium salt solutions. Soil Sci. Soc. Amer. Proc. 35(6):881-883. Nov-Dec 1971. 351
- Nielsen, D. R., Jackson, R. D., Cary, J. W., and Evans, D. D., Editors. SOIL WATER. 267 pp. Univ. of Calif. (Davis) Press, 1970. 339

- Reginato, R. J., and Jackson, R. D. Field measurement of soil-water content by Gamma-ray transmission compensated for temperature fluctuations. Soil Sci. Soc. Amer. Proc. 35(4):529-533. July-Aug 1971. 343
- Reginato, R. J., and Jackson, R. D. Field measurements of soil-water content and soil-water pressure. In Hydrology and Water Resources of Arizona and the Southwest, Vol. I. Pp. 143-151. (Univ. of Arizona Press, 1971). 366
- Replogle, John A. Critical-depth flumes for determining flow in canals and natural channels. Trans., Amer. Soc. Agric. Engin. 14(3):428-433:436. May-June 1971. 327
- Whisler, F. D., and Watson, K. K. Digest: Analysis of infiltration into draining porous media. Trans., Amer. Soc. Civil Engin. 136:215. 1971. 328
- Willardson, Lyman S., Boles, A. J., and Bower, Herman. Interceptor drain recovery of canal seepage. Trans., Amer. Soc. Agric. Engin. 14(4):738-741. July-Aug 1971. 385
- Prepared: Bower, Herman. Developing drainage design criteria. Chap. in "Drainage for Agriculture". Amer. Soc. Agronomy Monograph Series. (Submitted for publication). 379
- Bower, Herman, and Jackson, R. D. Determining soil properties. Chap. in "Drainage for Agriculture". Amer. Soc. Agronomy Monograph Series. (Submitted for publication). 384
- Cooley, Keith R., and Cluff, C. Brent Reducing pond evaporation with perlite ore. Jour. Irrig. and Drain. Div., Amer. Soc. Civil Engin. Proc. (Submitted for publication). 377

- Cooley, Keith R., Myers, Lloyd E., and Frasier, Gary W. Lower cost water harvesting methods. Proc., Symp. on Interdisciplinary Aspects of Watershed Management, Univ. of Montana, Bozeman, Mont., Aug 1970. (In press). 355
- DeBoer, D. W., Bucks, Dale A., Lembke, W. D., and Wiersma, J. L. Envelope performance in a coarse-silt base material. Proc., Natl. Drainage Symposium, Chicago, Ill., Dec 1971. (Submitted for publication). 381
- Ehrler, William L. Periodic nocturnal stomatal opening in a steady environment. Physiol. Plant. (In press). 363
- Ehrler, William L. Additions to transpiration data contained in "Biology Data Book", to be published by Fed. of American Societies for Experimental Biology. (Submitted for publication). 374
- Ehrler, William L. The water-use efficiency of Agave Americana L., and Zea Mays L., as affected by low soil-water potential. Agron. Jour. (Submitted for approval). 383
- Fink, Dwayne H., and Nakayama, F. S. Equation for describing the free-swelling of montmorillonite in water. Soil Sci. (Submitted for publication). 359
- Frasier, Gary W., and Myers, Lloyd E. Bonding films to soil surfaces for water harvesting. Trans., Amer. Soc. Agric. Engin. (Submitted for publication). 382
- Idso, Sherwood B. Solar radiation measurements augment air pollution studies. Jour. Air Pollution Control Assoc. (Submitted for publication). 358

MS No.

- Idso, Sherwood B. Systematic deviations of clear sky atmospheric thermal radiation from predictions of empirical formulae. Quart. Jour. Roy. Meteorol. Soc. (In press). 360
- Idso, Sherwood B. A comparison of the Funk and Idso techniques for measuring hemispherical all-wave radiation. Rev. Sci. Instr. (In press). 361
- Idso, Sherwood B. Solar and thermal radiation fluxes under cloudless skies during a dust storm. Weather. (Submitted for publication). 368
- Idso, Sherwood B. Calibration of soil heat flux plates by a radiation technique. Agric. Meteorol. (In press). 375
- Idso, Sherwood B. Simplifications in the transformation of net radiometers into hemispherical radiometers. Agric. Meteorol. (In press). 380
- Jackson, R. D. Diurnal soil-water content changes during drying. Field Moisture Regime Symp., Amer. Soc. Agron., New York, N.Y. Aug 1971. (Special pub., ASA) (Submitted for publication). 370
- Jackson, R. D. On the calculation of hydraulic conductivity. Soil Sci. Soc. Amer. Proc. (NOTE) (Submitted for publication). 376
- Lance, J. C. The natural way to clean wastewater. Amer. Horticulture Mag. (In press). 371
- Lance, J. C., and Whisler, F. D. Nitrogen balance in soil columns intermittently flooded with sewage water. Jour. Environ. Quality. (In press). 362

- Myers, Lloyd E., and Bucks, Dale A.  
Trickle irrigation with varying outlet  
sizes. Jour. Irrig. and Drain. Div.,  
Amer. Soc. Civil Engin. Proc. (Submitted  
for publication). 378
- Nakayama, F. S. The association of  
calcium with carbonates. Geochim. and  
Cosmochim. Acta. (In press). 348
- Nakayama, F. S. A simple method for  
estimating the solubility product of  
calcium carbonate. Soil Sci. (NOTE)  
(In press). 364
- Replogle, John A. Tailoring critical-  
depth measuring flumes. Symp. on Flow:  
Its measurement and control in science  
and industry. (Proc.) Pittsburgh, Pa.  
May 1971. (Submitted for publication). 356
- Watson, Keith K. Flow in porous media.  
4th Australasian Conf. on Hydraulics and  
Fluid Mechanics Proc., Melbourne, Aust.  
Dec 1971. (Submitted for publication). 372
- Watson, Keith K., and Whisler, F. D.  
Numerical analysis of drainage of a  
heterogeneous porous medium. Soil Sci.  
Soc. Amer. Proc. (Submitted for publication). 373

APPENDIX III

SUMMARY TABLE OF STATUS OF RESEARCH OUTLINES

	<u>Title</u>	<u>Code</u>
SWC-018-gG-4	Increasing and conserving agricultural and rural water supplies	
Ariz.-WCL 58-2	Consumptive use of water by crops grown in Arizona	C
Ariz.-WCL 61-4	Measurement and calculation of unsaturated conductivity and soil-water diffusivity	D
Ariz.-WCL 65-2	Materials and methods for water harvesting and water storage in the State of Hawaii	B
Ariz.-WCL 65-3	Integrating velocity profile meters	C
Ariz.-WCL 66-2	Irrigation outlet structures to distribute water onto erosive soils	B
Ariz.-WCL 67-1	Flow measurement in open channels with critical depth flumes	B
Ariz.-WCL 67-2	Physical and chemical characteristics of hydrophobic soils	B
Ariz.-WCL 67-4	Waste-water renovation by spreading treated sewage for groundwater recharge	B
Ariz.-WCL 68-1	Evaporation of water from soil	B
Ariz.-WCL 68-2	Fabricated-in-place, reinforced linings and ground covers	B
Ariz.-WCL 68-3	Column studies of chemical, physical, and biological processes of waste-water renovation by percolation through the soil	B
Ariz.-WCL 68-5	Assessing the energy environment of plants	D

	<u>Title</u>	<u>Code</u>
Ariz.-WCL 70-1	Computer simulation of greenhouses	B
Ariz.-WCL 70-2	Characterization of the soil microflora and biological processes occurring in the soil used for waste water renovation	B
Ariz.-WCL 70-3	Design and performance of trickle irrigation systems	B
Ariz.-WCL 71-1	Relative changes in transpiration and photosynthesis induced by soil water depletion in a constant environment	B
Ariz.-WCL 71-2	The effect of irrigation regimes and early cut-off of irrigation water on the yield of high population cotton	B
Ariz.-WCL 71-3	Heat and light transfer in ponds	B
Ariz.-WCL 71-4	Measurement and prediction of the solubility behavior of the calcium mineral constituents of soils	B
Ariz.-WCL 71-5	Water vapor movement through mulches under field conditions	B
Ariz.-WCL 71-6	Use of floating materials to reduce evaporation from water surfaces	B
Ariz.-WCL 71-7	Water adsorption properties of soil surfaces coated with organic compounds	B
Ariz.-WCL 71-8	The effect of air entrapment on water movement in soils	B
Ariz.-WCL 71-9	One-dimensional flow in scaled heterogeneous porous media	B
Ariz.-WCL 71-10	Assessment of biostimulation and eutrophication of reclaimed waste water	B

	<u>Title</u>	<u>Code</u>
Ariz.-WCL 71-11	Chemical treatment of irrigation water for the prevention of clogging and the removal of flow obstructions in trickle irrigation systems	B
Ariz.-WCL 71-12	Lower cost water harvesting systems	B
Ariz.-WCL 71-13	Modifying furrow irrigation practices for cabbage production	A
Ariz.-WCL 71-14	Evaluating trickle irrigation for cabbage production	A
Ariz.-WCL 71-15	Soil clogging during intermittent infiltration with secondary sewage effluent	B

	<u>Title</u>	<u>Code</u>
PL 480 Projects		
A10-SWC-20	Biology and consumptive water use of range plants under desert conditions	D
A10-SWC-75	Infiltration and rainfall runoff as affected by natural and artificial surface crusts	C
E30-SWC-4	Influence of irrigation on changes of physical properties of soil	B
E30-SWC-41	Depth, time and quantity of water for irrigation of cotton and corn (with depth and shallow root system)	B